Characterisation of the *Plasmodium falciparum* Hsp40 chaperones and their partnerships with Hsp70

A thesis submitted in fulfilment of
the requirements for the degree

of

DOCTOR OF PHILOSOPHY

of

RHODES UNIVERSITY

in the

FACULTY OF SCIENCE

DEPARTMENT OF BIOCHEMISTRY, MICROBIOLOGY & BIOTECHNOLOGY

by

MELISSA BOTHA

BSc (HONS) in BIOCHEMISTRY, RHODES UNIVERSITY, 2004

JANUARY 2009

ABSTRACT

Central to this research, 40 kDa Heat shock proteins (Hsp40s) are known to partner (or co-chaperone) 70 kDa Heat shock proteins (Hsp70s), facilitating the selection and transfer of protein substrate to Hsp70 and the stimulation of the protein folding ability of Hsp70. Members of the diverse Hsp70-Hsp40 protein complement of ***Plasmodium falciparum*** have been implicated in the cytoprotection of this malaria parasite, and are thought to facilitate the protein folding, assembly and translocation tasks required by the parasite to commandeer the infected human erythrocyte subsequent to invasion. In particular, the parasite has evolved an expanded and specialised 43-member suite of Hsp40 proteins, 19 of which bear an identifiable export motif for secretion into the infected erythrocyte cytoplasm where they potentially interact with human Hsp70. Although type ▮ Hsp40 proteins are representative of typical regulators of Hsp70 activity, only two of these proteins are apparent in the parasite's Hsp40 complement. These include a characteristic type ▮Hsp40 termed PfHsp40, and a larger, atypical type ▮Hsp40 termed Pfj1. Both Hsp40 proteins are predicted to be parasite-resident and are most likely to facilitate the co-chaperone regulation of the highly abundant and stress-inducible Hsp70 homolog, PfHsp70-▮ In this work, the co-chaperone functionality of PfHsp40 and Pfj1 was elucidated using ***in vivo*** and ***in vitro*** assays. Purified recombinant PfHsp40 was shown to stimulate the ATPase activity of PfHsp70-▮ in ***in vitro*** single turnover and steady state ATPase assays, and co-operate with PfHsp70-▮in ***in vitro*** aggregation suppression assays. In these ***in vitro*** assays, heterologous partnerships could be demonstrated between PfHsp70-▮and the human Hsp40, Hsj1a, and human Hsp70 and PfHsp40, suggesting a common mode of Hsp70-Hsp40 interaction in the parasite and host organism. The functionality of the signature Hsp40 domain, the J-domain, of Pfj1 was demonstrated by its ability to replace the equivalent domain of the ***A. tumefaciens*** Hsp40, ***Agt*** DnaJ, in interactions with the prokaryotic Hsp70, DnaK, in the thermosensitive ***dnaJ cbpA E. coli*** OD259 deletion strain. An H33Q mutation introduced into the invariant and crucial HPD tripeptide motif abrogated the functionality of the J-domain in the ***in vivo*** complementation system. These findings provide the first evidence for the conservation of the

prototypical mode of J-domain based interaction of Hsp40 with Hsp70 in ***P. falciparum.*** Immunofluorescence staining revealed the localisation of PfHsp40 to the parasite cytoplasm, and Pfj1 to the parasite cytoplasm and nucleus in cultured intraerythrocytic stage ***P. falciparum*** parasites. PfHsp70-▮ was also shown to localise to the parasite cytoplasm and nucleus in these stages, consistent with the literature. Overall we propose that PfHsp40 and Pfj1 co-localise with and regulate the chaperone activity of PfHsp70-▮ in ***P. falciparum***. This is the first study to identify and provide evidence for a functional Hsp70-Hsp40 partnership in ***P. falciparum***, and provides a platform for future studies to elucidate the importance of these chaperone partnerships in the establishment and survival of the parasite in the intraerythrocytic-stages of development.

DECLARATION

I, Melissa Botha, declare that this is my own unaided work hereby submitted for the degree of Doctor of Philosophy of Rhodes University in the Faculty of Science. It has not been submitted for any degree for examination in any other university.

_____

MELISSA BOTHA

DATED THIS _____ DAY OF _____ _____ AT _____.

TABLE OF CONTENTS

LIST OF FIGURES

LIST OF TABLES

DEDICATION

This thesis is dedicated to my parents, Gerrie and Maureen, for providing me with the opportunity to pursue a higher degree, and selflessly supporting me in every means throughout my studies.

PERSONAL ACKNOWLEDGEMENTS

Serge and Pandora the chocolate labrador

Thank-you for the immense support, love and encouragement!

ACKNOWLEDGEMENTS

I would like to recognise the following individuals for their contributions to this work:

My mentor, Professor Gregory Blatch, has endeavoured to share his passion and immense enthusiasm for Science with me over the past four years; inspiring me to remain motivated, and encouraging me to think creatively and independently as a Scientist in my own right.

Professor Rosemary Dorrington and Dr Brett Pletschke, for their guidance and helpful contributions as members of my PhD Steering Committee.

Dr. Heinrich Hoppe and members of the former Malaria Cell Biology Group, Department of Medicine, University of Cape Town, South Africa, for accommodating me in their laboratory and assistance with the localisation studies and preparation of the cultured P. falciparum-infected erythrocytes.

Dr. Vicky Longshaw and James Short for assistance with confocal microscopy.

Professor Jeff Brodsky, Dr Annette Chiang and members of the Brodsky Laboratory for accommodating me at the University of Pittsburgh, USA, and for invaluable input and assistance with the in vitro characterisation of the relevant malarial and human proteins detailed in this work. Plasmid construct pGEX-KG-Hlj1 was a kind gift from the Brodsky laboratory.

Purified recombinant human Hsp70 was a kind gift to the Brodsky laboratory from Professor Xiaojieng Chen and Dr. Michael Klein, University of the Department of Molecular and Computational Biology, University of Southern California, United States.

Dr Evelina Angov of the Walter Reed Army Institute for Research (WRAIR) of Maryland, USA, for assistance with codon harmonisation of the PfHsp40 coding sequence. Codon harmonisation was verified with use of the GeneSplitter software package, a kind gift from its developer, Professor Jaco de Ridder, University of Pretoria, South Africa.

Dr. William Nicoll for initiating codon optimisation and synthesis of the Pfj1 coding sequence. Dr. Addmore Shonhai for the kind gift of the pQPfHsp70-I plasmid construct and anti-PfHsp70-I antibody , and ***Caryn McNamara for the pQHsj1a plasmid construct.***

Professor Richard Zimmerman for production of the designed anti-PfHsp40 and anti-Pfj1 peptide antibodies.

Dr Jude Przyborski of Philipps University, Marburg, Germany for the Maurer's Clefts marker antibody, anti-PfSBP-1.

Professor Herman Bujard and Ute Woehlbier of the University of Heidelberg, Germany, for the kind gift of the anti-MSP-7 antibody.

Dr. Michael Cascio of the Department of Microbiology and Molecular Genetics, University of Pittsburgh School of Medicine, USA, for use of his facilities and thermo-controlled spectrophotometer for aggregation suppression assays.

ACKNOWLEDGEMENT OF FUNDING

Personal funding was provided by the German Academic Exchange Service (Deutscher Akademischer Austauchdienst - DAAD), a Prestigious PhD Scholarship granted by the South African National Research Foundation (NRF), and a Rhodes University Henderson Postgraduate Scholarship.

A research visit to the University of Pittsburgh, Pennsylvania, United States of America was supported by funding from the Rhodes University Joint Research Committee (JRC), a Wood-Whelan Research Fellowship granted by the International Union of Biochemistry and Molecular Biology (IUBMB), a travel allowance associated with an NRF Prestigious PhD Scholarship, and the NRF research grant of Professor Gregory Blatch.

LIST OF RESEARCH OUTPUTS

PUBLICATIONS

SHONHAI, A., BOTHA, M., DE BEER, T., BOSHOFF, A. and BLATCH, G.L. (2008). Structure-function analysis of the substrate binding cavity of ***Plasmodium falciparum*** heat shock protein 70. ***Protein and Peptide Letters***, 15, 1117-1125.

BOTHA, M., PESCE, E.R. and BLATCH, G.L. (2007). Review: The Hsp40 proteins of ***Plasmodium falciparum***: regulating chaperone power in the parasite and the host. ***International Journal of Biochemistry and Cell Biology***, 39, 1781-1803.

NICOLL, W.S.*, BOTHA, M.*, MCNAMARA, C., SCHLANGE, M., PESCE, E., BOSHOFF, A., LUDEWIG, M.H., ZIMMERMANN, R., CHEETHAM, M.E., CHAPPLE, J.P. and BLATCH, G.L. (2007). Cytosolic and ER J-domains of mammalian and parasitic origin can functionally interact with DnaK. ***International Journal of Biochemistry and Cell Biology***, 39, 736-751. * These authors contributed equally to this work.

LONGSHAW, V.M., NICOLL, W.S., BOTHA, M., LUDEWIG, M.H., SHONHAI, A., STEPHENS, L.L., and BLATCH G.L. (2006). Getting practical with molecular chaperones. ***Biotechnology International*** 18, 24-27.

In Progress:

BOTHA, M., CHIANG, A., HOPPE, H., BRODSKY, J.L. and BLATCH, G.L. (2009). Characterisation of an Hsp70-Hsp40 partnership of ***Plasmodium falciparum***. ***In Progress.***

CONFERENCE PROCEEDINGS

BOTHA, M., NICOLL, W.S. and BLATCH, G.L. (2006). Molecular Characterisation of the Major Type I Hsp40 Proteins from ***Plasmodium falciparum***. South African Society of Biochemistry and Molecular Biology Conference (20th Congress), University of Kwazulu-Natal, Pietermaritzburg Campus, South Africa.

BOTHA, M., HOPPE, H. and BLATCH, G.L. (2008). The Hsp40 Proteins of ***Plasmodium falciparum:*** understanding how the malaria parasite harnesses its chaperone power. ***Bio***-08 Conference (South African Society of Biochemistry & Molecular Biology, South African Society for Microbiology, and Biotech South Africa), Rhodes University, Grahamstown, South Africa.

BOTHA, M., HOPPE, H. and BLATCH, G.L. (2008). The Hsp40 Proteins of ***Plasmodium falciparum***: Exploiting Chaperone Power in the Malaria Parasite and Infected Human Erythrocyte. International Union of Biochemistry and Molecular Biology (IUBMB) First Advanced Summer School in Africa, Hermanus, South Africa.

BOTHA, M., HOPPE, H. and BLATCH, G.L. (2008). The Hsp40 Proteins of ***Plasmodium falciparum***: Exploiting Chaperone Power in the Malaria Parasite and Infected Human Erythrocyte. Cold Spring Harbor Meeting on Molecular Chaperones and Stress Responses, Cold Spring Harbor, Long Island, New York, United States of America.

APPENDIX A

LIST OF ABBREVIATIONS

<	Less than
α	Alpha
β	Beta
λ	Lambda
σ^{32}	Sigma-32
°C	Degrees Celsius
µ	Micro
µCi	Micro Curie
µg	Microgram(s)
µl	Microlitre(s)
µM	Micromolar
µmol	Micromole(s)
A	Absorbance
A_{600}	Absorbance at 600nm
A. gambiae	*Anopheles gambiae*
A. tumefaciens	*Agrobacterium tumefaciens*
ADP_R	Adenosine diphosphate
Amp	Ampicillin resistance (β-lactamase gene)
A-T	Adenosine - Thymine
ATP	Adenosine triphosphate
ATPase	Adenosine triphosphatase
APS	Ammonium Persulphate
BiP	Binding Protein
BLAST	Basic Local Alignment Search Tool
BSA	Bovine Serum Albumin
bp	Base pairs
C. hominis	*Cryptosporidium hominis*
C. parvum	*Cryptosporidium parvum*
C-	COOH-terminal
CAAX	C – Cysteine, A – Aliphatic Residue, X – Any Residue
CbpA	Curved DNA binding protein A
CHIP	Carboxyl terminus of the Hsc70 Interacting Protein
DAPI	4',6-diamidino-2-phenylindole
DMSO	Dimethyl sulfoxide
DNA	Deoxyribonucleic Acid
DnaJ	Prokaryotic Hsp40
DnaK	Prokaryotic Hsp70
dNTP	Deoxyribonucleotide Triphosphate
DSG	15-Deoxyspergualin
DTT	Dithiothreitol
E. coli	*Escherichia coli*
EDTA	Ethylene diamine tetra-acetic acid
ER	Endoplasmic reticulum
g	Gram(s)
GF-Region	Glycine-Phenylalanine rich region
GFP	Green Fluorescent Protein

GST	Glutathione-S-Transferase
H. sapiens	*Homo sapiens*
HEPES	N-2-hydroxyethyl-piperrazine-N'-2-ethanesulfonic acid
Hip	Hsc70 interacting protein
His_6	Hexahistidine tag
Hop	Hsp70/Hsp90 organising protein
HPD motif	Histidine-Proline-Aspartic acid motif
HRP	Horse Radish Peroxidase
HSF	Heat Shock Factor
Hsc70	70 kDa Heat shock cognate protein
Hsp	Heat shock protein
hsp	Heat shock protein gene
Hsp90	90 kDa Heat shock protein
Hsp70	70 kDa Heat shock protein
Hsp60	60 kDa Heat shock protein
Hsp40	40 kDa Heat shock protein
HT	Host Targeting Signal
IUBMB	International Union of Biochemistry and Molecular Biology
IUPAC	International Union of Pure and Applied Chemistry
IPTG	Isopropyl-β-D-thiogalactopyranoside
$iRBC_R$	Infected Red Blood Cell
Kan	Kanamycin resistance
kb	kilo base pairs
kDa	Kilo Daltons
l	Litre(s)
LB	Luria-Bertani media
m	Milli
M	Molar
mAb	Monoclonal antibody
MC	Maurer's Clefts
MESA	Mature parasite-infected Erythrocyte Surface Antigen
mol	Mole(s)
mg	Milligram(s)
ml	Millilitre(s)
mM	Millimolar
MSP-7	Merozoite Surface Protein 7
n	Nano
NaCl	Sodium chloride
Ni-NTA	Nickel nitrilotriacetic acid
ng	Nanogram(s)
nmol	Nanomole(s)
nM	Nanomolar
N-	NH_2-terminal
N.D.	Not determined
NEF	Nucleotide Exchange Factor
pI	Isoelectric point
P_i	Inorganic phosphate
pAb	Polyclonal antibody
P. berghei	*Plasmodium berghei*
P. chabaudi	*Plasmodium chabaudi*

P. falciparum	*Plasmodium falciparum*
P. knowlesi	*Plasmodium knowlesi*
P. vivax	*Plasmodium vivax*
P. yoelii yoelii	*Plasmodium yoelii yoelii*
PBS	Phosphate Buffer Saline
PCR	Polymerase Chain Reaction
PDB	Protein Data Bank
PDI	Protein Disulphide Isomerase
PEXEL	Plasmodium Export Element
PEI	Polyethyleneimine
PEG	Polyethylene glycol
PfBiP	*P. falciparum* binding protein
PfSBP-1	*P. falciparum* Skeleton Binding Protein-1
PHIST	Plasmodium helical interspersed subtelomeric family
PMSF	Phenyl Methyl Sulfonyl Fluoride
PV	Parasitophorous Vacuole
RESA	Ring-infected Erythrocyte Surface Antigen
RNA	Ribonucleic Acid
RNAse A	Ribonuclease A
rpm	Revolutions per minute
S. cerevisiae	*Saccharomyces cerevisiae*
S.D.	Standard Deviation
SDS	Sodium Dodecyl Sulphate
SDS-PAGE	Sodium Dodecyl Sulphate – Polyacrylamide Gel Electrophoresis
sHsp	Small Heat shock protein
SP	Signal Peptide
STCB	Single Turnover Complex Buffer
Sti1	Stress induced phosphoprotein-1
T. annulata	*Theileria annulata*
T. parva	*Theileria parva*
T. gondii	*Toxoplasma gondii*
TBE	Tris Borate EDTA buffer
TBS	Tris-Buffered Saline
TBS-T	Tris Buffer Saline – Tween 20
TE	Tris-EDTA buffer
TEMED	N,N,N',N'-tetramethylethylenediamine
TMD	Transmembrane domain
TPR	Tetratricopeptide Repeat
Tris	Tris-2-amino-2-hydroxymethyl-1,3-propanol
TRITC	Tetramethyl Rhodamine Iso-Thiocyanate
U	Unit(s)
UV	Ultraviolet
V	Volts
v/v	Volume to volume ratio
w/v	Weight to volume ratio
YT	Yeast-Tryptone media
*x*g	Gravitational force

APPENDIX B

AMINO ACID AND NUCLEOTIDE NOMENCLATURE

One- and three-letter codes were used to represent amino acids, and single letter codes were used to represent nucleotides as set forward by the Joint Commission of Biochemical Nomenclature (JBNC) of IUPAC (International Union of Pure and Applied Chemistry) and the IUBMB (International Union of Biochemistry and Molecular Biology):

NUCLEOTIDE	SINGLE-LETTER CODE
Adenine	A
Cytosine	C
Guanine	G
Thymine	T
Uracil	U
Any Nucleotide (A, C, G, T or U)	N

AMINO ACID	ONE-LETTER CODE	THREE-LETTER CODE	DNA CODONS
Alanine	A	Ala	GCT, GCC, GCA, GCG
Arginine	R	Arg	CGT, CGC, CGA, CGG, AGA, AGG
Asparagine	N	Asn	AAT, AAC
Aspartic acid	D	Asp	GAT, GAC
Cysteine	C	Cys	TGT, TGC
Glutamine	Q	Gln	CAA, CAG
Glutamic acid	E	Glu	GAA, GAG
Glycine	G	Gly	GGT, GGC, GGA, GGG
Histidine	H	His	CAT, CAC
Isoleucine	I	Ile	ATT, ATC, ATA
Leucine	L	Leu	CTT, CTC, CTA, CTG, TTA, TTG
Lysine	K	Lys	AAA, AAG
Methionine	M	Met	ATG
Phenylalanine	F	Phe	TTT, TTC
Proline	P	Pro	CCT, CCC, CCA, CCG
Serine	S	Ser	TCT, TCC, TCA, TCG, AGT, AGC
Threonine	T	Thr	ACT, ACC, ACA, ACG
Tryptophan	W	Trp	TGG
Tyrosine	Y	Tyr	TAT, TAC
Valine	V	Val	GTT, GTC, GTA, GTG
Stop	-	-	TAA, TAG, TGA
Any Amino Acid	X	-	-

APPENDIX C

C1: NUCLEOTIDE SEQUENCES IN FASTA FORMAT

>PfHsp40 (*Plasmodium falciparum* Hsp40) Harmonised Coding Sequence*

GGATCCATGTTCTTTAGCAGCGGCTTCCCATTCGATAGCATGGGCGGCCAGCAGGCCCGACGTAAACGTGAAGT
TAACAACAATAAATTCTATGAAGTTCTCAACCTGAAAAAAAACTGCACGACTGATGAAGTTAAAAAAGCCTACC
GAAAGCTCGCTATTATTCACCACCCAGACAAAGGCGGCGACCCAGAAAAGTTTAAAGAAATCAGCCGTGCTTAC
GAAGTTCTGAGCGACGAAGAAAAACGCAAACTCTACGACGAGTACGGCGAAGAAGGCCTGGAAAACGGCGAACA
GCCAGCTGACGCTACCGACCTGTTCGATTTCATTCTGAACGCTGGCAAAGGCAAGAAAAAGCGTGGCGAAGACA
TTGTGTCTGAAGTTAAAGTTACCCTCGAACAGCTGTACAACGGCGCTACCAAAAAGCTCGCTATCTCTAAAGAC
ATTATCTGCACCAACTGCGAAGGCCACGGCGGCCCAAAAGACGCTAAAGTTGACTGCAAACAATGCAACGGCCG
TGGCACGAAGACGTATATGCGTTACCACAGCTCGGTTCTGCACCAGACGGAAGTTACTTGCAACACCTGCCGAG
GCAAAGGCAAAATCTTCAACGAAAAAGACAAATGCGCTAACTGCAAAGGCATGTGCGTTCTCAAAACCCGCAAA
ATCATTGAAGTTTACATTCCAAAAGGCGCTCCAAACAAACATAAAATCGTTTTCAACGGCGAAGCTGACGAAAA
ACCAAACGTAATTACGGGCAACCTCGTTGTTATCCTGAACGAAAAGCAGCACCCAGTTTTCCGTCGTGAAGGCA
TTGACCTGTTCATGAACTATAAAATATCGCTGTACGAAAGCCTGACCGGCTTCGTTGCTGAAGTTACCCACCTC
GACGAACGCAAAATCCTGGTAAATTGTACTAATTCTGGCTTCATCCGTCACGGCGACATTCGTGAAGTTCTCGA
CGAAGGCATGCCAACCTACAAAGACCCATTTAAAAAAGGCAACCTGTACATTACCTTCGAGGTTGAATACCCAA
TGGACCTGATTATCACCAACGAAAATAAAGAAGTTCTCAAAATACTGAAAAAACAGAACGAAGTTGAAAAAAAA
TACGATCTGGAAAACTCTGAACTCGAAGTAGTATCGTGTAGCCCAGTTGACAAAGAATACATTAAAGTTCGTGT
TACGAAACAGCAGCAGCAGCAGCAGCAGGAAGCTTATGATGACGAAGACCACCAGCCAGAAATGGAAGGCGGCC
GTGTTGCTTGCGCTCAGCAGTGAAAGCTA

* The engineered flanking 5'-*BamHI* (GGATCC) and 3'-*HindIII* (AAGCTA) restriction sites are underlined

>Pfj1 (*Plasmodium falciparum* DnaJ protein 1) Optimised Coding Sequence**

GGATCCATGCTGGCGCTGCGTATCCTGCGTCGTAAAGTTTGCTCTGAACACTTCCTGTTCGAGCGTTCTTTCTT
CACCCAGTCTATCAAAGGTAAAAACGGTTGCCTGGTTACCCGTTACGACAAAAACAAACTGCTGTTCTACTACA
AACGTAACATCAACACCTCTCGTAAATGCCTGAACCAGGACCCGTACACCGTTCTGGGTCTGTCTCGTAACGCG
ACCACCAACGACATCAAAAAACAGTTCAGGCTGCTGGCGAAAAAATACCACCCGGACATCAACCCGTCTCCGGA
CGCGAAACAGAAAATGGCGTCTATCACCGCGGCGTACGAACTGCTGTCTGACCCGAAAAAGAAAGAATTCTACG
ACAAAACCGGTATGACCGACGACTCTAACTACCAGAACCACTCTTCTAACTTCGAAGGTGCGTTCTCTGGTTTC
GGTGACGCGTCTTTCATGTTCACCGACTTCGCGGAAATGTTCACCAACATGGCGGGTGGTAACAAAAACACCTC
TACCCGTGGTGAAGACATCCAGTCTGAAATCACCCTGAAATTCATGGAAGCGATCAAAGGTTGCGAAAAAAACT
CGCGACTGAACGTTAAAGTTTCTTGCAACAACTGCAACGGTTCTGGTAAAAAACCGGGCACCAACCTGACCATC
TGCAAAGTTTGCAACGGTTCTGGTATCCAGCGTATGGAACGTGGTCCGATCATCATCGGTGTTCCGTGCCGTAA
CTGCTCTGGTAACGGTCAGATCATCAACAACCCGTGCAAACACTGCTCTGGTTCTGGTGTTAAATTCCAGACCA
AAAACATCACCCTGGACATCCCGCCCGGGATCAAAAAAGGTATGCAGATGCGTATCCCGAACCAGGGTCACTGC
GGTTACCGTGGTGGTAAATCTGGTCACCTGTTCGTTACCATCAACATCGAACCGCACAAAATCTTCAAATGGGT
TGACGACAACATCTACGTTGACGTTCCGCTGACCATCAAACAGTGCCTGCTGGGTGGTCTGGTTACCGTTCCGA
CCCTGAACGGTGACATGGACCTGCTGATCAAACCGAAAACCTACCCGAACTCTGAAAAAATCCTGAAAGGTAAA
GGTCCGTGCAAAGTTGACTCTCACAACAACGGTGACCTGATCATCAAATTCTCTCTGAAAATCCCGGAAAAACT
GACCCCGCGTCAGGTTGAACTGATCGAAGAATTCAACACCATCGAACTGAACCTGCCGAACCCGCAGACCAACG
TTAAACAGAAAAAAAACATCTACGAAACCAAAGGTAACATCAACGAAAACATCTTCTCTATGAACAACACCTAC
AACAACATGAAAGGTCCGGAAGGTGAAACCTCTAACACCCAGGCGAAATCTATGAAAAACCAGAACTGGAACAA
CGAAAAATCTGTTAACAACAAAGGCACCATCTCTAAAGACGAAAAAAAACTGAACATGAAAAACAACCACATCA
ACGAAAAATCTAACCTGAAAAACTCTTCTCACATGGACACCAACAAAAACGAAGAAAACATGTCTGACGACGAA
AAAAAAAAAATCAAAAAAATCATCCCGGAACCGCCGATGCCGCACACCCACAAAATCGTTAACAACCTGGAATC
TAAAAACTCTTGCAACATCCCGATCCCGCCGCCGCCGCCGAAATCTTCTTCTAAACCGATCTCTGAAAACCAGA
ACATCTCTAACCGTGAACACAACGGTGTTACCAACAACTCTGCGAAACTGGACAACAACATCAACATGAACTAC
TCTTGCGACCCGTACAAAAACGTTACCCAGAACGACCTGAACAACAACGACAACATCAAAAACAAAATCTACAA
AGACAACACCAACATCTCTAACCACCACATCTTCAAAAACGACAACATCAACCAGCAGCAGTTCCACTGCGCGG
ACAACTCTTCTGAAAACAACAACGAATCTGACATGAACACCACCTCTACCTTCTCTTTCGCCAAAAAATGGATC
TCTGACAAACTGAAACCGAAAAACTAAGGTACCCTGCAG

** The engineered flanking 5'-*BamHI* (GGATCC) and 3'-*PstI* (CTGCAG) restriction sites are underlined, in addition to the *BstBI* site (TTCGAA) engineered between the encoded J-domain and GF-region for J-domain swapping, and the central *SmaI* site (CCCGGG) delineating the front and back halves of the Pfj1 coding sequence (Pfj1-Front and Pfj1-Back)

C2: PROTEIN SEQUENCES IN FASTA FORMAT

>PfHsp40 (*Plasmodium falciparum* Hsp40) [Accession: NP_702248.1]
MFFSSGFPFDSMGGQQARRKREVNNNKFYEVLNLKKNCTTDEVKKAYRKLAIIHHPDKGGDPEKFKEISRAYEV
LSDEEKRKLYDEYGEEGLENGEQPADATDLFDFILNAGKGKKKRGEDIVSEVKVTLEQLYNGATKKLAISKDII
CTNCEGHGGPKDAKVDCKQCNGRGTKTYMRYHSSVLHQTEVTCNTCRGKGKIFNEKDKCANCKGMCVLKTRKII
EVYIPKGAPNKHKIVFNGEADEKPNVITGNLVVILNEKQHPVFRREGIDLFMNYKISLYESLTGFVAEVTHLDE
RKILVNCTNSGFIRHGDIREVLDEGMPTYKDPFKKGNLYITFEVEYPMDLIITNENKEVLKILKKQNEVEKKYD
LENSELEVVSCSPVDKEYIKVRVTKQQQQQQQEAYDDEDHQPEMEGGRVACAQQ

>Pfj1 (*Plasmodium falciparum* DnaJ protein 1) [Accession: NP_702750.1]
MLALRILRRKVCSEHFLFERSFFTQSIKGKNGCLVTRYDKNKLLFYYKRNINTSRKCLNQDPYTVLGLSRNATT
NDIKKQFRLLAKKYHPDINPSPDAKQKMASITAAYELLSDPKKKEFYDKTGMTDDSNYQNHSSNFEGAFSGFGD
ASFMFTDFAEMFTNMAGGNKNTSTRGEDIQSEITLKFMEAIKGCEKNIRLNVKVSCNNCNGSGKKPGTNLTICK
VCNGSGIQRMERGPIIIGVPCRNCSGNGQIINNPCKHCSGSGVKFQTKNITLDIPPGIKKGMQMRIPNQGHCGY
RGGKSGHLFVTINIEPHKIFKWVDDNIYVDVPLTIKQCLLGGLVTVPTLNGDMDLLIKPKTYPNSEKILKGKGP
CKVDSHNNGDLIIKFSLKIPEKLTPRQVELIEEFNTIELNLPNPQTNVKQKKNIYETKGNINENIFSMNNTYNN
MKGPEGETSNTQAKSMKNQNWNNEKSVNNKGTISKDEKKLNMKNNHINEKSNLKNSSHMDTNKNEENMSDDEKK
KIKKIIPEPPMPHTHKIVNNLESKNSCNIPIPPPPPKSSSKPISENQNISNREHNGVTNNSAKLDNNINMNYSC
DPYKNVTQNDLNNNDNIKNKIYKDNTNISNHHIFKNDNINQQQFHCADNSSENNNESDMNTTSTFSFAKKWISD
KLKPKN

>*Agt* DnaJ (*Agrobacterium tumefaciens* DnaJ) [Accession: AAR84666.1]
MAKADFYETLGVSKTADEKELKSAFRKLAMKYHPDKNPDDADSERKFKEINEAYETLKDPQKRAAYDRFGHAAF
ENGGMGGGGGGFGGGGFANGGFSDIFEDIFGEMMGGGRARRSSGGRERGADLRYNMEITLEEAFTGKTAQIRVP
TSITCDVCSGSGAKPGTQPKTCATCQGSGRVRAAQGFFSVERTCPTCHGRGQTISDPCGKCHGQGRVTEERSLS
VNIPSGIEDGTRIRLQGEGEAGMRGGPAGDLYIFLSVRPHEFFQRDGADLYCTVPISMTTAALGGTFDVTTLDG
TKSRVTVPEGTQPGKQFRLKGKGMPVLRSAQTGDLYIQIQIETPQKLSKRQRELLQEFEQLSSKENNPESTGFF
ARMKKFFDG

>Pfj1-J-Agt-DnaJ Chimera (residues derived from the Pfj1 J-domain are underlined)
MAKQDPYTVLGLSRNATTNDIKKQFRLLAKKYHPDINPSPDAKQKMASITAAYELLSDPKKKEFYDKTGHAAFE
NGGMGGGGGGFGGGGFANGGFSDIFEDIFGEMMGGGRARRSSGGRERGADLRYNMEITLEEAFTGKTAQIRVPT
SITCDVCSGSGAKPGTQPKTCATCQGSGRVRAAQGFFSVERTCPTCHGRGQTISDPCGKCHGQGRVTEERSLSV
NIPSGIEDGTRIRLQGEGEAGMRGGPAGDLYIFLSVRPHEFFQRDGADLYCTVPISMTTAALGGTFDVTTLDGT
KSRVTVPEGTQPGKQFRLKGKGMPVLRSAQTGDLYIQIQIETPQKLSKRQRELLQEFEQLSSKENNPESTGFFA
RMKEFFEG

>Hsj1a (DnaJB2; *Homo sapiens* DnaJ Isoform 1a) [Accession: X63368]
MASYYEILDVPRSASADDIKKAYRRKALQWHPDKNPDNKEFAEKKFKEVAEAYEVLSDKHKREIYDRYGREGLT
GTGTGPSRAEAGSGGPGFTFTFRSPEEVFREFFGSGDPFAELFDDLGPFSELQNRGSRHSGPFFTFSSSFPGHS
DFSSSSFSFSPGAGAFRSVSTSTTFVQGRRITTRRIMENGQERVEVEEDGQLKSVTINGVPDDLALGLELSRRE
QQPSVTSRSGGTQVQQTPASCPLDSDLSEDEDLQLAMAYSLSEMEAAGKKPADVF

>Hlj1 J-domain (*Saccharomyces cerevisiae* ER transmembrane DnaJ-like protein) [Accession: NP_013884]
MSFTEDQEKIALEILSKDKHEFYEILKVDRKATDSEIKKAYRKLAIKLHPDKNSHPKAGEAFKVINRAFEVLSN
EEKRSIYDRIGR

>PfHsp70-1(*Plasmodium falciparum* Hsp70 Isoform 1) [Accession: AAA29626]
MASAKGSKPNLPESNIAIGIDLGTTYSCVGVWRNENVDIIANDQGNRTTPSYVAFTDTERLIGDAAKNQVARNP
ENTVFDAKRLIGRKFTESSVQSDMKHWPFTVKSGVDEKPMIEVTYQGEKKLFHPEEISSMVLQKMKENAEAFLG
KSIKNAVITVPAYFNDSQRQATKDAGTIAGLNVMRIINEPTAAAIAYGLHKKGKGEKNILIFDLGGGTFDVSLL
TIEDGIFEVKATAGDTHLGGEDFDNRLVNFCVEDFKRKNRGKDLSKNSRALRRLRTQCERAKRTLSSSTQATIE
IDSLFEGIDYSVTVSRARFEELCIDYFRDTLIPVEKVLKDAMMDKKSVHEVVLVGGSTRIPKIQTLIKEFFNGK

EACRSINPDEAVAYGAAVQAAILSGDQSNAVQDLLLLDVCSLSLGLETAGGVMTKLIERNTTIPAKKSQIFTTY
ADNQPGVLIQVYEGERALTKDNNLLGKFHLDGIPPAPRKVPQIEVTFDIDANGILNVTAVEKSTGKQNHITITN
DKGRLSQDEIDRMVNDAEKYKAEDEENRKRIEARNSLENYCYGVKSSLEDQKIKEKLQPAEIETCMKTITTILE
WLEKNQLAGKDEYEAKQKEAESVCAPIMSKIYQDAAGAAGGMPGGMPGGMPGGMPSGMPGGMNFPGGMPGAGMP
GNAPAGSGPTVEEVD

>HsHsp70 (HspA1A; *Homo sapiens* Hsp70 Protein 1A) [Accession: NP_005336]
MAKAAAIGIDLGTTYSCVGVFQHGKGERNVLIFDLGGGTFDVSILTIDDGIFEVKATAGDTHLGGEDFDNRLVN
HFVEEFKRKHKKDISQNKRAVRRLRTACERAKRTLSSSTQASLEIDSLFEGIDFYTSITRARFEELCSDLFRST
LEPVEKALRDAKLDKAQIHDLVLVGGSTRIPKVQKLLQDFFNGRDLNKSINPDEAVAYGAAVQAAILMGDKSEN
VQDLLLLDVAPLSLGLETAGGVMTALIKRNSTIPTKQTQIFTTYSDNQPGVLIQVYEGERAMTKDNNLLGRFEL
SGIPPAPRGVPQIEVTFDIDANGILNVTATDKSTGKANKITITNDKGRLSKEEIERMVQEAEKYKAEDEVQRER
VSAKNALESYAFNMKSAVEDEGLKGKISEADKKKVLDKCQEVISWLDANTLAEKDEFEHKRKELEQVCNPIISG
LYQGAGGPGPGGFGAQGPKGGSGSGPTIEEVD

APPENDIX D

COMMON PROTOCOLS FOR STANDARD MOLECULAR BIOLOGY TECHNIQUES

Standard molecular biology protocols were adapted from those described[1,2]. Sterile technique was employed where applicable. Specialised materials and reagents utilised are listed in *APPENDIX E.*

D1: ISOLATION OF PLASMID DNA

The protocol for isolation of plasmid DNA was adapted from that described for alkaline lysis[3]. In brief, *E. coli* cells transformed with the plasmid of interest were grown overnight (37°C, 200 rpm) in 5 ml cultures of 2x YT (1.6% tryptone, 1% yeast extract, 0.5% NaCl) or LB media (1% tryptone, 0.5% yeast extract, 1% NaCl) supplemented with the appropriate antibiotic for plasmid selection (100 $\mu g.ml^{-1}$ ampicillin for pQE30-based plasmids). The cells were harvested in a microcentrifuge (16 000 *x*g, 1 minute) and resuspended in 250 µl of Solution I (2 $mg.ml^{-1}$ lysozyme, 10 mM EDTA, 50 mM Glucose, 25 mM Tris-Cl, pH 8.0). To the resuspended cells, 250 µl of Solution II (1% (w/v) SDS, 0.2 M NaOH) was added and mixed by inversion, and subsequently 350 µl of Solution III (1.5 M potassium acetate, 12% (v/v) glacial acetic acid) was similarly added. This was followed by centrifugation (16 000 *x*g, 10 minutes) and precipitation of the DNA from the resulting supernatant with 500 µl of 100% isoproponal (10 minutes, room temperature). The precipitated DNA was pelleted by centrifugation (16 000 *x*g, 10 minutes) and washed with 800 µl of 70% ethanol (4°C). The ethanol was discarded and the pellet was allowed to dry for 20 minutes at room temperature, prior to resuspension in 50 µl of TE buffer (10 mM Tris, 20 $\mu g.ml^{-1}$ RNAse A, 1 mM EDTA, pH 8.0). The purified DNA was quantified at 260 nm in a Helios Alpha UV-Vis Spectrophotometer (Thermo Scientific).

D2: DNA DIGESTION WITH RESTRICTION ENZYMES

Plasmid DNA was digested with the appropriate restriction endonuclease(s) for two hours at the appropriate optimal temperature (37°C unless otherwise stated) in a digestion reaction comprising: 200 - 500 ng of plasmid DNA, 2 µl of the appropriate 10x restriction buffer, 1 - 2 U of restriction endonuclease enzyme (*APPENDIX E*) and distilled water to a final volume of 20 µl. The digested DNA

[1] SAMBROOK, J., FRITSCH, E.F. and MANIATIS, T. (1989). Molecular Cloning: A Laboratory Manual. Volumes I, II and III. Cold Spring Harbor Laboratory Press, Cold Spring Harbor, New York.

[2] SAMBOOK, J. and RUSSELL, D.W. (2001). Molecular Cloning: A Laboratory Manual. Volumes I, II and III. Cold Spring Harbor Laboratory Press, Cold Spring Harbor, New York.

[3] BIRNBOIM, H. and DOLY, J. (1979). A rapid alkaline extraction procedure for screening recombinant plasmid DNA. *Nucleic Acids Research*, 7, 1513-1523.

was resolved by agarose gel electrophoresis as described in *SECTION D3*. Double digestion with *Bam*HI/*Sma*I or *Sma*I/*Pst*I was achieved with sequential one hour incubations at 30°C and 37°C respectively. Restriction buffers for single and double restriction enzyme digestions were selected as per the supplier's recommendations.

*Pst*I-digested λDNA marker was prepared by the digestion of 20 µl of 526 µg.ml^{-1} λDNA (Promega) for two hours at 37°C in a reaction containing 5 U of *Pst*I restriction enzyme (Fermentas), 20 µl of the appropriate 10x restriction enzyme buffer (Fermentas) and distilled water to a final volume of 200 µl. The digested λDNA was treated with 6x DNA gel loading buffer (0.25% (w/v) bromophenol blue, 30% (v/v) glycerol) for use in subsequent agarose gel electrophoresis (*SECTION D3*).

D3: AGAROSE GEL ELECTROPHORESIS

Agarose gels were prepared by melting molecular grade agarose (0.8% or 1.5% (w/v)) in TBE Buffer (45 mM Borate, 1 mM EDTA, 45 mM Tris-Cl, pH 8.3) and supplementing ethidium bromide to a final concentration of 0.5 µg.ml^{-1} on cooling prior to casting. DNA samples for electrophoresis were treated with 6x DNA gel loading buffer (0.25% (w/v) bromophenol blue, 30% (v/v) glycerol) in a ratio of 5:1 respectively and loaded onto the gel with an appropriate marker of *Pst*I-digested λDNA (prepared as per *SECTION D2*). The samples were resolved at 100 - 120 V for one hour, and visualised under ultra-violet light with a Chemidoc Imaging System (Bio-Rad). For the visualisation of DNA fragments smaller than 500 bp, ethidium bromide staining (0.5 µg.ml^{-1} in TBE Buffer) was achieved subsequent to electrophoresis.

D4: EXTRACTION AND PURIFICATION OF DNA FROM AN AGAROSE GEL

Resolved DNA fragments were isolated subsequent to agarose gel electrophoresis using the GFX™ PCR DNA and Gel Band Purification Kit (GE Healthcare) as per the manufacturer's instructions. In brief, the DNA fragment of interest was identified by brief exposure to long-wave UV light, excised from the gel and incubated in Capture buffer (GE Healthcare; 10 µl per 10 mg of excised gel) at 60°C for 15 minutes. The sample was applied to a GFX™ spin column (GE Healthcare) and centrifuged at 16 000 *x*g for 1 minute. Bound DNA was washed with 500 µl of Wash buffer (GE Healthcare) passed through the column by centrifugation (16 000 *x*g, 1 minute). The DNA was eluted from the column with 20-30 µl of Elution buffer (GE Healthcare) by further centrifugation (16 000 *x*g, 1 minute). Quantification of the purified DNA was achieved in a Helios Alpha UV-Vis spectrophotometer (Thermo Scientific) at 260 nm.

D5: LIGATION OF DNA FRAGMENTS

DNA fragments intended for ligation (typically 500 ng of insert fragment to 100 ng of target plasmid) were incubated overnight at 4°C in a ligation reaction comprising 1 µl of 10x ligation buffer (Roche Applied Sciences), 1 U of T4 DNA Ligase (Roche Applied Sciences) and distilled water to a final volume of 10 µl. Following incubation at 4°C overnight, the ligation reaction was incubated at room temperature for 30 minutes prior to transformation into competent *E. coli* cells (*SECTION D8*).

D6: DNA SEQUENCING

Plasmid DNA was isolated for DNA sequencing using the QiaPrep Miniprep Kit (Qiagen) as per the manufacturer's instructions, with the exception that the final DNA elution was achieved with an equal volume of distilled water. Sequencing reactions comprised the plasmid DNA (200 - 500 ng), 3.2 pmol of primer (forward or reverse primer; *APPENDIX F3*), 2 µl of 5 x Big Dye® Terminator Sequencing Buffer (Big Dye Terminator Cycle Sequencing Kit version 3.1, Applied Biosystems), 4 µl of Big Dye Terminator (Applied Biosystems) and distilled water to a final volume of 10 µl. Thermal cycling was allowed to proceed in a GeneAmp PCR System 9700 (version 3.05; Applied Biosystems) as follows: one cycle of denaturation (96 °C, 10 seconds), 25 cycles of denaturation, annealing and extension (96 °C for 10 seconds, 52°C for 5 seconds, and 60°C for 4 minutes) and a final 4°C hold. Purification of the amplification product from unincorporated big dye terminators was achieved with Zymo-Spin I™ columns (Zymo Research) as per the manufacturer's instructions. The purified DNA was injected into an ABIPRISM 3100 Genetic Analyser (Applied Biosystems, USA) and analysed by capillary electrophoresis. DNA sequencing results were analysed using BioEdit Sequence Alignment Editor (version 7.0.4.1)[4].

D7: PREPARATION OF COMPETENT *E. COLT* CELLS

The protocol for the preparation of competent *E. coli* cells is adapted from that described for the calcium chloride method[5]. The strain of interest was grown overnight (37°C, 200 rpm) in 5 ml of 2x YT (1.6% tryptone, 1% yeast extract, 0.5% NaCl) or LB media (1% tryptone, 0.5% yeast extract, 1% NaCl) supplemented with the appropriate antibiotic for strain selection if required. The resulting overnight culture was diluted into 50 ml of 2x YT or LB media to an $_{A600}$ of 0.1 and growth was allowed to proceed until early log phase $_{(A600}$ of 0.3 - 0.6). The cells were harvested by

[4] HALL, T.A. (1999). BioEdit: a user-friendly biological sequence alignment editor and analysis program for Windows 95/98/NT. *Nucleic Acids Symposium Series,* 41, 95-98.

[5] DAGERT, M. and EHRLICH, S.D. (1979). Prolonged incubation in calcium chloride improves the competence of *Escherichia coli* cells. *Gene*, 6, 23-28.

centrifugation (5000 *x*g, 5 minutes, 4°C) and resuspended in 50 ml of ice-cold 0.1 M $MgCl_2$ (4°C). Following two minutes of incubation at 4°C the cells were pelleted by centrifugation as before and resuspended in 25 ml of ice-cold 0.1 M $CaCl_2$ (4°C). Following incubation at 4°C for one hour the cells were harvested by centrifugation as before and resuspended in 5 ml of 0.1 M $CaCl_2$ and 5 ml of 30% (v/v) glycerol. The competent cells were divided into aliquots and stored at -80°C prior to use. Supercompetent *E. coli* cells were sourced commercially as detailed in *APPENDIX E*.

D8: TRANSFORMATION OF COMPETENT *E. COLT* CELLS

Competent *E. coli* cells (100 µl; *SECTION D7*) were incubated with 100 ng of the plasmid DNA of interest (or 2 µl of ligation product) at 4°C for 30 minutes, followed by heat shock (42°C for 45 seconds) and subsequent cold shock (4°C for 2 minutes). The cells were diluted 1:10 with 2x YT (1.6% tryptone, 1% yeast extract, 0.5% NaCl) or LB media (1% tryptone, 0.5% yeast extract, 1% NaCl) pre-warmed to 37°C, and were subsequently incubated for 30 minutes with shaking (200 rpm, 37°C). The bacterial suspension (100 µl) was plated onto 2x YT- or LB-agar plates (1.5% agar in 2x YT or LB media) supplemented with the appropriate antibiotics (100 $\mu g.ml^{-1}$ ampicillin for pQE30-based plasmid selection; 50 $\mu g.ml^{-1}$ kanamycin for *E. coli* OD259 strain selection; 34 $\mu g.ml^{-1}$ chloramphenicol for *E. coli* Rosetta 2 strain selection). The plates were incubated overnight at 37°C. Transformation controls included a sterile control with sterile distilled water replacing the plasmid DNA in the incubation mixture, and a competence control with plasmid DNA of known concentration (10 ng of plasmid pUC18; Promega) transformed into the *E. coli* cells. For the thermosensitive *E. coli* OD259 strain, a temperature of 30°C was used for growth and incubation, and heat shock was achieved at 37°C.

D9: PROTEIN CONCENTRATION DETERMINATION BY BRADFORD'S ASSAY

Protein concentration determination was performed by Bradford's assay as previously described[6]. A volume of 200 µl of Bradford's reagent (Bio-Rad; diluted 1:4 with distilled water) was added to 10 µl of undiluted, 1:10 and 1:100 diluted protein samples of unknown concentration. Following incubation at room temperature for 10 minutes, the Absorbance of the samples was read at 595 nm in a PowerWave™ Microplate spectrophotometer (Biotek). Protein concentration was determined with the corresponding 0 - 250 $\mu g.ml^{-1}$ Bovine Serum Albumin (BSA) standard curve prepared for the assay (represented in *FIGURE D14* overleaf).

[6] BRADFORD, M.M. (1976). A Rapid and Sensitive Method for the Quantitation of Microgram Quantities of Protein Utilizing the Principle of Protein-Dye Binding. *Analytical Biochemistry*, 72, 248-254.

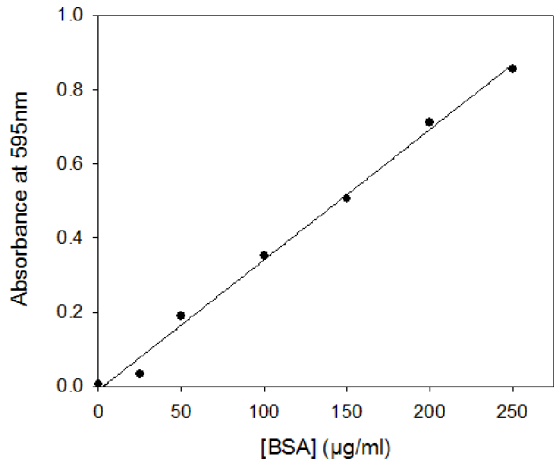

FIGURE D9. Representative Bovine Serum Albumin standard curve for protein concentration determination by Bradford's assay. The curve is represented by the linear equation: $y = 0.0035x - 0.0107$; $R^2 = 0.99$.

D10: SODIUM-DODECYL SULPHATE – POLYACRYLAMIDE GEL ELECTROPHORESIS (SDS-PAGE)

The protocol for SDS-PAGE analysis is adapted from that previously described[7]. Protein samples were treated with 5x SDS-PAGE sample buffer (10% glycerol, 2% SDS, 5% β-mercaptoethanol, 0.05% bromophenol blue, 0.0625 M Tris, pH 6.8) in a ratio of 4:1 respectively and loaded onto a polyacrylamide gel constituted by a resolving gel (10-12% (w/v) acrylamide, 0.1% (w/v) SDS, 0.05% (w/v) ammonium persulphate (APS), 0.005% (v/v) N,N,N',N'-tetramethylethylenediamine (TEMED), 0.375 M Tris, pH 8.8) and a stacking gel (4% (w/v) acrylamide, 0.1% (w/v) SDS, 0.05% (w/v) APS, 0.005% (v/v) TEMED, 0.125 M Tris, pH 6.8). The gel was resolved in a Mini Protean® ❚❚system (Bio-Rad) at 160 V for one hour and stained or used for Western analysis (*SECTION D11*). Staining of the SDS-PAGE gel was achieved in Coomassie Blue stain (40% (v/v) methanol, 7% (v/v) acetic acid, 0.25% (w/v) Coomassie Blue R250 in distilled water) for 30 minutes and subsequent destaining was achieved overnight in destain solution (40% (v/v) methanol, 7% (v/v) acetic acid in distilled water). Alternatively, the gel was stained with silver nitrate subsequent to electrophoresis. In brief, the gel intended for silver staining was fixed in fixative solution (50% (v/v) ethanol, 12% (v/v) acetic acid, 0.05% (v/v) formaldehyde) for 30 minutes and subsequently washed in 50% (v/v) ethanol for 20 minutes. Following brief incubation in 0.01% (w/v) $Na2S2O3$, the gel was washed twice in distilled water for 30 seconds. Subsequently the gel was stained in 0.1% (w/v) $AgNO_3$ prepared in distilled water for a further 20 minutes. Excess $AgNO_3$ was removed with a brief rinse in distilled water, followed by development in Developer Solution (7.5 g of Na_2CO_3, 0.12 ml of formaldehyde and 5 ml of 0.01% (w/v) $Na2S2O3$ per 250 ml of distilled water). Development was stopped with a 10 mM solution of EDTA and the gel was visualised.

[7] SHAPIRO, A.L., VIÑUELA, E. and MAIZEL, J.V. (1967). Molecular weight estimation of polypeptide chains by electrophoresis in SDS-polyacrylamide gels. *Biochemical and Biophysical Research Communications*, 28, 815-820.

D11: PROTEIN DETECTION BY WESTERN ANALYSIS

The protocol for the detection of proteins by Western analysis was adapted from that described[8]. Proteins were resolved by SDS-PAGE as per *SECTION D10* and transferred onto nitrocellulose membrane (Hybond C-extra; GE Healthcare) in transfer buffer (20% (v/v) methanol, 192 mM glycine, 25 mM Tris) at 100 V for 90 minutes in a Mini Protean® III Western trans-blot system (Bio-Rad). Protein transfer was verified with Ponceau S stain (0.5 % (w/v) Ponceau S, 1% (v/v) glacial acetic acid). The membrane was subsequently destained with distilled water and incubated overnight at 4°C in blocking solution comprised of 5% (w/v) fat-free milk powder in Tris Buffered Saline (TBS; 50 mM Tris, 150 mM NaCl, pH 7.5). The membrane was incubated with appropriate primary antibody (1:5000 in blocking solution unless otherwise stated in the text) for one hour at room temperature and subsequently washed three times with Tris Buffered Saline-Tween buffer (TBS-T; TBS containing 0.1% (v/v) Tween 20). The membrane was similarly incubated with the appropriate horse-radish peroxidise (HRP)-conjugated secondary antibody (1:5000 in blocking solution unless otherwise stated in the text) for one hour at room temperature and washed with TBS-T as before. Chemiluminescence-based protein detection was achieved using the ECL™ Western blotting kit (GE Healthcare) as per the manufacturer's instructions, and captured with a Chemidoc chemiluminescence imaging system (Bio-Rad).

D12: ANALYSIS OF RECOMBINANT PROTEIN EXPRESSION

A colony of the specified *E. coli* strain[9,10] transformed with the appropriate plasmid (pQPfHsp40 or pQPfj1; as per *SECTION D8*) was inoculated into 100 ml of the appropriate growth media[9] containing ampicillin selection pressure to the specified final concentration[9], and incubated overnight for approximately 16 hours at 200 rpm at the stated temperature[9]. The overnight culture was diluted to an $_{A600}$ of 0.1 in 1000 ml of the appropriate growth media[9] supplemented with the appropriate concentration of antibiotic[9] and incubated as before to a specified cell density $_{(A600)9.}$ Protein expression was induced with 1 mM IPTG in the presence or absence of selection pressure as indicated[9] and 1 ml aliquots of the induced cells were harvested at hourly intervals between 0 - 8 hours post-induction, and overnight at 16 hours post-induction. The harvested cells were pelleted by centrifugation (16 000 *x*g; 1 minute) and resuspended in phosphate buffered saline (PBS; 137

---

[8] TOWBIN, H., STAEHELIN, T. and GORDON, J. (1979). Electrophoretic transfer of proteins from Polyacrylamide gels to nitrocellulose sheets: procedure and some applications. *Proceedings of the National Academy of Sciences*, 76, 4350-4354.

[9] Variables used are specified in *TABLE 3.1*, *CHAPTER 3*.

[10] Selection of the *E. coli* Rosetta™ 2(DE3) strain was achieved with 34 µg.ml^{-1} chloramphenicol in the growth media

mM NaCl, 2.7 mM KCl, 10.3 mM Na_2HPO_4, 1.8 mM KH_2PO_4, pH 7.4) in volumes dependent on the cell density (150 µl of PBS per 0.5 recorded $_{A600}$ absorbance units). Samples were analysed for recombinant protein expression by SDS-PAGE as per *SECTION D10* and Western analysis using a mouse anti-His primary mAb (1:5000; GE Healthcare) and an HRP-conjugated sheep anti-mouse secondary antibody (1:5000; GE Healthcare) as per *SECTION D11*.

APPENDIX E

LIST OF MATERIALS AND SPECIALISED REAGENTS

REAGENT	SUPPLIER
[α ^{32}P]-Adenosine triphosphate	Perkin-Elmer Life Sciences, USA
β-mercaptoethanol	Merck, Germany
λDNA	Promega, USA
Acetic Acid	Saarchem, South Africa
Adenosine diphosphate (sodium salt)	Sigma-Aldrich, USA
Adenosine triphosphate (disodium salt)	Sigma-Aldrich, USA
Agar (Bacteriological)	Biolab Diagnostics, South Africa
Agarose	Hispanagar, Spain
Albumax ıı	Invitrogen, USA
Ammonium per sulphate	Saarchem, South Africa
Ampicillin	Fisher Scientific, UK
Aurion BSA	Electron Microscopy Sciences, USA
Bis-Acrylamide	Bio-Rad, US
Bovine Serum Albumin	Sigma-Aldrich, USA
Boric Acid	Saarchem, South Africa
Bradford's Reagent	Bio-Rad, USA
Bromophenol Blue	Sigma-Aldrich, Germany
Calcium chloride	Saarchem, South Africa
Centricon® Centrifugal Units	Millipore, Germany
Chloramphenicol	Sigma-Aldrich, USA
Coomassie Brilliant Blue R250	Sigma-Aldrich, Germany
DAPI (4',6-diamidino-2-phenylindole)	Invitrogen, USA
Diethiothreitol	BioVectra (DCI), Canada
Dimethyl sulfoxide (DMSO)	Sigma-Aldrich, Germany
dNTP mix	Roche Applied Sciences, Germany
EDTA, sodium salt	Saarchem, South Africa
Ethanol	Saarchem, South Africa
Ethidium bromide	Sigma-Aldrich, Germany
Formic Acid	Fisher Scientific, UK
Goat Serum	Calbiochem, USA
Gentamicin	Sigma-Aldrich, Germany
Glacial acetic acid	Saarchem, South Africa
Glucose	Sigma-Aldrich, Germany
Glutathione (reduced)	Sigma-Aldrich, USA
Glutathione agarose	Sigma-Aldrich, USA
Glycerol	EMD Chemicals, USA
Glycine	Sigma-Aldrich, Germany
HEPES	Fisher Scientific, UK
Hybond C-extra	GE Healthcare, UK
Hydrochloric Acid	Saarchem, South Africa
Hypoxanthine	Calbiochem, USA
Illustra™ NICK Sephadex G-50	GE Healthcare, UK
Imidazole	Sigma-Aldrich, Germany
Isopropyl-1-thio-β-D-galactopyranoside	Roche Applied Sciences, Germany
Kanamycin sulphate	Roche Applied Sciences, Germany
Leupeptin	Sigma-Aldrich, USA
Lithium chloride	Fisher Scientific, UK
LR White Resin	Electron Microscopy Sciences, USA
Lysine	Sigma-Aldrich, USA
Lysozyme	Sigma-Aldrich, USA
Methanol	Saarchem, South Africa

Magnesium acetate (MgOAc)	Sigma-Aldrich, USA
Magnesium chloride ($MgCl_2$)	Saarchem, South Africa
Malate Dehydrogenase (MDH)	Roche Applied Sciences, Germany
Ni-NTA column	Qiagen, USA
N-laurylsarcosine	Sigma-Aldrich, Germany
Pepstatin A	Sigma-Aldrich, USA
Percoll	Sigma-Aldrich, USA
Permafluor	Beckman Coulter, USA
Phenylmethylsulphonyl fluoride (PMSF)	Sigma-Aldrich, USA
Polyacrylamide	Bio-Rad, USA
Polyethylene Glycol 3000 (PEG-3000)	Sigma-Aldrich, Germany
Polyethyleneimine (PEI)	Sigma-Aldrich, USA
Ponceau S	Sigma-Aldrich, Germany
Potassium acetate (KOAc)	Fisher Scientific, UK
Potassium chloride (KCl)	Saarchem, South Africa
Potassium hydroxide (KOH)	Saarchem, South Africa
Potassium phosphate (K_2HPO4)	Merck, Germany
Potassium dihydrogen phosphate (KH_2PO4)	Merck, Germany
Protein G Sepharose	Sigma-Aldrich, Germany
Protein A/G PLUS Agarose™	Santa Cruz Biotechnology, USA
Q-Sepharose Fast Flow	Sigma-Aldrich, USA
RPMI-1640 Media	Highveld Biologicals, South Africa
Saponin	Sigma-Aldrich, Germany
Sepharose Fast Flow™ (uncharged)	GE Healthcare, UK
Sodium cacodylate ($NaCH_2H_6AsO_2$)	Sigma-Aldrich, Germany
Sodium carbonate (Na_2CO_3 / $NaHCO_3$)	Sigma-Aldrich, USA
Sodium chloride (NaCl)	Saarchem, South Africa
Sodium thiosulphate ($Na_2S_2O_3$)	Sigma-Aldrich, USA
Sodium dodecyl sulphate (SDS)	Sigma-Aldrich, USA
Sodium phosphate (NaH_2PO_4 / Na_2HPO_4)	Saarchem, South Africa
Sodium hydroxide (NaOH)	Saarchem, South Africa
Sorbitol	Sigma-Aldrich, USA
Silver nitrate ($AgNO_3$)	Fisher Scientific, UK
Snakeskin™ dialysis tubing	Thermo Scientific, USA
TEMED (N,N,N',N'-tetramethylethylenediamine)	Sigma-Aldrich, Germany
Tris (Tris-2-amino-2-hydroxymethyl-1,3-propanol)	Sigma-Aldrich, Germany
Triton X-100	Sigma-Aldrich, Germany
Tryptone	Oxoid, UK
Tween 20	Saarchem, South Africa
Urea	Sigma-Aldrich, Germany
Yeast extract	Oxoid, UK

ANTIBODIES

Alexa Fluor® 594 goat anti-rabbit	Invitrogen, USA
Alexa Fluor® 488 goat anti-mouse	Invitrogen, USA
Goat anti-GST pAb	GE Healthcare, UK
HRP-conjugated goat anti-sheep/goat	Exalpha Biologicals, USA
HRP-conjugated sheep anti-mouse	GE Healthcare, UK
HRP-conjugated goat anti-rabbit	GE Healthcare, UK
HRP-conjugated donkey anti-rabbit	GE Healthcare, UK
Mouse anti-His mAb	GE Healthcare, UK
Mouse anti-Penta-His mAb	Qiagen, USA
Rabbit anti-Hsp72/3 pAb	Upstate Biotechnology, USA
Rabbit anti-DnaJ pAb	Stressgen, USA
TRITC-conjugated anti-rabbit	Invitrogen, USA

RESTRICTION ENZYMES	
BamHI	Fermentas, Lithuania
BalI	Promega, USA
HindIII	Fermentas, Lithuania
SalI	Fermentas, Lithuania
EcoRV	GE Healthcare, UK
EcoRI	GE Healthcare, UK
NheI	GE Healthcare, UK
SacII	GE Healthcare, UK
SmaI	Roche Applied Sciences, Germany
PstI	Fermentas, Lithuania
DpnI	Promega, USA

E. COLT STRAINS	
E. coli BL21(DE3)pLysS	Promega, USA
E. coli DH5α	Gibco-BRL, USA
E. coli JM109™	Promega, UK
E. coli Rosetta™ 2(DE3)pLysS	Novagen, USA
E. coli RR1	ATCC, USA
E. coli XL1-Blue	Stratagene, USA
E. coli XL10-Gold	Strategene, USA

PLASMIDS	
pGEM-T Easy®	Promega, USA
pQE30	Qiagen, USA
pUC18	Promega, USA

ENZYMES	
Expand High Fidelity *Taq* Polymerase and 10x Buffer	Roche Applied Sciences, Germany
T4 DNA Ligase and 10x Buffer	Roche Applied Sciences, Germany
Pfu Dna Polymerase and 10x Buffer	Promega, USA

COMMERCIAL KITS	
Big Dye™ Terminator Cycle Sequencing Kit	Applied Biosciences, UK
ECL™ Western Blotting Kit	GE Healthcare, UK
GFX™ PCR DNA and Gel Band Purification Kit	GE Healthcare, UK
QiaPrep Miniprep™ Kit	Qiagen, USA
Zymo-Spin *I*	Zymo Research, USA

MARKERS	
Pageruler™ Protein Ladder	Fermentas, USA
SDS-PAGE Molecular Mass Marker	Bio-Rad, USA

PRIMERS	
All primers were synthesised by Integrated DNA Technologies (IDT, USA)	WhiteSci, South Africa

APPENDIX F

SEQUENCES OF PRIMERS USED IN PCR, MUTAGENESIS, AND DNA SEQUENCING

F1: PCR ASSEMBLY PRIMERS USED IN THE SYNTHESIS OF THE Pfj1 CODING SEQUENCE

PRIMER SET	PRIMER NAME	SEQUENCE (5' to 3')
FORWARD	Pfj1Fwd_1	GGATCCATGCTGGCGCTGCGTATCCTGCGTCGTAA
	Pfj1Fwd_2	AGTTTGCTCTGAACACTTCCTGTTCGAGCGTTCTTTCTTCACC
	Pfj1Fwd_3	CAGTCTATCAAAGGTAAAAACGGTTGCCTGGTTACCCGTTAC
	Pfj1Fwd_4	GACAAAAACAAACTGCTGTTCTACTACAAACGTAACATCAACACCT
	Pfj1Fwd_5	CTCGTAAATGCCTGAACCAGGACCCGTACACCGTTCTGG
	Pfj1Fwd_6	GTCTGTCTCGTAACGCGACCACCAACGACATCAAAAAACAGT
	Pfj1Fwd_7	TCAGGCTGCTGGCGAAAAAATACCACCCGGACATCA
	Pfj1Fwd_8	ACCCGTCTCCGGACGCGAAACAGAAAATGGCGTC
	Pfj1Fwd_9	TATCACCGCGGCGTACGAACTGCTGTCTGACCCGAAA
	Pfj1Fwd_10	AAGAAAGAATTCTACGACAAAACCGGTATGACCGACGACTCTAAC
	Pfj1Fwd_11	TACCAGAACCACTCTTCTAACTTCGAAGGTGCGTTCTCTGGTTT
	Pfj1Fwd_12	CGGTGACGCGTCTTTCATGTTCACCGACTTCGCG
	Pfj1Fwd_13	GAAATGTTCACCAACATGGCGGGTGGTAACAAAAACACCT
	Pfj1Fwd_14	CTACCCGTGGTGAAGACATCCAGTCTGAAATCACCCTGAAAT
	Pfj1Fwd_15	TCATGGAAGCGATCAAAGGTTGCGAAAAAAACTCGCGA
	Pfj1Fwd_16	CTGAACGTTAAAGTTTCTTGCAACAACTGCAACGGTTCTGGTA
	Pfj1Fwd_17	AAAAACCGGGCACCAACCTGACCATCTGCAAAGTTTGCA
	Pfj1Fwd_18	ACGGTTCTGGTATCCAGCGTATGGAACGTGGTCCGATC
	Pfj1Fwd_19	ATCATCGGTGTTCCGTGCCGTAACTGCTCTGGTAACGG
	Pfj1Fwd_20	TCAGATCATCAACAACCCGTGCAAACACTGCTCTGGTTCT
	Pfj1Fwd_21	GGTGTTAAATTCCAGACCAAAAACATCACCCTGGACATCC
	Pfj1Fwd_22	CGCCCGGGATCAAAAAAGGTATGCAGATGCGTATCCC
	Pfj1Fwd_23	GAACCAGGGTCACTGCGGTTACCGTGGTGGTAAATCTG
	Pfj1Fwd_24	GTCACCTGTTCGTTACCATCAACATCGAACCGCACAAAAT
	Pfj1Fwd_25	CTTCAAATGGGTTGACGACAACATCTACGTTGACGTTCCG
	Pfj1Fwd_26	CTGACCATCAAACAGTGCCTGCTGGGTGGTCTGGTTACC
	Pfj1Fwd_27	GTTCCGACCCTGAACGGTGACATGGACCTGCTGATCA
	Pfj1Fwd_28	AACCGAAAACCTACCCGAACTCTGAAAAAATCCTGAAAGGTA
	Pfj1Fwd_29	AAGGTCCGTGCAAAGTTGACTCTCACAACAACGGTGACCT
	Pfj1Fwd_30	GATCATCAAATTCTCTCTGAAAATCCCGGAAAAACTGACC
	Pfj1Fwd_31	CCGCGTCAGGTTGAACTGATCGAAGAATTCAACACCATC
	Pfj1Fwd_32	GAACTGAACCTGCCGAACCCGCAGACCAACGTTAAACAGA
	Pfj1Fwd_33	AAAAAAACATCTACGAAACCAAAGGTAACATCAACGAAAACATCTT
	Pfj1Fwd_34	CTCTATGAACAACACCTACAACAACATGAAAGGTCCGGAAGG
	Pfj1Fwd_35	TGAAACCTCTAACACCCAGGCGAAATCTATGAAAAACCAGAAC
	Pfj1Fwd_36	TGGAACAACGAAAAATCTGTTAACAACAAAGGCACCATCTCTAAAG
	Pfj1Fwd_37	ACGAAAAAAAAACTGAACATGAAAAACAACCACATCAACGAAAAA
	Pfj1Fwd_38	TCTAACCTGAAAAACTCTTCTCACATGGACACCAACAAAAACG
	Pfj1Fwd_39	AAGAAAACATGTCTGACGACGAAAAAAAAAAAATCAAAAAAATCA
	Pfj1Fwd_40	TCCCGGAACCGCCGATGCCGCACACC
	Pfj1Fwd_41	CACAAAATCGTTAACAACCTGGAATCTAAAAACTCTTGCAACATC
	Pfj1Fwd_42	CCGATCCCGCCGCCGCCGCC
	Pfj1Fwd_43	GAAATCTTCTTCTAAACCGATCTCTGAAAACCAGAACATCTCTAAC
	Pfj1Fwd_44	CGTGAACACAACGGTGTTACCAACAACTCTGCGAAACTGGA
	Pfj1Fwd_45	CAACAACATCAACATGAACTACTCTTGCGACCCGTACAAAAA
	Pfj1Fwd_46	CGTTACCCAGAACGACCTGAACAACAACGACAACATCAAAAA
	Pfj1Fwd_47	CAAAATCTACAAAGACAACACCAACATCTCTAACCACCACATCTTC
	Pfj1Fwd_48	AAAAACGACAACATCAACCAGCAGCAGTTCCACTGCGC
	Pfj1Fwd_49	GGACAACTCTTCTGAAAACAACAACGAATCTGACATGAACACCA
	Pfj1Fwd_50	CCTCTACCTTCTCTTTCGCCAAAAAATGGATCTCTGACAAACTG

PRIMER SET	PRIMER NAME	SEQUENCE (5'to 3')
REVERSE	Pfj1Rev_1	GGTACCTTAGTTTTTCGGTTTCAGTTTGTCAGAGATCCATTTTT
	Pfj1Rev_2	TGGCGAAAGAGAAGGTAGAGGTGGTGTTCATGTCAGATTCGT
	Pfj1Rev_3	TGTTGTTTTCAGAAGAGTTGTCCGCGCAGTGGAACTGCTG
	Pfj1Rev_4	CTGGTTGATGTTGTCGTTTTTGAAGATGTGGTGGTTAGAGATGT
	Pfj1Rev_5	TGGTGTTGTCTTTGTAGATTTTGTTTTTGATGTTGTCGTTGTTGT
	Pfj1Rev_6	TCAGGTCGTTCTGGGTAACGTTTTTGTACGGGTCGCAAG
	Pfj1Rev_7	AGTAGTTCATGTTGATGTTGTTGTCCAGTTTCGCAGAGTTGTTG
	Pfj1Rev_8	GTAACACCGTTGTGTTCACGGTTAGAGATGTTCTGGTTTTCAG
	Pfj1Rev_9	AGATCGGTTTAGAAGAAGATTTCGGCGGCGGC
	Pfj1Rev_10	GGCGGGATCGGGATGTTGCAAGAGTTTTTAGATT
	Pfj1Rev_11	CCAGGTTGTTAACGATTTTGTGGGTGTGCGGCATCG
	Pfj1Rev_12	GCGGTTCCGGGATGATTTTTTTGATTTTTTTTTTT
	Pfj1Rev_13	TCGTCGTCAGACATGTTTTCTTCGTTTTTGTTGGTGTCCATG
	Pfj1Rev_14	TGAGAAGAGTTTTTCAGGTTAGATTTTTCGTTGATGTGGTTGTT
	Pfj1Rev_15	TTTCATGTTCAGTTTTTTTTCGTCTTTAGAGATGGTGCCTTTGTTG
	Pfj1Rev_16	TTAACAGATTTTTCGTTGTTCCAGTTCTGGTTTTTCATAGATTTCG
	Pfj1Rev_17	CCTGGGTGTTAGAGGTTTCACCTTCCGGACCTTTCATGT
	Pfj1Rev_18	TGTTGTAGGTGTTGTTCATAGAGAAGATGTTTTCGTTGATGTTACC
	Pfj1Rev_19	TTTGGTTTCGTAGATGTTTTTTTTCTGTTTAACGTTGGTCTGCG
	Pfj1Rev_20	GGTTCGGCAGGTTCAGTTCGATGGTGTTGAATTCTTCGA
	Pfj1Rev_21	TCAGTTCAACCTGACGCGGGGTCAGTTTTTCCGGGA
	Pfj1Rev_22	TTTTCAGAGAGAATTTGATGATCAGGTCACCGTTGTTGTGAGAG
	Pfj1Rev_23	TCAACTTTGCACGGACCTTTACCTTTCAGGATTTTTTCAGAG
	Pfj1Rev_24	TTCGGGTAGGTTTTCGGTTTGATCAGCAGGTCCATGTCA
	Pfj1Rev_25	CCGTTCAGGGTCGGAACGGTAACCAGACCACCCAGC
	Pfj1Rev_26	AGGCACTGTTTGATGGTCAGCGGAACGTCAACGTAGATGT
	Pfj1Rev_27	TGTCGTCAACCCATTTGAAGATTTTGTGCGGTTCGATG
	Pfj1Rev_28	TTGATGGTAACGAACAGGTGACCAGATTTACCACCACGGTAAC
	Pfj1Rev_29	CGCAGTGACCCTGGTTCGGGATACGCATCTGCATAC
	Pfj1Rev_30	CTTTTTTGATCCCGGGCGGGATGTCCAGGGTGATGT
	Pfj1Rev_31	TTTTGGTCTGGAATTTAACACCAGAACCAGAGCAGTGTTTGC
	Pfj1Rev_32	ACGGGTTGTTGATGATCTGACCGTTACCAGAGCAGTTACGG
	Pfj1Rev_33	CACGGAACACCGATGATGATCGGACCACGTTCCATA
	Pfj1Rev_34	CGCTGGATACCAGAACCGTTGCAAACTTTGCAGATGGTC
	Pfj1Rev_35	AGGTTGGTGCCCGGTTTTTTACCAGAACCGTTGCAGTTG
	Pfj1Rev_36	TTGCAAGAAACTTTAACGTTCAGTCGCGAGTTTTTTTCGCAA
	Pfj1Rev_37	CCTTTGATCGCTTCCATGAATTTCAGGGTGATTTCAGACTG
	Pfj1Rev_38	GATGTCTTCACCACGGGTAGAGGTGTTTTTGTTACCACCC
	Pfj1Rev_39	GCCATGTTGGTGAACATTTCCGCGAAGTCGGTGAACA
	Pfj1Rev_40	TGAAAGACGCGTCACCGAAACCAGAGAACGCACCTTC
	Pfj1Rev_41	GAAGTTAGAAGAGTGGTTCTGGTAGTTAGAGTCGTCGGTCATACCG
	Pfj1Rev_42	GTTTTGTCGTAGAATTCTTTCTTTTTCGGGTCAGACAGCAGTT
	Pfj1Rev_43	CGTACGCCGCGGTGATAGACGCCATTTTCTGTTTCG
	Pfj1Rev_44	CGTCCGGAGACGGGTTGATGTCCGGGTGGTATTT
	Pfj1Rev_45	TTTCGCCAGCAGCCTGAACTGTTTTTTGATGTCGTTGGT
	Pfj1Rev_46	GGTCGCGTTACGAGACAGACCCAGAACGGTGTACGGGTC
	Pfj1Rev_47	CTGGTTCAGGCATTTACGAGAGGTGTTGATGTTACGTTTGTAG
	Pfj1Rev_48	TAGAACAGCAGTTTGTTTTTGTCGTAACGGGTAACCAGGCAA
	Pfj1Rev_49	CCGTTTTTACCTTTGATAGACTGGGTGAAGAAAGAACGCTCGA
	Pfj1Rev_50	ACAGGAAGTGTTCAGAGCAAACTTTACGACGCAGGATACGCAG

F2: PRIMERS USED IN THE AMPLIFICATION OF THE Pfj1-BACK CODING SEQUENCE

TARGET	PRIMER PRIMER NAME	PRIMER SEQUENCE (5′ to 3′)
Pfj1-Back	Forward Pfj1Fwd_21	GGTGTTAAATTCCAGACCAAAAACATCACCCTGGACATCC
	Reverse Pfj1-PstI Rev	CTGCAGGGTACCTTAGTTTTTCGGTTTCAG

The introduced PstI site is underlined on the 5' end of the reverse primer

F2: PRIMERS USED IN THE S248G MUTAGENESIS OF THE Pfj1 CODING SEQUENCE

MUTATION	PRIMER	PRIMER NAME	PRIMER SEQUENCE (5′ to 3′)
S248G	Forward	S248G-Fwd	GCTCTGGTAACGGTCAGATCATCAACAACC
	Reverse	S248G-Rev	GGTTGTTGATGATCTGACCGTTACCAGAGC

F3: PRIMERS USED IN DNA SEQUENCING

TARGET	PRIMER NAME	PRIMER SEQUENCE (5′ to 3′)
pQE30-based plasmids	pQE30-Forward	CGGATAACAATTTCACACAG
	pQE30-Reverse	CTGAGGTCATTACTGG
pGEM-T® Easy-based plasmids	pGEM/T-Forward	GGTTTTCCCAGTCACGAC
	pGEM/T-Reverse	GGAAACAGCTATGACCATG
Pfj1 coding sequence	S248G-Forward	GCACTGTTTGATGGTCAGC
Pfj1-Back coding sequence	Pfj1-Back-Forward	CCTGAAAGGTAAAGGTCCGTGC
	Pfj1-Back-Reverse	CGTCGTCAGACATGTTTTCTTCG

F4: PRIMERS USED IN THE MUTAGENESIS OF THE J-DOMAIN OF Pfj1

MUTATION	RESTRICTION SITE	PRIMER	PRIMER SEQUENCE (5′ to 3′)
F25A	EcoRV	Forward	CCACCAACGATATCAAGAAACAGGCCCGTCTGCTGG
		Reverse	CCAGCAGACGGGCCTGTTTCTTGATATCGTTGGTGG
R26A	BalI	Forward	GAAACAGTTCGCTCTGCTGGCCAAGAAATACC
		Reverse	GGTATTTCTTGGCCAGCAGAGCGAACTGTTTC
H33Q	EcoRV	Forward	CGAAGAAATACCAGCCAGATATCAACCCGTCTCC
		Reverse	GGAGACGGGTTGATATCTGGCTGGTATTTCTTCG
KFA	NheI	Forward	GCGAAACAGAAATTTGCTAGCATCACCGCGGC
		Reverse	GCCGCGGTGATGCTAGCAAATTTCTGTTTCGC
KMK	SacII	Forward	CGAAACAGAAAATGAAGTCTATCACAGCGGCGTACG
		Reverse	CGTACGCCGCTGTGATAGACTTCATTTTCTGTTTCG
KFK	SacII	Forward	CGAAACAGAAATTTAAGTCTATCACGGCGGCGTACG
		Reverse	CGTACGCCGCCGTGATAGACTTAAATTTCTGTTTCG
K62A	EcoRI	Forward	CCCGAAGAAGGCAGAGTTCTACGACAAAACC
		Reverse	GGTTTTGTCGTAGAACTCTGCCTTCTTCGGG
QKRAA	EcoRI	Forward	GTCTGACCCGCAGAAGCGCGCAGCCTACGACAAAACC
		Reverse	GGTTTTGTCGTAGGCTGCGCGCTTCTGCGGGTCAGAC

In the primer sequences, the nucleotide mutations introduced into the Pfj1 J-domain coding sequence are indicated in bold, and the restriction sites engineered or removed from the sequence are underlined.

APPENDIX G

SUPPLEMENTARY MULTIPLE PROTEIN SEQUENCE ALIGNMENTS

Alignments were performed using ClustalW (version 1.83)[11]. Protein sequences were retrieved from Genbank[12], PlasmoDB[13], CryptoDB[14] and ToxoDB[15]. Identical and similar conserved residues are indicated in with grey and black shading respectively, and with the symbols '*' and '.' in the consensus lines of the alignments.

---

[11] CHENNA, R., SUGAWARA, H., KOIKE,T., LOPEZ, R., GIBSON, T.J., HIGGINS, D.G. and THOMPSON, J.D. (2003). Multiple sequence alignment with the Clustal series of programs. *Nucleic Acids Research*, 31, 3497-3500.

[12] BENSON, D.A., KARSCH-MIZRACHI, I., LIPMAN, D.J., OSTELL, J. and WHEELER, D.L. (2008). GenBank. *Nucleic Acids Research*, 36, D25-D30.

[13] BAHL, A., BRUNK, B., CRABTREE, J., FRAUNHOLZ, M.J., GAJRIA, B., GRANT, G.R., GINSBURY, H., GUPTA, D., KISSINGER, J.C., LABO, P., LI, L., MAILMAN, M.D., MILGRAM, A.J., PEARSON, D.S., ROOS, D.S., SCHUG, J., STOECKERT, C.J. and WHETZEL, P. (2003). PlasmoDB: the *Plasmodium* genome resource. A database integrating experimental and computational data. *Nucleic Acids Research*, 31, 212-215.

[14] HEIGES, M., WANG, H., ROBINSON, E., AURRECOECHEA, C., GAO, X., KALUSKAR, N., RHODES, P., WANG, S., HE, C.Z., SU, Y., MILLER, J., KRAEMER, E. and KISSINGER, J.C. (2006). CryptoDB: a Cryptosporidium bioinformatics resource. *Nucleic Acids Research*, 34, D419-422.

[15] KISSINGER, J. C., GAJRIA, B., LI, L., PAULSEN, I. T. and ROOS, D. S. (2003). ToxoDB: accessing the *Toxoplasma gondii* genome. *Nucleic Acids Research*, 31, 234-236.

G1:

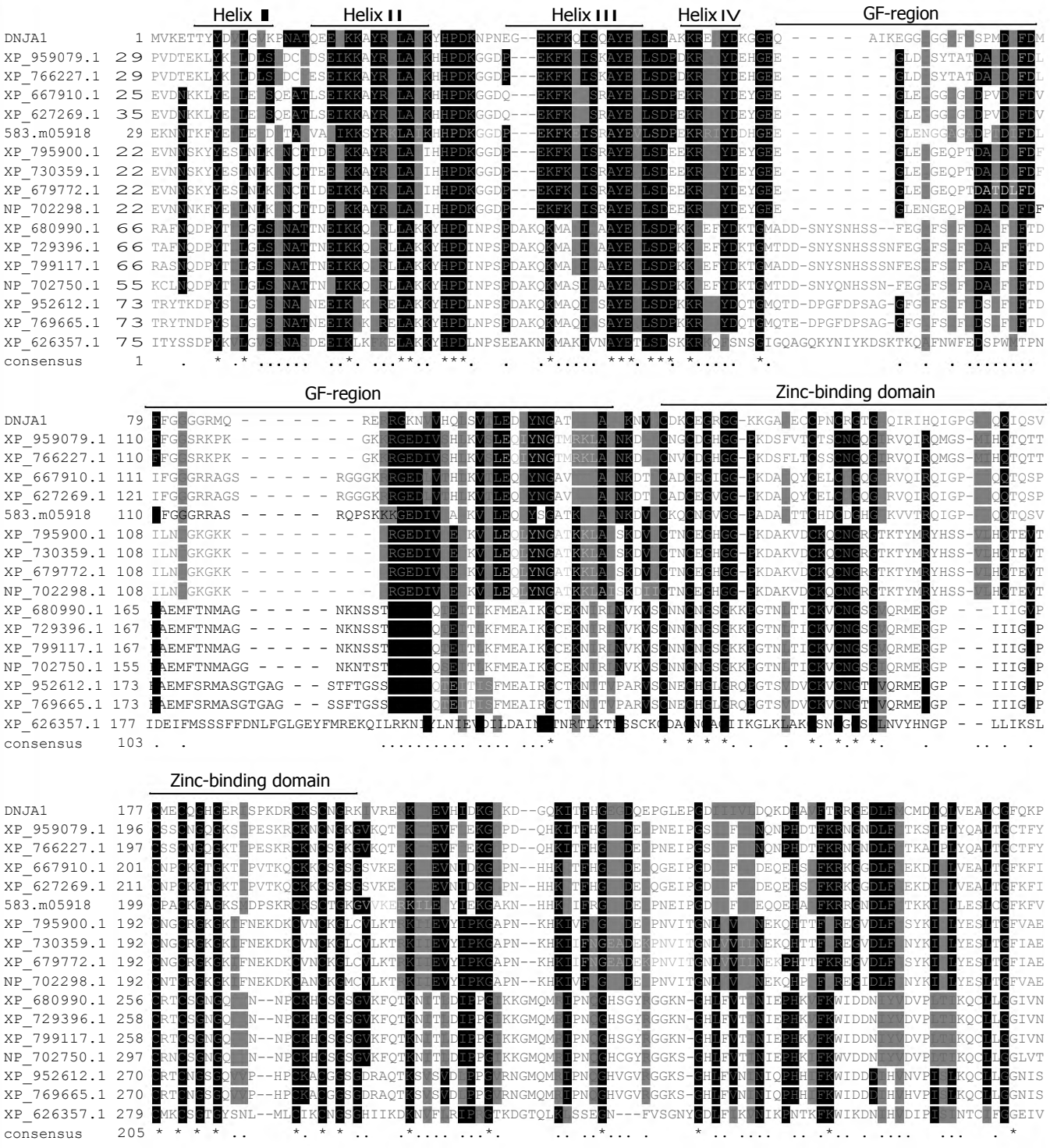
Helix I
Helix II
Helix III
Helix IV
GF-region
GF-region
Zinc-binding domain
Zinc-binding domain

FIGURE G1.../

.../FIGURE G1

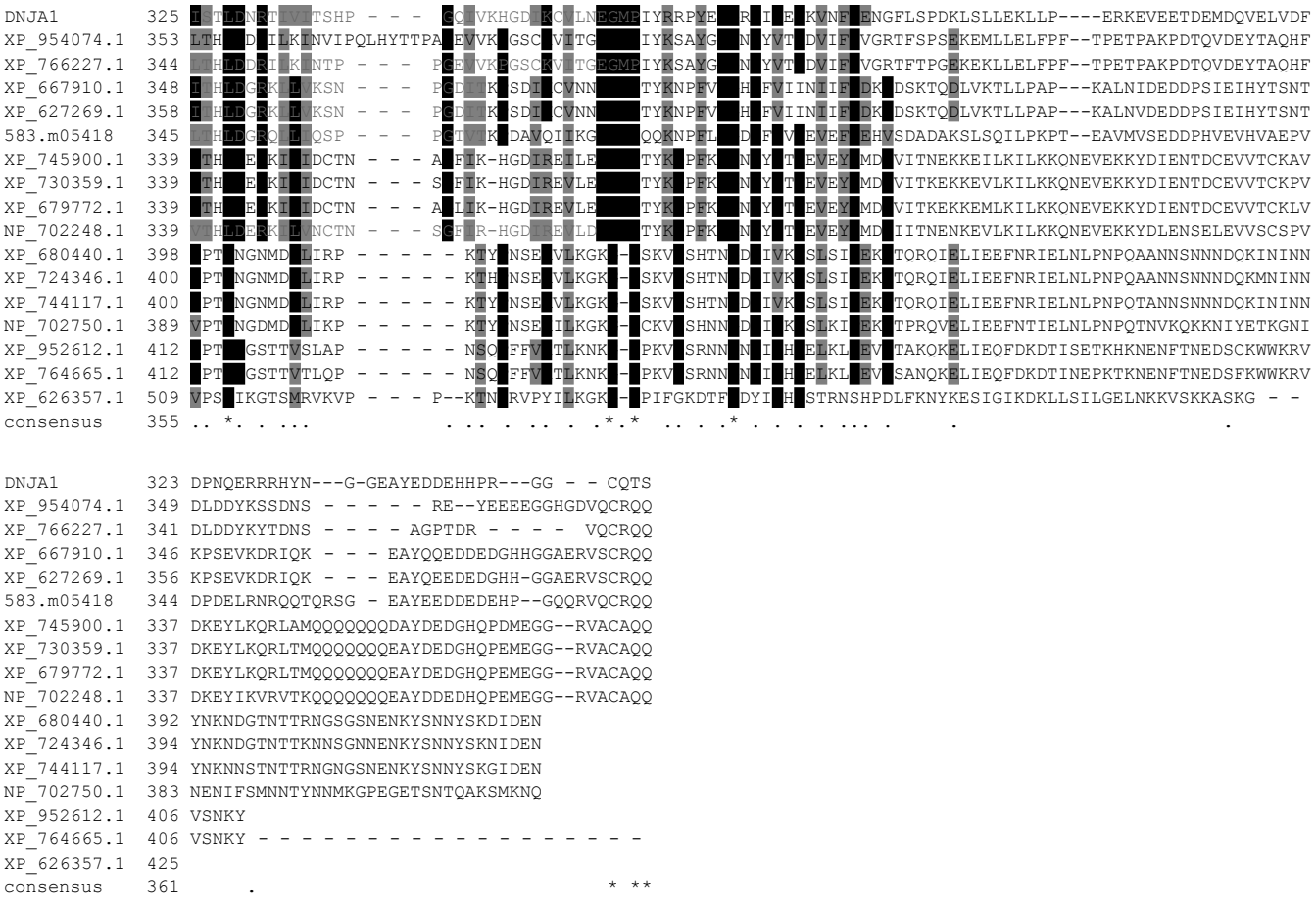

FIGURE G1 Protein sequence alignment of the type I Hsp40 proteins of *P. falciparum* and other apicomplexan parasites. Accession numbers: *P. falciparum* PfHsp40 (NP_702248.1) and Pfj1 (NP_702750.1), *C. hominis* (XP_667910.1), *C. parvum* (XP_627269.1 and XP_626357.1), *P. berghei* (XP_679772.1 and XP_680440.1), *P. chabaudi* (XP_745900.1 and XP_744117.1), *P. yoelii* (XP_730359.1 and XP_724346.1), *T. annulata* (XP_954074.1 and XP_952612.1), *T. parva* (XP_766227.1 and XP_764665.1), *T. gondii* (PlasmoDB locus number 583.05418) and *H. sapiens* DnaJA1 (NP_001530.1). Residues of helices I-IV of the J-domain, the GF region and the zinc-binding domain are indicated. N-terminal leader sequences of the apicomplexan Hsp40 proteins are not shown and C-terminal regions of XP_680440.1, XP_724346.1, XP_744117.1, NP_702750.1, XP_952612.1, XP_764665.1 and XP_626357.1 were truncated for the alignment. CAAX-box motifs and Gln repeat sequences are indicated in red and blue respectively.

G2:

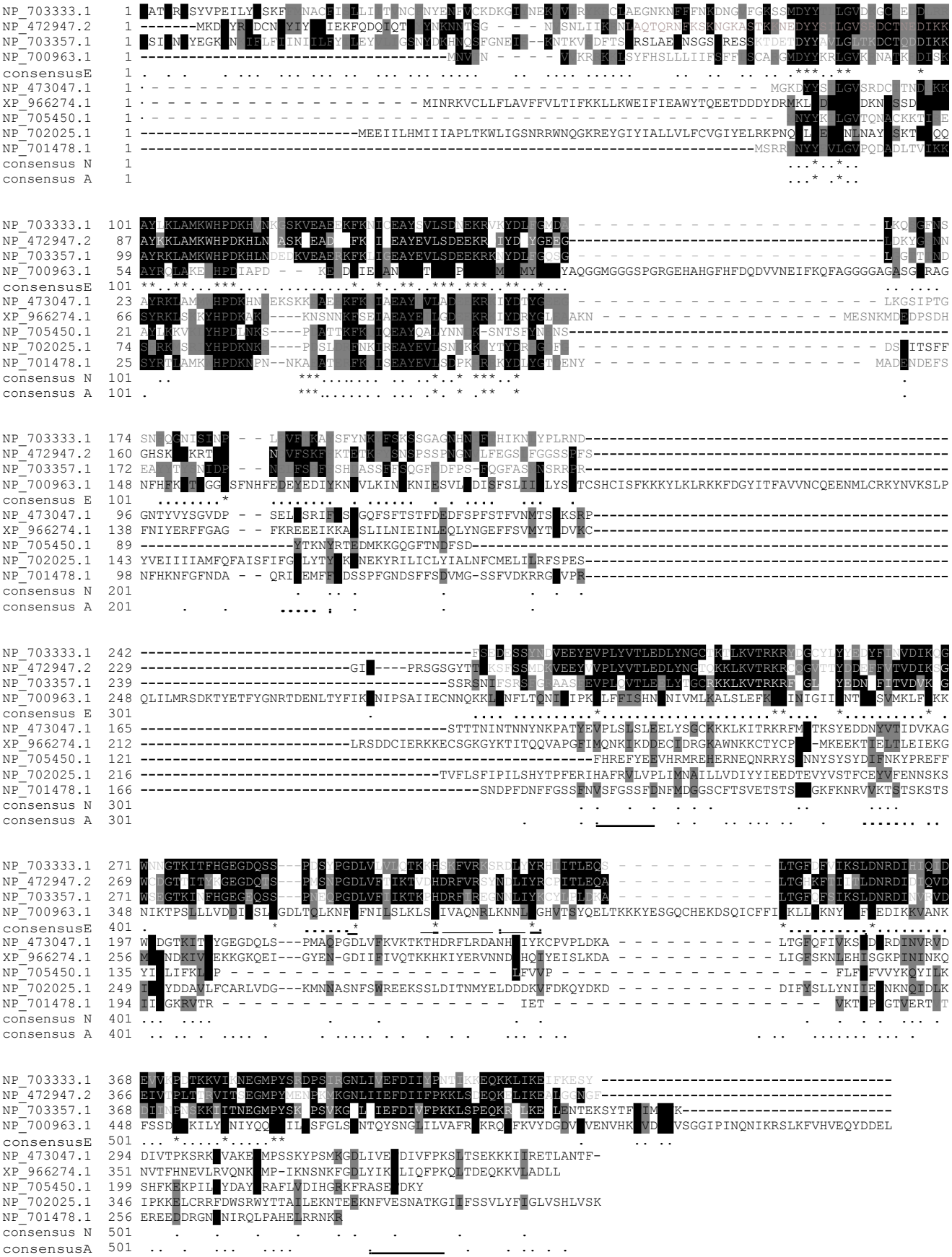
NP_703333.1
NP_472947.2
NP_703357.1
NP_700963.1
consensusE
NP_473047.1
XP_966274.1
NP_705450.1
NP_702025.1
NP_701478.1
consensus N
consensus A

FIGURE G2.../

../FIGURE G2 Protein sequence alignment of PEXEL/HT-positive and PEXEL/HT-negative type II Hsp40 proteins of *P. falciparum.* Accession numbers of the aligned protein sequences: PFA0660w (NP_703333.1), PFB0090c (NP_472947.2), PFE0055c (NP_703357.1), PF11_0099 (NP_700963.1), PFB0595w (NP_473047.1), PFF1415c (XP_966274.1), MAL13P1.277 (NP_705450.1), PF14_0137 (NP_702025.1) and PFL0565w (NP_701478.1). Putative PEXEL/HT sequences of the predicted exported proteins are indicated in red (SARGEANT *et al.*, 2006). Consensus A indicates the overall conserved residues of the protein sequences presented in the alignment, while consensus lines E and N indicate conserved residues of the PEXEL/HT-positive and PEXEL/HT-negative proteins respectively.

G3:

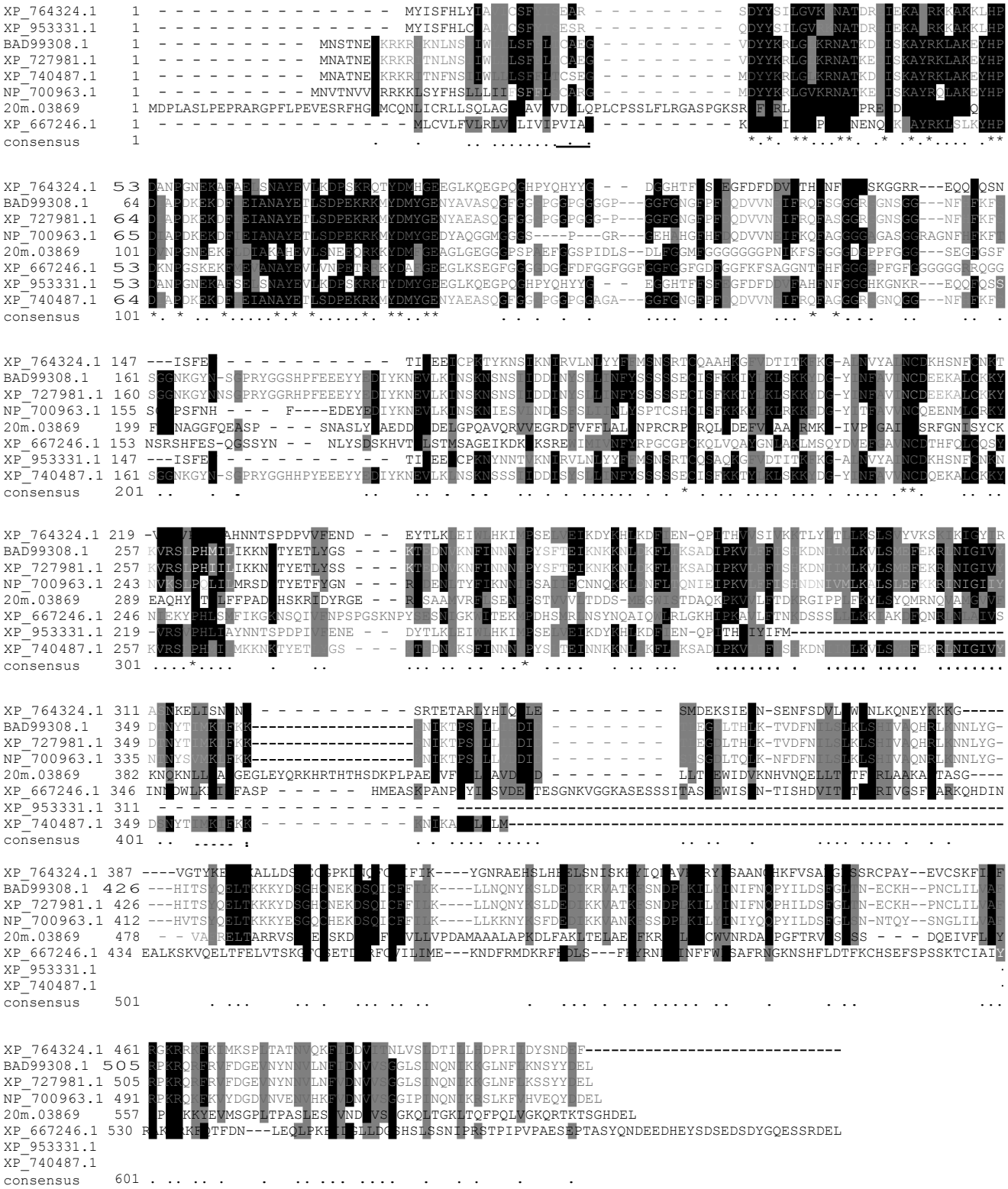

FIGURE G3 Protein sequence alignment of the *P. falciparum* type II Hsp40, Pfj2, and its apicomplexan homologs. Homologous proteins to Pfj2 (NP_700963.1) were identified in *C. hominis* (XP_667246.1), *C. parvum* (CryptoDB locus cgd2_3230), *P. berghei* (BAD99308.1), *P. chabaudi* (XP_740487.1), *P. yoelii* (XP_727981.1), *T. annulata* (XP_953331.1), *T. parva* (XP_764324.1) and *T. gondii* (20m.03869). The putative PEXEL/HT sequence of Pfj2 (RQLAK) and potential PEXEL/HT sequences of the homologous proteins are indicated in red.

G5:

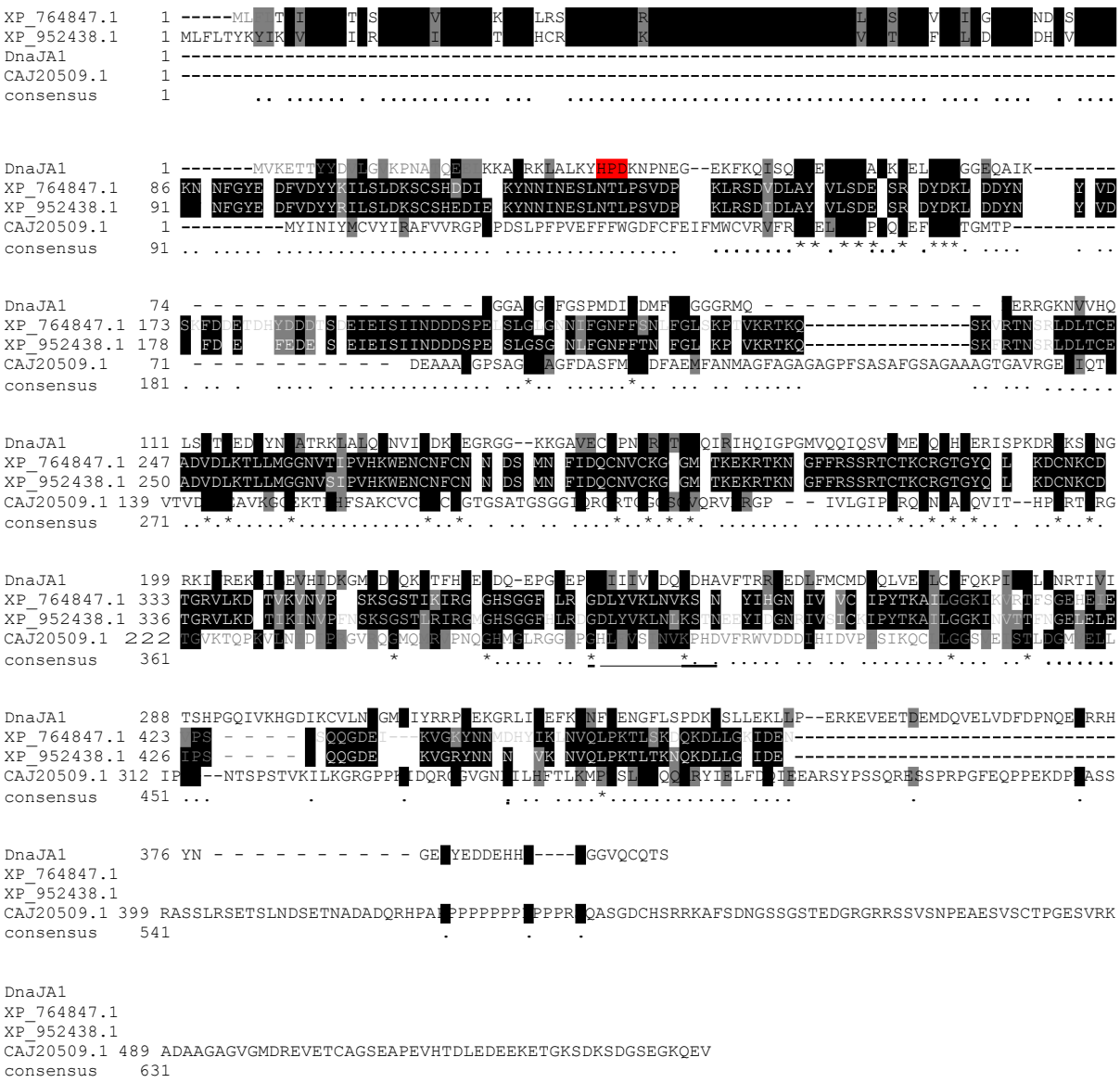

FIGURE G5 Protein sequence alignment of the type III Hsp40 proteins of the apicomplexa. Aligned sequences: *T. parva* (XP_764847.1), *T. annulata* (XP_952438.1) and *T. gondii* (CAJ20509.1) with the sequence of human DnaJA1 (NP_001530.1) as a reference. The HPD motif of DnaJA1 is indicated in red.

G6:

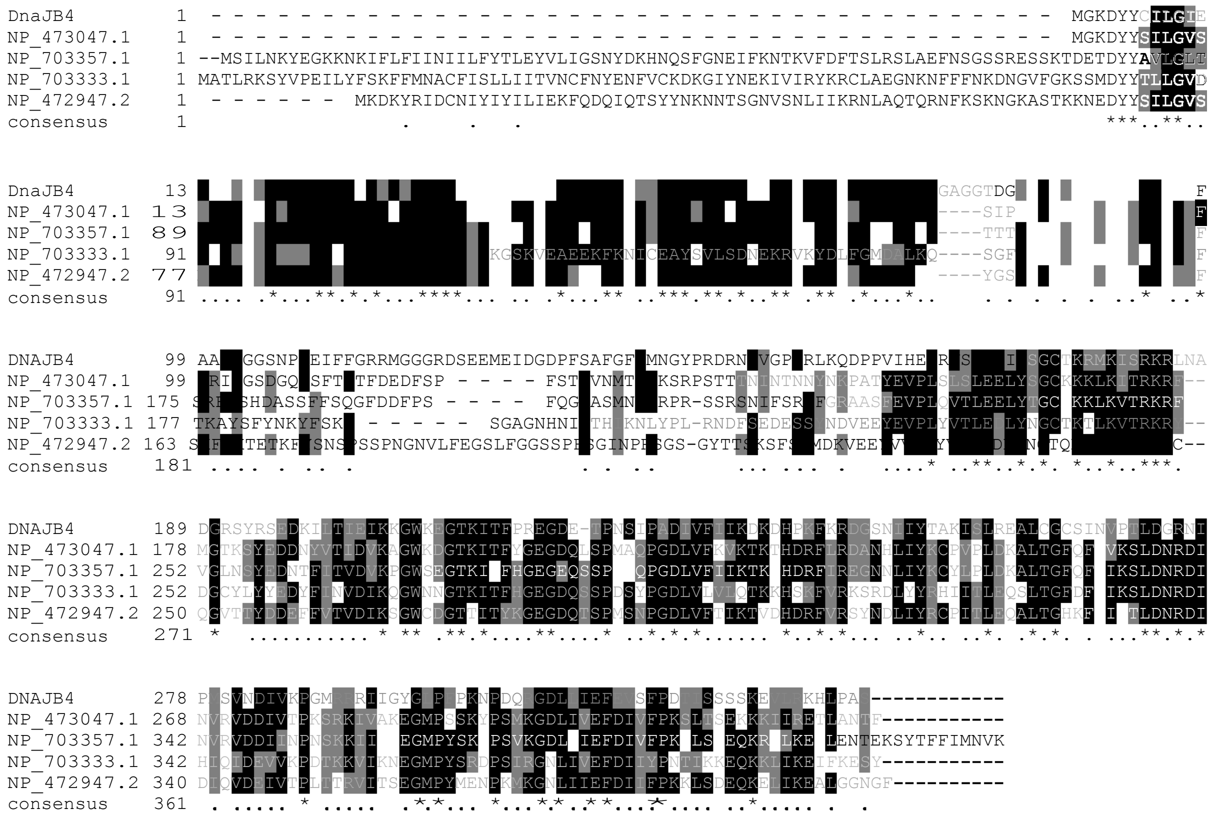

FIGURE G6 Protein sequence alignment of the human type II Hsp40 protein DnaJB4 and homologous type II Hsp40 proteins of *P. falciparum*. Accession numbers: DnaJB4 (NP_008965.2) and type II Hsp40 proteins of *P. falciparum* PFB0505w (NP_473047.1), PFA0660w (NP_703333.1), PFE0055c (NP_703357.1) and PFB0090c (NP_472947.2). The putative PEXEL/HT motifs of the proposed exportome type II Hsp40 proteins are indicated in red.

G7:

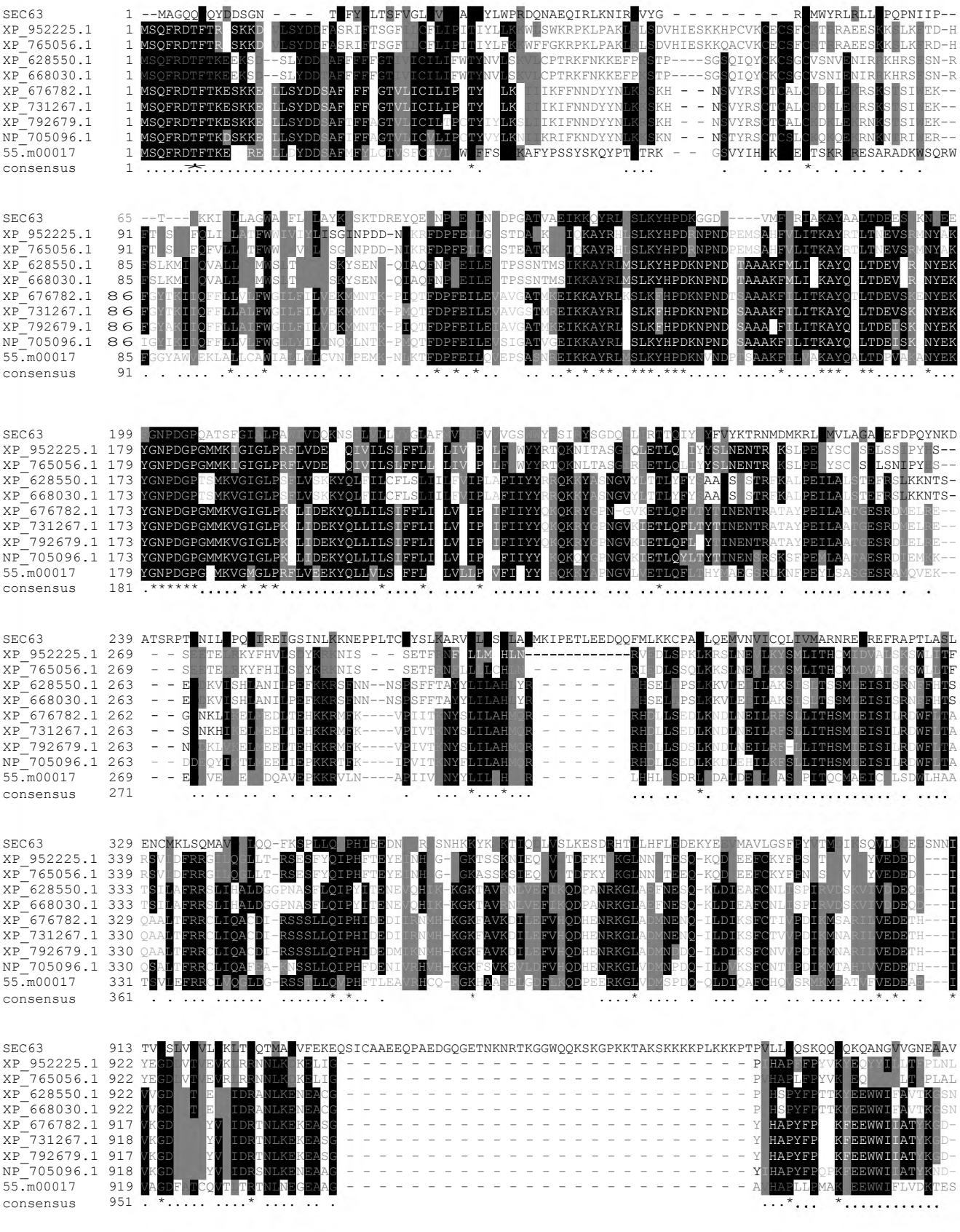
SEC63
XP_952225.1
XP_765056.1
XP_628550.1
XP_668030.1
XP_676782.1
XP_731267.1
XP_792679.1
NP_705096.1
55.m00017
consensus

FIGURE G7.../

.../FIGURE G7

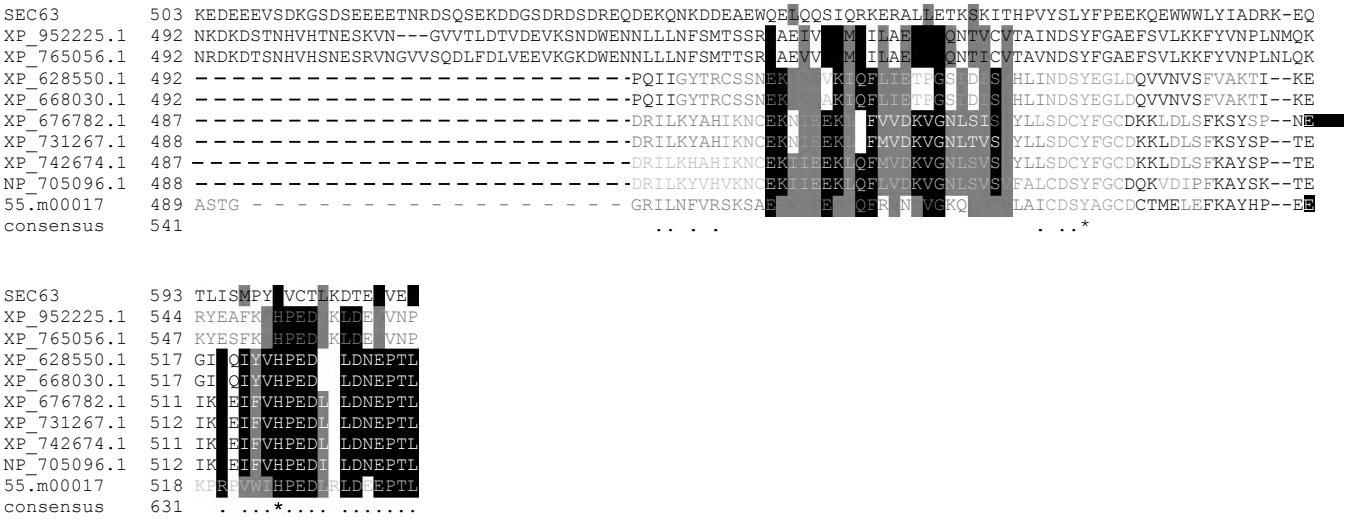

FIGURE G7 Protein sequence alignment of the human endoplasmic reticulum membrane type III Hsp40 protein, Sec63, and homologous apicomplexan proteins. Accession numbers of the Sec63 proteins: *H. sapiens* (AAC83375.1), *P. falciparum* (NP_705096.1), *C. hominis* (XP_668030.1), *C. parvum* (XP_628550.1), *P. berghei* (XP_676782.1), *P. chabaudi* (XP_742674.1), *P. yoelii* (XP_731267.1), *T. annulata* (XP_952225.1), *T. parva* (XP_765056.1) and *T. gondii* (PlasmoDB locus 55.m00017).

APPENDIX H

CLASSIFICATION OF HSP40 PROTEINS FROM THE APICOMPLEXA

Apicomplexan	Hsp40 Type			
	Type I	Type II	Type III	Type IV
P. falciparum	NP_702248.1, NP_702750.1	NP_703333.1, NP_472947.2, NP_703357.1, NP_700963.1, NP_705450.1, NP_702025.1, NP_473047.1, XP_966274.1, NP_701478.1	NP_700851.1, NP_701358.1, NP_473112.2, NP_701376.1, NP_704176.1, NP_704316.1, NP_704487.1, NP_700506.1, NP_700532.1, NP_701133.1, NP_701239.1, NP_704971.1, NP_705096.1, NP_702589.1, NP_703373.1, NP_703578.1, NP_705208.1, NP_704730.1, NP_704740.1, NP_701527.1	NP_700854.1, NP_700899.1, NP_701354.1, NP_701357.1, NP_701901.1, NP_703225.1, NP_703336.1, NP_472946.1, NP_473113.2, NP_703354.1, NP_701868.1, CAA00077.1, NP_701301.1
P. berghei	XP_680440.1, XP_679772.1	XP_677556.1, XP_678015.1, XP_675336.1, XP_677966.1, BAD99308.1	XP_680251.1, XP_674936.1, XP_679805.1, XP_679581.1, XP_678174.1, XP_676782.1, XP_676168.1, XP_674789.1, XP_674078.1, XP_672208.1, XP_678535.1, XP_675745.1	XP_676696.1, XP_676292.1, XP_673844.1, XP_674629.1
P. chabaudi	XP_744117.1, XP_745900.1	XP_745867.1, XP_733846.1, XP_740487.1, XP_744229.1, XP_742984.1, XP_741048.1	XP_741274.1, XP_743132.1, XP_745623.1, XP_745623.1, XP_743352.1, XP_743161.1, XP_742782.1, XP_742674.1, XP_742418.1, XP_742282.1, XP_741054.1, XP_739007.1, XP_738064.1, XP_738063.1, XP_733803.1, XP_744850.1	XP_745038.1, XP_743387.1, XP_740905.1
P. yoelli	XP_730359.1, XP_724346.1	XP_728950.1, XP_727981.1, XP_726085.1, XP_730944.1, XP_727897.1, XP_723708.1	XP_724808.1, XP_726262.1, XP_731267.1, XP_723904.1, XP_730811.1, XP_730442.1, XP_729659.1, XP_729396.1, XP_729337.1, XP_729014.1, XP_725782.1, XP_724990.1, XP_724674.1, XP_724439.1, XP_723878.1, XP_723695.1, YP_294151.1	XP_724488.1
C. parvum	XP_626357.1, XP_627269.1	cgd2_3230, CAD98554.1, XP_625863.1	cgd1_2280, XP_627481.1, CAD98666.1, XP_628550.1, XP_628113.1, XP_628029.1, XP_627375.1, XP_627186.1, XP_627182.1, XP_626829.1, XP_626673.1, XP_626430.1, XP_626267.1, XP_626230.1, XP_626839.1, XP_627223.1, XP_626275.1, XP_625506.1	XP_626276.1
C. hominis	XP_667910.1, XP_668107.1	XP_667385.1, XP_667246.1, XP_667435.1, XP_667885.1	XP_667991.1, XP_666401.1, XP_668519.1, XP_668107.1, XP_668094.1, XP_668014.1, XP_667995.1, XP_667828.1, XP_667820.1, XP_667421.1, XP_666859.1, XP_666569.1, XP_666525.1, XP_666306.1, XP_666126.1, XP_665120.1, XP_668030.1, XP_665309.1	XP_664887.1, XP_667829.1
T. annulata	XP_952612.1, XP_954074.1	XP_954671.1, XP_952090.1, XP_953331.1, XP_954119.1	XP_955331.1, XP_952494.1, XP_954744.1, XP_952203.1, XP_952078.1, XP_952068.1, XP_952363.1, XP_954418.1, XP_953620.1, XP_953068.1, XP_952378.1, XP_952302.1, XP_952225.1, XP_952907.1	XP_952438.1
T. parva	XP_766227.1, XP_764665.1	XP_765562.1, XP_765191.1, XP_764324.1, XP_766186.1	XP_766250.1, XP_764922.1, XP_764980.1, XP_766673.1, XP_765837.1, XP_765214.1, XP_765204.1, XP_765080.1, XP_765056.1, XP_764787.1, XP_764037.1, XP_763870.1, XP_762749.1, XP_763339.1	XP_766587.1, XP_764847.1
T. gondii	25.m01777, 583.m05418	55.m00016, 57.m00015	20.m03665, 26.m00247, 33.m02195, 37.m00768, 44.m02699, 49.m00059, 55.m04854, 59.m03598, 59.m06079, 76.m01546, 76.m01596, 80.m02164, 80.m02203, 80.m02292, 583.m05553, 583.m05701, CAJ20508.1, 20m.03869, 55.m11052, 20.m05961, 55.m00017, 50.m00025, 583.m00680, 57.m01857, 162.m00513, 641.m02560	CAJ20509.1, 52.m01602

CHAPTER 1:

INTRODUCTION:

Literature Review

&

Hypothesis, Broad Objectives and Approach

1.1 THE CHALLENGES OF PROTEIN FOLDING IN THE CELL

The biogenesis of proteins in the cell is an intricate process, requiring the folding and translocation of nascent proteins emerging from the ribosomes for maturation into functional products. It is known that the complete specification for the folding of a protein into tertiary and quaternary structure is contained within its primary structure, or amino acid sequence, and that the process of protein folding into the native conformation may be spontaneous (ANFINSEN, 1973). However the correct folding of proteins *in vivo* is fraught with challenges owing to the complexity of the cellular environment. In particular, macromolecular crowding contributes to the aggregation and degradation of improperly folded proteins (ELLIS, 2001; ZIMMERMAN and MINTON, 1993) which in turn are associated with the onset of numerous disease states (DOBSON, 2003). Moreover, it is known that protein aggregation and unfolding are promoted by varied conditions of physiological stress. Consequently, cells have addressed the need for orchestrated protein folding by evolving specialised protein folding machinery comprised predominantly of molecular chaperone proteins (FELDMAN and FRYDMAN, 2000; SMITH *et al.*, 1998). While such coordination does not necessarily increase the rate of protein folding, it serves to minimise non-productive interactions and interference from other cellular components which hinder protein folding. In this context, molecular chaperones may be seen as protein folding 'catalysts' which lessen non-productive intra- and inter-molecular interactions by sequestering proteins for the folding process (FINK, 1999; THULASIRAMAN *et al.*, 1999).

1.2 MOLECULAR CHAPERONE PROTEINS ARE FOLDING CATALYSTS

The term 'molecular chaperones' coined by LASKEY *et al.* (1978) is used to define a class of ubiquitous proteins that are responsible for the correct folding and/or refolding of nascent, denatured, misfolded or aggregated proteins into functional conformations in the cell (ELLIS, 1987). This mediated folding is crucial to the prevention of the unfavourable consequences associated with protein misfolding and aggregation in eukaryotic and prokaryotic cells, and viral particles (DEUERLING and BUKAU, 2004; FELDMAN and FRYDMAN, 2000; YOUNG *et al.*, 2004). In addition to the mediation of correct protein folding in the cytosol, mitochondria and endoplasmic reticulum of the cell, molecular chaperones have been implicated in numerous additional and diverse roles including protein translocation to distinct subcellular compartments, the assembly and degradation of multiprotein complexes, cell signalling, protein activation and the facilitation of proteolytic degradation (BECKER and CRAIG, 1994; FINK *et al.*, 2003; SŐTI *et al.*, 2005; YOUNG *et al.*, 2003). The essentiality of the 'protein quality control' activity of molecular chaperones is emphasised in their involvement in the prevention of protein-folding diseases. The corruption of chaperone protein

function has been described in the onset of numerous of these diseases, ranging from cancer to neurodegenerative disorders (BARRAL *et al*., 2004; BRODSKY and CHIOSIS, 2006; DOBSON, 2003).

Chaperone activity is comprised of successive cycles of binding and release of non-native protein substrates which are recognised by the exposure of hydrophobic residues. In particular, chaperone proteins are known to exhibit both holdase and (re)foldase activity, binding and stabilising proteins in a manner that is conducive to folding (FELDMAN and FRYDMAN, 2000). The regulation of this activity is achieved by a sub-set of chaperone proteins termed 'co-chaperones'. In essence, co-chaperones function by (i) targeting partner chaperone proteins to specific pathways, (ii) mediating the specificity of chaperone protein folding activity by serving as substrate selectors, and/or (iii) regulating the nucleotide-bound state of chaperone proteins which governs conformation and hence activity (BLATCH, 2006; CAPLAN, 2003). Moreover, certain co-chaperones have been shown to possess dual chaperone/co-chaperone capabilities, exhibiting the holdase or refoldase activity required to facilitate protein folding (KELLEY, 1998; LU and CYR, 1998a, 2006).

Based on the ability of molecular chaperones to function both independently and in combination, it is proposed that the folding of nascent proteins and the refolding of misfolded proteins in the cell is coordinated by the successive involvement of chaperone protein networks (GEORGOPOULOS and WELCH, 1993; HENDRICK and HARTL, 1993, 1995). Consistent with this, certain molecular chaperones are designated to the preliminary folding of nascent proteins, while others appear to be employed for the processing of later protein folding intermediates and the assembly of higher order protein structures (BUCHBERGER *et al*., 1995; FRYDMAN *et al*., 1994; HARTL, 1996). It has also been argued that protein folding intermediates may be cycled in a less coordinated manner by available chaperone proteins in the cytosol (FELDMAN and FRYDMAN, 2000; YOUNG *et al*., 2004). Such proteins may include heat shock proteins, protein disulfide isomerases and peptidyl prolyl isomerases as reviewed by FINK (1999).

1.3 HEAT SHOCK PROTEINS FUNCTION AS MOLECULAR CHAPERONES

Heat shock proteins (Hsps) comprise a major portion of the molecular chaperone protein class and represent a highly abundant and conserved group of proteins that are responsible for the maintenance of cellular viability under varied conditions of cellular stress (GEORGEOPOULOS and WELCH, 1993; HENDRICK and HARTL, 1993, 1995; BECKER and CRAIG, 1994). These proteins were first identified by RITOSSA (1962) in *Drosophila melanogaster* cells exposed to elevated temperatures. Hsp expression is upregulated in response to numerous cellular or environmental stress stimuli including temperature elevation (heat shock) or decline (cold shock), the deprivation of oxygen, water or nutrients, or the accumulation of cytotoxic compounds such as free radicals, antibiotics or

heavy metals. The upregulated heat shock proteins function as molecular chaperones by assisting in the refolding of misfolded proteins that accumulate in response to the respective stress conditions, allowing for the restoration of homeostasis (BECKER and CRAIG, 1994; HENDRICK and HARTL, 1995).

In contrast to the stress-inducible Hsp class of proteins, homologous heat shock cognate (Hsc) proteins are constitutively expressed under typical cellular conditions and are proposed to facilitate de novo protein folding and general cellular 'house-keeping' processes (INGOLIA and CRAIG, 1982). The Hsp and Hsc classes are often referred to collectively as heat shock proteins, due to the high degree of shared structural and functional features between these classes and the reported dual constitutive and stress-inducible upregulation of certain Hsc proteins (BECKER and CRAIG, 1994). Differences in the roles of the inducible and constitutive chaperone proteins may be dictated by subtle differences in these protein classes. In particular, the role of Hsp proteins is more pronounced in the presence of stress stimuli, attributed to differential client binding and co-chaperone regulation (CALLAHAN et al., 2002; TUTAR et al., 2005).

Classification of the members of the heat shock protein class is according to average molecular weight, with each heat shock protein family designated a term – Hsp*X* – where *X* represents the molecular weight in kDa. ATP-dependent high molecular weight heat shock proteins including those of the Hsp100 (100 kDa), Hsp90 (90 kDa), Hsp70 (70 kDa) and Hsp60 (60 kDa) families require co-chaperone proteins to modulate their ATP-bound state. The majority of general folding processes in the cell appear to be mediated by the Hsp70 and Hsp60 classes and their associated co-chaperones (DEUERLING and BUKAU, 2004; FINK, 1999). Hsp40 proteins (40 kDa) are known to serve as co-chaperones to Hsp70 proteins and are suspected to function as chaperones in their own right (LU and CYR, 1998b; ROSSER and CYR, 2006). In contrast to the large ATP-dependent chaperones, members of the small heat shock protein family (sHsp) are in the order of 9-43 kDa in size and function as chaperones in an ATP-independent manner (JAKOB et al., 1993).

Variations exist in the functions of the different Hsp protein families, and evidence suggests that particular protein substrates may be directed to particular heat shock protein networks in the cell for folding (DEUERLING and BUKAU, 1994). In general, Hsp100 and sHsps are implicated in thermotolerance, the prevention of protein aggregation and the stabilisation of misfolded proteins; Hsp90 is known to regulate cell signalling, stabilise misfolded proteins and process more mature protein folding intermediates; Hsp70 functions in conjunction with Hsp40 to mediate a wide range of chaperone tasks including nascent protein folding, protein translocation and cytoprotection

during cellular stress; and Hsp60 proteins are concerned with the folding and refolding of particular protein substrates and higher order proteins (SMITH et al., 1998; YOUNG et al., 2003, 2004).

1.3.1 The Small Heat Shock Proteins – α-Crystallins

The diverse roles of the ATP-independent small heat shock proteins (sHsps) range from the mediation of signal transduction, to cell differentiation, morphological development and the inhibition of apoptosis of the cell (DE JONG et al., 1993; GUSEV et al. 2002; JAKOB et al., 1993). Most importantly, the sHsps play a major role in thermotolerance, typically functioning in large flexible oligomeric complexes which passively bind and stabilise compromised proteins with high affinity (HORWITZ, 1992; JAKOB et al., 1993; LELJ-GAROLLA and MAUK, 2005). Active disaggregation and renaturation of the compromised proteins is achieved by subsequent transferral to ATP-dependent chaperones, such as Hsp70 as further described in SECTION 1.3.5 (GUSEV et al., 2002 ; MOGK et al., 2003). The mechanism by which sHsps exhibit chaperone activity and co-operate in synergy with other chaperone networks to promote thermotolerance is not entirely understood (GUSEV et al., 2002).

Proteins of the sHsp class are characterised by the presence of an 80-100 residue α-crystallin domain in the C-terminal region, initially identified in the vertebrate eye lens proteins, αA- and αB-crystallin (DE JONG et al., 1993; HORWITZ, 1992). The domain is thought to be comprised of flexible interacting beta sheets, which participate directly in the oligomerisation of the sHsps (GUSEV et al., 2002; LELJ-GAROLLA and MAUK, 2005). Importantly, sHsps of variant sizes are known to form mixed oligomers via the α-crystallin domain and may function in unison (GUSEV et al., 2002). Evidence suggests that phosphorylation may disrupt sHsp oligomerisation, providing a clue to the regulation of the chaperone activity of this heat shock class or to their proposed involvement in cell signalling (DE JONG et al., 1993; GUSEV et al., 2002). The N-terminal region of the sHsp class preceding the α-crystallin domain is highly varied and may be key to the functional specialisation and substrate specificities of the diverse sHsp proteins (BASHA et al., 2004; DE JONG et al., 1993).

1.3.2 The Hsp100 Proteins – Stress Tolerance Factors

Molecular chaperones of the Hsp100 or caseinolytic protease (Clp) class are classified in the AAA^{+} superfamily of proteins (ATPases associated with various cellular activities) and may be distinguished from other chaperones by their unfoldase and translocase activity. These activities are employed in the disassembly and remodelling of higher order protein complexes, the disruption of large protein aggregates and the targeting of improperly folded proteins for degradation (MOGK et al. 1999; PAK and WICKNER, 1997). SANCHEZ and LINDQUIST (1990) demonstrated that S. cerevisiae

cells deficient in Hsp100 were significantly prone to induced heat stress, highlighting the importance of this protein class in the promotion of thermotolerance. As described for the sHsp class of proteins, Hsp100 chaperones rely on co-operation with more conventional chaperones such as Hsp70 to promote protein refolding. In particular, the co-operation of sHsps, Hsp100 and Hsp70 has been described in the facilitation of protein disaggregation (GLOVER AND LINDQUIST, 1998; GOLOUBINOFF et al., 1999; MOGK et al., 2003). The unfoldase activity of Hsp100 appears to be driven by ATP hydrolysis by the six-member ring-like subunits comprising the proteins of this class. ATP-dependent conformational changes in the subdomains are thought to prise protein aggregates or protein complex subunits apart (GLOVER and TKACH, 2001) or 'thread' them through the central cavity formed by the Hsp100 subdomains (LUM et al., 2004).

1.3.3 The Hsp90 Proteins – Cell Signalling Chaperones

In addition to demonstrating a general role in protein folding and translocation, the highly conserved and abundant Hsp90 proteins may be distinguished from other chaperones by their involvement in the regulation of cell differentiation and development, protein trafficking, apoptosis and intra- and inter-cellular communication (ALIGUE et al., 1994; YOUNG et al., 2001). In particular, Hsp90 proteins are known to be responsible for the activation and regulation of cell signalling transduction proteins, such as kinases and steroid receptors (PICARD et al., 1990; PRATT and TOFT, 1997, 2003; XU and LINDQUIST, 1993). Moreover, the Hsp90 class have been implicated in protein quality control tasks in the cell through the targeting of damaged proteins for degradation by the proteasome (CONNELL et al., 2001; MCDONOUGH and PATTERSON, 2003).

Hsp90 proteins are characterised by the presence of three highly conserved domains, including a 25 kDa nucleotide-binding N-terminal domain, a 35 kDa central domain thought to contribute to the ATPase and substrate binding activity of the protein, and a 12 kDa C-terminal domain crucial to dimerization and interaction with numerous Hsp90 co-chaperone proteins (MEYER et al., 2003; NEMOTO et al., 1995; PRODROMOU et al., 1997). Hsp90 promotes protein folding in the dimeric form, the conformation of which is governed by nucleotide-dependent changes and complex inter- and intra-domain communication (RICHTER et al., 2008; SHIAU et al., 2006). In the absence of bound nucleotide, the Hsp90 dimer adopts an open conformation that may bind and stabilise protein substrate in a manner that is not conducive to folding (BUCHNER et al., 1999). This is achieved by the presentation of hydrophobic residues from each of the three conserved domains into the large interdomain cleft formed by the dimer (SHIAU et al., 2006). Upon the binding of ATP, transient dimerization of the N-terminal and central domains facilitates the clamping of the Hsp90 monomers into a closed conformation, which may promote subsequent protein folding (ALI et al.,

2006; PRODROMOU et al., 2000). Release of the substrate is governed by hydrolysis of the bound ATP (PRODROMOU et al., 1997; YOUNG and HARTL, 2000) facilitated by the interaction of the nucleotide-binding and central-domains (ALI et al., 2006; SHIAU et al., 2006).

The regulation of Hsp90 activity is proposed to be dependent on various co-chaperone proteins which, by the most part, are thought to bind the C-terminus of the chaperone via tetratricopeptide repeat (TPR) motifs (YOUNG et al., 1998). These co-chaperones include the Hsp70-Hsp90 organising protein, Hop (also referred to as the stress induced phosphoprotein-1; Sti1), protein phosphatase-5 (PP5), Aha1 (Activator of Hsp90 ATPase activity) and the immunophilins FKBP52, FKBP51/54 and cyclophilin 40 (BARENT et al., 1998; CHEN et al., 1996; HOFFMANN and HANDSCHUMACHER, 1995; LOTZ et al., 2003; SILIGARDI et al., 2002). The immunophilins are known to connect Hsp90 to protein trafficking machinery in the cell (PRATT and TOFT, 1997). Hop is known to mediate substrate transfer from Hsp70 to Hsp90, by forming a physical link between these two proteins via its tetratricopeptide repeat (TPR) domain (CHEN and SMITH, 1998; ODUNUGA et al., 2004; SCHEUFLER et al., 2000). The co-operation between Hsp90 and Hsp70 is proposed to facilitate the processing of later protein folding intermediates and specific client proteins in the cell (FRYDMAN and HÖHFELD, 1997). Moreover, the TPR-bearing carboxyl terminus of the Hsc70-interacting protein (CHIP) represents an E3 ubiquitin ligase that has been shown to connect Hsp90 to the ubiquitination pathway for the designation of proteins for degradation by the proteasome (BALLINGER et al., 1999; CONNELL et al., 2001; MCDONOUGH and PATTERSON, 2003). Hsp90 has also been shown to be responsible for the maintenance of the 26S proteasome, highlighting a crucial role for the chaperone in the degradation of damaged proteins in the cell (IMAI et al., 2003). Co-chaperones Cdc37/p50 and p23 have also been shown to bind Hsp90 and regulate its activity despite the lack of a recognisable TPR domain (ROE et al., 2004; MCLAUGHLIN et al., 2006). In particular, p23 is important in the regulation of the ATPase cycle of Hsp90; the co-chaperone is proposed to recognise ATP-bound Hsp90 and promote the dissociation of substrate (YOUNG and HARTL, 2000) or stabilise Hsp90 in a multi-chaperone complex as further discussed in SECTION 1.3.7.

1.3.4 The Hsp60 Chaperonins

Members of the Hsp60 protein family, represented by prokaryotic GroEL (VIITANEN et al., 1990) and eukaryotic T-complex polypeptide-1 (TCP-1; MCCALLUM et al., 2000) are also referred to as chaperonins (ELLIS, 1990). In addition to facilitating general protein folding processes and the prevention of the aggregation of partially folded protein intermediates, chaperonins are known to assist the unfolding and refolding of improperly folded proteins and the assembly of higher order or multidomain protein structures (HOURY et al., 1999). Chaperonins are typically oligomeric and ring-

shaped, bearing a central cavity responsible for the binding non-native protein substrates (XU et al., 1997; XU and SIGLER, 1998). This cavity provides a sequestered environment in which protein folding proceeds unimpeded by the interference of external cellular factors (APETRI and HORWICH, 1998).

The chaperone activity of GroEL is mediated by ATP binding and co-chaperone intervention. The binding of substrate to the apical domain of GroEL is alternated by the binding of a 10 kDa co-chaperone, chaperonin 10 (cpn10) in eukaryotic organisms or the equivalent prokaryotic GroES to the same domain (TODD et al., 1994; VIITANEN et al., 1990). The latter is coupled by the binding of ATP to the equatorial domain of GroEL. An intermediate domain housed between the apical and equatorial domains of GroEL, induces conformational changes to the central cavity on the binding of ATP, influencing the hydrophobic nature of the substrate binding site (RANSON et al., 1998). In this manner, the binding of ATP and GroES lessens the hydrophobicity and enlarges the central GroEL cavity, promoting release of the substrate following the promotion of folding into the native state. Studies have demonstrated that the GroEL-GroES chaperone system is essential to the viability of E. soli (FAYET et al., 1989).

1.3.5 The Hsp70 Proteins –Multifunctional 'House-keeping' Chaperones

It is known that at least 15-20 % of nascent proteins are processed by the well conserved ATP-dependent members of the Hsp70 chaperone machinery, termed DnaK in prokaryotic organisms (DEUERLING et al., 1999; THULASIRAMAN et al., 1999). DnaK is termed as such due to initial implications of the protein in the replication of bacteriophage λ DNA (GEORGOPOULOS and WELCH, 1993). Under typical eukaryotic cellular conditions, constitutively expressed Hsc70 is responsible for the folding of nascent polypeptide chains (BUKAU et al., 2000; HARTL and HAYER-HARTL, 2002), quaternary assembly and disassembly (CHAPPELL et al., 1986; CHROMY et al., 2003), protein translocation (JENSEN and JOHNSON, 1999; RYAN and PFANNER, 2002), cell signalling (PRATT and TOFT, 2003) and the activation of transcriptional and replication factors (HOFFMAN et al., 1992). In the presence of stress stimuli, inducible Hsp70 functions in a similar manner to Hsc70 with enhanced affinity for client protein, and enables the refolding of accumulated denatured and misfolded proteins (CALLAHAN et al., 2002; HARTL, 1996; MAYER and BUKAU, 1998). In particular, Hsp70 proteins are crucial to the maintenance of cellular viability during thermal stress, promoting the disruption of protein aggregates that form from intermolecular interactions between exposed hydrophobic residues. Moreover, Hsp70 proteins appear to participate in the targeting of compromised proteins for degradation (HÖHFELD et al., 2001) through the lysosomal pathway (AGARRABERES and DICE, 2001) or the ubiquitination pathway via association with CHIP (BALLINGER et al., 1999; BERCOVICH et al., 1997; HÖHFELD et al., 2006).

In contrast to the Hsp60 chaperonins which are capable of encompassing entire proteins, Hsp70 chaperones recognise and preferentially bind smaller hydrophobic peptide segments, 7-9 amino acids in length (FLYNN *et al.,* 1991; GRAGEROV *et al*., 1994). These differences highlight the synergistic co-operation of chaperone networks in the facilitation of protein folding; Hsp70 may promote the folding of a protein in the earlier stages of maturation or refolding, while the successive involvement of chaperonins or Hsp90 may promote the folding of the protein into its final native conformation (BUCHBERGER *et al*., 1996; BUKAU *et al*., 2000; GAITANARIS *et al*., 1994; HENDRICK and HARTL, 1995). Moreover, different Hsp70 proteins exhibit bias in interaction with particular protein substrates, and this is thought to be mediated by Hsp40 co-chaperone partners (GRAGEROV and GOTTESMAN, 1994; MISSELWITZ *et al.,* 1998). Substrate bias may be indicative of the functional diversification of Hsp70 proteins through evolution (KABANI and MARTINEAU, 2008; MAYER and BUKAU, 2005) and is of particular significance in eukaryotic organisms, where certain Hsp70 proteins appear to be confined to distinct subcellular compartments for specific protein folding and translocation tasks (CRAIG *et al*., 1994; GRAGEROV and GOTTESMAN, 1994).

1.3.5.1 Hsp70 Domain Organisation

Hsp70 proteins are comprised of two conserved domains, including a 45 kDa N-terminal ATPase domain, and a 15-30 kDa substrate binding domain which is linked to a 10 kDa C-terminal region. The domain organisation of Hsp70 proteins is schematically represented in *FIGURE 1.1A* overleaf. Importantly, Hsp70 function requires co-operation between the ATPase and substrate binding domains as further discussed. The monomeric form of Hsp70 is proposed to favour ATP and substrate binding, while the oligomeric form of Hsp70 is proposed to act as a reserve in the cell for the monomeric form (GAO *et al*., 1996).

1.3.5.1.1 The ATPase Domain

The ATPase domain is constituted by four subdomains comprising two lobes and an upper and lower cleft (*FIGURE 1.1B*; BORK *et al*., 1992; FLAHERTY *et al.,* 1990, 1991). The nucleotide binding site of the ATPase domain is housed in the upper cleft constituted by subdomains IB and IIB (FLAHERTY *et al.,* 1990). The hydrolysis of ATP to ADP in this cleft is known to induce conformational changes which regulate the substrate binding capabilities of the substrate binding domain (BUCHBERGER *et al*., 1995; FUNG *et al*., 1996). The linker region adjoining the ATPase and substrate binding domains (*FIGURE 1.1A*) is thought to be crucial to such interdomain communication (JIANG *et al*., 2005). Consistent with this, the linker region was shown to bring the ATPase domain in close proximity with the structural elements of the peptide binding pocket in the partial full length structure of bovine Hsc70 (JIANG *et al.,* 2007) and substitution of residues in this region have been shown to

affect Hsp70 activity (HAN and CHRISTEN, 2001). The lower cleft of the ATPase domain constituted by subdomains IA and IIA, has been proposed to mediate Hsp40 co-chaperone binding (GÄSSLER *et al.*, 1998; SUH *et al.*, 1998). This was disputed by subsequent findings that the interdomain interface between the ATPase and substrate binding domains of bovine Hsc70 serves as a binding site for the Hsp40 protein, auxilin (JIANG ***et al.***, 2007) as further discussed in ***SECTION 2.3.2, CHAPTER 2***. Moreover, subdomain IIB has been recognised as a potential binding site for prokaryotic nucleotide exchange factors, as detailed in *SECTION* ***1.3.5.2.2*** (SCHÖNFELD *et al.*, 1995; SONDERMANN ***et al.***, 2001).

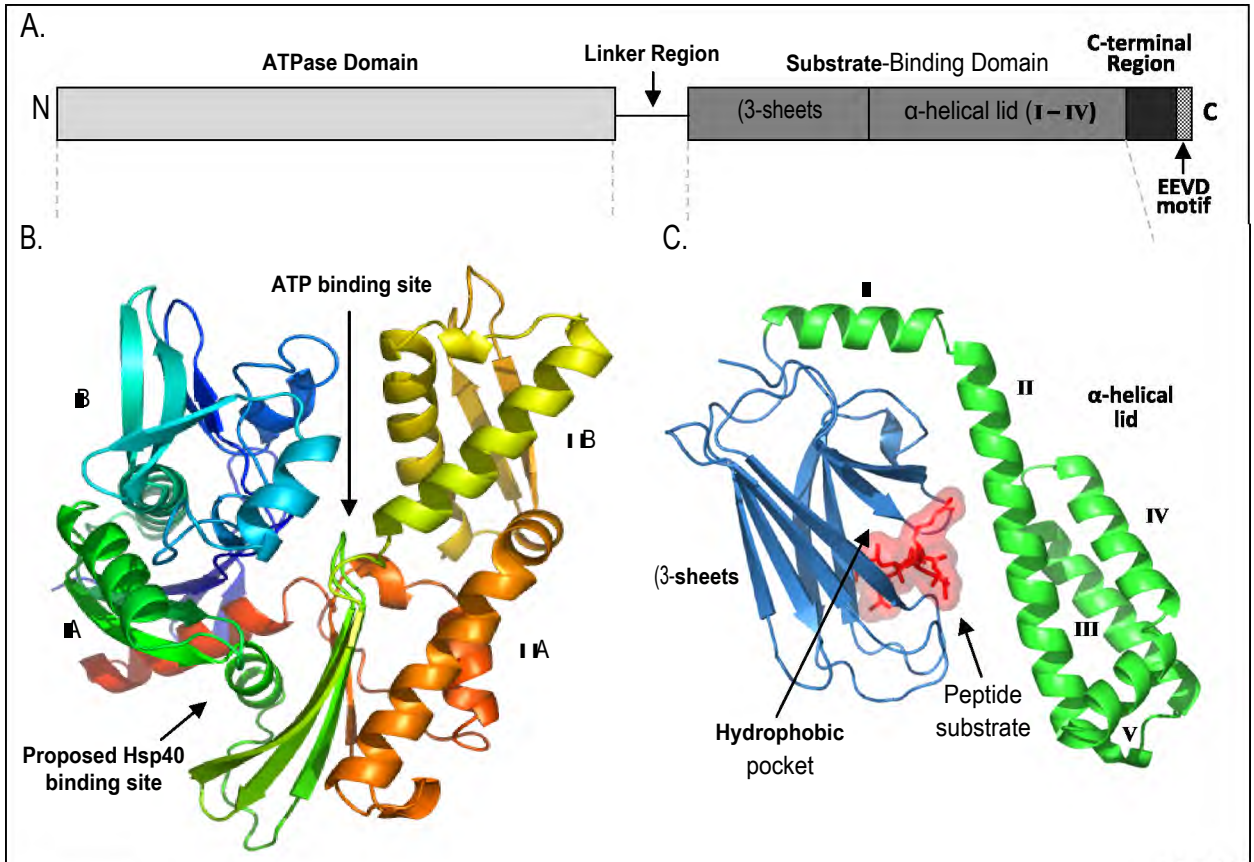

FIGURE 1.1 Domain organisation and structure of Hsp70 proteins. (A) Schematic representation of Hsp70 domain organisation. The ATPase domain of approximately 45 kDa is followed by a substrate binding domain of approximately 15-30 kDa linked to a C-terminal region in the order of 10 kDa. The ATPase and substrate binding domains are adjoined by a linker region. The EEVD motif identified on the C-terminal end of certain eukaryotic Hsp70 proteins is indicated (DEMAND *et al.*, 1998). Domains and motifs are not drawn to scale and are listed from the N- to the C-terminus of the protein as indicated. (B) Structure of the *Bos taurus* (bovine) Hsc70 ATPase domain (PDB: 3HSC; FLAHERTY *et al.*, 1990). The domain is divided into two lobes which in turn are divided into two subdomains (right lobe: IA and IB, left lobe: IIA and IIB; BORK *et al.*, 1992). A proposed Hsp40 binding site (GÄSSLER *et al.*, 1998; SUH *et al.*, 1998) and nucleotide binding site (FLAHERTY *et al.*, 1990) are indicated in the lower and upper clefts of the domain respectively. (C) Structure of the substrate binding domain of the prokaryotic Hsp70, *E. coli* DnaK (PDB: 1DKX; ZHU *et al.*, 1996). β-sheets comprising the hydrophobic peptide binding pocket are indicated in blue with the bound peptide substrate 'NRLLLTG' shown in red. The α-helical lid structure, comprised of helices IV and shown in green, locks the peptide substrate into place in the hydrophobic pocket. Co-ordinate files of the structures in (B) and (C) were obtained from the Protein Data Bank (PDB; BERMAN *et al.*, 2003) and visualised using PyMol (version 0.95; DELANO, 2005). The structure of the C-terminal region following the α-helical lid has not been resolved.

1.3.5.1.2 The Substrate Binding Domain

The substrate binding domain is similarly comprised of subdomains, including a hydrophobic peptide binding pocket constituted by a sandwich of β-sheets and a flexible α-helical lid structure (*FIGURE 1.1C*, ZHU *et al.,* 1996). Residues comprising the binding cavity of the β-subdomain have been shown to bind and stabilise the backbones and side-chains of exposed hydrophobic residues of the substrate in an extended conformation, in a manner that is conducive to folding (*FIGURE 1.1C*, BRODSKY, 1996; RUDIGER *et al*., 2001; ZHU *et al*., 1996). The α-helical lid appears to latch the peptide into the binding pocket and is also suggested to mediate substrate specificity (*FIGURE 1.1C*; MAYER *et al*., 2000; ZHU *et al*., 1996). Ionic interactions between the α- and β-subdomains are proposed to mediate entry to the peptide binding pocket (FERNANDEZ-SÁIZ *et al.* 2006) with dynamic opening and closing of the pocket promoted in the ATP and ADP bound states of Hsp70 respectively (FERNANDEZ-SÁIZ *et al.* 2006; MAYER *et al*., 2000). Perplexingly though, interdomain communication between the substrate binding and ATPase domains was shown to be preserved in the absence of an α-helical subdomain in *E. coli* DnaK (PELLECCHIA *et al*., 2000).

1.3.5.1.3 The C-terminal Region

The 10 kDa C-terminal region essentially constitutes a part of the substrate-binding domain of Hsp70 proteins, but is often referred to as a distinct region as it is known to facilitate interactions with other chaperone proteins (DEMAND *et al.,* 1998). In particular, the C-terminal EEVD motif of eukaryotic cytosolic Hsp70 proteins (*FIGURE 1.1A*) is proposed to mediate interactions with Hsp90 (via the adaptor protein Hop) and the co-chaperones CHIP and Hsp40 (*FIGURE 1.1A;* BRINKER *et al*., 2002; DEMAND *et al.,* 1998; FREEMAN *et al*., 1995; LI *et al*., 2006). The structure of this C-terminal region remains to be resolved.

1.3.5.2 Co-chaperone Regulation of the ATPase Cycle and Chaperone Activity of Hsp70

The affinity of Hsp70 for protein substrate is governed by ATP binding, hydrolysis and exchange as depicted in *FIGURE 1.2* overleaf (MCCARTY *et al.,* 1995). The hydrolysis of ATP to ADP and inorganic phosphate (P_i) represents the rate limiting step of the ATPase cycle (BURKHOLDER *et al*., 1994; RUSSELL *et al.,* 1999) in the absence of mediation by Hsp40 co-chaperone proteins (*SECTION 1.3.5.2.1*; BANECKI *et al*., 1996; HENDRICK *et al*., 1993; SZABO *et al*., 1994). The subsequent exchange of ADP for ATP is in certain circumstances facilitated by nucleotide exchange factors (NEF; *SECTION 1.3.5.2.2*).

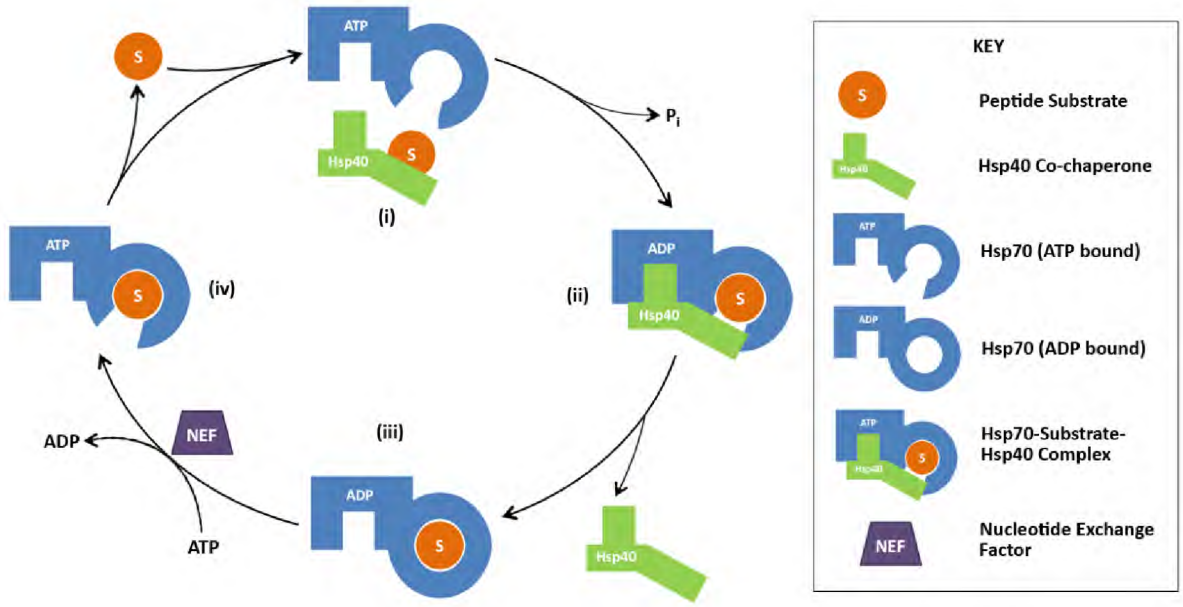

FIGURE 1.2 The Hsp40/Nucleotide Exchange Factor-mediated ATPase cycle of Hsp70 protein folding activity. Hsp70 folding activity is characterised by repeated cycles of substrate binding and release, as follows: (i) Protein substrate (S) is recruited to Hsp70 by the co-chaperone Hsp40, or Hsp70 interacts with substrate independently. Hsp40 promotes the ATPase activity of Hsp70, enabling the latter to hydrolyse ATP; (ii) In an ADP-bound state, Hsp70 adopts a conformation with increased affinity for protein substrate thereby facilitating (iii) folding of the substrate; (iv) The exchange of Hsp70-bound ADP for ATP is facilitated by a nucleotide exchange factor (NEF)*, thereby decreasing the Hsp70 affinity for substrate and allowing the release of the folded protein, or protein folding intermediate. Several cycles of Hsp40/NEF-mediated folding by Hsp70 are required for folding to continue until completion. In the most likely scenario, the protein folding intermediate is transferred to a complementary chaperone system such as the Hsp60/Cpn10 (GroEL/GroES) system for the completion of protein folding (GEORGOPOULOS and WELCH, 1993; HARTL, 1996; HENDRICK and HARTL, 1993, 1995). It is suggested that Hsp40 and NEFs function at substoichiometric levels to Hsp70 (LAUFEN *et al*., 1999; PIERPAOLI *et al*., 1998). *Characterised Nucleotide Exchange Factors include GrpE (prokaryotes), Snl1, Fes1, Sse1, Sil1 and Sls1 (*Saccharomyces cerevisiae*), HspBP1, BAG-1, Hsp110 and Hsp105α (mammals) (BRODSKY and BRACHER, 2006). The figure was adapted from MAYER and BUKAU (1998) and SZABO *et al.* (1994).

1.3.5.2.1 Regulation by Hsp40 Co-chaperones

The Hsp70-Hsp40 interaction represents the most ubiquitous chaperone protein partnership (LINDQUIST, 1986; KELLEY and SCHLESINGER, 1982). Evidence suggests that particular Hsp40-Hsp70 partnerships are dedicated to the folding of specific client protein subsets in distinct subcellular compartments (BRODSKY and SCHEKMAN 1993; KELLEY, 1998, 1999; NGOSUWAN *et al*., 2003). The number of Hsp40 proteins typically outweighs the number of Hsp70 proteins in any given organism, suggesting that Hsp70 is the more promiscuous protein in the partnership and may be regulated by numerous Hsp40 co-chaperones (BOTHA *et al*., 2007; HENNESSY *et al.,* 2005b; QIU *et al*., 2006).

The co-chaperone activity of Hsp40 serves two probable purposes, including the targeting of substrate to Hsp70 and the stabilisation of substrate-bound Hsp70 in the presence of ATP (FAN *et*

al., 2003; LAUFEN et al., 1999; MINAMI et al., 1996; SUH et al., 1999). This may be achieved through interaction with both the substrate-binding and ATPase domains of Hsp70 (AUGER and ROUDIER, 1997; SUH et al., 1998). Hsp40 functions by promoting ATP hydrolysis by Hsp70 (SUH et al., 1998) enabling the latter to adopt an ADP-bound conformation with increased affinity for substrate (FLYNN et al., 1989; GREENE et al., 1998; SUH et al., 1998). Substrate transfer from Hsp40 to Hsp70 is proposed to involve the formation of an $(ATP.Hsp70)_m$-substrate-$(Hsp40)_n$ ternary complex involving binding to independent segments of the substrate (HAN and CHRISTEN, 2003). Consistent with this, the displacement of a target substrate from the peptide binding domain of Hsp40 by D-amino peptides was shown to impede refolding of the substrate by the Hsp70/Hsp40/NEF system (BISCHOFBERGER et al., 2003). The shared features that exist between the substrate binding domains of Hsp40 and Hsp70 proteins suggests that Hsp40 serves as a substrate 'scanning factor' for Hsp70 (MISSELWITZ et al. 1998; RÜDIGER et al., 2001). Moreover, Hsp40 appears to have a lower substrate binding affinity which may promote the transfer of substrate to Hsp70 (RÜDIGER et al., 2001).

An alternate mechanism for the independent association of Hsp70 with peptide substrate and the subsequent docking of Hsp40 has also been hypothesised (PIERPAOLI et al., 1997, 1998; SUH et al., 1999). This emanates from the enhanced ability of Hsp40 to stimulate Hsp70 ATPase activity in the presence of bound substrate in the Hsp70 substrate binding site (BUKAU and HORWICH, 1998; MAYER et al., 1999). Moreover, peptide sequences have been shown to stimulate the ATPase activity of Hsp70, albeit at insignificant levels in comparison to Hsp40 (JORDAN and MCMACKEN, 1995).

The significance of the Hsp70-Hsp40 partnership is further emphasized in its role in the regulation of the heat shock response. Heat shock protein expression is known to be induced by the σ^{32} subunit of RNA Polymerase in prokaryotes (STRAUS et al., 1987) and the heat shock transcription factor (HSF) in eukaryotes (BIENZ and PELHAM, 1987). In both cases, heat shock protein expression appears to be regulated by the negative modulation of these transcription factors by Hsp70 and Hsp40 (ABRAVAYA et al., 1992; STRAUS et al., 1990; TOMOYASU et al., 2002). As previously discussed, the strong propensity of proteins to aggregate and adopt unfavourable conformations in the presence of stress stimuli is countered by the binding of Hsp70. This diminishes the amount of unbound Hsp70 in the cell, warranting the induction of additional heat shock protein expression. This is initiated by the binding of σ^{32} to hsp gene promoters in prokaryotes or the binding of HSF to heat shock elements (HSE) of hsp promoter sites in eukaryotes (GROSSMAN et al., 1987; PELHAM, 1982). Autorepression of further Hsp expression is achieved by the Hsp40-assisted sequestration of σ^{32}/HSF by Hsp70, and the subsequent targeting of the transcription factor for proteolytic degradation (BALER et al., 1992; RODRIGUEZ et al., 2008).

1.3.5.2.2 The Facilitation of Nucleotide Exchange

Nucleotide exchange factors (NEFs) facilitate the release of Hsp70-bound ADP, allowing for subsequent binding of the chaperone to ATP with the net effect of nucleotide exchange. This decreases Hsp70 affinity for substrate, allowing the release of protein folding intermediates in the Hsp70-protein folding cycle (*FIGURE 1.2*; LIBEREK *et al*., 1991; PIERPAOLI *et al*., 1997). In essence, NEFs function as nucleotide release factors rather than participating directly in the exchange of bound ADP for ATP (BRODSKY and BRACHER, 2006).

The structure of the prokaryotic nucleotide exchange factor, GrpE, in complex with DnaK has been resolved (HARRISON *et al*., 1997). It is suggested that this co-chaperone binds in dimeric form to the IB subdomain of the Hsp70 ATPase domain (SCHÖNFELD *et al.,* 1995; SONDERMANN *et al*., 2001) inducing a conformational change in the upper cleft that mediates nucleotide binding (*FIGURE 1.1B*; BRODSKY and BRACHER, 2006). Nucleotide exchange factors in the eukaryotic cytosol differ both structurally and functionally from prokaryotic GrpE (BRODSKY and BRACHER, 2006). While eukaryotic GrpE homologs have been identified, they appear to be confined to the mitochondria and chloroplast (CHOGLAY *et al*., 2001; NAYLOR *et al*., 1998). In the mammalian cytosol, nucleotide exchange is thought to be facilitated by the Hsp70-binding protein (HspBP1) and BCL2-associated athanogene (BAG-1) co-chaperones (BREHMER *et al*., 2001; HÖHFELD and JENTSCH 1997). Consistent with this, BAG-1 has been shown to interact with the ATPase domain of cytosolic Hsp70 proteins (TAKAYAMA *et al*., 2001). The interaction of these proteins is mediated by a domain termed the BAG domain; additional proteins bearing this domain have been identified and are thought to be involved in more specialised mediation of nucleotide exchange (BRODSKY and BRACHER, 2006). These include the BAG-1 homologue, Snl1, in the cytoplasm of *S. cerevisiae*. An additional cytoplasmic nucleotide exchange factor in yeast, Fes1, was shown to facilitate nucleotide exchange and inhibit the ATPase activity of the Hsp70 protein, Ssa1p (KABANI *et al*., 2002, 2003). A further two nucleotide exchange factors, Sls1 and Sil1, were identified in the lumen of the yeast endoplasmic reticulum, and are thought to facilitate nucleotide exchange of the endoplasmic reticulum Hsp70 protein, BiP (Binding Protein; BRODSKY and BRACHER, 2006; KABANI *et al*., 2000). Similarly, an Sls1-related nucleotide exchange factor, BAP (BiP associated protein), was identified in the mammalian endoplasmic reticulum and was shown to interact with mammalian BiP (CHUNG *et al*., 2002).

1.3.5.2.3 Additional Co-chaperone Regulation in Eukaryotes

The TPR-containing Hsc70 interacting protein (Hip) represents an additional co-chaperone that is responsible for the regulation of eukaryotic Hsc70 (FRYDMAN and HÖHFELD, 1997; HÖHFELD *et al.*, 1995). Hip is thought to function in oligomeric form by binding the ATPase domain of Hsc70

following the activation of ATP hydrolysis by Hsp40. This is thought to maintain Hsc70 in an ADP conformation with high affinity for client protein, and may represent the subsequent co-operation of Hsc70 with other chaperone systems (DEMAND *et al.,* 1998; HÖHFELD *et al*., 1995). The interaction of Hip with Hsc70 appears to be independent of nucleotide exchange, demonstrating that Hsp70 activity is not the entirely dependent on the cycling of the ATP- and ADP-bound states (NOLLEN *et al*., 2001). Hip has also been shown to bind to unfolded proteins, highlighting its potential to serve as a chaperone protein in its own right (BRUCE and CHURCHICH, 1997).

1.3.6 The Hsp40 Proteins – Co-chaperones of Hsp70

1.3.6.1 Hsp40 Domain Organisation and Classification

Molecular chaperones of the Hsp40 family, termed DnaJ in prokaryotes, exhibit greater structural diversity than their Hsp70 counterparts (QIU *et al*., 2006; WITTUNG-STAFSHEDE *et al.,* 2003) and are characterised by the presence of four domains, schematically represented in *FIGURE 1.3A*. These domains include a highly conserved N-terminal J-domain, flanked by a glycine/phenylalanine-rich region (GF-region), a cysteine-rich zinc-binding domain and a lesser conserved C-terminal substrate binding domain. The categorisation of Hsp40 proteins into types I-III has previously been proposed, based on the varied conservation of the four primary domains (*FIGURE 1.3A;* CHEETHAM and CAPLAN, 1998). Notably, the minimum requirement for characterisation as an Hsp40 protein is the presence of the signature J-domain (WALSH *et al.,* 2004). Type I Hsp40 proteins are representative of a prototypical Hsp40 bearing all four conserved domains, while type II Hsp40 proteins lack the zinc-binding domain, and type III Hsp40 proteins exhibit only the signature J-domain in a position that is not necessarily N-terminal (CHEETHAM and CAPLAN, 1998). Differences in domain structure contribute significantly to the specificity of Hsp40 function *in vivo* (CHEETHAM and CAPLAN, 1998; WALSH *et al*., 2004).

Type I and II Hsp40 proteins have been implicated in the facilitation of protein folding processes, making the functional distinction between these protein classes subtle (KELLEY *et al*., 1998; WALSH *et al.,* 2004) and yet distinct (FAN *et al*., 2004; LU AND CYR, 1998b). Type I Hsp40 proteins have been shown to exhibit holdase chaperone activity by binding non-native peptide substrates and preventing their aggregation (CHAE *et al*., 2004; LU and CYR, 1998b). In contrast, type II Hsp40 proteins have been shown to bind peptide substrate but are incapable of aggregation suppression activity in the absence of Hsp70 (CHAE *et al*., 2004; FAN *et al*., 2003; FREEMAN and MORIMOTO, 1996; LU AND CYR, 1998b).

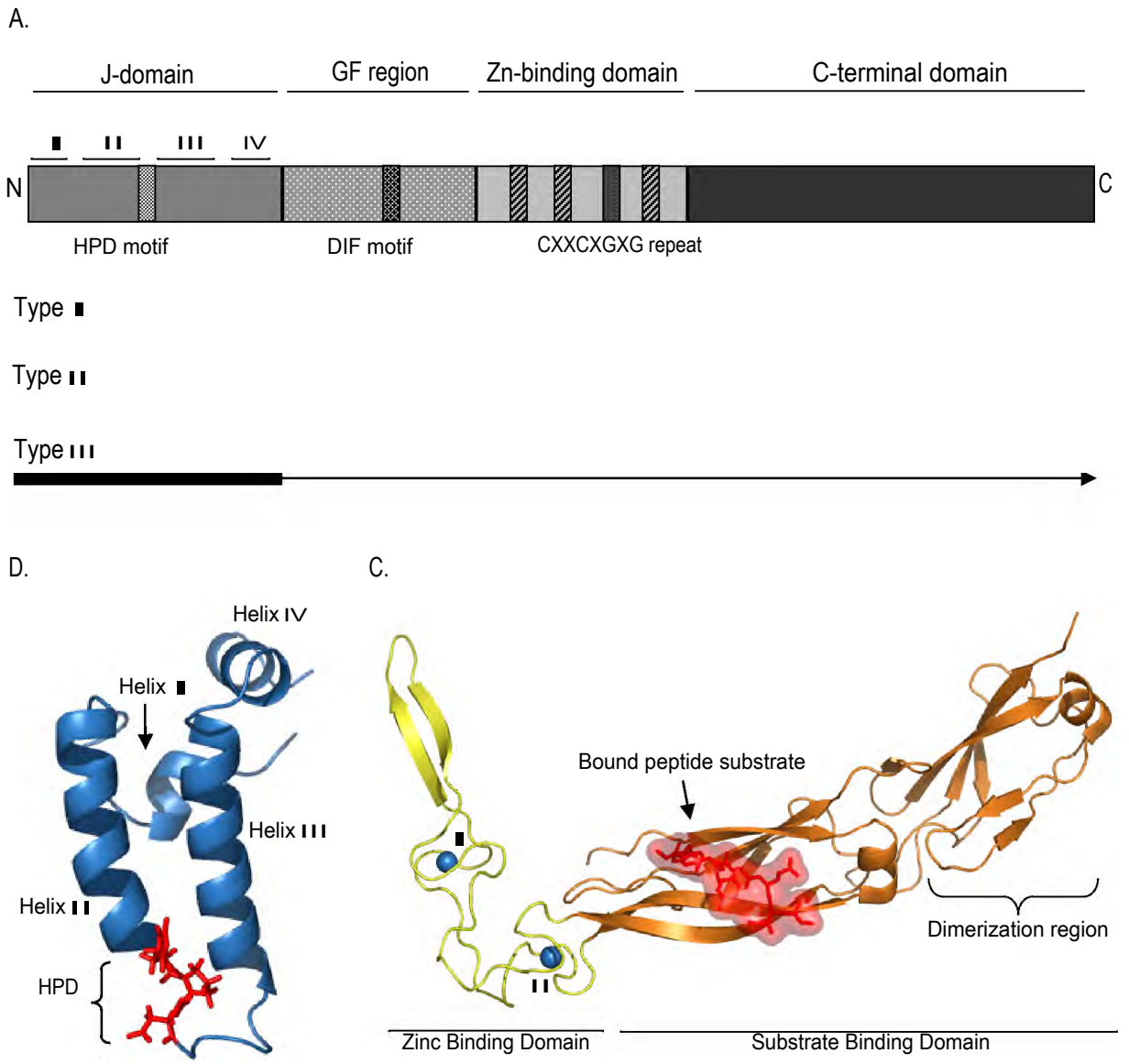

FIGURE 1.3 Classification, domain organisation and structure of Hsp40 proteins. (A) Proteins of the Hsp40 family are characterised by the presence of four domains: a highly conserved N-terminal J-domain, a glycine/phenylalanine-rich region (GF-domain), a cysteine-rich zinc-binding domain and a lesser conserved C-terminal substrate-binding domain. The minimum requirement for Hsp40 characterisation is the presence of the signature J-domain (WALSH *et al*., 2004). The categorisation of Hsp40 proteins has previously been described (CHEETHAM and CAPLAN, 1998): type I Hsp40 proteins are representative of a typical Hsp40 bearing all four conserved domains, while type II Hsp40 proteins lack the zinc-binding domain, and type III Hsp40 proteins exhibit only the signature J-domain in a position that is not necessarily N-terminal. The GF-region may also be followed by a GM (Glycine/Methionine-rich) in type II Hsp40 proteins. The highly conserved HPD motif of the J-domain, the DIF motif of the GF-region and the Cysteine repeat sequences of the zinc-binding domain (CXXCXGXG) are indicated. Domains and motifs are not drawn to scale, and are listed from the N to C-terminus as indicated. (B) Structure of the J-domain of the prokaryotic Hsp40, *E. coli* DnaJ (PDB: 1BQ0; HUANG *et al.,* 1998). Helices I- IV of the domain are indicated. The highly conserved HPD motif in the loop region between helices II and III is shown in red. (C) Structure of the zinc-binding domain (yellow) and substrate binding domain (orange) of the *S. cerevisiae* Hsp40, Ydj1 (PDB: 1NLT; LI *et al*., 2003) with the bound peptide substrate 'GWLYEIS' (red). The two zinc centres of the zinc-binding domain are indicated (I and II) with bound zinc atoms shown in blue. The dimerization region of the substrate binding domain is indicated. Co-ordinate files of the structures in (B) and (C) were obtained from the Protein Data Bank (PDB; BERMAN *et al*., 2003) and visualised using PyMol (version 0.95; DELANO, 2005).

Type III Hsp40 proteins tend to be more structurally and functionally divergent and are thought to recruit Hsp70 proteins to more specialised roles (CHEETHAM and CAPLAN, 1998; KELLEY, 1999; WALSH *et al*., 2004). In general, type III Hsp40s lack the ability to bind peptide substrate (WALSH *et al*., 2004) although certain members of this Hsp40 class are known to bear specialised domains for the recovery of specific substrates, for subsequent delivery to Hsp70 (CHEETHAM and CAPLAN, 1998). The most apparent example includes the co-operation of the type III Hsp40, auxilin, with Hsc70 in clathrin uncoating (UNGEWICKELL *et al*., 1995). The human endoplasmic reticulum type III Hsp40, ERdj5 (DnaJC10), has recently been shown to function in the process of endoplasmic reticulum associated degradation (ERAD; USHIODA *et al*., 2008). In addition to co-operating with the endoplasmic reticulum Hsp70 protein, BiP, ERdj5 has been shown to exert disulphide reductase activity via its thioredoxin domain to cleave the disulphide bonds of misfolded proteins destined for retrograde translocation (CUNNEA *et al*., 2003; USHIODA *et al*., 2008). The co-chaperone ability of type III Hsp40 proteins lacking the ability to bind substrate was initially in question (WALSH *et al*., 2004). Recently however, the function of these proteins was placed into context with the discovery that the stimulation of Hsp70 ATPase activity represents the minimum requirement for certain roles of the Hsp70 chaperones in the cytosol of *S. cerevisiae* (SAHI and CRAIG, 2007). Although type III Hsp40 proteins possess only the J-domain of typical Hsp40 proteins, they may be capable of such stimulation (refer to *SECTION 1.3.6.1.1*).

1.3.6.1.1 The J-domain Defines the Hsp40 Class

The highly conserved J-domain (*FIGURE 1.3B*) is crucial to the interactions of Hsp40 co-chaperones with Hsp70 partner proteins (MAYER *et al*., 1999; PELLECHIA *et al*., 1996; WITTUNG-STAFSHEDE *et al*., 2003). Studies have shown that the J-domain alone is sufficient to stimulate the ATPase activity of Hsp70 (WALL *et al*., 1994) through electrostatic interactions with the ATPase domain of Hsp70 (GREENE *et al*., 1998). The high degree of J-domain conservation is highlighted in the numerous resolved structures of the J-domains of diverse origin, as documented in the Protein Data Bank (BERMAN *et al*., 2003) and summarised in *TABLE 1.1.* Comprised of approximately seventy amino acid residues, the J-domain exhibits four α-helices (I-IV) and is stabilised by an internal core of hydrophobic residues. A highly conserved His-Pro-Asp (HPD) tripeptide motif is housed in the loop region between helices II and III (*FIGURE 1.3B;* QIAN *et al*., 1996) and is known to be indispensable to interactions with Hsp70 chaperone partners. The alteration of residues of this motif has consistently been shown to result in loss in interaction with Hsp70 (GENEVAUX *et al*., 2002; LAUFEN *et al*., 1999; MAYER *et al*., 1999; TSAI and DOUGLAS, 1996; WITTUNG-STAFSHEDE *et al*., 2003).

TABLE 1.1 Resolved Structures of Hsp40 J-domains of Diverse Origin

Organism	Hsp40	PDB Code [1]	Reference
E. coli	DnaJ	1BQ0; 1BQZ; 1XBL	HUANG *et al.* (1998); PELLECCHIA *et al.* (1996)
	Hsc20/HscB	1FPO	CUPP-VICKERY and VICKERY (1997); CUPP-VICKERY and VICKERY (2000); FÜZERY *et al.* (2008)
S. cerevisiae	Sis1	2O37	*Unpublished* [2]
	Tim14-Tim16	2GUZ	MOKRANJAC *et al.* (2006)
H. sapiens [3]	DnaJB1 (HDJ1)	1HDJ	QIAN *et al.* (1996)
	DnaJB8	2DMX	*Unpublished*
	DnaJB9	2CTR	*Unpublished*
	DnaJB12	2CTP	*Unpublished*
	DnaJA3 (Tid-1)	2DN9	*Unpublished*
	DnaJC29 (Sacsin)	1IUR	*Unpublished*
Mus musculus	DnaJC5	2CTW	*Unpublished*
	DnaJ-like protein	1WJZ	*Unpublished*
	DnaJ-like protein	2CUG	*Unpublished*
Caenorhabditis elegans	DnJ-12	2OCH	*Unpublished*
Murine polyomavirus	T antigen	1FAF	BERJANSKII *et al.* (2000)
Simian Virus 40	T antigen	1GH6	KIM *et al.* (2001)
B. taurus	Auxilin	1NZ6	GRUSCHUS *et al.* (2004); JIANG *et al.* (2003)

[1] Protein Data Bank (PDB; BERMAN *et al.,* 2003); [2] *Unpublished* – currently unpublished structures; [3] The nomenclature of the human Hsp40 proteins is as described by HIGHTOWER *et al.* (2009).

Additional residues of the J-domain implicated in binding to partner Hsp70s appear to be less precisely defined, although residues of helices II and III and the intermediate trans-helix loop region are thought to form the primary catalytic interface of the domain (GENEVAUX *et al.*, 2002, 2003; PELLECHIA *et al.*, 1996). In certain instances, the presence of the HPD motif and positively charged residues on helix II appears to be the minimum requirement for productive J-domain based stimulation of Hsp70 ATPase activity (GREENE *et al.*, 1998). Residues Tyr[25] and Lys[26] of helix II of the J-domain of *E. coli* DnaJ were flagged as candidate catalytic residues comprising the interaction surface with DnaK (GENEVAUX *et al.*, 2002). The importance of corresponding residues in numerous Hsp40 homologs has been confirmed, indicating the evolutionary conservation of the interaction between Hsp70 and Hsp40 (reviewed in HENNESSY *et al.*, 2005b). A conserved KFK motif in helix III of the J-domain may also be important to interactions with Hsp70; it is suggested that the phenylalanine residue of this motif may interact with and stabilise the histidine residue of the HPD motif in the loop region (HENNESSY *et al.*, 2000, 2005a).

Other residues of the J-domain are gradually being implicated in structural roles, the mediation of the interaction with Hsp70 and the enhancement of the specificity of the Hsp70-Hsp40 partnership (GARIMELLA *et al.*, 2006; GENEVAUX *et al.*, 2002, 2003; LU and CYR, 1998a; SUH *et al.*, 1999). In particular, the residues of helix IV which were previously argued to be dispensable to the co-chaperone function of *E. coli* DnaJ (GENEVAUX *et al.,* 2002) have been implicated in key structural or functional

roles in other Hsp40 homologs (GARIMELLA *et al*., 2006; HENNESSY *et al*., 2005a). The helix sports a conserved QKRAA pentapeptide motif proposed to play a role in enhancing the specificity of interactions with Hsp70 (AUGER and ROUDIER, 1997; HENNESSY *et al*., 2005b).

It is generally accepted that the J-domain is tailored to make significant contributions to the affinity and specificity of the binding of a specific Hsp40 protein to its partner Hsp70 (GARIMELLA *et al*., 2006; HENNESSY *et al*., 2005b). This emanates from the fact that not all Hsp40 proteins or their J-domains appear to be interchangeable with respect to function and interaction with distinct Hsp70 proteins (reviewed in HENNESSY *et al*., 2005b). Residues implicated in determining the specificity of the Hsp70-Hsp40 partnership tend to be less conserved (GENEVAUX *et al*., 2002; GREENE *et al*., 1998; HENNESSY *et al*., 2000; HENNESSY *et al*., 2005B; KELLEY, 1998). In particular, the loop regions between the four α-helices of the J-domain appear to be divergent and may serve a role in mediating Hsp70-Hsp40 specificity. The auxilin J-domain bears an extended loop region between helices I and II which is proposed to mediate the specificity of interaction with Hsc70 in the process of clathrin uncoating (JIANG *et al.*, 2007). Moreover, the last segment of helix III and the intermediate loop region between helices III and IV have been suggested to contribute to the specificity of the J-domain of the murine polyomavirus large T antigen (GARIMELLA *et al*., 2006).

Helix I of the J-domain is fairly conserved in type I Hsp40s, but becomes divergent in type II and III Hsp40s (HENNESSY *et al*., 2000). A number of highly conserved hydrophobic residues have been identified in helix I and are suggested to be of importance to the functional integrity of the J-domain (HENNESSY *et al*., 2005a; NICOLL *et al*., 2007). Interestingly, substitutions performed on a leucine-rich region of helix I of the J-domain of murine polyomavirus large T antigen were shown to diminish the replication of the virus *in vivo*, but did not affect J-domain based interaction of the large T antigen with Hsc70. This implies that helix I may mediate a distinct function of the large T antigen (LI *et al*., 2001).

1.3.6.1.2 The GF Domain May Confer Functional Specificity

The role of the GF-region, termed according to the prevalence of glycine and phenylalanine residues, appears to be somewhat elusive. The domain is thought to be significant in the regulation of the substrate-binding capabilities of Hsp70 (MAYER *et al*., 1999; PELLECCHIA *et al.,* 1996) although it does not participate directly in the stimulation of Hsp70 ATPase activity (CHAMBERLAIN and BURGOYNE, 1997). The region may facilitate substrate transfer from Hsp40 to Hsp70 or serve to stabilise of the Hsp70-substrate complex (BANECKI *et al*., 1996; GENEVAUX *et al*., 2002; HAN and CHRISTEN, 2003; ROSSER and CYR, 2006). Furthermore, the involvement of the region in the

optimisation of substrate selection by Hsp40 has been proposed (KELLEY, 1999). The GF-region was initially thought to act as a linker between the J-domain and the remaining Hsp40 domains, but this is disputed by its high degree of sequence conservation. A conserved Asp-Ile-Phe (DIF) motif has been identified in the domain and is thought to play a significant structural or functional role, possibly in the regulation of the Hsp70 chaperone cycle subsequent to ATP hydrolysis (CAJO *et al.*, 2006; WALL *et al.*, 1995).

Differences in the GF-regions of type I and II Hsp40 proteins may contribute to the differences observed in the chaperone functions of these Hsp40 classes (FAN *et al.*, 2004; RAMOS *et al.*, 2008; ROSSER and CYR, 2006). YAN and CRAIG (1999) demonstrated the loss of functionality of the *S. cerevisiae* type II Hsp40 protein, Sis1, when the GF-region of the protein was interchanged with that from the corresponding type I Hsp40, Ydj1. In contrast, the functionality of Ydj1 was maintained when the GF-region of the type I Hsp40 was replaced with that from Sis1 (YAN and CRAIG, 1999). It was later concluded that the GF-region of Sis1 and type II Hsp40s may serve to specify unique cellular functions (ARON *et al.*, 2005; FAN *et al.*, 2004). In particular, the GF-region of type II Hsp40 proteins appears to be critical to function and in certain instances, the segment flanking the GF-region is proposed to constitute a glycine-methionine (GM)-region which may similarly serve to specify function (FAN *et al.*, 2003). This region is thought to mediate the ability of Sis1 to function in prion formation in yeast (LOPEZ *et al.*, 2003). Recently, RAMOS et al. (2008) demonstrated an exchange in the functionality of Ydj1 and Sis1 when the zinc-binding domain of Ydj1 and the GM-rich region of Sis1 were interchanged.

1.3.6.1.3 The Zinc-binding Domain Influences Substrate Binding

The zinc-binding domain found exclusively in type I Hsp40 proteins (*FIGURES 1.3A* and *1.3C*) is characterised by the presence of four cysteine-repeat sequences (CXXCXGXG, where X represents any amino acid) capable of coordinating the binding of two Zn(II) ions. This implies a possible role for the region in the stabilisation of Hsp40 tertiary or quaternary structure (GREENE *et al.*, 1998; MARTINEZ-YAMOUT *et al.*, 2000). The two zinc-binding centres of the domain (I and II; *FIGURE 1.3B*) exist in reduced state and are comprised of the two outermost and the two innermost cysteine-repeat sequences with respect to primary structure. An investigation into the individual roles of the two centres revealed that both are responsible for enhanced Hsp40 co-chaperone activity but the zinc-binding centre comprised of the two innermost cysteine repeat sequences (zinc centre II) is crucial to Hsp70 substrate binding (LINKE *et al.*, 2003). Mounting evidence suggests that the presence of the zinc-binding domain may be a prerequisite for substrate binding by the latter C-terminus (GREENE *et al.*, 1998; HAN and CHRISTEN, 2003; SZABO *et al.*, 1996) or the facilitation of

substrate transfer to Hsp70 (BANECKI et al., 1996; FAN et al., 2005; LINKE et al., 2003). The zinc-binding domain of Ydj1 was previously reported to be crucial to the protein's role in targeting Hsp70 for hormone receptor activation (FLISS et al., 1999). It is more likely that the domain permits substrate transfer by mediating productive interactions with Hsp70, as opposed to exhibiting direct involvement in substrate binding (ROSSER and CYR, 2006).

The crystal structure of the zinc- and substrate binding domains of the S. cerevisiae type I Hsp40, Ydj1 with the peptide substrate 'GWLYEIS' (FIGURE 1.3C) demonstrated the proximity of zinc centre II to the antiparallel β-sheets comprising the peptide binding surface of the substrate binding domain (LI et al., 2003; LI and SHA, 2005). Both zinc-binding centres of Ydj1 have been shown to be crucial to the transfer of bound substrate to Hsp70, but only zinc-binding centre II was revealed to be important to interactions with Hsp70 in the suppression of protein aggregation under conditions of heat stress (FAN et al., 2005).

Contrary to the typical cysteine-repeat motifs of prototypical type I Hsp40 proteins, the human endoplasmic reticulum lumenal type I Hsp40, ERdj3, exhibits an uncharacteristic cysteine-repeat domain, bearing CXC and CXXC motifs more commonly encountered in thioredoxin and Protein Disulphide Isomerase (PDI) related proteins (MARCUS et al., 2007). These motifs were shown to exist in oxidised state, promoting the formation of intramolecular disulphide bridges between the respective cysteine residues. Disruption of the disulphide bonds was shown to compromise the conformation of ERdj3 and its ability to bind protein substrate (MARCUS et al., 2007). Thus, the cysteine-repeat sequences of this zinc-finger like region appear to be important to substrate binding capabilities, in line with the function of cysteine-repeat sequences of Hsp40 proteins in general.

1.3.6.1.4 The C-terminal Substrate Binding Domain

The C-terminal substrate binding domain of Hsp40 co-chaperones is conserved to a lesser degree than the first three primary domains and is required to mediate substrate selection and transfer to Hsp70 (BANECKI et al., 1996; MINIMANI et al., 1996; LU and CYR, 1998a). Consistent with this, Hsp70 and Hsp40 demonstrate a similar affinity for peptides rich in hydrophobic and aromatic residues (RUDIGER et al., 1997, 2001). Hsp40 is proposed to bind the side-chains of protein substrates while Hsp70 binds both side- and main-chains (RÜDIGER et al., 1997, 2001; ZHU et al., 1996). These similarities and differences highlight the involvement of the Hsp40 substrate binding domain in initial substrate selection for Hsp70 (BISCHOFBERGER et al., 2003; HAN and CHRISTEN, 2003; RÜDIGER et al., 2001).

Evidence suggests that the substrate binding domains of type I and II Hsp40s may share crucial yet overlapping functions and compensate for each other *in vivo* (JOHNSON AND CRAIG, 2001). The resolved structures of the substrate binding domains of the *S. cerevisiae* type I and II Hsp40 proteins, Ydj1 (*FIGURE 1.3C;* LI *et al*., 2003) and Sis1 (SHA *et al*., 2000) reveal a structurally similar peptide binding pocket constituted by β-sheets. This supports the notion that Hsp40 function may be specified by the aforementioned central GF- and zinc-binding domains (FAN *et al*., 2004; LU and CYR, 1998b; YAN and CRAIG, 1999). As previously discussed, type I Hsp40s are distinguished from type II Hsp40s by their ability to bind and suppress the aggregation of proteins. Studies suggest that this chaperone activity is confined to the zinc- and substrate-binding domains, and implicated residues have been identified in *E. coli* DnaJ and *S. cerevisiae* Ydj1 (GOFFIN and GEORGOPOULOS, 1998; LU and CYR, 1998b). The substitution of residues comprising the hydrophobic peptide binding pocket of Ydj1 was shown to compromise substrate binding and co-operation with Hsp70 in protein refolding *in vitro* (LI and SHA, 2005). Certain type II Hsp40 proteins, such as Sis1, are suggested to exhibit an additional substrate binding module termed the C-terminal domain 1 (CTD1) in a region flanking the GF/GM-region, corresponding to the position of zinc-binding domain of type I Hsp40s (FAN *et al*., 2003; LEE *et al*., 2002). Recently, the flexibility of this domain in the human type II Hsp40, DnaJB1, was demonstrated and an "anchoring and docking" model was proposed for use of the domain in substrate capture and transfer to Hsp70 (HU *et al*., 2008).

In addition to being implicated in the capture of protein substrate, the C-terminal domain is involved in dimerization which is thought to be imperative to Hsp40 function (BORGES *et al*., 2005; SHA *et al*., 2000; SHI *et al.,* 2005). Loss of functionality has been demonstrated following truncation of the Hsp40 motif that mediates dimerization (indicated in *FIGURE 1.3C;* SHA *et al*., 2000). WU *et al.* (2005) have demonstrated significant differences in the dimer structures of type I and II Hsp40 proteins from *S. cerevisiae*, and have proposed that these differences may account for their distinct functions *in vivo*. In agreement with this, the quaternary structures of human type I and II Hsp40s were suggested to confer Hsp40 functional specialisation (BORGES *et al.,* 2005). The dimerization of both type I and II Hsp40 proteins sees the substrate binding domains of two monomers come together to shape a large intermediate cleft. In type I Hsp40 dimers, the zinc-binding domains have been shown to point directly towards each other creating a larger cleft than type II Hsp40 dimers (BORGES *et al*., 2005; SHI *et al*., 2005; WU *et al*., 2005). This cleft may accommodate the unbound portion of the protein substrate (SHI *et al*., 2005) or constitute the site of Hsp70 docking prior to substrate transfer (SHA *et al*., 2000; WU *et al*., 2005). The latter is consistent with the notion that the interaction of Hsp40 with Hsp70 is bipartite (AUGER and ROUDIER, 1997; SUH *et al*., 1998). The C-terminal EEVD motif of Hsp70 may serve as an anchor in this interaction; the peptide binding region

of the S. cerevisiae type ❙❙Hsp40, Sis1, and the human type ❙❙Hsp40, DnaJB1 have been shown to contact the EEVD motif in partner Hsp70s (FREEMAN et al., 1995; LI et al., 2006). The Hsp40 C-terminal residues implicated in this interaction appear to be conserved in type ❙❙Hsp40s and semi-conserved in type ❙Hsp40s (LI et al., 2006). It has further been suggested that the lid region of the Hsp70 substrate binding domain may interact with the upper region of the cleft formed in the Sis1 dimer (QIAN et al., 2002).

The substrate binding domain may also implicate certain Hsp40 proteins in membrane interactions or the processing of distinct substrates in the cell. The C-terminal end of certain type ❙Hsp40 proteins specifies a CAAX-box motif sequence (C-cysteine, A-aliphatic amino acid, X-any amino acid) that is known to be farnesylated in vivo (CAPLAN et al., 1992b). This involves the proteolytic cleavage of the last three amino acids and the addition of a hydrophobic 15-carbon farnesyl moiety from farnesylpyrophosphate to the cysteine residue of the motif by a farnesyltransferase enzyme (CLARKE, 1992; FARH et al., 1995). The farnesylation of Ydj1 has been shown to facilitate the association of the protein with the endoplasmic reticulum and perinuclear membranes in S. cerevisiae consistent with its role in protein translocation across intracellular membranes (BECKER et al., 1996; CAPLAN et al., 1992a). Recently, FLOM et al. (2008) demonstrated that farnesylation of Ydj1 is required for its role in the maturation of Hsp90 client proteins, through associations with the Hsp90/Hsp70 multi-chaperone complex (FLISS et al., 1999; JOHNSON and CRAIG, 2000).

1.3.7 The Hsp90/Hsp70 Multi-chaperone Complex

The crucial co-operation between Hsp90 and Hsp70 in the maturation of client proteins in the cell is proposed to involve the formation of a dynamic multi-chaperone and co-chaperone complex (reviewed by WEGELE et al., 2004). In eukaryotic cells, this complex is essential to the activation of steroid receptors and kinases; reconstitution of a functional complex to this effect in vitro showed the minimum components to include Hsp90, Hsp70, Hop, Hsp40 and p23 (PRATT and TOFT, 2003). In this system, recognition of the client protein is initially achieved by Hsp40 (DITTMAR et al., 1996; MURPHY et al., 2003) which recruits Hsp70 to the client protein, and stimulates the chaperone protein's ATPase activity for client processing (CINTRON and TOFT, 2006). The association of the Hsp70-Hsp40 partnership to the client may be stabilised by Hip (HÖHFELD et al., 1995). Subsequent recruitment of Hsp90 to the client occurs via association with Hsp70, mediated by the adaptor protein Hop (ODUNUGA et al., 2004; SCHEUFLER et al., 2000). The binding of Hsp70 to Hop appears to be enhanced by Hsp40 (HERNÁNDEZ et al., 2002). Following this, p23 interacts with Hsp90 in a manner that is thought to stabilise the association of the Hsp90-Hop-Hsp70-Hsp40 complex with the client (MORISHIMA et al., 2003). ATP-dependent processing of the client is promoted by Hsp90

following release of Hsp70 and its associated co-chaperones (MURPHY *et al*., 2003; PRATT and TOFT, 2003).

1.4 THE HUMAN CEREBRAL MALARIA PARASITE, PLASMODIUM FALCIPARUM

Malaria illness in humans is prompted by infection with eukaryotic protozoan parasites of the *Plasmodium* genus; in particular, *P. falciparum*, *P. vivax, P. malariae*, *P. ovale* and simian malaria parasites such as *P. knowlesi* (TUTEJA, 2007a; WHITE, 2008). *P. falciparum* is the causative agent of cerebral malaria, the most acute and fatal form of the illness, distinguished from other forms of malaria by the sequestration of parasitized erythrocytes in the cerebral vascular tissue (ADAMS *et al*., 2002). The adhesion of infected erythrocytes to receptors on the endothelial lining of this tissue ultimately disrupts the functionality of the blood-brain barrier, underlining the severity of the illness (BROWN *et al.* 1999; SHERMAN *et al*., 1995).

The World Health Organisation (WHO) Malaria Report for 2008[1] estimated the global incidence of human malaria infection in 2006 at 247 million cases of the 3.3 billion people considered to be at risk. Of these infections, close to a million resulted in death with 85% of deaths occurring in children under five years of age. Moreover, 86% of all infections and 91% of the resultant deaths were reported for the African continent. Current approaches to contend with malaria include physical avoidance and chemoprophylaxis. Avoidance strategies have had partial success in affected areas where chemotherapeutic agents may be limited for infected individuals. However, the increasing emergence of resistant *Plasmodium* strains has rendered certain chemoprophylaxis strategies ineffective (TUTEJA, 2007a). Irrespective of this, chemoprophylaxis does not serve as a continuous solution for populations residing in high risk malaria areas. A combinatorial approach is crucial to the design of future strategies to contend with the global burden of malaria; this includes a comprehensive understanding of the biological mechanisms governing the success of the *Plasmodium* parasites, for the identification of novel antimalarial targets (KOOIJ, 2006).

1.4.1 The Biology and Lifecycle of P. falciparum

P. falciparum exhibits a complex multihost lifecycle comprised of numerous morphologically distinct developmental stages, schematically represented in *FIGURE 1.4*. The ability of the parasite to survive within the *Anopheles gambiae* mosquito vector and the *Homo sapiens* host is attributed to the complexity of its protein expression mechanisms (KUMAR *et al*., 2004; MILITELLO *et al*., 2004). Proteomic analyses of the developmental stages of the parasite's lifecycle revealed the occurrence of stage- and strategy-specific protein expression (FLORENS *et al*., 2002; KOOIJ *et al*., 2006). A

[1] http://www.who.int/malaria/wmr2008/

significant portion of the proteome appears to be designated to host-parasite interactions, enabling this intracellular apicomplexan parasite to successfully invade and adapt to a variety of vector and host cells (KOOIJ ***et al.***, 2006).

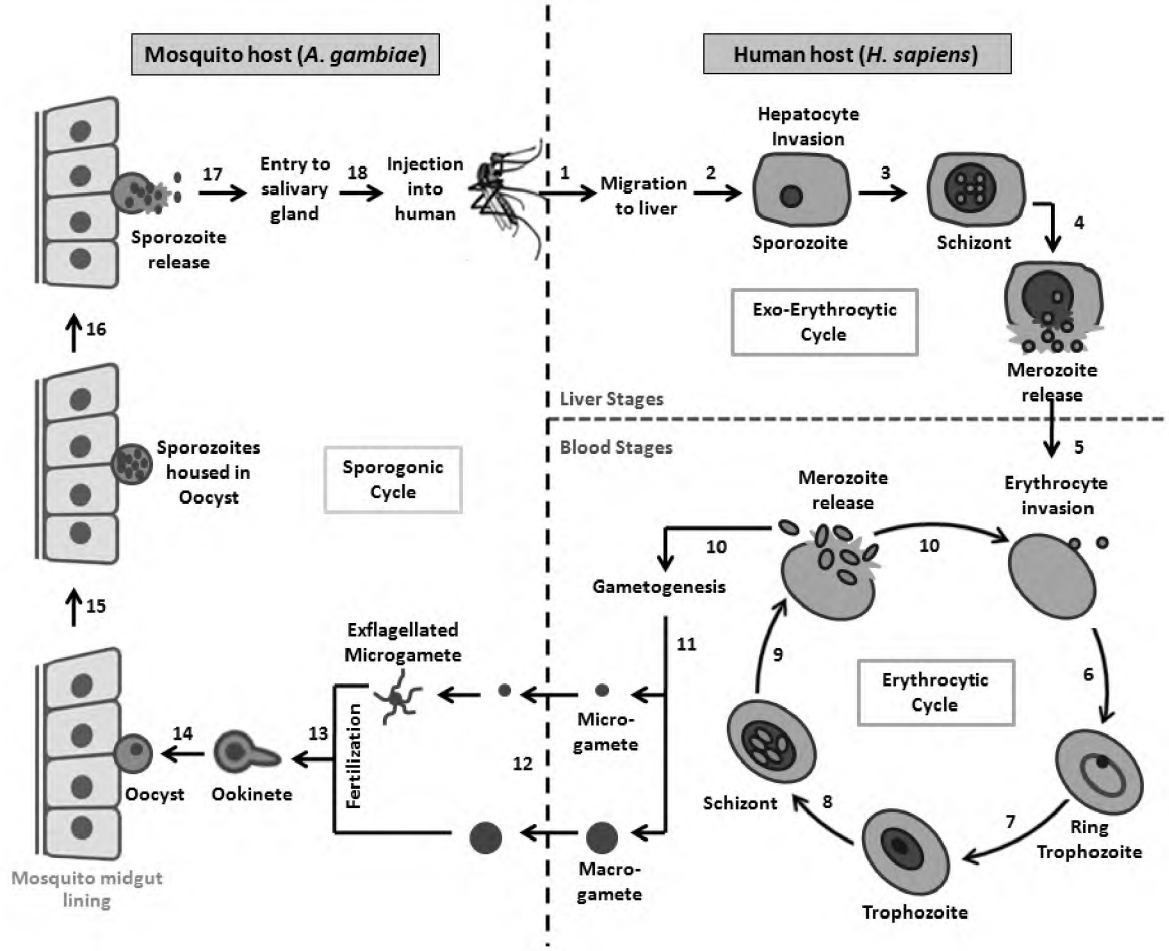

FIGURE **1.4** **Schematic representation of the** P. falciparum lifecycle **in the human host and invertebrate** vector. **(1) Sporozoites are transmitted to the vertebrate host from the female *A. gambiae* mosquito upon feeding. The transmitted sporozoites migrate to the liver via the circulatory system and invade hepatocytes.** (3) In **the exo-erythrocytic schizogony** (5-**15 days), the sporozoites propagate asexually to form schizonts** of **individual merozoites. (4) The hepatocyte is ruptured releasing the merozoites, which (5) subsequently enter** the **circulatory system and invade** individual **erythrocytes. (6) Within the infected erythrocyte, a merozoite establishes itself as a ring trophozoite and degrades the haemoglobin of the host cell.** (7) **The erythrocytic schizogony (48 hours) includes the maturation of the ring trophozoite into a mature trophozoite, and** (8) asexual **replication to form a schizont of individual merozoites. (9) The erythrocyte is ruptured releasing the merozoites, which (10) reinvade erythrocytes or (11) undergo Gametogenesis to form macro- and micro-gametes. (12) These gametes are taken up by the invertebrate host, the female *A. gambiae* mosquito**, upon **feeding from an infected human. (13) The microgamete becomes exflagellated and fertilises the macrogamete, resulting in the development of a zygote and subsequent motile** ookine**te** within 18-**24 hours** (14). **In the sporogonic schizogony** (10-24 days), **t**he o**okinete establishes itself as an** o**ocyst in the mosquito** midgut **cell lining between the epithelium and bas**olateral **lamina,** and **(15)** replicates asexually to **produce sporozoites**. (16) **The mature oocyst ruptures releas**ing the **motile sporozoites which (17) migrate through the haemolymph to invade the epithelial cells of the salivary glands of the mosquito. (18) The lifecycle is thus continued by transmission of the sporozoites to the human host by mosquito feeding. The figure was adapted from FUJIOKA and AIKAWA (2002) and WIRTH (2002).**

The considerable resilience of the parasite is highlighted in its ability to demonstrate gene expression versatility within the human host (LOVEGROVE *et al.*, 2007) and the occurrence of numerous antigenically variable *var* genes on the *P. falciparum* genome (SU *et al.*, 1995). In addition to strengthening the parasite's ability to evade the adaptive host immune response, these attributes have posed as obstacles to the discovery and development of vaccines and contemporary prophylactic and therapeutic agents for malaria. Interestingly, approximately 60% of the *P. falciparum* proteome appears to lack identifiable orthologs in known eukaryotic organisms including other *Plasmodium* and apicomplexan parasites; this suggests that a large portion of the biological mechanisms of this parasite may be novel (GARDNER *et al.*, 2002). Transcriptomic and proteomic data imply that at least 60% of the genes encoded on the parasite's genome are expressed during the asexual blood stages with approximately 24% expressed exclusively during these stages (BOZDECH *et al.*, 2003; LE ROCH *et al.*, 2003). Recently, attention has been drawn to the importance of the erythrocytic stages of the parasite's development, as further discussed in *SECTION 1.4.1.1*.

1.4.1.1 Cell Biology of the P. falciparum-infected Human Erythrocyte

In essence, the human erythrocyte represents a highly specialized host cell which offers very little for the *P. falciparum* parasite to harness in terms of the fundamental components of a typical eukaryotic cell (PASINI *et al.*, 2006). During the development of human reticulocytes into erythrocytes, the organelles and proteins redundant to the mature erythrocyte are discarded by lysosomal degradation and extracellular expulsion. This process sees the loss of the erythrocyte nucleus, mitochondria, protein synthesis machinery including the ribosomes, and secretory organelles including the endoplasmic reticulum and Golgi apparatus which govern protein trafficking (BLANC *et al.*, 2005; FADER *et al.*, 2005). Consequently, the barren eukaryotic cell undergoes extensive structural and functional remodelling subsequent to *P. falciparum* invasion, suited to the devices of the parasite. This includes the establishment of parasite processes implicated in the development of virulence, the acquisition of nutrients, protein trafficking, protein degradation, replication and evasion of the host immune response (PRZYBORSKI and LANZER, 2005). Such modifications are brought about by the export of a range of proteins of parasite origin – collectively termed the secretome or exportome – across the parasitophorous vacuole (PV) in which the parasite resides and into the erythrocyte cytoplasm (HALDAR *et al.*, 2005; LINGELBACH and PRZYBORSKI, 2006; TEMPLETON and DEITSCH, 2005; WISER *et al.*, 1999). The development of the parasitophorous vacuole occurs during parasite invasion of the erythrocyte; the vacuolar membrane serves as a selective semi-permeable barrier between the parasite and the erythrocyte cytoplasm facilitating nutrient acquisition and ion exchange (ANSORGE *et al.*, 1996; JOINER, 1991).

With the advancement of its intra-erythrocytic development, the parasite generates membranous structures termed Maurer's clefts in the erythrocyte cytoplasm beneath the plasma membrane (SPYCHER et al., 2006). These structures are believed to serve as specialized secretory organelles crucial to the trafficking of exported parasite proteins to the host cell membrane (PRZYBORSKI et al., 2003; WICKERT et al., 2004). Modifications of the erythrocyte membrane are of particular importance to P. falciparum. The parasite is known to produce and export a series of parasite proteins that constitute a cytoadherence complex at the erythrocyte membrane in the proximity of electron dense structures termed knobs (SHARMA, 1991). This is known to mediate the adherence of the infected erythrocyte to the endothelial lining of the vascular system as previously described, thereby averting splenic clearance (CRAIG and SCHERF, 2001).

The export of proteins to the host cytoplasm is proposed to be dependent on the presence of a conserved signal sequence motif termed the Plasmodium export element (PEXEL; MARTI et al., 2004) or host targeting signal (HT; HILLER et al., 2004) determined by independent studies. The manner in which the motif mediates export into the erythrocyte is not yet entirely understood, however recent research has provided insight into its processing in the parasite (BODDEY et al., 2008; CHANG et al., 2008). It is also speculated that more than one mode of protein export may be utilised by the parasite, as represented in FIGURE 1.5 (GORMLEY et al., 1992; HORROCKS and MUHIA, 2005; VINCENSINI et al., 2005). Prior to export, the trafficking of proteins within the parasite may be mediated by the traditional secretory pathway; proteins bearing a hydrophobic N-terminal signal sequence are thought to be routed via the ER to a Golgi-resembling membranous structure and subsequently to the PV (ADISA et al., 2003). Proteins bearing the PEXEL/HT motif are subsequently routed beyond the confines of the vacuolar membrane to erythrocytic locations (COOKE et al., 2004; RÖMISCH, 2005). Notably, the presence of an export signal is only a prediction of actual export, and proteins lacking identifiable export signals have also been found to be secreted (BLISNICK et al., 2000; DIXON et al., 2008; SPIELMANN et al., 2006; SPYCHER et al., 2003). Contrary to the model of the utilisation of the traditional secretory pathway, the involvement of a distinct ER-like organelle in the sorting and secretion of proteins destined for export to extra-parasitic sites via an 'alternate secretory pathway' has been put forward (WISER et al., 1997).

Numerous proteins bearing the PEXEL/HT motif have been identified and thus prospectively constitute a part of the exportome; the export status of certain of these proteins has been validated experimentally (HILLER et al., 2004; MARTI et al., 2004; SARGEANT et al., 2006). Several members of the molecular chaperone proteins, and in particular, members of the Hsp40 family are predicted to be exported and comprise a significant portion of the exportome (HILLER et al., 2004; MARTI et al., 2004; SARGEANT et al. 2006). This is consistent with the need for the establishment of

parasite **protein trafficking, translocation, folding and assembly processes** in the **host cell** (**BANUMATHY** et al., **2002**; MARTI **et al.**, 2004; **LINGELBACH and PRZYBORSKI**, 2006).

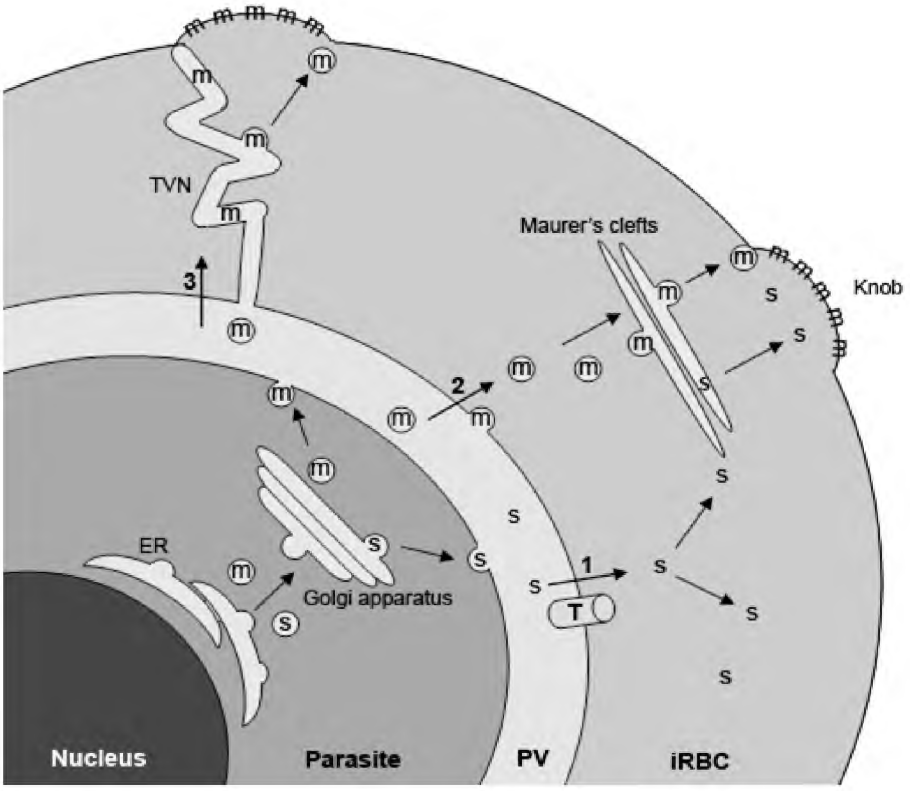

FIGURE 1.5 **Schematic representation of** a P. falciparum-**infected erythrocyte illustrating the potential export mechanisms of parasite proteins to erythrocytic destinations. It is thought that** parasite **proteins destined for export into the infected erythrocyte (iRBC; infected red blood cell) and those bearing a hydrophobic N-terminal signal sequence are transferred from the parasite endoplasmic reticulum (ER) to a rudimentary Golgi apparatus and secreted into the parasitophorous vacuole (PV) via the traditional secretory pathway (A**DISA **et al.**, 2003). **Proteins bearing export motifs, in addition to certain exceptions, are subsequently routed beyond the confines of the vacuolar membrane to erythrocytic destinations** (B**ARNWELL**, 1990; SPIELMANN **et al.**, 2006) **via alternate mechanisms indicated by the numbered arrows 1-3. (1) Soluble proteins 's' are potentially shuttled across the PV membrane into the erythrocyte cytosol through an ATP dependent translocon system 'T' or via an alternate active process requiring ATP** (A**NSORGE** et al., 1996)**. Subsequently the exported proteins may associate with knob structures on the erythrocyte membrane, potentially via the Maurer's clefts, or localise to the erythrocyte cytoplasm** (BANNISTER et al., 2004; **GORMLEY et al.**, 1992; **WICKERT** et al., **2004**). **(2) Membrane proteins 'm' are thought to be trafficked to the erythrocyte via a vesicular-based transport system to the Maurer's clefts and subsequently to the erythrocyte membrane where they may associate with the cytoadherence complex in the knob structures** (**BARNWELL**, 1990; **TARASCHI et al.** 1991; **GORMLEY** et al., **1992; WICKERT** et al., **2004). (3) Membrane proteins may also traverse a tubulovesicular network (TVN) branched from the PV, to reach the erythrocyte membrane (ELMENDORF** and **HALDAR, 1994). This may involve lateral diffusion through the network or the budding of vesicles from the TVN (BARNWELL, 1990).**

Moreover, molecular chaperones were shown to comprise 34% of the proteins identified in the parasitophorous vacuole (NYALWIDHE and LINGELBACH , 2006). The presence of these chaperones in the interface between the parasite and erythrocyte implies that they may play an important role in the functional refolding, processing and tran slocation of additional exportome proteins across the

vacuolar membrane (NYALWIDHE and LINGELBACH, 2006, RÖMISCH, 2005). Consistent with this, recent work has established that protein unfolding is a requirement for the translocation of certain exportome proteins across this membrane into the erythrocyte (GEHDE et al., 2009). The presence of parasite chaperones in the Maurer's clefts has also been proposed, consistent with the need for compensation for the lack of protein transport machinery in the host erythrocyte (LANZER et al., 2006; PRZYBORSKI et al., 2003; VINCENSINI et al., 2005).

In addition to the molecular chaperones, the exportome of the parasite was shown to comprise a significant number of protein kinases and phosphatases, in addition to the protein products of numerous *var*, *rif* (repetitive interspersed family) and *stevor* (sub-telomeric variable open reading frame) genes implicated in cytoadherence (HILLER et al., 2004; MARTI et al., 2004). Interestingly, the parasite genome appears to encode fewer genes assigned to standard 'house-keeping' processes such as transport and metabolism, in comparison to that of classical eukaryotic organisms (KOOIJ et al., 2006). In contrast, the parasite genome exhibits a significant expansion of the genes encoding the molecular chaperones and kinases destined for export to the erythrocyte cytosol (SARGEANT et al., 2006). This is indicative of the significant specialisation for the parasite to the demands of intracellular parasitism (reviewed by NYALWIDHE et al., 2003).

1.4.2 Molecular Chaperones in the Context of Malaria

Numerous members of the diverse chaperone protein complement of *P. falciparum* have been identified and implicated in cytoprotection of the parasite (BANUMATHY et al., 2003; MATAMBO et al., 2004; SHARMA, 1992). It is likely that the parasite undergoes significant exposure to oxidative stress and heat shock as its lifecycle alternates between the cold-blooded invertebrate vector (25°C at ambient temperature) and the warm-blooded human host (37°C), resulting in the coordinated upregulation of heat shock protein expression (JOSHI et al., 1992; PAVITHRA et al., 2007). Moreover, successive cycles of temperature elevation encountered in the recurrent febrile episodes synonymous with malaria (41°C) have been shown to promote heat shock-mediated cytoprotection and development of the intra-erythrocytic stages of the parasite (OAKLEY et al., 1997; PAVITHRA et al., 2004). In particular, enhanced expression of Hsp40, Hsp70 and Hsp90 proteins has been reported in the trophozoite, schizont and merozoite erythrocytic stages of development (OAKLEY et al., 1997; SHARMA et al., 1992). These Hsps are thought to be indispensible to the stress response and survival of apicomplexan parasites in general (VONLAUFEN et al., 2008). A comparison of the upregulation of these proteins in the lifecycle of *P. falciparum* suggests that they may be most critical in development within the human host (PAVITHRA et al., 2007). Heat shock proteins of the parasite have also been implicated in the immune response of the human host (KUMAR et al., 1990).

Moreover, evidence suggests that the parasite may exploit host chaperones for its devices in the intraerythrocytic stages of development; human Hsp90, Hsp70 and Hsp60 are known to be recruited in membrane bound complexes in the infected erythrocyte (BANUMATHY *et al.*, 2002). It is possible that the exported parasite proteins function in concert with host chaperones to facilitate the trafficking and assembly of the cytoadherence complexes at the erythrocyte surface. Consistent with this, the association of the host chaperones with the membrane bound complexes appears to be ATP-dependent. Furthermore, none of the Hsp90 and Hsp70 homologs of parasitic origin appear to be exported to the erythrocyte cytoplasm (BANUMATHY *et al.*, 2002).

1.4.2.1 Thermotolerance Factors - sHsps and Hsp100

To date only two small heat shock proteins have been identified in the parasite (PAVITHRA *et al.*, 2007) including a polyubiquitin protein (PfUB) which is induced in response to heat shock associated with the intraerythrocytic phases of the parasite's development (HORROCKS and NEWBOLD, 2000). Notably, serial analysis of gene expression from the *P. falciparum* genome suggests that PfUB may be one of the most highly expressed proteins in the parasite, highlighting a pronounced role for this protein (PATANKAR *et al.*, 2001). Four putative Hsp100 proteins have been identified including a protein termed Cg4 which may be linked to chloroquine resistance (PAVITHRA *et al.*, 2007).

1.4.2.2 The P. falciparum Hsp90 Proteins and Associated Co-Chaperones

The induction of cytosolic *P. falciparum* Hsp90, PfHsp90 (gene accession PF07_0029) has been demonstrated in response to the recurrent heat shock associated with the intraerythrocytic stages of the parasite's development (PAVITHRA *et al.*, 2004). The chaperone is suggested to be indispensable to the progression and cytoprotection of the intraerythrocytic stages, and is accompanied by PfHsp70-I (*SECTION 1.4.2.4*) and numerous co-chaperone proteins in multi-chaperone complexes in the parasite (BANUMATHY *et al.*, 2003; PAVITHRA *et al.*, 2004). This has placed PfHsp90 as a prime antimalarial target and has resulted in efforts to identify specific inhibitors of this chaperone protein (KUMAR *et al.*, 2007). An identified Hsp90 inhibitor, geldanamycin, has been shown to serve as an antimalarial compound and is proposed to act through specific inhibition of the ATP-binding capability of PfHsp90 (BANUMATHY *et al.*, 2003) and the ability of the chaperone to promote intraerythrocytic parasite growth and development subsequent to the establishment of the ring stage (PAVITHRA *et al.*, 2004). Three additional Hsp90 homologs have been identified in *P. falciparum* including the endoplasmic reticulum Hsp90 homolog, Grp94, and two tumor necrosis factor receptor-associated protein-1 (Trap-1) related proteins (PAVITHRA *et al.*, 2007).

Putative homologs of characterised Hsp90 co-chaperones have similarly been established in the parasite (KUMAR *et al*., 2007), including p23 (Pfp23), PP5 (PfPP5; DOBSON *et al*., 2001, LINDENTHAL and KLINKERT, 2002), Aha1 (PfAha1; LACOUNT *et al*., 2005) and the cyclophilins FKBP35 (PfFKBP35; MONAGHAN and BELL, 2005), FKBP (PfFKBP) and Cyp19 (PfCyp19). PfPP5 has been implicated in the PfHsp90 multi-chaperone complex of the parasite (PAVITHRA *et al*., 2004) and co-immunoprecipitation experiments have demonstrated the interaction between this co-chaperone and PfHsp90 (DOBSON *et al*., 2001). The peptidyl–prolyl *cis–trans* isomerase and protein aggregation suppression activity of PfFKBP35 has been demonstrated *in vitro*, and the protein is known to be inhibited by antimalarial compounds FK506 and rapamycin (MONAGHAN and BELL, 2005). Moreover, putative parasite homologs of the Hsp70-Hsp90 adaptor protein, Hop (PfHop) and the E3 ubiquitin ligase CHIP (PfCHIP) have been recognised (PAVITHRA *et al*., 2007). PfHop may mediate interactions of PfHsp90 with Hsp70 homologs of the parasite (PfHsp70; described in *SECTION 1.4.2.4*), while PfCHIP may associate with PfHsp90 and PfHsp70 proteins to facilitate the targeting of proteins for degradation via the ubiquitination pathway. The interaction of Hsp90 with the protein phosphatase, calcineurin, has also been documented (KUMAR *et al*., 2005)

1.4.2.3 The P. falciparum Hsp60 Chaperonins

The parasite genome appears to encode two Hsp60 homologs, including PfHsp60 (SYIN and GOLDMAN, 1996) and PfCpn60 (HOLLOWAY *et al*., 1994), in addition to nine TCP-1 related proteins (PAVITHRA *et al*., 2007). Enhanced transcription of the *pfhsp60* gene has been described in response to heat shock (SYIN and GOLDMAN, 1996). Irrespective of this, the expression of the protein appears to be remain constitutive in all stages of the parasite's development (DAS *et al*., 1997; FUJIOKA *et al*., 1998). PfHsp60 was shown to localise to the parasite cytoplasm in all stages of development, and to the mitochondria in the gametocyte, erythrocytic and exo-erythrocytic stages, suggesting a role for the protein in the facilitation of translocation in this organelle (DAS *et al*., 1997). Moreover, the protein was shown to co-precipitate with numerous parasitic proteins including a 70 kDa protein suggested to be a PfHsp70 homolog (DAS *et al*., 1997). This would be consistent with the successive co-operation of Hsp70 and Hsp60 in protein folding as previously discussed in *SECTION 1.3.5*.

1.4.2.4 The P. falciparum Hsp70 Proteins

P. falciparum appears to be equipped with six Hsp70 homologs, three of which have been described (PETERSON *et al*., 1988; SHONHAI *et al*., 2007; refer to *TABLE 2.4*, *CHAPTER 2*). These homologs have been implicated in assorted roles in the parasite, ranging from cytoprotection (MATAMBO *et al*., 2004) to the progression of the exo-erythrocytic schizogony (KAISER *et al*., 2003), the regulation of

actin polymerisation (TARDIEUX *et al*., 1998) and the trafficking of proteins to distinct organelles such as the apicoplast (FOTH *et al*., 2003).

The most abundant and well characterised of the Hsp70 homologs in the parasite includes the 75 kDa PfHsp70-I protein, which is upregulated in erythrocytic-stage parasites in response to heat shock (BISWAS and SHARMA, 1994; JOSHI *et al*., 1992). The protein was initially identified as a 75 kDa protein termed 'p75' on the surface of the merozoite stage of the parasite (ARDESHIR *et al*., 1987). Subsequent work has shown that the protein is among the most abundant proteins produced in *P. falciparum* (LE ROCH *et al*., 2003; PATANKAR *et al.* 2001) and localises to the parasite cytosol, nucleus (KUMAR *et al*., 1991) and PV (NYALWIDHE AND LINGELBACH, 2006). PfHsp70-I has been shown to occur in complex with PfHsp90, suggesting a related role in the cytoprotection, growth and development of the parasite (BANUMATHY *et al*., 2003; MATAMBO *et al*., 2004). The immunogenicity of PfHsp70-I has been described, and attention has been drawn to its potential to serve as a vaccine candidate (QAZI *et al.* 2005; SHARMA, 1992). Moreover, the chaperone capabilities of PfHsp70-I have been validated experimentally (MATAMBO *et al*., 2004; RAMYA *et al*., 2006; SHONHAI *et al*., 2008) and the protein has been shown to suppress the thermosensitivity of a DnaK mutant strain of *E. coli*, consistent with its proposed role in cytoprotection (SHONHAI *et al*., 2005). Interestingly, domain swapping experiments have revealed that the substrate binding domain, but not the ATPase domain, of PfHsp70-I is functionally equivalent to that of *E. coli* DnaK (SHONHAI *et al*., 2005).

A 72 kDa homolog of the endoplasmic reticulum Hsp70, BiP (termed PfBiP, PfGrp78 or PfHsp70-II) is conserved in the *Plasmodium* genus (DE OLIVEIRA-FERREIRA *et al*., 1999) and is reported to be upregulated in the intra- and exo-erythrocytic stages of *P. falciparum* in response to heat shock (KUMAR and ZHENG, 1992; SHARMA, 1992). Recently, this protein has been implicated in interactions with exportome proteins in the stages prior to export (SARIDAKI *et al*., 2008). Interestingly, both PfHsp70-I and PfBiP are thought to undergo phosphorylation during the course of the parasite's intraerythrocytic development (KAPPES *et al*., 1993). An additional Hsp70 homolog termed PfHsp70-III has similarly been identified in the asexual blood-stages of the parasite (SHARMA, 1992) and is suggested to localise to the mitochondria and PV (NYALWIDHE and LINGELBACH, 2006; ŠLAPETA and KEITHLY, 2004). The outstanding three Hsp70 homologs in the parasite – termed PfHsp70-x, PfHsp70-y and PfHsp70-z – remain to be characterised (SHONHAI *et al*., 2007).

1.4.2.5 The P. falciparum Hsp40 Proteins

Initial bioinformatics studies indicate that the *P. falciparum* genome encodes an expanded Hsp40 protein complement comprised of at least forty three member proteins. Nineteen of these proteins

are predicted to be exported to the host erythrocyte and are implicated in erythrocyte remodelling (SARGEANT *et al*., 2006). The export status of certain of these Hsp40 proteins has been verified experimentally (BROWN *et al*., 1985; COPPEL *et al*., 1988; HILLER *et al*., 2004; SARGEANT *et al*., 2006). An analysis of the complete Hsp40 complement of *P. falciparum* is provided in *CHAPTER 2*.

WATANABE (1997) initially identified and described four Hsp40 proteins, termed Pfj1-4, and the abundance of corresponding mRNA transcripts in erythrocytic stage parasites. Prior to heat shock, Pfj2 (gene accession PF11_0099), Pfj4 (PFL0565w), Pfj3 (PF10_0378) and Pfj1 (PFD0462w) mRNA transcripts were found in order of decreasing abundance in the parasite respectively. Following the induction of heat shock at 43°C for 2 hours, Pfj2 mRNA was observed to decrease, with a considerable increase in the abundance of Pfj3 mRNA and a lesser increase in that of Pfj1 and Pfj4 (WATANABE, 1997). The upregulation of Pfj3 production in the parasite in response to heat shock was later confirmed (OAKLEY *et al*., 2007) and the protein was shown to bear an identifiable PEXEL/HT motif (SARGEANT *et al*., 2006). Recently, the upregulation of Pfj4 production under heat shock conditions was also verified (PESCE *et al*., 2008).

Hsp40 proteins constituting a part of the exportome were identified prior to the discovery of the PEXEL/HT motif. These include the J-domain bearing members of the ring-infected erythrocyte surface antigen (RESA) protein family (DA SILVA *et al*., 1994; FOLEY *et al*., 1991). These proteins are known to be exported to the erythrocyte cell membrane where they interact with components of the membrane skeleton, such as spectrin, to facilitate the formation of the knob structures implicated in cytoadherence (FOLEY *et al*., 1991; DA SILVA *et al*., 1994). Data from the disruption of the gene encoding the original RESA protein (PFA0110w) suggests that the protein plays a role in supporting resistance against heat shock (SILVA *et al*., 2005). Intriguingly, the RESA proteins lack the crucial HPD motif in the J-domain, and thus the role of this domain remains uncertain. In light of this, WATANABE (1997) suggested that the RESA proteins belong to independent subgroups of Hsp40-like proteins in contrast to the 'true' J-domain bearing proteins Pfj1-4. DA SILVA *et al.* (1994) have suggested a role of the RESA J-domain in the stabilisation of spectrin interactions. OAKLEY *et al.* (2007) identified a PRESAN domain (*Plasmodium* RESA N-terminal domain) preceding the J-domain in RESA proteins, suggested to mediate protein-protein interactions. This domain was subsequently identified in other exportome proteins (OAKLEY *et al*., 2007). The mature parasite-infected erythrocyte surface antigen (MESA) protein, also referred to as *P. falciparum* erythrocyte membrane protein 2 (PfEMP-2), represents an additional Hsp40 protein in the parasite and similarly associates with the erythrocyte membrane skeleton (COPPEL *et al*., 1988) in the formation of the

knobs (SHARMA, 1991). RESA and MESA represent typical exportome proteins, bearing an identifiable PEXEL/HT motif in the N-terminal region preceding the J-domain (SARGEANT *et al.*, 2006).

The essentiality of the proposed exportome Hsp40 proteins of the parasite was recently explored using a gene knockout strategy (MAIER *et al.*, 2008). The genes encoding three Hsp40 proteins could not be disrupted potentially implying an essential role for these proteins; these include the Sis1 homolog encoded by PFA0660w, the Hsp40-like protein encoded by PF11_0034, and the Ring-infected Erythrocyte Surface Antigen (RESA) related protein encoded by PF11_0509 (MAIER *et al.*, 2008). Moreover, the Hsp40-like protein encoded by PF10_0381 was found to be essential to the formation of the cytoadherence complexes on the erythrocyte surface (MAIER *et al.*, 2008).

Of the parasite Hsp40 complement, only two type ▮Hsp40 proteins are apparent, bearing all four conserved domains characteristic of a prototypical Hsp40 protein. This includes a typical type ▮ Hsp40 identified in this work (termed PfHsp40, encoded by PF14_0359), thought to be crucial to the parasite's protein folding processes by inference. Moreover, Pfj1 identified by WATANABE (1997) represents a larger, atypical type ▮ Hsp40 (encoded by PFD0462w), the function of which is tentative. Both co-chaperone proteins are predicted to be parasite-resident as they lack a putative PEXEL/HT export motif; this suggests potential associations of these proteins with parasite-resident Hsp70 homologs such as the most abundant parasite-resident Hsp70 protein, PfHsp70-▮ Moreover, the possible upregulation of Pfj1 as a consequence of heat shock in infected erythrocytes (WATANABE, 1997) suggests that this protein may play a role in the stress response of the parasite and associate with other inducible components of the chaperone machinery, such as PfHsp70-▮

1.5 RESEARCH HYPOTHESIS, BROAD OBJECTIVES AND APPROACH

Knowledge pertaining to the Hsp70-Hsp40 partnerships of the *P. falciparum* molecular chaperone protein system is currently lacking. In addition to six Hsp70 homologs, the *P. falciparum* genome appears to encode forty-three Hsp40 proteins, bringing to light the numerous possible associated chaperone partnerships of the parasite. In keeping with the lower proportion of 'house-keeping' genes encoded on the *P. falciparum* genome, the existence of only two type ▮Hsp40 proteins in the parasite could represent an inherent weakness in its makeup, considering that type ▮ Hsp40 proteins represent typical regulators of Hsp70 chaperone activity. Disruption or inhibition of these proteins could have severe implications for the viability of the malaria parasite. The attributes, activities and interactions of these Hsp40 proteins could thus be valuable in the pursuit of novel antimalarial targets. This warrants the biochemical characterisation of these putative co-chaperone

proteins, including the elucidation of their interaction with Hsp70 chaperone partner and substrate proteins, and their role in the developmental stages of the *P. falciparum* lifecycle.

Co-chaperone partners of the most abundant parasite-resident Hsp70 homolog, PfHsp70-1, have not been validated in the parasite. It is most likely that PfHsp40 and Pfj1 serve this purpose, deduced from the known associations of homologous Hsp70 and Hsp40 proteins in characterised organisms, including *E. coli* DnaK-DnaJ, human HspA1A-DnaJA1 and *S. cerevisiae* Ssa1-Ydj1. Importantly, PfHsp70-1 is thought to promote resistance to heat shock and has been implicated in association with the PfHsp90 multi-chaperone machinery, highlighting a role in the cytoprotection of the malaria parasite (BANUMATHY *et al*., 2003; SHONHAI *et al*., 2005). Moreover, the chaperone activity of PfHsp70-1 has been demonstrated, suggesting the importance of this chaperone to general protein folding and processing tasks in the parasite (MATAMBO *et al*., 2004; SHONHAI *et al*., 2008). By inference, co-chaperone partners of PfHsp70-1 may be implicated in these indispensable tasks in the parasite.

The research detailed in the dissertation is thus centred about deciphering the type I Hsp40–Hsp70 partnerships of *P. falciparum*. In particular, it is hypothesised that:

PfHsp40 and Pfj1 are responsible for the regulation of the chaperone activity of PfHsp70-1

The broad research objectives and approach may be summarised as follows (*i-vi*):

i. Prediction of the biochemical properties and functions of PfHsp40 and Pfj1 in the P. falciparum parasite

In silico bioinformatics analyses were used to investigate and infer the potential biological functions, interactions and localisations of PfHsp40 and Pfj1 relative to PfHsp70-1 in *P. falciparum*. To place these proteins into context in the parasite, an analysis was performed to identify and explore members of the full Hsp70-Hsp40 complement encoded on the parasite's genome. Details of these analyses are provided in *CHAPTER 2.*

ii. Heterologous production and isolation of recombinant PfHsp40 and Pfj1 for subsequent characterisation

Numerous factors including codon bias and the AT-richness of the *P. falciparum* genome are known to pose difficulties to the production and purification of recombinant malarial proteins in heterologous expression systems. Synthetic genes encoding PfHsp40 and Pfj1 were constructed by PCR assembly using the approaches of codon-optimisation and codon-harmonisation. Approaches to the optimisation of the heterologous production and

isolation of PfHsp40 and Pfj1 for subsequent *in vitro* characterisation are detailed in *CHAPTER 3*.

iii. Elucidation of the presence and localisation of PfHsp40 and Pfj1 in P. falciparum in the intraerythrocytic stages of development

In view of the importance of chaperone proteins in the intraerythrocytic stages of the parasite's development, localisation studies were employed in cultured *P. falciparum*-infected erythrocytes to establish the presence, localisation and potential roles of the type I Hsp40 proteins of the parasite relative to PfHsp70-I These localisation studies are detailed in *CHAPTER 4*.

iv. Assessment of the co-chaperone abilities of PfHsp40 and Pfj1 in an in vivo complementation system

The *in vivo* functionality of recombinant PfHsp40 and Pfj1 was assessed in a prokaryotic complementation system. Using this heterologous platform, the co-chaperone properties of the more atypical Hsp40 protein, Pfj1, were explored by the approach of J-domain swapping and rational site-directed mutagenesis. Experiments pertaining to this *in vivo* characterisation are detailed in *CHAPTER 5*.

v. Assessment of the co-chaperone regulation of PfHsp70-I activity in vitro

The ability of the more typical type IHsp40, PfHsp40, to stimulate the chaperone activity of PfHsp70-I was assessed using *in vitro* Adenosine triphosphatase (ATPase) assays and protein aggregation suppression assays using a model thermolabile substrate. The latter approach was similarly used to investigate the ability of PfHsp40 to exert holdase chaperone activity in its own right. This activity was gauged relative to previously characterised co-chaperone proteins of eukaryotic origin. Details of this *in vitro* characterisation are provided in *CHAPTER 6*.

vi. Comparison of Hsp70-Hsp40 Partnerships of P. falciparum and human origin

The activities of PfHsp70-Iand PfHsp40 were gauged against an established human Hsp70-Hsp40 partnership using in the *in vitro* assays detailed above in (*v*). The interchangeability of human and parasite Hsp70 and Hsp40 proteins was assessed to substantiate the potential for host-parasite heterologous chaperone interactions in the *P. falciparum*-infected erythrocyte, and to explore the potential conservation of Hsp70-Hsp40

mechanisms in the parasite. This provided a platform from which to evaluate the potential Hsp70-Hsp40 partnerships of the parasite to serve as specific anti-malarial targets. A model system was established using the human and *P. falciparum* heterologous and homologous Hsp70-Hsp40 associations, to screen for small molecular modulators specific to the parasite chaperone and co-chaperone proteins. Details of this work are provided in *CHAPTER 6*.

CHAPTER 2:

BIOINFORMATICS ANALYSIS:

The Hsp40 Proteins of P. falciparum and other

Apicomplexan Parasites

2.1 INTRODUCTION

The integration of information technology and molecular biology has resulted in the emergence of the field of *Bioinformatics*, which encompasses *s*tatistical, mathematical and computational approaches to the organisation and interpretation of biological data *in silico*. A fundamental application of this field is the prediction of biological function by extrapolation from developed algorithms or existing biological knowledge (KANEHISA and BORK, 2003; YANG *et al.*, 2008). In this manner, genome mapping and annotation, protein and DNA sequence alignments, protein structure prediction, phylogenetic analyses, the interpretation of gene expression profiles and the development of protein interaction networks, may all be used to complement or direct traditional experimental approaches to understanding biological processes (SEARLS, 2000).

The emergence of *Bioinformatics* was prompted by the exponential increase in data generated by numerous genome sequencing projects and the application of novel tools developed for large-scale transcriptomic and proteomic analyses (KANEHISA and BORK, 2003). This has seen the integration of vast amounts of bioinformatics data in online public access 'databanks' and the development of countless computational tools - collectively termed the 'Resourceome' - for the interpretation of this data (CANNATA *et al.*, 2005; ROOS, 2001). In February 2008, the online nucleotide database, GenBank, housed by the National Center for Biotechnology Information (NCBI)[1] was reported to hold approximately 83 million nucleotide sequence records derived from more than 260 000 organisms (BENSON *et al.*, 2008). GenBank is a constituent of the International Nucleotide Sequence Database collaboration (INSD) which amalgamates nucleotide records from the NCBI with two other major databases including the DNA DataBank of Japan (DDBJ; SUGAWARA *et al.*, 2008) and that of the European Molecular Biology Laboratory (EMBL; FLICEK *et al.*, 2008).

The sequencing of the *P. falciparum* genome has been completed (GARDNER *et al.*, 2002); this includes 14 nuclear chromosomes, a 6 kb mitochondrial genome and a 35 kb circular apicoplast genome. Moreover, numerous high-throughput transcriptomic and proteomic studies have provided insight into the stage-specific gene expression of the parasite's lifecycle (FLORENS *et al.*, 2002; LE ROCH *et al.*, 2003; BOZDECH *et al.*, 2003). Experimental and *in silico* data relating to the parasite are continually assembled and made available in online resources such as the *Plasmodium* database, PlasmoDB (BAHL *et al.*, 2003; TUTEJA, 2007a). Such efforts have appropriately been dubbed 'databases towards the virtual parasite' (KOOIJ *et al.*, 2006) and have proven useful in characterising some of the many proteins encoded on the *P. falciparum* genome that are of unknown function (DATE and STOECKERT,

[1] www.ncbi.nlm.nih.gov/GenBank/

2006). These efforts have become key elements in the discovery of novel antimalarial drug targets (KUMAR *et al*., 2007).

Bioinformatic analysis reveals that the genome of *P. falciparum* encodes a diverse chaperone complement including at least forty three members of the Hsp40 family, and six members of the Hsp70 family. Nearly half of the Hsp40 proteins of *P. falciparum* are predicted to contain a PEXEL/HT (*Plasmodium* export element/host targeting signal) sequence motif, and hence, are likely to constitute a part of the exportome implicated in the extensive structural and functional remodelling of infected erythrocytes. In contrast, none of the Hsp70 proteins bear a recognisable export motif and are thus predicted to be parasite-resident (HILLER *et al*., 2004; MARTI *et al*., 2004; SARGEANT *et al*., 2006). The broad objectives of this study were to draw on available bioinformatics resources to investigate the potential functions, localisation and interactions of PfHsp40 and Pfj1 in *P. falciparum*, and to place these proteins into the context of the entire Hsp70-Hsp40 complement of the parasite. The classification, sequence similarity and clustering, and possible interactors of the Hsp40 proteins of the parasite were critically evaluated, and potential associations with Hsp70 proteins were identified. Moreover, parallels were drawn with the Hsp40 chaperone machinery of other apicomplexan parasites and the human host for insight into the conserved and divergent functions of the *P. falciparum* Hsp40 proteins. Considering the upregulation of parasite heat shock proteins in the intraerythrocytic stages of development (JOSHI *et al.* 1992), the Hsp70 and Hsp40 proteins referred to in this study are discussed specifically in the context of these stages (refer to *FIGURE 1.5*, *CHAPTER 1*). Specifically, the objectives of this study were to (*i-vii*):

i. Infer biological roles and potential localisations of PfHsp40 and Pfj1 from available knowledge pertaining to homologous Hsp40 proteins

ii. Predict the tertiary structures of PfHsp40, Pfj1 and PfHsp70-I and identify conserved residues potentially important to the structural and functional integrity of the proteins

iii. Identify and categorise members of the complete Hsp40 chaperone complement of *P. falciparum*

iv. Establish protein interactors of the *P. falciparum* Hsp40 proteins to predict their assignment to key biological processes

v. Assess the phylogenetic clustering of the Hsp40 proteins of *P. falciparum*

vi. Identify apicomplexan and human homologs of the *P. falciparum* Hsp40 proteins, and investigate differences and similarities in the Hsp40 complements of these organisms

vii. Identify Hsp70 homologs of *P. falciparum* and identify potential Hsp70-Hsp40 associations in the parasite

2.2 INSIGHT FROM MULTIPLE PROTEIN SEQUENCE ALIGNMENTS

Elements of Hsp40 conservation and divergence were revealed in a comparison of the protein sequences of PfHsp40 and Pfj1 with that of well-characterised type ▮Hsp40 proteins derived from *E. coli*, *Agrobacterium tumefaciens, S. cerevisiae* **and the human (***FIGURE 2.1***). In comparison to PfHsp40, Pfj1 demonstrates a lower degree of protein sequence conservation and appears to be more distantly related to the typical type ▮Hsp40 proteins of eukaryotic origin. This suggests a potential divergence in chaperone function. In contrast, PfHsp40 represents a more characteristic eukaryotic type ▮Hsp40 and may be implicated in standard 'house-keeping' chaperone roles in the parasite.**

A.

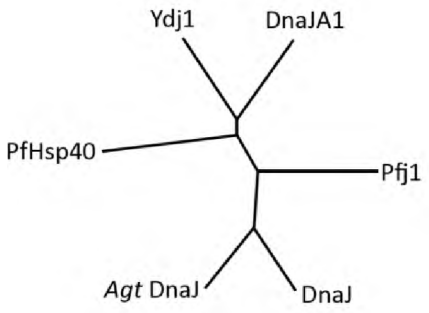

B.

	DnaJ	AgtDnaJ	Ydj1	DnaJA1	PfHsp40	Pfj1
DnaJ	-	57.2	27.0	27.5	22.4	17.4
Agt DnaJ	57.2	-	30.3	28.2	22.7	17.8
Ydj1	27.0	30.3	-	47.0	32.5	16.0
DnaJA1	27.5	28.2	47.0	-	35.9	13.7
PfHsp40	22.4	22.7	32.5	35.9	-	13.5
Pfj1	17.4	17.8	16.0	13.7	13.5	-

FIGURE 2.1 Comparison of PfHsp40 and Pfj1 with type ▮Hsp40 proteins of eukaryotic and prokaryotic origin. **(A) Unrooted radial tree diagram and (B) percentage protein sequence identity matrix illustrating the similarly of PfHsp40 and Pfj1 to previously characterised type ▮Hsp40 proteins of eukaryotic and prokaryotic origin. Eukaryotic proteins: Ydj1 (***S. cerevisiae***; CAA95937.1) and DnaJA1 (***H. sapiens***; NP_001530.1). Prokaryotic proteins:** *Agt* **DnaJ (***A. tumefaciens***; AAR84666.1) and DnaJ (***E. coli***; P08622.3). The tree diagram was generated using TreeView (version 1.6.6; Page, 1996) based on the multiple protein sequence alignment of the respective proteins depicted in** *FIGURE 2.2***. Protein sequences were retrieved from GenBank (BENSON** *et al.***, 2008). Values of percentage protein sequence identity were calculated using BioEdit Sequence Alignment Editor (version 7.0.4.1; HALL, 1999).**

The corresponding protein sequence alignment in *FIGURE 2.2* **highlights the identification of unique and conserved residues, motifs and domains thought to be important for the functionality of the** *P. falciparum* **type ▮Hsp40 proteins. Notably, PfHsp40 and Pfj1 bear an N-terminal extension preceding the J-domain, but lack a PEXEL/HT motif or signal sequence required for secretion into the parasitophorous vacuole or erythrocyte cytosol respectively (HILLER** *et al.*, **2004; MARTI** *et al.*, **2004; NIELSEN** *et al.*, **1997). Although this does not exclude the possibility of export, it supports the notion that these Hsp40 proteins serve as parasite-resident co-chaperones. PSortII protein localisation predictions suggest that Pfj1 may localise to the parasite nucleus, while PfHsp40 may be predominantly cytosolic (NAKAI and HORTON, 1999).**

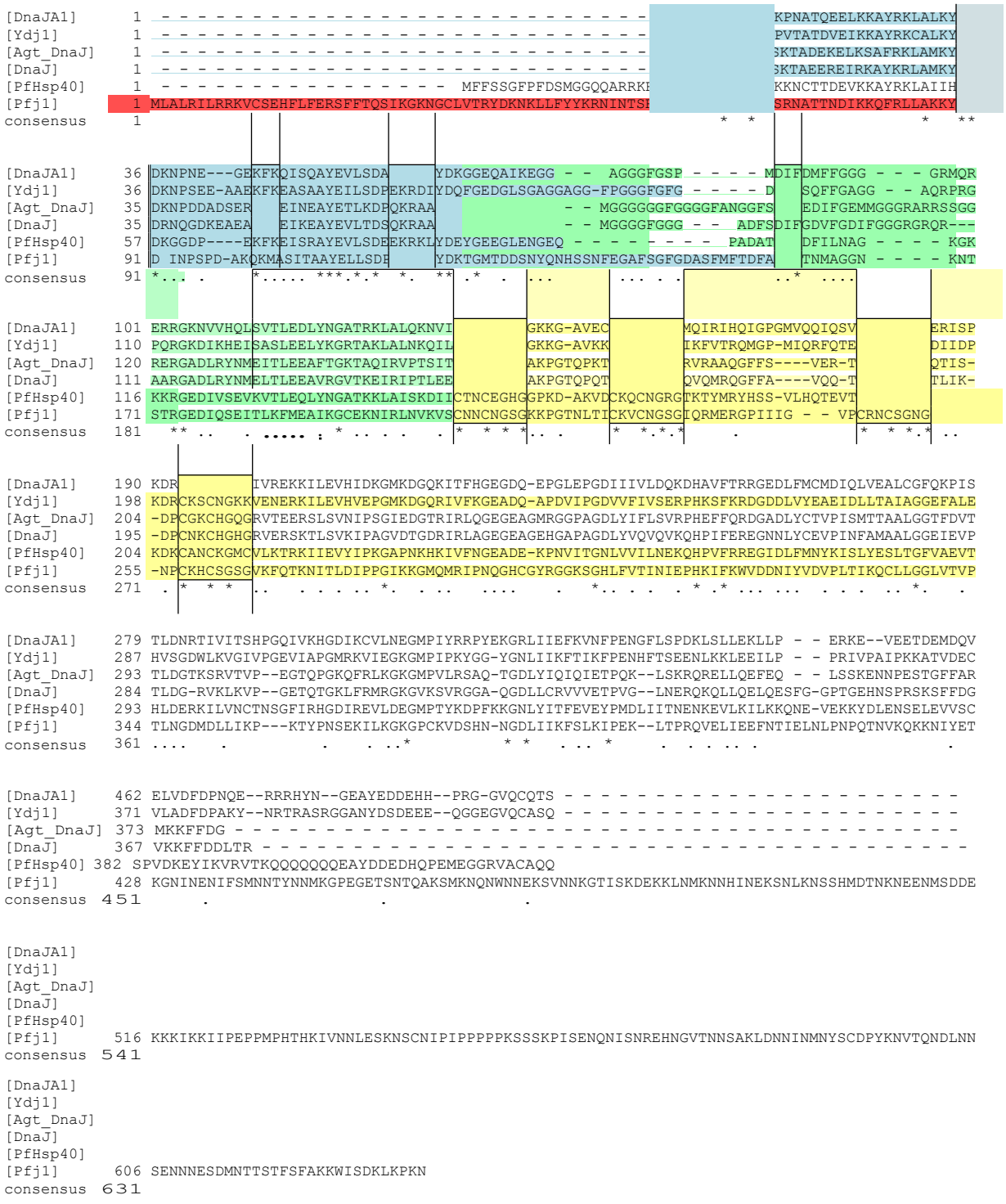

FIGURE 2.2 Protein sequence alignment of PfHsp40, Pfj1 and type ▮Hsp40 proteins of eukaryotic and prokaryotic origin. **Protein sequences aligned include that of the *H. sapiens* Hsp40, DnaJA1 (NP_001530.1), *S. cerevisiae* Hsp40, Ydj1 (CAA95937.1), *A. tumefaciens* DnaJ (*Agt* DnaJ; AAR84666.1), *E. coli* DnaJ (DnaJ; P08622.3), and the *P. falciparum* Hsp40 proteins, PfHsp40 (PF14_0359; NP_702248.1) and Pfj1 (PFD0462w; NP_702750.1). The N-terminal extensions of PfHsp40 and Pfj1 are highlighted in red boxes. The highly conserved J-domain is indicated in blue with the conserved HPD, KFK and QKRAA motifs indicated in black boxes. The GF-region is indicated in green with the conserved DIF motif highlighted in a black box (CAJO *et al.*, 2006). The zinc-finger motifs of the zinc-binding domain (yellow) are similarly indicated in black boxes. Residues indicated in red align to the Ydj1 residues proposed to comprise the interaction surface with non-native polypeptide substrates (LI and SHA, 2005). The CAAX-box motifs of PfHsp40, Ydj1 and DnaJA1 are highlighted in grey. Conserved identical and similar residues are indicated in the consensus line by the symbols '*' and '.' respectively. The alignment was performed using ClustalW (version 1.83; CHENNA *et al.*, 2003).**

The protein sequence of PfHsp40 reveals a putative C-terminal CAAX-box motif which may implicate the protein in intracellular membrane interactions or associations with the Hsp90 multi-chaperone complex following post-translational farnesylation (FARH *et al*., 1995; FLOM *et al*., 2008). CAAX-box motifs are evident in the related eukaryotic type I Hsp40 proteins of *S. cerevisiae* (Ydj1) and *H. sapiens* (DnaJA1), and are similarly accompanied by an incomplete fourth cysteine repeat sequence in the zinc-binding domain (CXXCXGXC). Loss of Ydj1 function in the absence of farnesylation of the CAAX-box motif has been demonstrated (CAPLAN *et al*., 1992; FLOM *et al*., 2008) suggesting a related critical role for the CAAX-box motif of PfHsp40 (refer to *SECTION 1.3.6.1.4, CHAPTER 1*). Importantly, farnesyltransferase enzymes responsible for CAAX-box farnesylation have been identified in *P. falciparum*, and inhibitors of these enzymes have proven successful as anti-malarial compounds (SCHLITZER, 2005). An additional distinguishing feature of the PfHsp40 C-terminus includes a glutamine repeat sequence of unknown function preceding the CAAX-box motif (*FIGURE 2.2*).

In line with the proposed divergent function of Pfj1, the protein exhibits an extended C-terminus characterised by regions of low complexity that do not align to the characteristic C-termini of more typical type I Hsp40 proteins (*FIGURE 2.2*). These regions are rich in lysine, proline and asparagine residues and appear to be predominantly helical in structure based on the CHOU-FASMAN and GARNIER-ROBSON methods of secondary structure prediction (CHOU and FASMAN, 1974; GARNIER *et al*., 1978, 1996).

2.3 HOMOLOGY MODELLING

2.3.1 Modelling of the Domains of PfHsp40 and Pfj1

Homology modelling was employed in the prediction of the tertiary structure of the J-domains, zinc-binding domains and substrate-binding domains of Pfj1 and PfHsp40 respectively, shown in *FIGURE 2.3*. The homology models were generated using the software package Modeller (version 8.2; FISER *et al*., 2000; MARTI-RENOM *et al*., 2000; SALI and BLUNDELL, 1993) and the protein modelling server SWISS -MODEL (SCHWEDE *et al*., 2003). Protein structure templates were identified using fold recognitions servers 3D-PSSM (version 2.6.0; KELLEY *et al*., 2000) and GenTHREADER (version 8.1; JONES, 1999) and the corresponding co-ordinates were retrieved from the Protein Data Bank (BERMAN *et al.,* 2003). The generated homology models do not incorporate portions of the N- and C-termini of PfHsp40 and Pfj1 that do not align with the specified homology modelling templates, evident in the alignment in *FIGURE 2.2*. The position of the conserved catalytic residues of the HPD motif and the peptide binding pocket of these two Hsp40 proteins, lends itself to their potential conserved co-chaperone roles.

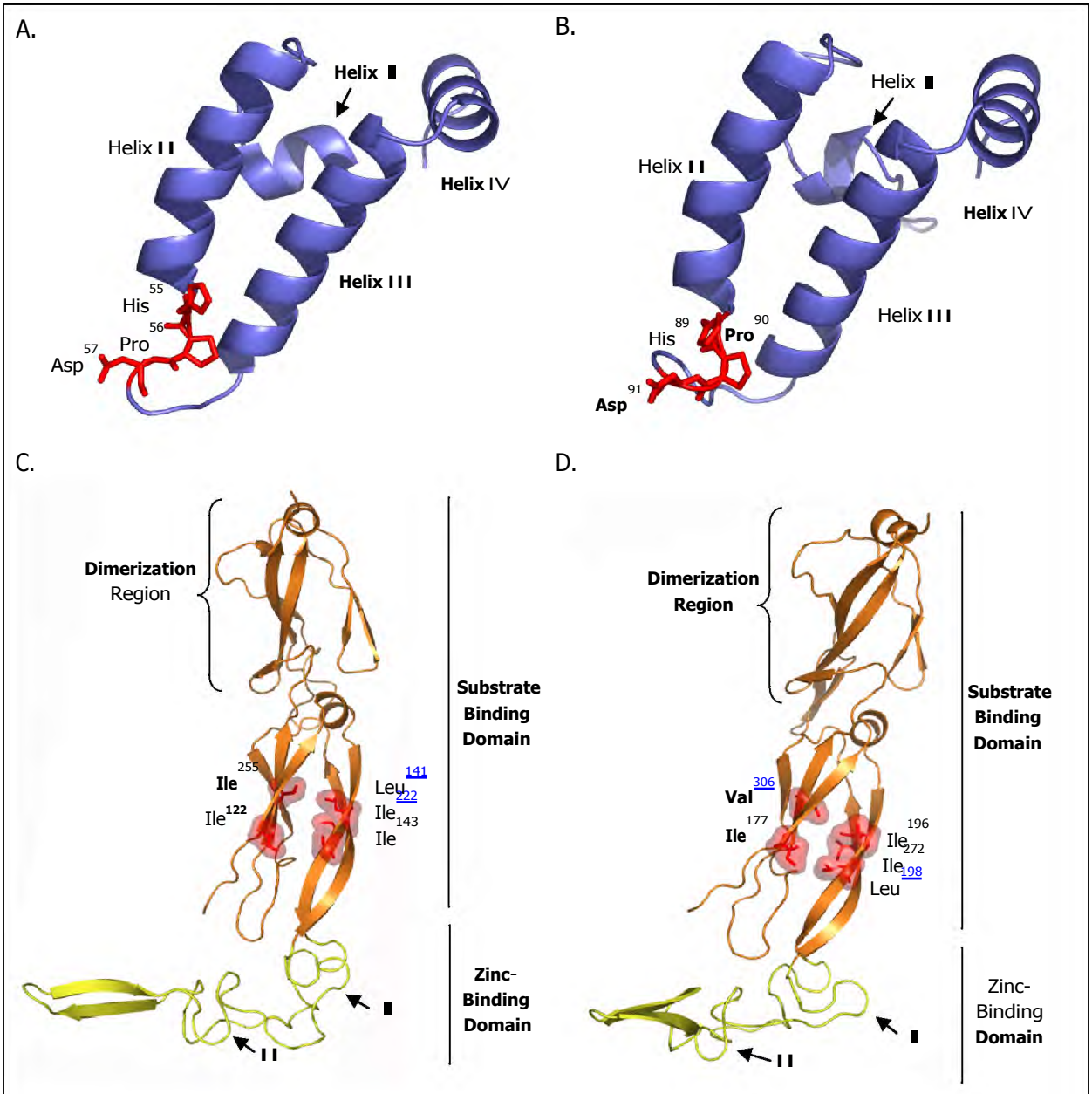

FIGURE **2.3 Homology** models **of the conserved Hsp40 domains of PfHsp40 and Pfj1. Models of the J-domain (blue), zinc-binding domain (yellow) and substrate-binding domain (orange) of Pf Hsp40 (A and C) and Pfj1 (B and D) are indicated. Modelling of the J-domains was performed using crystal structures of the J-domain of** E. coli **DnaJ (PDB: 1XBL, IBQ0 and 1BQZ; HUANG** et al., **1999; PELLECHIA et al., 1996) and the human Hsp40, DnaJB1 (PDB: 1HDJ; Q IAN** et al., **1996) as templates (TABLE 1.1,** CHAPTER 1**). Positions of the four helices (I- IV) comprising the J-domains are indicated (A and B). Residues of the highly conserved HPD motif of the J-domain are indicated in red in the loop region between helices II and III. The modelling of the zinc- and substrate-binding domains (C and D) was performed using the crystal structure of the C-terminus of the S. cerevisiae Hsp40 protein, Ydj1 , as a template (PDB: 1NLT; LI** et al., **2003). Indicated in red are the residues of PfHsp40 (Ile^{122}, Leu^{141}, Ile^{143}, Ile^{222}, Ile^{255}) and Pfj1 (Ile^{177}, Ile^{196}, Leu^{198}, Ile^{272}, Val^{306}) which correspond to residues proposed to comprise the substrate binding site of Ydj1 to the peptide 'GWLYEIS' (Ile^{116}, Leu^{135}, Leu^{137}, Leu^{216} and Phe^{249} respectively; LI and SHA, 2005). The two zinc-binding centres of the zinc-binding domain are indicated (I and II) comprised of the two outermost and two innermost cysteine-repeat sequences with respect to primary amino acid sequence. Models were generated using the homology modelling software Modeller (version 8.2; FISER et al., 2000; MARTI-RENOM** et al., **2000; SALI and BLUNDELL, 1993) and validated through use of the homology modelling server, SWISS-MODEL (SCHWEDE** et al., **2003). Stereochemical quality of the models was validated with ProSA (SIPPL, 1993) and Procheck (version 3.5; LASKOWSKI** et al., **1993). Images of the homology models were rendered using PyMol (version 0.95; DELANO , 2005).**

2.3.2 Modelling of the Proposed Hsp70 Partner of PfHsp40 and Pfj1

The crystal structure of bovine Hsc70 complexed with the J-domain of bovine auxilin has revealed Hsp70 residues thought to comprise the interaction surface with partner Hsp40 proteins (JIANG *et al.*, 2007). An alignment of the protein sequence of PfHsp70-I with bovine Hsc70 (*FIGURE 2.4*) indicates the conservation of corresponding residues in the vicinity of the interdomain interface. The protein sequence of the prokaryotic Hsp70, *E. coli* DnaK was included as a reference in the alignment, to highlight residues implicated in interactions with the J-domain of the *E. coli* Hsp40 protein, DnaJ.

```
[PfHsp70-I]     1 MASAKGSKPNLPESNIAIGIDLGTTYSCVGVWRNENVDIIANDQGNRTTPSYVAFT-DTERLIGDAAKNQVARNPENTVFDAKRLIGRKF
[BtHsc70]       1 --MSKGP - - - - AVGIDLGTTYSCVGVFQHGKVEIIANDQGNRTTPSYVAFT-DTERLIGDAAKNQVAMNPTNTVFDAKRLIGRRF
[DnaK]          1 --MGK - - - - - IIGIDLGTTNSCVAIMDGTTPRVLENAEGDRTTPSIIAYTQDGETLVGQPAKRQAVTNPQNTLFAIKRLIGRRF
consensus       1   ..*.          ..*******.***...    .....*..*.*****..*.* *.*.*.*..**.*.. ** **.*..******.*

                                                                                          Y ND
[PfHsp70-I]    90 TESSVQSDMKHWPFTVKSGVDEKPMIEVTYQGEKKLFHPEEISSMVLQKMKENAEAFLGKSIKNAVITVPAYFNDSQRQATKDAGTIAGL
[BtHsc70]      79 DDAVVQSDMKHWPFMVVNDAG-RPKVQVEYKGETKSFYPEEVSSMVLTKMKEIAEAYLGKTVTNAVVTVPAYFNDSQRQATKDAGTIAGL
[DnaK]         78 QDEEVQRDVSIMPFKIIAADNGDAWVEVK--GQK--MAPPQISAEVLKKMKKTAEDYLGEPVTEAVITVPAYFNDAQRQATKDAGRIAGL
consensus      91  .  **.*....** .. .   .. ..* . *... . *...*..** ***. **..**      **.********.*********.****

               LR  N  T                                          I
[PfHsp70-I] 180 NVMRIINEPTAAAIAYGLHKKGKGEKNILIFDLGGGTFDVSLLTIEDG----IFEVKATAGDTHLGGEDFDNRLVNFCVEDFKRKNRGKD
[BtHsc70]   168 NVLRIINEPTAAAIAYGLDKKVGAERNVLIFDLGGGTFDVSILTIAAG----IFEVKSTAGDTHLGGEDFDNRMVNHFIAEFKRKHK-KD
[DnaK]      164 EVKRIINEPTAAALAYGLDK-GTGNRTIAVYDLGGGTFDISIIEIDEVDGEKTFEVLATNGDTHLGGEDFDSRLINYLVEEFK-KDQGID
consensus   181 .*.**********.****.*.......... ********.*...*...    .***..*.***********.*..*. ...**.* ...*

[PfHsp70-I] 266 LSKNSRALRRLRTQCERAKRTLSSSTQATIEIDSLFEGID----YSVTVSRARFEELCIDYFRDTLIPVEKVLKDAMMDKKSVHEVVLVG
[BtHsc70]   253 ISENKRAVRRLRTACERAKRTLSSSTQASIEIDSLYEGID----FYTSITRARFEELNADLFRGTLDPVEKALRDAKLDKSQIHDIVLVG
[DnaK]      252 LRNDPLAMQRLKEAAEKAKIELSSAQQTDVNLPYITADATGPKHMNIKVTRAKLESLVEDLVNRSIEPLKVALQDAGLSVSDIDDVILVG
consensus   271 .. . .*..**....*.**..***..*.............    . ....**..*.*  *... ...*....*.** .... .....***

                                                  IL  S  V
[PfHsp70-I] 352 GSTRIPKIQTLIKEFFNGKEACRSINPDEAVAYGAAVQAAILSGDQSNAVQDLLLLDVCSLSLGLETAGGVMTKLIERNTTIPAKKSQIF
[BtHsc70]   339 GSTRIPKIQKLLQDFFNGKELNKSINPDEAVAYGAAVQAAILSGDKSENVQDLLLLDVTPLSLGIETAGGVMTVLIKRNTTIPTKQTQTF
[DnaK]      342 GQTRMPMVQKKVAEFF-GKEPRKDVNPDEAVAIGAAVQGGVLTGD----VKDVLLLDVTPLSLGIETMGGVMTTLIAKNTTIPTKHSQVF
consensus   361 *.**.*..*... .**.*** ...*******.*****...*.** . *.*.*****..****.**.***** ** .*****.*..*.*

[PfHsp70-I] 442 TTYADNQPGVLIQVYEGERALTKDNNLLGKFHLDGIPPAPRKVPQIEVTFDIDANGILNVTAVEKSTGKQNHITITNDKGRLSQDEIDRM
[BtHsc70]   429 TTYSDNQPGVLIQVYEGERAMTKDNNLLGKFELTGIPPAPRGVPQIEVTFDIDANGILNVSAVDKSTGKENKITITNDKGRLSKEDIERM
[DnaK]      427 STAEDNQSAVTIHVLQGERKRAADNKSLGQFNLDGINPAPRGMPQIEVTFDIDADGILHVSAKDKNSGKEQKITIKASSG-LNEDEIQKM
consensus   451 .*. ***..*.*.*..***....**..**.* *.**.****..**********.***.*.*..*..**...***....*.*. ..*..*

[PfHsp70-I] 532 VNDAEKYKAEDEENRKRIEARNSLENYCYGVKSSLEDQKIKEKLQPAEIETCMKTITTILEWLEKNQLAGKDEYEAKQKEAESVCAPIMS
[BtHsc70]   519 VQEAEKYKAEDEKQRDKVSSKNSLESYAFNMKATVEDEKLQGKINDEDKQKILDKCNEIINWLDKNQTAEKEEFEHQQKELEKVCNPIIT
[DnaK]      516 VRDAEANAEADRKFEELVQTRNQGDHLLHSTRKQVE--EAGDKLPADDKTAIESALTALETALKGE---DKAAIEAKMQELAQVSQKLME
consensus   541 *..**.....*....... ..*... . . .. ..*. .. .*.. ...  ..  .. .. .*.... ..*...*....*.. *

[PfHsp70-I] 622 KIYQDAAGAAGGMPGGMPGGMPGGMPSGMPGGMNFPGGMPGAGMPGNAPAGSGPTVEEVD
[BtHsc70]   609 KLYQ----SAGGMPGGMPGGMPG - - - - - -  GFPGGGAPPSGGASSGPTIEEVD
[DnaK]      601 IAQQQ---HAQQQTAGAD---AS - - - - - - -  ANNAKDDDVVDAEFEEVKDKK
consensus   631 ...*     *     *                    . .... . . ----------
```

FIGURE 2.4 Identification of potential Hsp40 interaction residues of PfHsp70-I **Alignment of the protein sequences of PfHsp70-I (locus PF08_0054), bovine Hsc70 (*B. taurus* BtHsc70; NP_776770) and the prokaryotic Hsp70, *E. coli* DnaK (BAA01595). Conserved and semi-conserved residues indicated in red align to residues of bovine Hsc70 proposed to mediate interaction with the J-domain of bovine auxilin, a type III Hsp40 (JIANG *et al.*, 2007). These residues are either conserved, semi-conserved or not conserved in *E. coli* DnaK as indicated. Conserved residues highlighted in blue correspond to residues of *E. coli* DnaK suggested to mediate interaction with the J-domain of the *E. coli* type I Hsp40 protein, DnaJ (GÄSSLER *et al.*, 1998; SUH *et al.*, 1998). PfHsp70-I aligns with greater similarity to bovine Hsc70; both proteins bear GGMP repeat sequences (grey) in the C-terminal region, and a C-terminal EEVD motif (black) characteristic of eukaryotic Hsp70 proteins. The EEVD motif is suggested to mediate Hsp70 interactions with Hop and Hsp40 partner proteins, and has been shown to affect Hsp70 substrate binding and ATPase activity (BRINKER *et al.*, 2002; DEMAND *et al.*, 1998; FREEMAN *et al.*, 1995). Conserved identical and similar residues are indicated in the consensus line by the symbols '*' and '.' respectively. The alignment was performed using ClustalW (version 1.83; CHENNA *et al.*, 2003).**

Homology modelling was employed to predict the full length tertiary structure of PfHsp70-I (FIGURE 2.5). Residues corresponding to the proposed Hsp40-interaction surface of bovine Hsc70 are indicated in the model . It is possible that PfHsp40 and Pfj1 interact with these indicated residues of PfHsp70-I

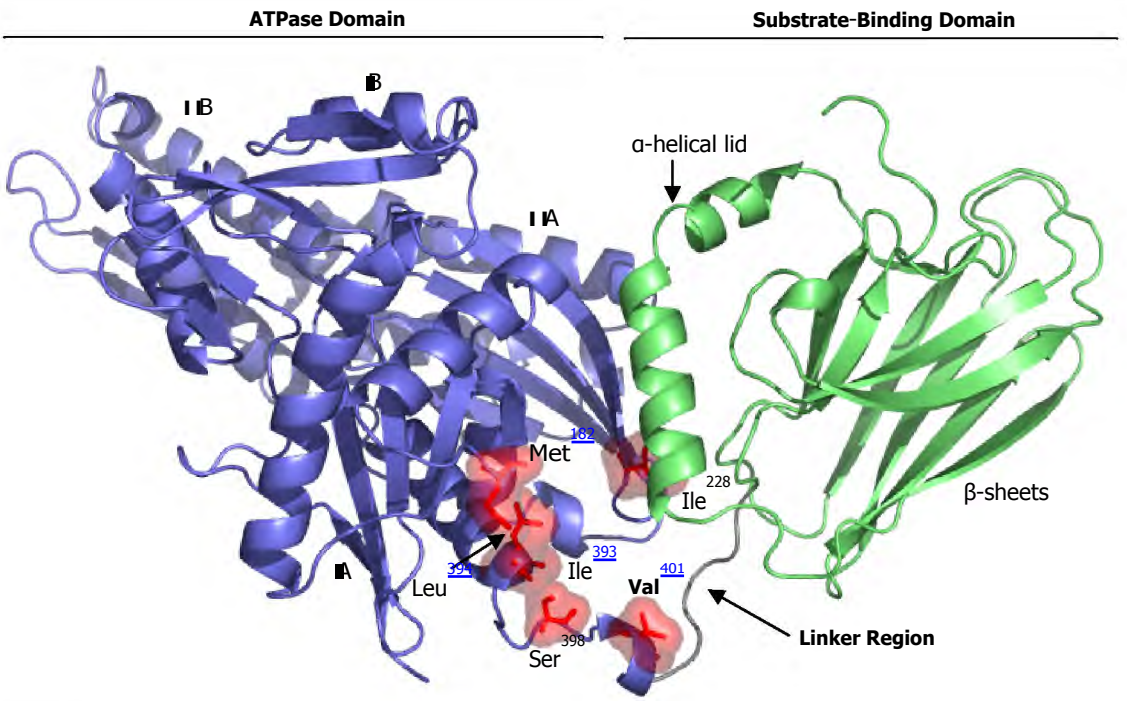

FIGURE 2.5 Homology model of partial full length PfHsp70-I The ATPase domain of the protein is shown in blue with the position of the four lobes of the domain indicated (IA, IIA, IB IIB). The substrate binding domain is shown in green with the β- sheet and α-helical lid subdomains indicated. The ATPase and substrate binding domains are connected by a linker region shown in grey. The model encompasses residues 12 - 567 of the PfHsp70 - I protein sequence, presented in the alignment in FIGURE 2.4. Residues indicated in red (Met^{182}, Ile^{228}, Ile^{393}, Leu^{394}, Ser^{398}, Val^{401}) are thought to comprise the interaction surface with Hsp40 co-chaperone proteins, as they correspond to residues of the crystal structure of bovine Hsc70 complexed with the J-domain of bovine auxilin (JIANG et al., 2007). The model was generated using Modeller (version 8.2; FISER et al., 2000; MARTI-RENOM et al., 2000; SALI and BLUNDELL, 1993) using t he full length crystal structure of bovine Hsc70 as a template (PDB: 1YUW; JIANG et al., 2007). Stereochemical quality of the model was validated with WHAT CHECK (version 4.99g; HOOFT et al. 1996) and the image was rendered using PyMol (DELANO, 2005).

PfHsp70-I residues Leu^{394} and Ile^{393} correspond to residues of bovine Hsc70 that are proposed to exhibit hydrophobic interactions with the His and Asp residues of the HPD motif of auxilin, and a Phe residue of helix III of the J-domain potentially corresponding to the KFK motif (not conserved in the auxilin J-domain). The residues flanking this J-domain Phe residue are proposed to contact the side - chain of the bovine Hsc70 residue corresponding to Val^{401} of PfHsp70-I The carbonyl of the bovine Hsc70 residue corresponding to Met^{182} of PfHsp70-I is thought to exhibit hydrogen bond contacts with the imidazole ring of the His residue of the auxilin HPD motif. Similarly, the side-chain of the bovine Hsc70 residue corresponding to Ser^{398} of PfHsp70 - I is thought to exhibit hydrogen bond interactions with the side-chain of the Asp residue of the HPD motif. Finally, residue Ile^{228} of

PfHsp70-I potentially contacts residues in the loop region preceding helix III of Hsp40 partners. Not shown in *FIGURE 2.5*, residues Ile^{193} and Tyr^{384} of PfHsp70-I correspond to residues of bovine Hsp70 that are suggested to induce a chemical shift to the ATPase domain upon the binding of the auxilin J-domain (JIANG *et al.*, 2007).

It cannot be excluded that the Hsp40-interaction surface of PfHsp70-I differs to that described for the association of bovine Hsc70 with the auxilin J-domain (JIANG *et al.*, 2007). Importantly, auxilin represents a type III Hsp40 protein, and an alignment of the lesser-conserved auxilin J-domain with that of the proposed type I Hsp40 interactors of PfHsp70-I (not shown) reveals distinct differences in residue composition. It is possible that a typical J-domain characteristic of type I Hsp40 proteins may interact with different Hsp70 residues. The proposed position of the Hsp40-interaction surface in the locality of the Hsp70 interdomain interface has been contrasted by previous studies suggesting that the *E. coli* type I Hsp40, DnaJ, interacts with residues on the lower cleft of the ATPase domain of the corresponding Hsp70 protein, DnaK (*FIGURE 2.4;* GÄSSLER *et al.*, 1998; SUH *et al.*, 1998). Corresponding conserved residues implicated in this interaction were identified in the underside cleft of the ATPase domain of PfHsp70-I, including Tyr^{161}, Asn^{163}, Asp^{164}, Glu^{230}, Val^{231} (GÄSSLER *et al.*, 1998), Arg^{183}, Asn^{186} and Thr^{189} (SUH *et al.*, 1998). Notably, residues Met^{182}, Ile^{228} and Ser^{398} of PfHsp70-I are not conserved in the *E. coli* DnaK sequence, but correspond to residues of the proposed bovine Hsc70-Hsp40 interaction surface (*FIGURE 2.4*; JIANG *et al.*, 2007). Moreover, the complex revealed in the bovine Hsc70-auxilin J-domain crystal structure was achieved by disulfide linkage, raising the concern of the presence of non-functional or false residue associations in the complex (JIANG *et al.*, 2007). The underside cleft of the bovine Hsc70 ATPase domain may serve as a more appropriate docking site for the J-domain of auxilin, as shown *in silico* by GRUSCHUS *et al.* (2004). Nevertheless, the findings of the JIANG *et al.* (2007) study support suggestions that elements of J-domain conservation, such as the HPD motif and Phe residue of the KFK motif, are crucial to interactions with Hsp70 partners in general (GENEVAUX *et al.*, 1997, HENNESSY *et al.*, 2000, 2005a,b; TSAI and DOUGLAS, 1996) and these elements were identified in both PfHsp40 and Pfj1 (*FIGURES 2.2* and *2.3*).

2.4 ANALYSIS OF GENE EXPRESSION

Genome studies have suggested that the organisation of genes in a eukaryotic genome is not random, lending itself to co-ordinated gene co-expression and in certain cases indicating gene co-functionality (MICHALAK *et al.*, 2008). Mechanisms underlying the regulation of gene expression in *P. falciparum* appear to be complex and multi-factorial (GUNASEKERA *et al.*, 2007) however transcriptomic data from gene expression profiles have provided insight into the expression of various proteins during the developmental stages of the parasite's lifecycle (LE ROCH *et al.*, 2003). The gene expression

profiles of PfHsp70-I (PF08_0054) and PfHsp40 (PF14_0359) were extracted from the representation of this data in the PlasmoDB database (BAHL *et al.*, 2003) as shown in *FIGURE 2.6*. The expression profile of the type II Hsp40 Sis1 homolog encoded by PFB0595w was included as a reference.

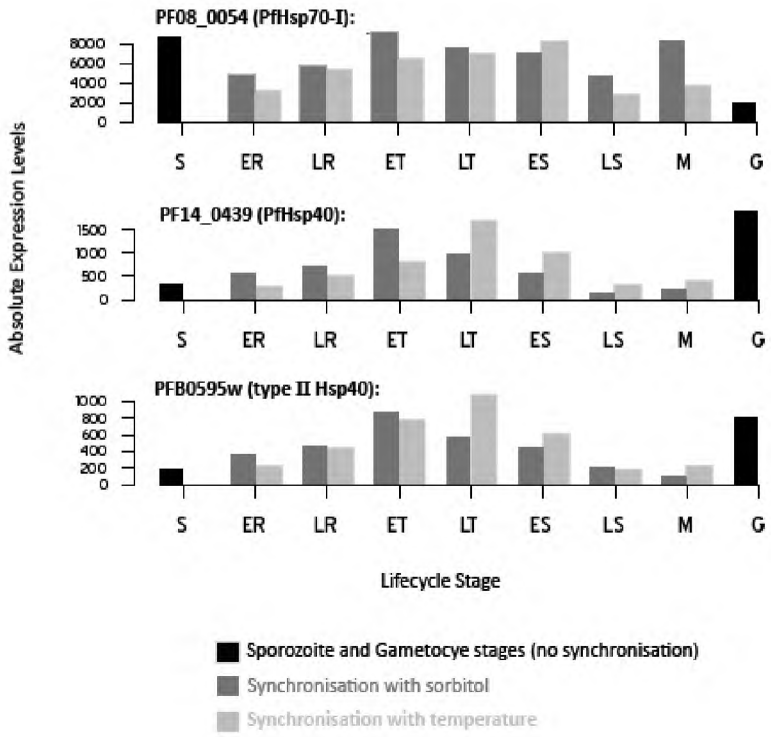

FIGURE 2.6 Gene expression profiles of PfHsp70-I and PfHsp40 during the course of *P. falciparum* development. **Stage-specific expression levels of PfHsp70-I (upper panel; PF08_0054) PfHsp40 (middle panel; PF14_0359) and a type II Hsp40 identified as a Sis1 homolog (lower panel; PFB0595w) in cultured *P. falciparum* 3D7 parasites. Lifecycle stages of the parasite are abbreviated as follows: *S* – sporozoite, *ER* – early ring, *LR* – late ring, *ET* – early trophozoite, *LT* – late trophozoite, *ES* – early schizont, *LS* – late schizont, *M* – merozoite, and *G* – gametocyte. Parasite cultures were synchronised as specified with sorbitol or temperature, with the exception of the sporozoite and gametocyte stages. Lifecycle stages are listed in order of development. The data was extracted from a study of *P. falciparum* gene expression profiling (LE ROCH *et al.*, 2003). The figure adapted from that presented in PlasmoDB (BAHL *et al.*, 2003).**

Interestingly, PfHsp70-I (PF08_0054) and PfHsp40 (PF14_0359) appear to follow similar patterns of transcriptional upregulation, with the exception of the gametocyte and sporozoite stages of development. Absolute expression levels show a steady increase from the early ring stages, with most expression proposed to be occurring in the intraerythrocytic trophozoite stages (*FIGURE 2.6*). The expression levels appear to taper off in the schizont stages, with lessened PfHsp40 expression anticipated in the merozoite stage. This is suggestive of similar patterns of upregulation in the erythrocytic stage parasites and is potentially indicative of the proposed interaction between PfHsp70-I and PfHsp40. Notably, the absolute expression levels of PfHsp70-I emphasise that this protein is amongst the most abundant produced by the parasite (PATANKAR *et al.*, 2001). A corresponding expression profile for gene PFD0462w encoding Pfj1 was unavailable, however

transcriptional data derived from a different study indicated that the protein may be consistently expressed in the ring, trophozoite and schizont intraerythrocytic stages of development (BOZDECH *et al.*, 2003). Moreover, this was initially proposed by WATANABE (1997). Cautiously, it must be noted that the protein expression levels depicted in *FIGURE 2.6* are based on the assumption that transcriptional upregulation is indicative of the upregulation of protein expression. Confirmation of the production of PfHsp70-1, PfHsp40 and Pfj1 in the intraerythrocytic stages of *P. falciparum* development is provided in *CHAPTER 4*.

The protein encoded by gene PFB0595w has been identified as the only typical parasite-resident type II Hsp40 protein in *P. falciparum* (referred to as PfSis1 in this study; *SECTION 2.5.1.2*). PfHsp40 and PfSis1 therefore represent the only typical type I and II parasite-resident Hsp40 proteins respectively, suggesting implications for these proteins in the facilitation of general protein folding processes in the parasite with the highly abundant PfHsp70-1. Consistent with this, the gene expression profile of PFB0595w presented in *FIGURE 2.6* appears to match that of PF14_0359 (PfHsp40) and similarly corresponds to the expression profile of PF08_0054 (PfHsp70-1) in the erythrocytic stage parasites.

2.5 BIOINFORMATIC ANALYSIS OF THE ENTIRE HSP40 COMPLEMENT OF *P. FALCIPARUM*

2.5.1 Identification and Classification of P. falciparum Hsp40 Proteins

Hsp40 proteins were initially identified from the genome sequence of *P. falciparum* by a BLAST search (Basic Local Alignment Search Tool; ALTSCHUL *et al.*, 1997) using the classical J-domain of *E. coli* DnaJ as a reference (Pfam accession PF00226). The Hsp40 protein complement of the organism was determined to be comprised of forty-three member proteins, categorised in *TABLE 2.1*. Here, the further categorisation of Hsp40 proteins has been proposed, complementary to the classification described by CHEETHAM and CAPLAN (1998). Hsp40 proteins exhibiting variation in the highly conserved HPD motif of the J-domain were classed into an independent category (type IV). It is known that the alteration of residues of the HPD motif abolishes interaction with Hsp70 partner proteins (GENEVAUX *et al.*, 2001; LAUFEN *et al.*, 1999; MAYER *et al.*, 1999; TSAI and DOUGLAS, 1996; WITTUNG-STAFSHEDE *et al.*, 2003), suggesting that the type IV Hsp40 proteins exert their *in vivo* functionality via a different mechanism. In contrast, it has been suggested that Hsp40 proteins that exhibit non-conservative substitutions in the HPD motif imitate 'true' J-domain proteins resulting in a more complex regulation of Hsp70 (WALSH *et al.*, 2004). Interestingly, the majority of the type IV Hsp40 proteins of *P. falciparum* are predicted to be exported to the erythrocyte cytoplasm (*TABLE 2.1*), thus the latter argument could have profound implications for the manner in which these proteins potentially interact with host cell proteins during erythrocyte remodelling or associated parasite processes.

TABLE 2.1 The *P. falciparum* Hsp40 Protein Complement: Classification, Prediction of Export and Localisation

Type[1]	Locus[2]	Protein[3]	Protein description[3,4]	Export / Secretory Signal			TMD[8]	Localisation		
				PEXEL[5]	HT[6]	SP[7]		PSortII[9]	Putative / Other	Reference
I	PF14_0359	NP_702248.1	DnaJ homolog, PfHsp40	-	-	-	0	Cytoplasm	N.D.	
	PFD0462w	NP_702750.1	DnaJ homolog, Pfj1	-	-	-	0	Nucleus	Apicoplast	10
II	PFA0660w	NP_703333.1	DnaJ homolog, Dnj1/Sis1 family	+	-	-	0	Mitochondria	iRBC	5, 11
	PFB0090c	NP_472947.2	Hypothetical protein	+	-	-	0	Nucleus	iRBC	5, 11
	PFE0055c	NP_703357.1	Heat shock protein, putative	+	+	-	1	Nucleus	Apicoplast, iRBC Maurer's clefts	5, 6, 10, 11, 12
	PF11_0099	NP_700963.1	DnaJ homolog Pfj2, similar to PDIa and ERdj5 protein family	+	-	+	1	Golgi apparatus	iRBC, ER, Mitochondria	5, 11
	MAL13P1.277	NP_705450.1	DnaJ-like protein, putative	-	-	-	0	Cytoplasm	Mitochondria	13
	PF14_0137	NP_702025.1	Hypothetical protein	-	-	+	5	Plasma membrane	Apicoplast	10
	PFB0595w	NP_473047.1	Dnj1/Sis1 homolog, PfSis1	-	-	-	0	Nucleus	N.D.	
	PFF1415c	XP_966274.1	DnaJ protein	-	-	-	0	Extracellular	Apicoplast	10
	PFL0565w	NP_701478.1	DnaJ homolog Pfj4	-	-	-	0	Nucleus	N.D.	17
III	PF10_0378	NP_700851.1	DnaJ homolog Pfj3	+	-	+	1	Plasma membrane	Apicoplast, iRBC, Mitochondria	5, 10, 11, 13
	PF11_0513	NP_701358.1	Hypothetical protein	+	-	-	0	Nucleus / Cytoplasm	iRBC	11
	PFB0920w	NP_473112.2	Hypothetical protein with HRPI/III region	+	+	-	2	Nucleus	iRBC, Mitochondria	5, 6, 11, 13
	PFL0055c	NP_701376.1	DnaJ protein (RESA-like), putative	+	-	-	1	Nucleus	iRBC, Mitochondria	5, 11, 13
	PF07_0103	NP_704176.1	Chaperone protein, putative	-	-	+	0	Cytoplasm	Apicoplast	10
	PF08_0032	NP_704316.1	Hypothetical protein, similar to PDIa and ERdj5	-	-	-	3	Plasma membrane	N.D.	
	PF08_0115	NP_704487.1	Hypothetical protein	-	-	-	0	Nucleus	N.D.	
	PF10_0032	NP_700506.1	Hypothetical protein	-	-	-	1	Nucleus	N.D.	
	PF10_0058	NP_700532.1	Hypothetical protein with Dcp and ZUO1 regions	-	-	-	0	Nucleus	Mitochondria, Nucleus	4, 13
	PF11_0273	NP_701133.1	Hypothetical protein	-	-	-	0	Nucleus	N.D.	
	PF11_0380	NP_701239.1	Hypothetical protein	-	-	-	1	Nucleus / ER	N.D.	
	PF13_0036	NP_704971.1	DnaJ protein, putative	-	-	-	0	ER	N.D.	
	PF13_0102	NP_705096.1	DnaJ protein, Sec63 homolog	-	-	-	3	ER	ER membrane	4, 14
	PF14_0700	NP_702589.1	Hypothetical protein	-	-	-	0	Nucleus	N.D.	

TABLE 2.1.../

/...TABLE 2.1

III	PFE0135w	NP_703373.1	Hypothetical protein	-	-	-	0	Nucleus	N.D.	
	PFE1170w	NP_703578.1	Hypothetical protein with MRS6 region	-	-	-	2	ER	N.D.	
	PFF1290c	NP_705208.1	Hypothetical protein	-	-	-	0	Mitochondria	Apicoplast, Mitochondria	10, 13
	PFI0935w	NP_704730.1	DnaJ protein, putative	-	-	+	6	ER	N.D.	
	PFI0985c	NP_704740.1	Chaperone protein	-	-	-	0	ER	Mitochondria	13
	PFL0815w	NP_701527.1	Putative DNA-binding chaperone with ZUO1 region	-	-	-	0	Nucleus	Nucleus, Ribosomes	4
IV	PF10_0381	NP_700854.1	Hypothetical protein	+	-	-	1	Nucleus	iRBC, Mitochondria	5, 11, 13
	PF11_0034	NP_700899.1	Hypothetical protein	+	-	-	1	ER	iRBC, Mitochondria	5, 11, 13
	PF14_0013	NP_701901.1	Hypothetical protein	+	-	-	0	Nucleus	iRBC	11
	PFB0085c	NP_472946.1	Hypothetical protein	+	-	+	1	Golgi apparatus	iRBC, Mitochondria	5, 11, 13
	PFL2550w	NP_701868.1	Hypothetical protein	+	+	+	0	Nucleus	Apicoplast, iRBC	5, 6, 10, 11
	PFB0925w	NP_473113.2	Hypothetical protein	+	-	+	0	Plasma membrane	Apicoplast, iRBC	5, 10, 11
	PFE0040c	NP_703354.1	Mature parasite-infected erythrocyte surface antigen (MESA or PfEMP2)	+	+	-	0	Nucleus	iRBC membrane	5, 6, 11, 15
	RESA / PFA0110w	CAA00077.1 /NP_703225.1	Ring-infected erythrocyte surface antigen, RESA / RESA precursor protein	+	-	-	0	Mitochondria	iRBC, Mitochondria	5, 11, 13, 16
	PFA0675w	NP_703336.1	RESA-like protein	+	-	-	0	Nucleus	iRBC	11
	PF11_0509	NP_701354.1	RESA protein, putative	+	-	-	0	Nucleus	iRBC, Mitochondria	5, 11, 13
	PF11_0512	NP_701357.1	Ring-infected erythrocyte surface antigen 2, RESA-2	+	-	-	1	Nucleus	iRBC, Mitochondria	5, 11, 13
	PF11_0443	NP_701301.1	Hypothetical protein	-	-	+	2	Cytoplasm	Apicoplast	10

[1] CHEETHAM and CAPLAN (1998); [2] BAHL *et al.* (2003); [3] BENSON *et al.* (2008); [4] MARCHLER-BAUER and BRYANT (2004); [5] MARTI *et al.* (2004); [6] HILLER *et al.* (2004); [7] NIELSEN *et al.* (1997), NIELSEN and KROCH (1998); [8] KROGH *et al.* (2001); [9] NAKAI and HORTON (1999); [10] ZUEGGE *et al.* (2001); [11] SARGEANT *et al.* (2006); [12] VINCENSINI *et al.* (2005); [13] BENDER *et al.* (2003); [14] FELDHEIM *et al.* (1992); [15] COPPEL *et al.* (1988); [16] BROWN *et al.* (1985); [17] PESCE *et al.* (2008); N.D. – not determined; PEXEL – Protein Export Element; HT – Host-targeting Signal; SP – Signal Peptide; TMD – Transmembrane Domain; iRBC – infected red blood cell (erythrocyte); ER – Endoplasmic reticulum.

2.5.1.1 Type I Hsp40 Proteins

The presence of only two identified type I Hsp40 proteins in *P. falciparum* (*TABLE 2.1*) contrasts with the six reported type I Hsp40 proteins in the human host (QIU *et al*., 2006). Importantly, the two corresponding type I Hsp40 proteins identified in the apicomplexan parasites (*TABLE 2.2*) appear to be homologous to PfHsp40 and Pfj1 respectively, suggesting distinct and crucial roles for these proteins in the respective parasitic organisms. An alignment of the homologous protein sequences is provided in *APPENDIX G1*, illustrating Hsp40 domain conservation in relation to the human type I Hsp40, DnaJA1. The presence of only two type I Hsp40 proteins may represent an inherent weakness of the apicomplexa, considering that this Hsp40 class is crucial to protein folding processes.

Apicomplexan orthologs of PfHsp40 (PF14_0359; *TABLE 2.2*) are similarly predicted to be cytosolic and may be engaged in the maintenance of standard 'house-keeping' co-chaperone processes in the respective apicomplexa. As observed for PfHsp40, these homologs exhibit a glutamine repeat sequence in the C-terminal domain preceding the conserved CAAX-box motif, in addition to an incomplete fourth cysteine-repeat sequence in the zinc-binding domain (*APPENDIX G1*). Apicomplexan homologs of Pfj1 (PFD0462w; *TABLE 2.2*) similarly exhibit a lengthier N-terminal extension and an extended C-terminal domain rich in proline, lysine and asparagine residues. It is possible that these proteins exhibit a more specialised role in interaction with Hsp70 partner proteins, perhaps in distinct subcellular compartments.

Interestingly, in the Pfj1 homologs and in the majority of the *P. falciparum* type II Hsp40 proteins, the absence of a conserved DIF motif in the GF region (WALL *et al*., 1995; CAJO *et al*., 2006) appears to be consistent with the prevalence of Ser residues, comprising a GFS-rich region (*APPENDICES H1 and H2*). An abundance of serine residues has similarly been observed in the GF region of the *Drosophila* Hsp40 protein and related orthologs including human DnaJ136, and is proposed to signify the evolutionary specialisation of these proteins (FAYAZI *et al*., 2006). In contrast, PfHsp40 and its homologs exhibit a conserved DIF or DLF motif in the absence of serine residues in the GF region (*APPENDIX G1*). These distinguishing features may represent significant differences in the manner in which these different type I Hsp40 proteins facilitate substrate transfer and therefore regulate the substrate-binding capabilities of Hsp70 proteins.

2.5.1.2 Type II Hsp40 Proteins

Four of the type II Hsp40 proteins of *P. falciparum* are predicted to be exported to the host erythrocyte (*TABLE 2.1*). Three of these proteins - encoded by PFA0660w, PF130090c and PFE0055c - resemble the *S. cerevisiae* type II Hsp40, Sis1, and exhibit a high degree of sequence identity

TABLE 2.2 Apicomplexan Protein Homologs of *P. falciparum* Hsp40 and Hsp40-like proteins

Type	Export[1]	Accession Number[2] Locus	Accession Number[3] Protein	Accession Numbers of Identified Apicomplexan Protein Homologs[2,3,4] *C. hominis*	*C. parvum*	*P. berghei*	*P. chabaudi*	*P. yoelii*	*P. vivax*	*T. annulata*	*T. parva*	*T. gondii*
I	-	PF14_0359	NP_702248.1	XP_667910.1	XP_627269.1	XP_679772.1	XP_745900.1	XP_730359.1	Pv084650	XP_954074.1	XP_766227.1	583.m05418
		PFD0462w	NP_702750.1	-	XP_626357.1	XP_680440.1	XP_744117.1	XP_724346.1	-	XP_952612.1	XP_764665.1	CAJ20509.1
II	+	PFA0660w	NP_703333.1	-	-	-	-	-	-	-	-	-
		PFB0090c	NP_472947.2	-	-	-	-	-	-	-	-	-
		PFE0055c	NP_703357.1	-	-	-	-	-	-	-	-	-
		PF11_0099	NP_700963.1	XP_667246.1	cgd2_3230	BAD99308.1	XP_740487.1	XP_727981.1	Pv091110	XP_953331.1	XP_764324.1	20m.03869
	-	PFF1415c	XP_966274.1	XP_667385.1	XP_625863.1	XP_678015.1		XP_723708.1	-	XP_954671.1	XP_765562.1	55.m00016
		PFB0595w	NP_473047.1	XP_667435.1	-	XP_675336.1	XP_745867.1	XP_730944.1	-	XP_952090.1	XP_765191.1	57.m00015
		MAL13P1.277	NP_705450.1	-	-	-	-	-	-	-	-	-
		PF14_0137	NP_702025.1	XP_667991.1	XP_627182.1	XP_677556.1	XP_742984.1	XP_726085.1	Pv085755	-	-	-
		PFL0565w	NP_701478.1	XP_667885.1	CAD98554.1	XP_676696.1	XP_741048.1	XP_728950.1	Pv084600	XP_954119.1	XP_766186.1	-
III	+	PF10_0378	NP_700851.1	-	-	-	-	-	-	-	-	-
		PFB0920w	NP_473112.2	-	-	-	-	-	-	-	-	-
		PF11_0513	NP_701358.1	-	-	-	-	-	-	-	-	-
		PFL0055c	NP_701376.1	-	-	-	-	-	-	-	-	-
	-	PFE0135w	NP_703373.1	-	-	XP_678174.1	XP_743161.1	XP_724990.1	-	-	-	-
		PF07_0103	NP_704176.1	XP_667828.1	XP_626275.1	XP_678535.1	XP_741054.1	XP_729396.1	Pv096125	XP_952363.1	-	20.m05961
		PF08_0032	NP_704316.1	XP_666525.1	XP_626829.1	-	-	XP_724808.1	-	-	-	-
		PF10_0032	NP_700506.1	-	-	-	-	-	-	-	-	-
		PF10_0058	NP_700532.1	-	-	-	-	-	-	-	-	-
		PF11_0273	NP_701133.1	-	-	-	-	-	-	-	-	-
		PF11_0380	NP_701239.1	XP_667820.1	XP_626267.1	XP_672208.1	XP_733803.1	XP_726262.1	Pv092455	-	-	-
		PF13_0036	NP_704971.1	XP_666126.1	XP_625506.1	XP_680251.1	XP_741274.1	XP_730442.1	-	-	-	-
		PF13_0102	NP_705096.1	XP_668030.1	XP_628550.1	XP_676782.1	XP_742674.1	XP_731267.1	-	XP_952225.1	XP_765056.1	55.m00017
		PFF1290c	NP_705208.1	-	-	-	-	-	-	-	-	-
		PFE1170w	NP_703578.1	XP_668519.1	XP_627223.1	XP_674936.1	XP_743132.1	XP_723904.1	-	XP_952494.1	XP_764787.1	50.m00025
		PFI0985c	NP_704740.1	-	-	-	-	-	-	-	-	-
		PFL0815w	NP_701527.1	-	-	XP_679805.1	XP_744850.1	XP_729337.1	-	XP_953068.1	XP_764037.1	-
		PF14_0700	NP_702589.1	XP_665120.1	CAD98666.1	-	-	XP_723878.1	-	XP_952907.1	XP_763870.1	-
		PF08_0115	CAD51306.1	-	-	-	-	-	-	-	-	583.m00680
		PFI0935w	NP_704730.1	XP_668014.1	XP_628113.1	XP_675745.1	XP_743352.1	XP_725782.1	-	-	-	57.m01857

TABLE 2.2.../

/...TABLE 2.2

IV	+	PF10_0381	NP_700854.1	-	-	-	-	-	-	-	-	-
		PF11_0034	NP_700899.1	-	-	-	-	-	-	-	-	-
		PFB0925w	NP_473113.2	-	-	-	-	-	-	-	-	-
		PFB0085c	NP_472946.1	-	-	-	-	-	-	-	-	-
		PF11_0509	NP_701354.1	-	-	-	-	-	-	-	-	-
		RESA	CAA00077.1	-	-	-	-	-	-	-	-	-
		PF11_0512	NP_701357.1	-	-	-	-	-	-	-	-	-
	+	PFA0675w	NP_703336.1	-	-	-	-	-	-	-	-	-
		PF14_0013	NP_701901.1	-	-	-	-	-	-	-	-	-
		PFL2550w	NP_701868.1	-	-	-	-	-	-	-	-	-
		PFE0040c	NP_703354.1	-	-	-	-	-	-	-	-	-
	-	PF11_0443	NP_701301.1	-	-	-	XP_740905.1	-	-	-	-	-

[1] MARTI *et al.* (2004), HILLER *et al.* (2004); [2] BAHL *et al.* (2003); [3] BENSON *et al.* (2008), MARCHLER-BAUER and BRYANT (2004); [4] ALTSCHUL *et al.* (1997), CHENNA *et al.* (2003), HEIGES *et al.* (2006) KISSINGER *et al.* (2003), PENKETT *et al.* (2006).

(*APPENDIX G2*). The export status of PFE0055c[2] has been experimentally validated (BHATTACHARJEE *et al*., 2008; HILLER *et al*., 2004). The essentiality of these proteins was investigated with a gene knockout strategy, revealing that only one of the three genes, PFA0660w, could not be disrupted without lethality (MAIER *et al*., 2008). It is not apparent as to which subtle, yet crucial, differences in the exported type II Hsp40 proteins govern the differences in their roles in the erythrocyte. Nevertheless it is evident that certain co-chaperone processes appear to be more essential to the parasite than others, as previously suggested (MAIER *et al*., 2008, WALSH *et al*., 2004). The parasite genome appears to encode a single parasite-resident Sis1 homolog, PfSis1 (PFB0595w) as discussed in *SECTION 2.4*. The protein aligns with significant identity to PFA0660w, PFB0090c and PFE0055c, but lacks a recognisable export motif and N-terminal extension preceding the J-domain (*APPENDICES H2 and H6*). This suggests that the protein may be implicated in general folding and disaggregation processes in the parasite, in partnership with an Hsp70 homolog such as PfHsp70-I.

It is questionable as to whether the fourth putative exportome type II Hsp40 protein, Pfj2 (PF11_0099) bears a true PEXEL/HT motif for localisation to the erythrocyte cytosol. The protein is known to be constitutively expressed in erythrocytic-stage parasites, with a potential decrease in production following heat shock (WATANABE, 1997). The proposed PEXEL/HT motif of Pfj2 is not positioned in the N-terminal extension preceding the J-domain, but rather overlaps with helix II of the J-domain (*APPENDIX G2*). Moreover, Pfj2 has a number of apicomplexan homologs, unlike the other PEXEL/HT-bearing type II Hsp40 proteins (*TABLE 2.2*), and an alignment of these homologs reveals the similar positioning of a PEXEL/HT-like motif in helix II of the J-domain (*APPENDIX G3*). This argument does not exclude the possibility that these proteins are exported to the erythrocyte, but necessitates the experimental validation of export status and the dependence of export, if any, on the putative PEXEL/HT motif. SARGEANT *et al.* (2006) described three type II Hsp40 proteins from *Plasmodium* species other than *P. falciparum*, with potential PEXEL/HT sequences: Pv1 (Pv11869), Pv2 (Pv081840) and Py1 (Py07104). Interestingly, none of these proteins appear to be orthologous to any of the PEXEL/HT-containing *P. falciparum* type II Hsp40 proteins. This implies the potential evolution of specialised exportome proteins tailored to the devices of each parasite.

2.5.1.3 Type III and IV Hsp40 Proteins

The type III Hsp40 proteins of *P. falciparum* appear to be far more divergent than the type I and II Hsp40 proteins, consistent with the notion that members of the type III Hsp40 proteins exhibit more specialized roles in interactions with Hsp70 proteins (KELLEY, 1999; YOUNG *et al*., 2004). The regions of similarity of these type III Hsp40 proteins extend only as far as their J-domains. Four of the type III

[2] For unequivocal comparison of the *P. falciparum* proteins discussed in this study the unitalicised gene loci have been used to denote the corresponding encoded proteins

Hsp40 proteins of the parasite are predicted to contain PEXEL/HT motifs, and may therefore be exported to the host erythrocyte (*TABLE 2.1*). This includes Pfj3 (PF10_0378; WATANABE, 1997) which is known to be induced upon heat stress (OAKLEY *et al*., 2007). Interestingly, only predicted exportome type III and IV Hsp40 proteins appear to be upregulated in response to the febrile episodes synonymous with malaria (OAKLEY *et al*., 2007).

The *P. falciparum* genome encodes twelve type IV Hp40 proteins, eleven of which are predicted to contain a PEXEL/HT sequence for export to extra-parasitic locations. These include four members of the ring-infected erythrocyte surface antigen (RESA) protein family, the mature erythrocyte surface antigen (MESA) and six hypothetical proteins. As previously discussed in *CHAPTER 1*, RESA and MESA associate and interact with the erythrocyte membrane skeleton (COPPEL *et al*., 1988; FOLEY *et al*., 1991; DA SILVA *et al*., 1994). The RESA protein encoded by PFA0110w is suggested to support parasite resistance against heat shock (SILVA *et al*., 2005) while the type IV Hsp40 RESA protein encoded by gene PF11_0509 could not be disrupted in gene knockout experiments, highlighting its essentiality to the parasite (MAIER *et al.,* 2008). RESA-2 (PF11_0512) and the RESA-like proteins encoded by PFL0055c and PFA0675w may similarly support resistance against heat shock, as suggested by their heat inducibility (OAKLEY *et al*., 2007).

The identification of putative transmembrane domains in three of the hypothetical exportome type IV Hsp40 proteins (*TABLE 2.1*) may suggest similar interactions with the erythrocyte membrane as described for RESA and MESA. Consistent with this, the disruption of gene PF10_0381 revealed implications for the encoded type IV Hsp40 in knob formation on the erythrocyte surface (MAIER *et al*., 2008). Moreover, the disruption of the gene encoding the transmembrane domain-bearing type IV Hsp40 protein encoded by PF11_0034 proved lethal (MAIER *et al*., 2008). In agreement with this, the heat-inducibility of the protein was demonstrated with the febrile response associated with malaria, suggesting an important role in defence against heat shock (OAKLEY *et al*., 2007). The same was reported for the third type IV Hsp40 protein exhibiting a transmembrane domain (PFB0085c; OAKLEY *et al*., 2007).

The PEXEL/HT-containing protein encoded by the gene designated PFB0925w has been classified as a type IV Hsp40 (*TABLE 2.1*) as it exhibits a semi-conservative HPE motif in place of the typical HPD motif of the J-domain. Substitution of the HPD motif for an HPE motif was previously shown to abolish the J-domain based interaction of the *Agrobacterium tumefaciens* DnaJ protein with DnaK (HENNESSY *et al*., 2005a). In contrast, Hsp40 proteins that naturally contain an HPE motif in this position are known to interact with a specialized Hsp70 partner; the *E. coli* Hsp40 protein, DjlC, is known to interact with *E. coli* HscC (reviewed in HENNESSY *et al*., 2005b). It is therefore possible that

the HPE-containing type IV Hsp40 of *P. falciparum* may have evolved interactions with a more specialised Hsp70 protein, warranting alternate classification as a type III Hsp40.

2.5.2 Functional Insight From the Clustering of Similar Hsp40 Proteins

In terms of protein similarity there is a distinct clustering of the putative exportome (PEXEL/HT-containing) and non-exportome (PEXEL/HT-negative) Hsp40 proteins of *P. falciparum* (*FIGURE 2.7*) which may be indicative of functional equivalence. WATANABE (1997) was the first to suggest that the RESA protein family belongs to an independent Hsp40 subgroups than Pfj1-4 (*TABLE 2.1*).

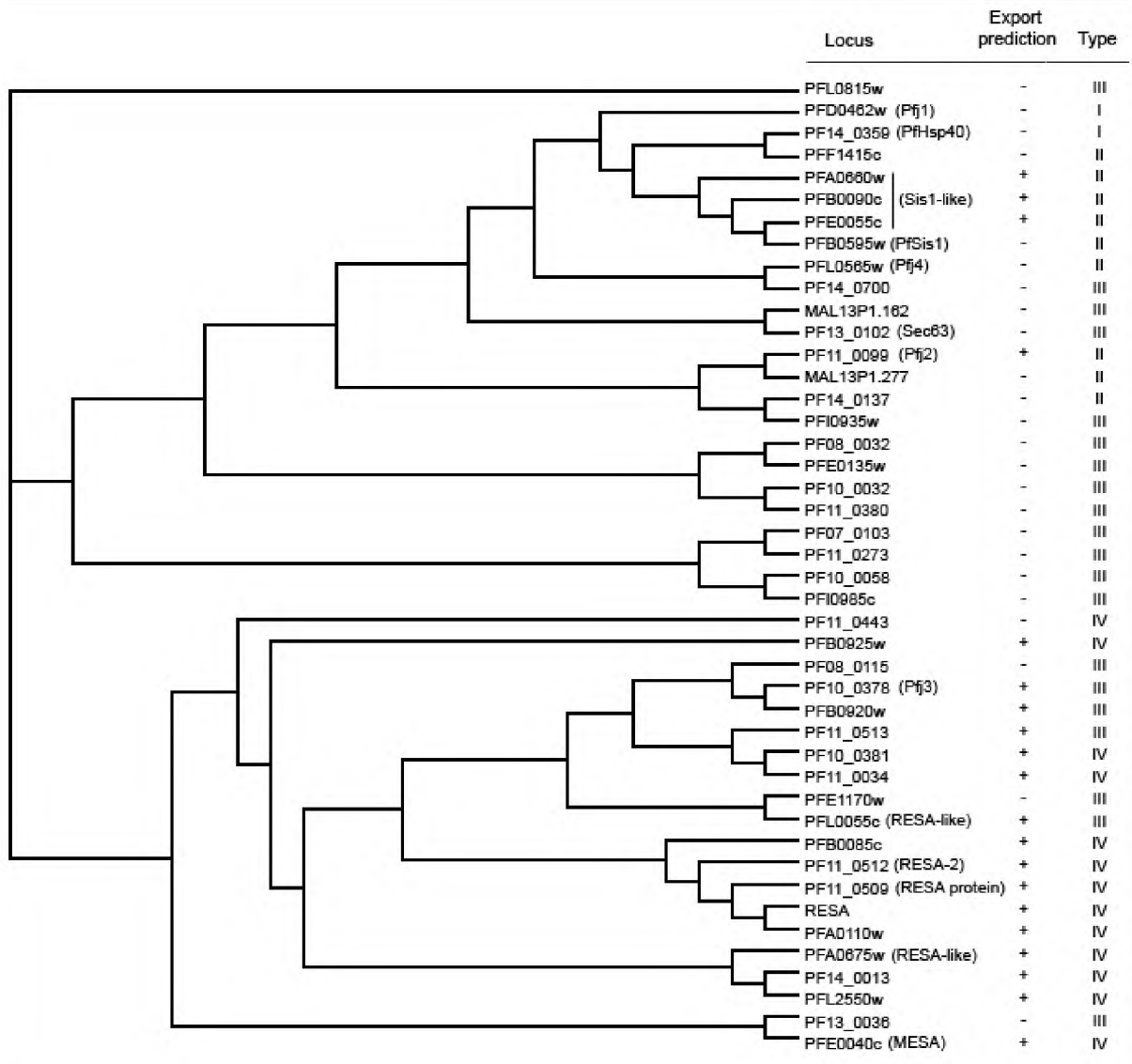

FIGURE 2.7 Phylogenetic analysis of the *P. falciparum* Hsp40 protein complement**. The similarly of the respective Hsp40 proteins is represented as a tree diagram. Locus numbers are given as retrieved from PlasmoDB (BAHL *et al.*, 2003). The prediction of protein export (+) or no export (-) into the human erythrocyte cytosol was determined from the presence or absence of a PEXEL/HT motif respectively (HILLER *et al.*, 2004; MARTI *et al.*, 2004). Hsp40 classification for each protein (type I–IV) is indicated. The protein sequences were aligned using ClustalW (version 1.8.3; CHENNA *et al.*, 2003) and imported into TreeView (version 1.6.6; PAGE, 1996) for generation of the tree diagram.**

The clustering of type I and II Hsp40 proteins is consistent with the proposed joint role of these classes in protein folding processes (KELLEY *et al.*, 1998; WALSH *et al.*, 2004). Interestingly, the type II Hsp40 proteins encoded by PF14_0137, PF11_0099 and MAL13P1.277 appear to cluster in a sub-class. This may be attributed to the presence of a degenerate C-terminal substrate-binding domain which may functionally distinguish these proteins from the more typical type II Hsp40 proteins.

The type II Hsp40 protein encoded by PFF1415c bears apparent similarity to the type I Hsp40, PfHsp40 (*FIGURE 2.7*) and significant similarity to the human type I Hsp40, DnaJA2 (*TABLE 2.3*). The protein and its apicomplexan homologs (*TABLE 2.2*) exhibit a degenerate zinc-binding domain with a single putative zinc centre (*APPENDIX G4*). LINKE *et al.* (2003) proposed that both zinc centres of a typical Hsp40 zinc-binding domain are responsible for enhanced co-chaperone activity, but the centre comprised of the two innermost cysteine repeat sequences in terms of primary structure (zinc centre II) is crucial to mediating Hsp70 substrate binding. In light of this, PFF1415c and its homologs may represent a distinct subclass of type I/II Hsp40 proteins capable of interaction with Hsp70 through appropriate use of the degenerate zinc-finger like domain. In contrast it may be argued that the region represents the atypical cysteine-rich domain of the human type I Hsp40, ERdj3. With this in mind, the degenerate cysteine-repeat motifs of PFF1415c may be oxidised and form disulphide bridges crucial to structure and function as described for ERdj3 (MARCUS *et al.*, 2007).

The majority of the predicted PEXEL/HT-containing Hsp40 proteins are categorised into the type III and IV Hsp40 classes, consistent with the proposed functional specialisation of these proteins. Interestingly, the putative PEXEL/HT-containing type III Hsp40 protein encoded by PFL0055c is annotated as a RESA-like protein, indicating that there may be shared features in the J-domains of the exported type III and IV Hsp40 proteins in general. Moreover, the apparent clustering of PEXEL/HT-containing type III and IV Hsp40 proteins (*FIGURE 2.7*) may be indicative of these shared features. SARGEANT *et al.* (2006) described certain of the type III Hsp40s (encoded by PFL0055c, PF10_0378 and PF130920w) and type IV Hsp40s (RESA and those encoded by PF130085c, PF11_0509 and PF11_0512) as members of the PHIST (*Plasmodium* helical interspersed subtelomeric) protein family. Members of this family are characterised by the presence of a unique conserved PHIST domain of unknown function comprised of four α-helices.

2.5.3 The Hsp40 Protein Interactome of P. falciparum

The protein interaction network of *P. falciparum* has been assessed using a yeast two-hybrid approach as previously described (LACOUNT *et al.*, 2005). Notably, the majority of protein interactions detected by this study are suggested to be unique to *P. falciparum* as they appear to lack homologous associations, or interologs, in other characterised eukaryotic organisms (DATE and

STOECKERT, 2006; PAVITHRA *et al.*, 2007; SUTHRAM *et al.*, 2005). Use of the yeast two-hybrid data enabled the construction of a *P. falciparum* Hsp40 protein interaction network, shown in *FIGURE 2.8*.

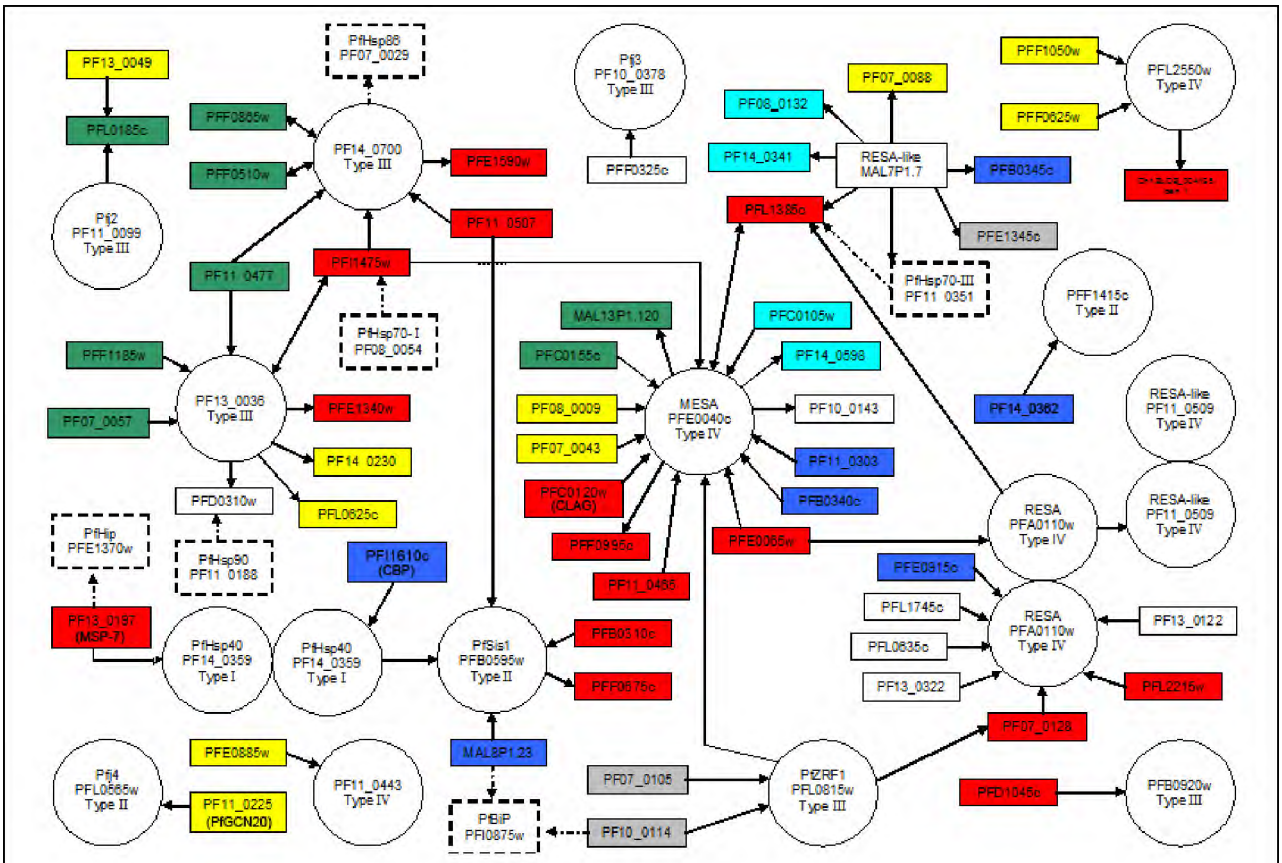

FIGURE 2.8 Schematic representation of the predicted *P. falciparum* Hsp40 protein interaction network. **The predicted protein-protein interactions involving members of the *P. falciparum* Hsp40 protein family were extracted from a yeast two-hybrid analysis (LACOUNT *et al.*, 2005). Hsp40 proteins are indicated in circles with a common name if designated, a locus accession number, and classification according to Hsp40 type (I - IV). Members of the Hsp70, Hsp90 and Hip protein families of *P. falciparum* are indicated in dashed boxes. Potential protein interactors are indicated by locus accession number in solid boxes and classified into functional categories as indicated by colour: *red* - cytoskeletal and membrane proteins, *blue* - the proteasome and proteolytic enzymes, *yellow* - translational machinery, *green* - transcriptional machinery, *turquoise* - enzymes involved in cellular physiology, *grey* - DNA repair and replication machinery, and *white* - unclassified. The association of prey with bait proteins in the yeast two-hybrid assays is indicated with directional arrows pointing to the prey for single associations (bait → prey), and double headed arrows indicating reciprocal associations (↔). Double circles were drawn to indicate self-association of Hsp40 proteins. The abbreviated common names for certain of the *P. falciparum* (Pf) proteins are defined as follows: Pfj2-4 - the Hsp40 proteins described by Watanabe (1997), PfZRF1 - a protein similar to the human zuotin-related factor 1, PfBiP - immunoglobulin binding protein or endoplasmic reticulum Hsp70 homolog, PfHip - Hsp70-interacting protein homolog, PfHsp90 - heat shock protein 90 homolog, PfHsp86 - heat shock protein 86 homolog, MSP-7 - Merozoite Surface Protein-7, CBP - Calcyclin Binding Protein, and CLAG - cytoadherence linked asexual protein. The non-Hsp40 RESA-like protein, MAL7P1.7, and its associated set of interactors was included because of its similarity to the RESA protein family, and its potential interaction with PfHsp70-III.**

Analysis of the network suggests (i) that the type III and type IV Hsp40 proteins are either better represented as an artefact of the yeast two-hybrid system constraints, or do indeed have a greater number of interactions *in vivo* than the type I and II Hsp40 proteins, and (ii) that a number of the

Hsp40 proteins form a network involving direct (Hsp40-Hsp40) and indirect interactions (Hsp40-interactor-Hsp40) with one another. The potential interactors were categorized broadly into cytoskeletal and membrane proteins, transcriptional machinery, DNA repair and replication machinery, translational machinery, the proteasome and proteolytic enzymes, and enzymes involved in cellular physiology (metabolism and phosphorylation pathways). It is possible that a number of the interactors detected represent substrates of the Hsp90, Hsp70 and/or Hsp40 proteins, as opposed to partner proteins of the chaperone machinery implicated in the cellular processes categorised. The validity and nature of the protein interactions described remains to be assessed biochemically.

The type I and II Hsp40 interactions may be under-represented in the yeast two-hybrid screen, since many expected interactions were not detected. This may reflect the transient nature of interactions with Hsp70 partner and substrate proteins, as it is possible that such interactions were too transient for detection in the yeast two-hybrid system. PfHsp40 (PF14_0359) is the only type I Hsp40 represented in the interactome, and appears to be networked directly and indirectly to cytoskeletal and membrane proteins (*FIGURE 2.8*). Of particular interest is the proposed direct interaction of the C-terminal domain of PfHsp40 with that of PfSis1 (PFB0595w), which similarly exhibits associations with cytoskeletal and membrane proteins (*FIGURE 2.8;* LACOUNT *et al*., 2005). As previously discussed, PfHsp40 and PfSis1 represent the only putative parasite-resident, typical type I and type II Hsp40 proteins of *P. falciparum*, and are thus prime candidates for the facilitation of general folding processes in the parasite (equivalent to Ydj1 and Sis1 of *S. cerevisiae* respectively). Consistent with the theme of Hsp40-Hsp40 interactions, PFB0595w appears to be indirectly networked to the type III Hsp40 proteins encoded by PFL0815w (similar to the human zuotin-related factor 1; ZRF1 or DnaJC2) and PF14_0700. PAVITHRA *et al.* **(2007) suggested that PF14_0700 may serve as a co-chaperone in an Hsp90-Hsp70 multi-chaperone complex in the parasite, based on its proposed association with PfHsp70-I and PfHsp90 (*FIGURE 2.8*). PfHsp90 and PfHsp70-I were previously shown to occur in complex in the parasite (BANUMATHY *et al*., 2003).**

The yeast two-hybrid data suggests that PfHsp40 may self-associate via the zinc-finger and C-terminal substrate binding domains (LACOUNT *et al*., 2005). In line with this, these domains encompass the region suggested to mediate Hsp40 dimerization (BORGES *et al*., 2005; SHI *et al*., 2005; WU *et al*., 2005). Moreover, PfHsp40 is proposed to interact with the hypothetical protein encoded by PFF0565c and the lysine-rich C-terminal fragment of the hypothetical mitochondrial protein encoded by PFL0130c (not illustrated in *FIGURE 2.8*; LACOUNT *et al*., 2005). Both hypothetical proteins are of unknown function but are conserved in the *Plasmodium* genus (PlasmoDB; BAHL *et al*., 2003). The suggested interaction of these proteins with the C-terminal domain of PfHsp40 suggests that they

may represent protein substrates of this chaperone protein. Interestingly, elements of the J-domain and GF-region of PfHsp40 were suggested to mediate interactions with the putative protein encoded by PFI1610c, resembling a calcyclin binding protein, and Merozoite Surface Protein-7 (MSP-7, encoded by PF13_0197). MSP-7 represents a membrane precursor protein that is targeted to the membrane of developing merozoite-stage parasites following synthesis and proteolytic processing in the schizont stage. The protein is thought to exhibit a role in the invasion of the human erythrocyte by the merozoite stage (PACHEBAT *et al*., 2007) highlighting the importance of elucidating associated protein interactions. Perhaps related to the proposed PfHsp40-MSP-7 association, PfHsp70-I was initially located on the surface of the merozoite stage of *P. falciparum* (ARDESHIR *et al*., 1987). It is possible that PfHsp70-I and PfHsp40 co-operate in the processing of MSP-7. Cautiously though, interactions proposed to involve the J-domain may represent artefacts of the yeast two-hybrid system rather than true associations, and the association of MSP-7 and PfHsp40 need to be validated.

The lesser-conserved type II Hsp40s may be remotely associated with the Hsp40-translation machinery network as suggested by the interaction of Pfj4 (PFL0565w) with the translation initiation factor, PfGCN20, and the interaction of Pfj2 (PF11_0099) with a putative nucleosome assembly protein. Consistent with this, Pfj4 has been shown to localise to the parasite nucleus and its association with the PfHsp90/PfHsp70-I multi-chaperone complex has been proposed (PESCE *et al*., 2008).

The MESA and RESA proteins potentially form a major network with cytoskeletal and membrane proteins, consistent with their known localisation and function. In particular, the interactions of MESA with the cytoadherence linked asexual protein (CLAG; PFC0120w) and the skeleton binding protein (PFE0065w) which also interacts with RESA, provide support to its role in cytoadherence. The RESA-like protein (MAL7P1.7) is not classified as an Hsp40 protein, but was included in the Hsp40 interactome analysis due to its potential interaction with the Hsp70 homolog, PfHsp70-III (PF11_0351) and indirect interaction with RESA. Since the interaction of this RESA-like protein with PfHsp70-III would not be J-domain-based, the protein could represent a substrate of the Hsp70. This further highlights the possibility that the other Hsp70 interactions reflected in the interaction network represent substrate associations (*FIGURE 2.8*).

Also worth mentioning, the Hsp40 protein interactome network derived from the work by LACOUNT *et al.* (2005) is limited to proteins of *P. falciparum*. In light of the export of parasite proteins to the erythrocyte cytosol (SARGEANT *et al*., 2006) and the potential utilisation of host chaperones for parasite processes (BANUMATHY *et al*., 2002), it would be of interest to apply similar protein

interaction studies to investigate the association of putative exportome proteins with proteins of the human erythrocyte proteome (described by PASINI *et al.*, 2006).

2.5.4 The Conservation of Hsp40 Proteins in the Apicomplexa

Members of the Hsp40 complements of numerous apicomplexan parasites were identified and classified, as presented in *FIGURE 2.9*. A complete list of identified proteins is provided in *APPENDIX H*. To date, genome sequences have been published for *P. falciparum* (GARDNER *et al.*, 2002), *P. berghei*, *P. chabaudi* (HALL *et al.*, 2005), *P. yoelii* (CARLTON *et al.*, 2002), *Cryptosporidium hominis* (XU *et al.*, 2004), *C. parvum* (ABRAHAMSEN *et al.*, 2004), *Theileria annulata* (PAIN *et al.*, 2005) and *T. parva* (GARDNER *et al.*, 2005). Sequencing of the genomes of *Toxoplasma gondii* and *P. vivax* is in progress (CARLTON *et al.*, 2003; KOOIJ *et al.*, 2006). Each apicomplexan genome investigated appears to encode two type I Hsp40 proteins as previously detailed and a fairly consistent number of type III Hsp40 proteins, with the exception of *T. gondii* (*FIGURE 2.9*). The presence of type IV Hsp40 proteins appears to be a phenomenon, although not unique, in the apicomplexa, with a considerably larger type IV Hsp40 class in *P. falciparum*.

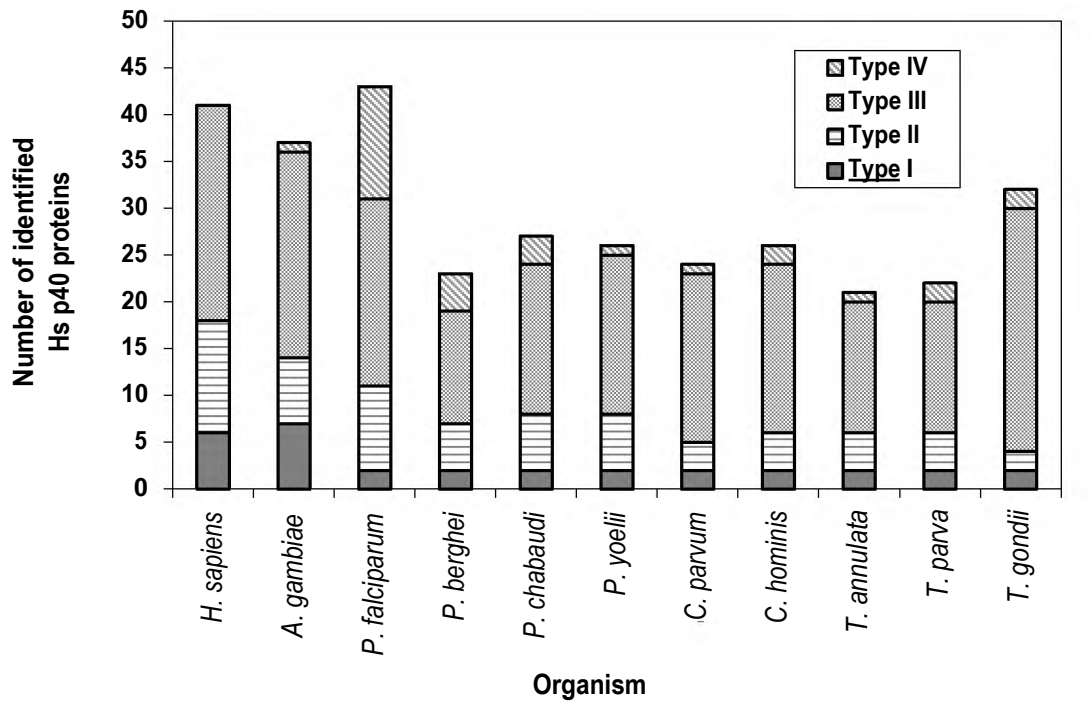

FIGURE 2.9 Comparison of the Hsp40 make-up of *P. falciparum* to that of related apicomplexan parasites. **The number of identified Hsp40 proteins in *P. falciparum* contrasted to the human host (*H. sapiens*), mosquito vector (*A. gambiae*) and specified apicomplexan parasites is represented as a bar graph. Classification of the Hsp40 proteins (types I- IV) is indicated. In comparison to its host organisms and to the other apicomplexa, *P. falciparum* exhibits the largest number of Hsp40 proteins, with a larger specialised Hsp40 class of type IV Hsp40s. Classification of the human Hsp40 proteins is as described by QIU *et al.* (2006). The Hsp40 proteins of *A. gambiae* were derived from the genome sequence of the organism reported by HOLT *et al.* (2002).**

As previously discussed, approximately 60% of the *P. falciparum* proteome is thought to be novel as it does not share significant homology to known proteomes of eukaryotic origin (GARDNER *et al.*, 2002). Consistent with this, members of the *P. falciparum* Hsp40 chaperone machinery were found to outnumber those of the human host (*H. sapiens*; QIU *et al.*, 2006), mosquito host (*A. gambiae*) and other apicomplexa (*FIGURE 2.9*). Apicomplexan homologs were identified for only nineteen members of the *P. falciparum* Hsp40 protein complement (*TABLE 2.2*) with an apparent absence of homologs for the predicted PEXEL/HT-containing proteins. Interestingly, the number of non-PEXEL/HT Hsp40 proteins in *P. falciparum* is approximately equivalent to the total number of Hsp40 proteins identified in the other *Plasmodium* species. The expansion of Hsp40 proteins in *P. falciparum* and the roles of the PEXEL/HT-containing proteins may be of relevance to species-specific attributes of this parasite. Interestingly, *P. falciparum* is distinguished from the other human malarial counterparts by its ability to occupy mature erythrocytes in addition to immature reticulocytes (RAYNER *et al.*, 2005). The appropriateness of comparative analyses between human and rodent malaria models is thus questionable, as proposed by KOOIJ *et al.* (2006). The lack of Hsp40 protein conservation between *P. falciparum* and the less virulent human malarial species *P. vivax* is also notable (*TABLE 2.2*) although the incomplete status of the sequencing of the *P. vivax* genome must be considered (CARLTON *et al.*, 2003).

In certain instances, Hsp40 orthologs were identified but categorised into different classes (types I-IV). The *P. berghei* protein designated XP_676696.1 bears an FVD motif in place of the HPD motif of the J-domain, and was thus categorised as a type IV Hsp40 (*TABLE 2.2*) despite its similarity to the *P. falciparum* type II Hsp40, Pfj4 (PFL0565w). Although these proteins may be functionally equivalent, the notion that type IV Hsp40 proteins exert their *in vivo* functionality differently to type I-III Hsp40 proteins suggests that the role of XP_676696.1 has diverged significantly from the HPD-established functions of Pfj4. The induction of Pfj4 expression in erythrocytic-stage *P. falciparum* parasites following heat shock has been described, implying a significant role for Pfj4 in cytoprotection (PESCE *et al.*, 2008; WATANABE, 1997).

An additional subclass of type IV Hsp40 proteins was identified in *T. gondii*, *T. annulata* and *T. parva* (*APPENDIX G5*). These proteins exhibit the typical domains of a type I Hsp40 protein, but lack a conserved HPD motif in the J-domain. A type IV protein was identified in *T. gondii* (52.m01602) bearing a weak GF region and degenerate zinc-binding domain with two cysteine repeat sequences. As previously indicated, the presence of a single zinc-binding centre may be sufficient to mediate Hsp70 substrate binding (LINKE *et al.*, 2003) but interactions with Hsp70 in the absence of an HPD motif are questionable.

2.5.5 Functional Insight From Homologous Host Hsp40 Proteins

Insight into the prospective functions of the *P. falciparum* Hsp40 proteins was achieved through comparison with similar or homologous proteins of the human host. Significantly similar human proteins, potentially representing homologs, were identified for twelve members of the *P. falciparum* Hsp40 protein complement as summarised in *TABLE 2.3*.

TABLE 2.3 Identified Human Homologs of the *P. falciparum* Hsp40 Proteins

P. falciparum Hsp40 Protein				Human Homolog			
Type	Locus	Protein	Export	Name *	Localisation	Description / Function	Ref.
I	PF14_0359	NP_702248.1	-	DnaJA1	Cytosol	Co-operates with Hsc70 to facilitate protein folding; Exhibits potential membrane interactions following farnesylation; Facilitates protein import into mitochondria; Functionally equivalent to DnaJA2	2,5
	PFD0462w	NP_702750.1	-	DnaJA3	Mitochondria	Regulates apoptosis signalling	6
II	PFA0660w	NP_703333.1	+	DnaJB4	Cytosol	Sis1 homolog; expression is induced following heat shock	7,8
	PFB0090c	NP_472947.2	+				
	PFE0055c	NP_703357.1	+				
	PFB0595w	NP_473047.1	-				
	PFF1415c	XP_966274.1	-	DnaJA2	Cytosol	Functionally equivalent to DnaJA1	4
	PFL0565w	NP_701478.1	-	DnaJB6	Nucleus	Facilitates protein folding	4, 9
III	PF11_0380	NP_701239.1	-	DnaJB12	Membrane	Putative type I membrane protein	2
	PF13_0102	NP_705096.1	-	DnaJC23 (SEC63)	ER	Facilitates protein translocation across ER membrane	2,4, 10
	PFE0135w	NP_703373.1	-	DnaJC24 (ZCSL3)	-	CSL-type zinc finger- protein 3	2
	PFL0815w	NP_701527.1	-	DnaJC2 (ZRF1)	Ribosomes	Regulates translation and the folding of peptides emerging from the ribosomes	4, 11

[1] BAHL *et al.* (2003), [2] Potential human homologs or significantly similar proteins, displaying overall domain conservation or a minimum of 30% sequence identity; Benson *et al.* (2008); MARCHLER-BAUER and BRYANT (2004), [3] Predicted to be exported (+) or not exported (-) due to the presence or absence of a PEXEL/HT motif, respectively; HILLER *et al.* (2004); MARTI *et al.* (2004), [4] QIU *et al.* (2006), [5] TERADA and MORI (2000), [6] SYKEN *et al.* (1999), [7] HOE *et al.* (1998), [8] ANCEVSKA-TANEVA *et al.* (2006), [9] HANAI and MASHIMA (2003), [10] FELDHEIM *et al.* (1992), [11] OTTO *et al.* (2005); * The nomenclature of the Hsp40 homologs is as described by HIGHTOWER *et al.* (2009).

Proteomic analysis of the human erythrocyte revealed the presence of a single Hsp40 protein, DnaJC5, bound to the membrane of this specialised host cell (PASINI *et al.*, 2006). The significant deficiency of Hsp40 proteins in the erythrocyte may shed light on the export of Hsp40 proteins by the parasite. The putative exportome type II Hsp40 proteins PFA0660w, PFB0090c and PFE0055c were found to be significantly similar to the human type II Hsp40, DnaJB4. Although DnaJB4 is not evident in the human erythrocyte, the homologous *P. falciparum* exportome proteins may be tailored to mimic DnaJB4 to establish associated or homologous roles in the infected erythrocyte. The heat-inducible DnaJB4 protein is predominantly cytosolic, interacting with human Hsp70 to facilitate protein folding (HOE *et al.*, 1998; QIU *et al.*, 2006).

The conservation of the endoplasmic reticulum Hsp40 protein, Sec63 (ERdj2) in the apicomplexa (*APPENDIX G7*) lends itself to the preservation of certain elements of the traditional secretory pathway (COOKE *et al*., 2004; FELDHEIM *et al*., 1992; RÖMISCH, 2005). Consistent with this, additional core elements of the sec protein translocation complex have been identified in *P. falciparum* including homologs of the α-, β- and γ-subunits of Sec61, and Sec62 (TUTEJA *et al*., 2007b). Elements of both post- and co-translational protein translocation have been identified in *P. falciparum*. In particular, identified conserved components of the signal recognition particle (SRP) complex and its associated receptor required for co-translational translocation in the parasite have been described (TUTEJA *et al*., 2007b).

Interestingly, apicomplexan homologs of additional endoplasmic reticulum Hsp40 proteins such as ERdj1, ERdj3, ERdj4 and ERdj5 were not identified. It is possible that protein folding tasks in the parasite endoplasmic reticulum are facilitated by Protein Disulfide Isomerases (PDI) as previously described (MAHAJAN *et al*., 2006). Notably, Pfj2 and its identified apicomplexan homologs (*TABLE 2.2*) bear a PDI-related domain (accession cd02961; MARCHLER-BAUER and BRYANT, 2004) suggesting a role for these proteins in chaperone activity in the endoplasmic reticulum. In agreement with this, Pfj2 exhibits a C-terminal motif, DDEL (*APPENDIX G3*), similar to the endoplasmic reticulum retention motif, KDEL (MUNRO and PELHAM, 1987). The occurrence of this motif appears to be consistent in the Pfj2 homologs (*APPENDIX G3*). PDI-related domains were similarly identified in the *P. falciparum* type III Hsp40 protein encoded by PF08_0032 (*TABLE 2.1*) and its apicomplexan homologs (*TABLE 2.2*), and in a *T. gondii* type III Hsp40 protein (37.m00768). These proteins all belong to the same J-domain bearing subset of the PDI protein family as ERdj5 (CUNNEA *et al*., 2003) suggesting functional equivalence and co-operation with the endoplasmic reticulum Hsp70, PfBiP (*TABLE 2.4*). Interestingly, apicomplexan homologs of the type III Hsp40, p58^{IPK} (VAN HUIZEN *et al*., 2003), or equivalent proteins bearing a tetratricopeptide repeat (TPR) domain (BLATCH and LÄSSLE, 1999) were not identified. The expression of p58^{IPK} is thought to be upregulated in the endoplasmic reticulum during stress conditions, where the protein is involved in the inhibition of eIF2α signalling to alleviate protein aggregation and the accumulation of unfolded proteins (VAN HUIZEN *et al*., 2003). Moreover, PAVITHRA *et al*. (2007) noted the absence of orthologs of the calcium-dependent endoplasmic reticulum chaperones calnexin and calreticulin from the parasite genome.

In contrast, the translation machinery and the manner in which emerging proteins are folded and assembled from the ribosomes in eukaryotic organisms appears to be conserved in the apicomplexa. Two type III Hsp40 proteins with similarity to the human zuotin-related factor 1 (ZRF1; DnaJC2) were identified in *P. falciparum*, PFL0815w (*TABLE 2.3*) and PF10_0058, and other apicomplexa (*TABLE 2.2*).

ZRF1 (equivalent to human DnaJC2) is known to associate with the ribosomes and interact with Hsp70 to facilitate the folding of newly translated proteins (OTTO *et al.*, 2005).

2.5.6 Deciphering the Potential Hsp70-Hsp40 Partnerships of P. falciparum

Five of the six Hsp70 proteins encoded on the *P. falciparum* genome appear to be homologous to members of the human Hsp70 protein family (SARGEANT *et al.*, 2006; SHONHAI *et al.*, 2007). The human homologs, predicted localisations and possible Hsp40 partners of the *P. falciparum* Hsp70 proteins are summarised in *TABLE 2.4*.

TABLE 2.4 Putative Localisation, Human Homologs and Potential Hsp40 Partners of *P. falciparum* Hsp70s

Locus[1]	Protein[2]	Human homolog[3]	Localisation	References	Potential partner[1,2]
PF08_0054	PfHsp70-I (AAA29626)	HspA1A (Hsp70-1)	Cytosol	3, 4, 10	NP_702248.1 (PF14_0359)
			Nucleus	4, 10	NP_701478.1 (PFL0565w)
			Maurer's cleft	5	NP_703357.1 (PFE0055c)
			PV	6	NP_700851.1 (PF10_0378)
PFI0875w	PfBiP (PfGrp78) / PfHsp70-II (NP_704718)	HspA5 (Grp78/BiP)	ER lumen	3, 4	NP_705096.1 (PF13_0102)
			Maurer's cleft	5	NP_703357.1 (PFE0055c)
PF11_0351	PfHsp70-III (NP_701211)	HspA9B	Apicoplast	8	NP_702750.1 (PFD0462w)
			Maurer's cleft	5	NP_703357.1 (PFE0055c)
			Mitochondria	3, 7, 12	NP_705208.1 (PFF1290c)
			PV	6	NP_700851.1 (PF10_0378)
MAL13P1.540	PfHsp70-y	-	Apicoplast	8	NP_702750.1 (PFD0462w)
			ER	3, 9	NP_705096.1 (PF13_0102)
MAL7P1.228	PfHsp70-x	HspA6 (Hsp70B)	Cytoplasm, Nucleus	3, 11	NP_701478.1 (PFL0565w)
PF07_0033	PfHsp70-z (NP_704032)	HspA14 (Hsp70-4)	ER, Cytoplasm	3, 11	NP_705096.1 (PF13_0102)

[1] BAHL *et al.* (2003); [2] BENSON *et al.* (2008), [3] MARCHLER-BAUER and BRYANT (2004), [4] SHONHAI *et al.* (2007); [5] NAKAI and HORTON (1999); [6] KUMAR *et al.* (1991); [7] VINCENSINI *et al.* (2005); [8] NYALWIDHE and LINGELBACH (2006); [9] BENDER *et al.* (2003); [10] FOTH *et al.* (2003); [11] MUNRO and PELHAM (1987); [12] PESCE *et al.* (2008); SARGEANT *et al.* (2006); ŠLAPETA and KEITHLY (2004).

As previously detailed, the production of PfHsp70-I is upregulated in erythrocytic-stage parasites in response to heat shock (BISWAS and SHARMA, 1994; JOSHI *et al.*, 1992; KUMAR and ZHENG, 1992). The protein is significantly abundant in the parasite and is known to localise to the parasite cytosol and nucleus (KUMAR *et al.*, 1991; PESCE *et al.*, 2008), and potentially to the PV (NYALWIDHE AND LINGELBACH, 2006). The putative parasite-resident, typical type I Hsp40, PfHsp40 (PF14_0359) and type II Hsp40, PfSis1 (PFB0595w) may co-operate with PfHsp70-I in general protein folding processes as previously suggested. Moreover, PfHsp70-I may be partnered by the additional type I Hsp40, Pfj1 (PFD0462w). It is further possible that the ZRF1 homolog, PFL0815w, interacts with PfHsp70-I to facilitate the folding of nascent proteins emerging from the ribosomes during translation in the parasite. PfHsp70-x appears to be closely related to PfHsp70-I and is similarly proposed to localise to the parasite cytoplasm (SHONHAI *et al.*, 2007). With this in mind, PfHsp70-x may co-operate with the above-mentioned Hsp40 proteins similarly to PfHsp70-I.

PfBiP and the Hsp70 protein encoded by MAL13P1.540 (*TABLE 2.4*) exhibit putative C-terminal endoplasmic reticulum retention signals ('SDEL' and 'KDEL', respectively; MUNRO and PELHAM, 1987) and are thus predicted to localise to this organelle where they may interact with the Sec63 homolog encoded by PF13_0102. The putative endoplasmic reticulum Hsp70 proteins may similarly co-operate with the PDI-related Hsp40 proteins previously discussed in *SECTION 2.5.5* (Pfj2 and the protein encoded by PF08_0032). These potential Hsp70-Hsp40 partnerships may facilitate the folding and assembly of proteins in the endoplasmic reticulum and mediate subsequent protein transport out of the organelle. In particular, the homology of PfBiP to human BiP may implicate the protein in multimeric protein complex assembly in the endoplasmic reticulum (KUMAR and ZHENG, 1992). The *P. falciparum* interactome did not reveal any direct interactions of PfBiP with any of the predicted endoplasmic reticulum Hsp40 proteins (*FIGURE 2.8*) but indirect interactions were detected with the ZRF1-like Hsp40 protein, PFL0815w, via a common interactor (the DNA repair protein RAD23; PF10_0114), and the typical type II Hsp40, PfSis1 (PFB0595w) via a common interactor (ubiquitin-protein ligase 1; MAL8P1.23).

PfHsp70-III (PF11_0351) is similarly expressed in the asexual blood stages of *P. falciparum* (SHARMA, 1992) and is homologous to the human Hsp70 protein, HspA9B (*TABLE 2.4*). HspA9B is reported to be ubiquitous in the mitochondria, endoplasmic reticulum, cytoplasm and plasma membrane where it facilitates the trafficking of proteins, particularly in response to cellular stress. Moreover, the protein is proposed to be involved in the processing of antigens (WADHWA *et al.*, 2002) which may suggest a similar role for PfHsp70-III in the processing of *P. falciparum* antigens destined for export to the parasite surface or to the host erythrocyte membrane. Consistent with this, PfHsp70-III is proposed to exhibit a direct associations with the RESA-like protein (MAL7P1.7), and the 101 kDa malaria antigen (referred to as ABRA or MSP-9; PFL1385c).

A proteomic study revealed the potential localisation of PfHsp70-I, PfBip and PfHsp70-III to the Maurer's clefts (VINCENSINI *et al.*, 2005). Moreover, the study revealed the possible localisation of the exportome type II Hsp40 protein, PFE0055c, to these proposed secretory organelles, in agreement with experimental validation of the presence of this protein in the erythrocyte cytoplasm (BHATTACHARJEE *et al.*, 2008; HILLER *et al.*, 2004; SARGEANT *et al.*, 2006). Consistent with the requirement of protein unfolding prior to membrane translocation, the latter protein might co-operate with PfHsp70-I, PfBiP and/or PfHsp70-III in facilitating the secretion of exportome proteins from the clefts into the erythrocyte cytosol. Contradictory to the findings of VINCENSINI *et al.* (2005), BANUMATHY *et al.* (2002) were unable to detect PfHsp70-I in the erythrocyte cytoplasm, and it has been suggested that PfBiP is restricted to the parasite endoplasmic reticulum (KUMAR *et al.*, 1991; KUMAR and ZHENG, 1992). Notably, approximately one third of the proteins identified in ghost preparations of the

Maurer's clefts were suspected contaminants of the proteomic study (VINCENSINI et al., 2005). This questions the localisation of the aforementioned Hsp70 proteins to the Maurer's clefts and suggests the need for experimental validation. VINCENSINI et al. (2005) proposed that the roles of the heat shock proteins found in the Maurer's clefts may be predicted from the roles that these proteins perform in their typical subcellular locations; this might rationalise the need for the presence of three distinct Hsp70 proteins in the clefts. In favour of either argument, it may be possible for parallels to be drawn between the role of the endoplasmic reticulum and Maurer's clefts in the facilitation of protein secretion; the movement of a protein from the parasite cytosol to a final secreted destination in the infected erythrocyte via the Maurer's clefts could be analogous to the movement of a protein from the cytosol to a final secreted destination via the endoplasmic reticulum in typical eukaryotic systems (LANZER et al., 2006).

PfHsp70-I and PfHsp70-III have also been proposed to localise to the PV of blood-stage parasites. To date the presence of P. falciparum Hsp40 proteins in the PV has not been reported despite chaperone proteins representing over a third of the protein complement experimentally detected in the vacuole (NYALWIDHE and LINGELBACH, 2006). It may be possible that chaperone processes other than those of the Hsp70-Hsp40 partnership govern protein translocation across the PV membrane. It is known that parasite proteins bearing an N-terminal signal sequence potentially gain entry to the PV via a traditional secretory pathway (NYALWIDHE and LINGELBACH, 2006; WICKHAM et al., 2001); consequently signal sequence-bearing Hsp40 proteins (TABLE 2.1) may be responsible for the co-chaperone regulation of PfHsp70-I and PfHsp70-III in the vacuole. Notably, numerous P. falciparum proteins lacking a PEXEL/HT and signal sequence were identified in the PV and the Maurer's clefts (NYALWIDHE and LINGELBACH, 2006; VINCENSINI et al., 2005) further emphasising the potential export of additional Hsp40 proteins to these compartments, other than those specified in TABLE 2.1.

2.5.7 A Model for the Recruitment of Chaperone Power in the Erythrocyte Cytoplasm

Compartmentalisation of the PV has been suggested, implying the separation of PV-transit proteins (exportome proteins) from PV-resident proteins and a clear distinction between their roles (COOKE et al., 2004). It is likely that the translocation of exportome proteins across the PV membrane could involve a vesicular- or translocon-based transport process as previously suggested (BANNISTER et al., 2004; LINGELBACH and PRZYBORSKI, 2006). Proteins homologous to the sec61 translocon machinery and associated chaperones such as sec63 and PfBiP have identified in the parasite, but have not been detected in the PV. Notably, the involvement of the Sec62-like translocation protein (PF14_0361) in this process has been proposed (OAKLEY et al., 2007). It is also possible that the parasite encodes a novel translocon system, or one of functional equivalence to the sec61 complex, with the

involvement of PV- and erythrocyte-resident chaperones to facilitate the transport of PV-transit proteins to the erythrocyte cytosol. This could be mechanistically analogous to retrograde protein translocation as is observed for endoplasmic reticulum associated degradation (ERAD), considering the potential involvement of Hsp70-Hsp40 chaperone machinery on either side of the membrane and the export of proteins into a cytosolic compartment. Consistent with this, it was recently reported that the transport of specific exportome proteins across the PV membrane requires protein unfolding (GEHDE *et al.*, 2009). Moreover, the transport of model exportome proteins across the PV membrane was previously shown to require ATP and protein components of the infected erythrocyte (ANSORGE *et al.*, 1996).

Regardless as to the process and mechanism of protein export, it is anticipated that refolding of exportome proteins into functional conformations or transport to distinct subcellular compartments will be required subsequent to secretion into the erythrocyte cytosol. The involvement of exported parasite chaperone proteins in the assembly of protein complexes in various locations within the infected erythrocyte has been proposed (WISER *et al.*, 1999). Moreover, the recruitment of host chaperones for the assembly of proteins of parasite origin has been suggested (BANUMATHY *et al.*, 2002). The deficiency of host Hsp40 chaperone machinery in the mature erythrocyte may account for the proposed export of nineteen parasite Hsp40s into the host cell. These proteins may work in concert with the host chaperones to permit the assembly of the cytoadherence complexes. In accordance with this notion, the substrate specificities of the parasite Hsp40 proteins may be better tailored to capture protein substrates of parasitic origin for delivery to human Hsp70 for processing. Importantly, none of the Hsp70 proteins of *P. falciparum* bear a recognisable export motif for localisation to the host erythrocyte. Consistent with this, BANUMATHY *et al.* (2002) failed to detect Hsp70 of parasitic origin in the parasitized erythrocyte cytoplasm as previously described.

A model was devised for chaperone-mediated translocation, folding and assembly of *P. falciparum* exportome proteins in erythrocytic-stage parasites involving the Hsp40 protein complement of the parasite. A schematic representation of the proposed model is provided in *FIGURE 2.10*. It is possible that the parasite Hsp70 proteins might remain in the PV and Maurer's clefts to mediate the translocation of exportome proteins into the erythrocyte, while exported parasite Hsp40 proteins might capture the secreted exportome proteins as they enter the erythrocyte cytosol and deliver them to human Hsp70 (HsHsp70) proteins for folding and assembly. In particular, exported type II Hsp40 parasite proteins could be implicated in these general folding and assembly processes. The exported type III parasite Hsp40 proteins could be involved in more specialized and regulatory processes, such as the assembly and regulation of proteinaceous structures during the remodelling of the infected erythrocyte.

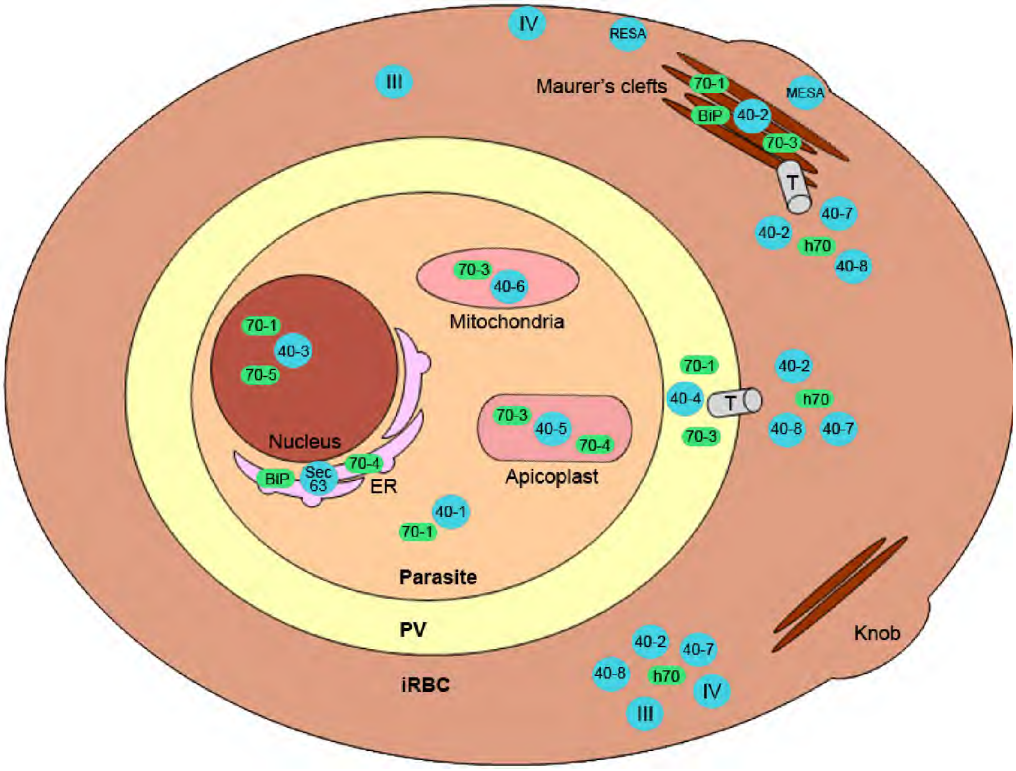

FIGURE 2.10 Schematic representation of the potential Hsp70-Hsp40 partnerships in the *P. falciparum*-infected erythrocyte. **Only organelles and compartments of interest are indicated (erythrocyte membrane and cytosol, Maurer's clefts, parasite nucleus, endoplasmic reticulum (ER), apicoplast, mitochondria, and the parasitophorous vacuole (PV) in which the parasite resides). Abbreviations:** *40-1* **– PfHsp40 (locus PF14_0359),** *40-2* **- PFE0055c,** *40-3* **- PFL0565w,** *40-4* **- PF10_0378,** *40-5* **– Pfj1 (PFD0462w),** *40-6* **- PFF1290c,** *40-7* **- PFA0660w,** *40-8* **- PFB0090c,** *40-9* **– PfSis1 (PFB0595w),** *Sec63* **- PF13_0102,** *RESA* **- Ring-infected erythrocyte surface antigen proteins (PFA0110w, PFA0675w, PF11_0512, PF11_0509),** *MESA* **- Mature parasite-infected erythrocyte surface antigen (PFE0040c),** *III* **- PEXEL/HT-containing type III Hsp40 proteins (refer to** *TABLE 2.1*), *IV* **- PEXEL/HT-containing type IV Hsp40 proteins (refer to** *TABLE 2.1*), *70-1* **- PfHsp70-I (PF08_0054),** *BiP* **- PfBip/PfGrp78 (PFI0875w),** *70-3* **- PfHsp70-III (PF11_0351),** *70-4* **- MAL13P1.540,** *70-5* **- MAL7P1.228, and** *h70* **- human Hsp70. In the parasite cytosol, PfHsp70-I might co-operate with the typical type I and II Hsp40s, PfHsp40 (PF14_0359) and Pfsis1 (PFB0595w) to facilitate general 'house-keeping' protein folding processes. Cytosolic PfHsp70-I may also interact with the ZRF1-like protein encoded by PFL0815w, to mediate the folding of nascent proteins emerging from the ribosomes. In the parasite nucleus, PfHsp70-I and the protein encoded by MAL7P1.228 could be co-chaperoned by Pfj4 (PFL0565w). In the parasite endoplasmic reticulum, PfBiP and the Hsp70 protein encoded by MAL13P1.540 may interact with the Sec63 homolog (PF13_0102) or PDI-related Hsp40 proteins Pfj2 (PF11_0099) and PF08_0032, thought to be functionally equivalent to ERdj5. PfHsp70-III is predicted to localise to the parasite mitochondria and apicoplast where it might co-operate with the Hsp40 proteins PFF1290c and Pfj1 (PFD0462w) respectively. PfHsp70-I and PfHsp70-III may localise to the PV where they might interact with signal sequence-bearing Hsp40 proteins, such as Pfj3 (PF10_0378) which exhibits a putative transmembrane domain. The type II Hsp40 encoded by PFE0055c and the parasite Hsp70 proteins PfHsp70-I, PfBiP and PfHsp70-III, have been suggested to localise to the Maurer's clefts and mediate the translocation of exportome proteins into the erythrocyte cytosol. Contradictory data implies that these proteins are not exported from the parasite, consequently necessitating experimental validation of their localisation. Proposed Hsp70-Hsp40 controlled translocons representing active transport across the Maurer's clefts and PV membranes are indicated by 'T'. The chaperone machinery potentially involved in protein translocation is indicated either side of each membrane. In the erythrocyte cytosol, the parasite type II Hsp40 proteins encoded by PFA0660w, PFB0090c and PFE0055c, might functionally mimic human DnaJB4 in interactions with human Hsp70 to facilitate the general folding of exportome proteins. Exported type III Hsp40 proteins could be involved in specialized processes using their J-domains for the recruitment of human Hsp70 proteins for the assembly and regulation of parasite proteins in the erythrocyte cytosol. The type IV Hsp40 protein MESA is known to interact with elements of the erythrocyte cytoskeleton where it is involved in the formation of knobs. Members of the RESA protein family similarly associate with the erythrocyte membrane. This potentially implicates additional type IV exportome Hsp40 proteins in similar interactions with the erythrocyte membrane. It is possible that the exported type IV Hsp40 proteins could modulate the chaperone machinery in the erythrocyte, through negative regulation of the manner in which exported type II and III parasite Hsp40 proteins co-operate with host chaperone proteins.**

The exported type II and III Hsp40 proteins might interact closely with the type IV Hsp40 proteins such as MESA and RESA, assisting in interactions with the erythrocyte cytoskeleton. One could envisage that MESA and RESA with their non-HPD-containing J-domains would rely on the type II and/or type III Hsp40 proteins for the recruitment of human Hsp70 for the formation of the cytoadherence complexes. Alternatively, the type IV Hsp40s may negatively regulate or modulate the type II and III Hsp40 J-domain-based stimulation of the human Hsp70 chaperone activity. MOKRANJAC *et al.* (2006) demonstrated the ability of the non-HPD-containing Hsp40 protein, Tim16, of the *S. cerevisiae* mitochondrial import motor to complex with its HPD-containing counterpart, Tim14 thereby inhibiting the ability of Tim14 to stimulate the ATPase activity of mitochondrial Hsp70.

2.6 CONCLUSIONS

This study has drawn emphasis to the importance of PfHsp40 and Pfj1 as the only type I Hsp40 proteins of the forty-three member Hsp40 complement of the parasite. The existence of only two type I Hsp40s - of which only one is representative of a typical Hsp40 protein - may represent an inherent weakness of the parasite and is consistent with the fewer 'house-keeping' proteins encoded on its genome. Both of these co-chaperone proteins are predicted to be parasite-resident and may be implicated in general folding and chaperone processes in the parasite. Consistent with this, the conservation of PfHsp40 and Pfj1 in other apicomplexan parasites suggests that these chaperones are important to this phylum in general. Co-chaperone roles for PfHsp40 and Pfj1 were inferred through comparison with analogous, classical Hsp40 proteins of human, yeast and bacterial origin. Placed together with gene expression profiles, this was used to substantiate potential interactions with the abundant and putative parasite-resident Hsp70 protein, PfHsp70-I. Based on localisation prediction, it is possible that PfHsp40 and Pfj1 interact with PfHsp70-I in the parasite cytosol and nucleus respectively, consistent with the previously reported localisation of this Hsp70 homolog. Residues potentially important to the proposed Hsp70-Hsp40 interactions were identified in the respective partner proteins, providing a basis from which to explore these associations experimentally. Importantly, elements of Hsp70 and Hsp40 conservation appear to be conserved in these proteins in *P. falciparum*. Experimental work pertaining to the proposed interactions is detailed in *CHAPTERS 4 - 6*.

Overall, the bioinformatics analysis presented in this study suggests that *P. falciparum* has evolved an expanded and highly specialized Hsp40 protein machinery, for the purposes of chaperone-mediated translocation, folding, assembly and regulation of both parasite and host proteins in the intraerythrocytic stages of development. In addition to the type I, II and III Hsp40 proteins exhibiting the signature J-domain, specialized *P. falciparum* Hsp40 proteins with a J-like domain have been

described here and categorized as type IV Hsp40 proteins founded on the absence of a conserved HPD motif. The export of these type IV Hsp40 proteins into the human erythrocyte appears to be crucial to the parasite's establishment, growth and survival in this specialised host cell. Interestingly, the PEXEL/HT-containing type III and IV putative exportome Hsp40 proteins appear to form a distinct subset of Hsp40 proteins in the parasite consistent with their specialised roles. These roles appeared to have diverged from the apicomplexa and other *Plasmodium* species, as suggested by the lack of orthologs of these putative exportome Hsp40s. In contrast, a few *P. falciparum* Hsp40 proteins appear to have human and apicomplexan homologs, suggesting implications in fundamental biological processes. These include the type I, II and III putative parasite-resident Hsp40 proteins classed into a distinct subset from the exportome type III and IV Hsp40s.

Notably, not all of the Hsp40 proteins of the parasite may be expressed during the intraerythrocytic stages of the lifecycle. However, the upregulation of the exported type III and IV Hsp40 proteins has previously been described (OAKLEY *et al*., 2007) and the participation of certain of these proteins in erythrocyte remodelling has been validated (DA SILVA *et al*., 1994; SHARMA, 1991). This has lead to the notion that the parasite may use its specialised Hsp40 machinery to harness the chaperone potential of Hsp70 proteins of the human host in addition to that of its own chaperone protein complement. The elucidation of the proposed heterologous interactions between *P. falciparum* Hsp40 proteins and human chaperones is of fundamental interest and remains to be validated experimentally. Related to this, the elucidation of the protein transport mechanisms operating within the parasite, and between the parasite and the host at the erythrocytic stage, represents a major challenge in malaria research in the near future. The facilitation of protein translocation through the membranes of the PV and the Maurer's clefts into the erythrocyte cytosol may be crucial to the survival of the parasite, and the proposed involvement of chaperone proteins in these processes may lead to the identification of candidate protein drug targets. Of further importance is the molecular basis of heterologous and homologous chaperone-substrate interactions, and particularly those involved in the erythrocyte membrane protein rearrangements. An analysis of the putative *P. falciparum* protein interaction network highlighted the significant functional diversity of the Hsp40 proteins in the parasite and their involvement with potential protein substrates. Connections were revealed predominantly with cytoskeletal and membrane proteins, transcriptional machinery, DNA repair and replication machinery, translational machinery, the proteasome and proteolytic enzymes, and enzymes involved in cellular physiology. While these associations remain to be validated, they too provide new avenues for the identification of novel anti-malarial targets.

CHAPTER 3:

FOUNDATION WORK:

Approaches to the Production and Isolation of

Recombinant PfHsp40 and Pfj1

3.1 INTRODUCTION

It is well documented that numerous *P. falciparum* proteins tend to be recalcitrant to heterologous expression for an array of reasons (BIRKHOLTZ *et al*., 2008; MEHLIN *et al*., 2006; SATI *et al*., 2002). Many of the parasite's proteins prove to be aggregation-prone following heterologous production or are prematurely truncated due to their significantly larger sizes. This is complicated by the significant AT-richness and comparatively rare codon usage of the *P. falciparum* genome which sees numerous codons coupled to minor tRNA species in heterologous expression systems (GARDNER *et al*., 2002; MEHLIN *et al.,* 2006). Many *P. falciparum* proteins bear lower-complexity stretches of Asn and Gln residues that are prone to trigger aggregation or mistranslation (PIZZI and FRONTALI, 2001; SCHNEIDER *et al*., 2005) in addition to N- and C-terminal extensions that appear to influence protein folding and solubility (SATI *et al*., 2002). Moreover, the parasite appears to utilise certain unique post-translational modification patterns which may not be recognised or appropriately processed in heterologous systems (CHANG *et al*., 2008; GOWDA and DAVIDSON, 1999). These challenges have impeded the characterisation of numerous *P. falciparum* proteins and in particular, many prospective vaccine candidates.

Approaches to overcome the problem of *P. falciparum* codon-bias in heterologous expression systems have been described (reviewed by BIRKHOLTZ *et al*., 2008). Firstly, plasmids encoding rare tRNA species may be introduced into the heterologous host organisms to avert translational stalling of the target mRNA bearing the corresponding codons. In particular, the RIG plasmid encoding rare tRNA species corresponding to Arg (R), Ile (I) and Gly (G) codons (BACA AND HOL, 2000) has been used for the successful production of PfHsp70-I in *E. coli* (MATAMBO *et al*., 2004). In a second approach termed 'codon-optimisation', the codons of the gene of interest may be altered by whole gene synthesis to complement the codon preference of the heterologous expression host. More specifically, lower frequency codons may be replaced with higher frequency codons corresponding to more abundant tRNA species in the heterologous host to avoid tRNA depletion and associated truncation of the target protein on expression. The success of this approach has been demonstrated in relation to use of the RIG plasmid, and for the expression of numerous *P. falciparum* vaccine candidates in both heterologous prokaryotic and eukaryotic systems (YADAVA and OCKENHOUSE, 2003; ZHOU *et al*., 2004). Notably however, the success of the described strategies appears to differ for each target protein (FLICK *et al*., 2004; ZHOU *et al*., 2004). Contrasted to the approach of codon-optimisation, a novel strategy termed 'codon-harmonisation' attempts to match the codon rhythm of the synthetic gene to that of the wildtype gene, for the maintenance of the rate of expression in the heterologous system as is encountered in the source organism (ANGOV *et al*., 2008; HILLIER *et al.*,

2005; NICOLL *et al*., 2005). In this manner, the preservation of rare codons representing translational pause sites may theoretically promote the correct co-translational folding of secondary structures and domains as they emerge from the ribosome (KOMAR *et al*., 2008; MARIN *et al*., 2008). The higher incidence of lower frequency codons may thus serve to enhance the solubility of heterologous protein products as demonstrated for the 42 kDa subunit of the *P. falciparum* vaccine candidate, Merozoite Surface Protein-1 ($MSP\text{-}1_{42}$; ANGOV *et al*., 2008).

Previously, only one third of 1000 selected *P. falciparum* open reading frames were shown to be expressible in *E. coli* in a large scale expression study, with the majority of these proteins sequestered in inclusion bodies due to their insolubility (MEHLIN *et al*., 2006). This is thought to be attributed to the potential toxicity posed by the plasmodial proteins to the heterologous host organism (MEHLIN *et al*., 2006; VEDADI *et al*., 2007). Notably, the gene encoding PfHsp40 could not be expressed in *E. coli* in the described expression study, potentially attributed to the 71% AT-richness of the open reading frame (MEHLIN *et al*., 2006). Adding to this, the overproduction of Hsp40 proteins in prokaryotic heterologous expression systems has consistently been shown to pose toxicity problems to the bacterial host resulting in a reduction in cell viability, potentially through the disruption of the endogenous Hsp70:Hsp40 ratio (AL-HERRAN and ASHRAF, 1998; NICOLL *et al*., 2006).

Placed together, these factors warranted the need for alternative approaches to the heterologous expression and production of the *P. falciparum* Hsp40 proteins, PfHsp40 and Pfj1. In this study, the approaches of codon-harmonisation and codon-optimisation were used to design synthetic genes encoding PfHsp40 and Pfj1 respectively. Notably, synthesis of the codon-optimised Pfj1 synthetic gene was initiated prior to the emergence of the concept of codon-harmonisation. The genes were synthesised and cloned into the pQE30 expression vector (Qiagen) for subsequent heterologous expression and purification of the respective recombinant proteins for characterisation studies. Specifically, the aims of this study were to:

i. Employ codon-harmonisation and codon-optimisation for the design of synthetic genes encoding recombinant PfHsp40 and Pfj1 respectively

ii. Assemble the PfHsp40 and Pfj1 synthetic genes and clone them into the pQE30 expression vector (Qiagen)

iii. Optimise the heterologous expression of PfHsp40 and Pfj1 in a prokaryotic *E. coli* expression system

iv. Isolate recombinant PfHsp40 and Pfj1 from the heterologous expression system by Nickel-affinity chromatography for subsequent *in vitro* characterisation studies

3.2 MATERIALS AND METHODS

3.2.1 Construction of Expression Plasmids Encoding Recombinant PfHsp40 and Pfj1

Codon-harmonised PfHsp40 and codon-optimised Pfj1 coding regions were synthesised and cloned into the pQE30 expression vector (Qiagen) as further described to constitute plasmids pQPfHsp40 and pQPfj1 respectively. Expression from the pQE30 plasmid results in fusion with an N-terminal hexahistidine-tag (His_6) for subsequent purification of the recombinant protein of interest by Nickel affinity chromatography and detection by Western analysis with an anti-His antibody.

3.2.1.1 Codon-Harmonisation, Synthesis and Cloning of the PfHsp40 Synthetic Gene

Codon-harmonisation of the PfHsp40 coding sequence for heterologous expression in *E. coli* K12 was performed by Dr. Evelina Angov of the Walter Reed Army Institute of Research (WRAIR, Maryland, USA) and verified with use of the GeneSplitter software package, kindly provided by the developer, Professor Jaco de Ridder (University of Pretoria, South Africa). The algorithm used for the codon-harmonisation procedure was recently described (ANGOV *et al.*, 2008). The preservation of the codon frequency rhythm in the codon-harmonised PfHsp40 coding sequence relative to the wildtype sequence is graphically represented in *FIGURE 3.1A*. The codon-harmonised PfHsp40 coding sequence is provided in *APPENDIX C1*. Flanking 5'-*BamHI* an 3'-*HindIII* restriction sites were engineered into the sequence for subsequent cloning purposes as indicated.

The codon-harmonised PfHsp40 coding sequence was synthesised by Inqaba Biotechnical Industries (South Africa) and inserted into the PCR-Smart cloning vector (Lucigen) to produce plasmid pPCR-Smart-PfHsp40 (*FIGURE 3.1B*). The insert was excised from the plasmid with *BamHI* and *HindIII* restriction enzymes (Fermentas), purified subsequent to agarose gel electrophoresis, and ligated into the *BamHI*/*HindIII*-digested pQE30 expression vector (Qiagen) as per *APPENDICES D2-D5* to produce plasmid pQPfHsp40 (*FIGURE 3.1C*). The ligation product was transformed into *E. coli* JM109 (Promega) as per *APPENDIX D8*. Plasmid DNA was isolated from the resulting colonies as per *APPENDIX D1* and verified by restriction digestion analysis as detailed in *FIGURE 3.3A.* Subsequent DNA sequencing was employed to verify the coding sequence as per *APPENDIX D6* using the pQE30-specific sequencing primers detailed in *APPENDIX F3*.

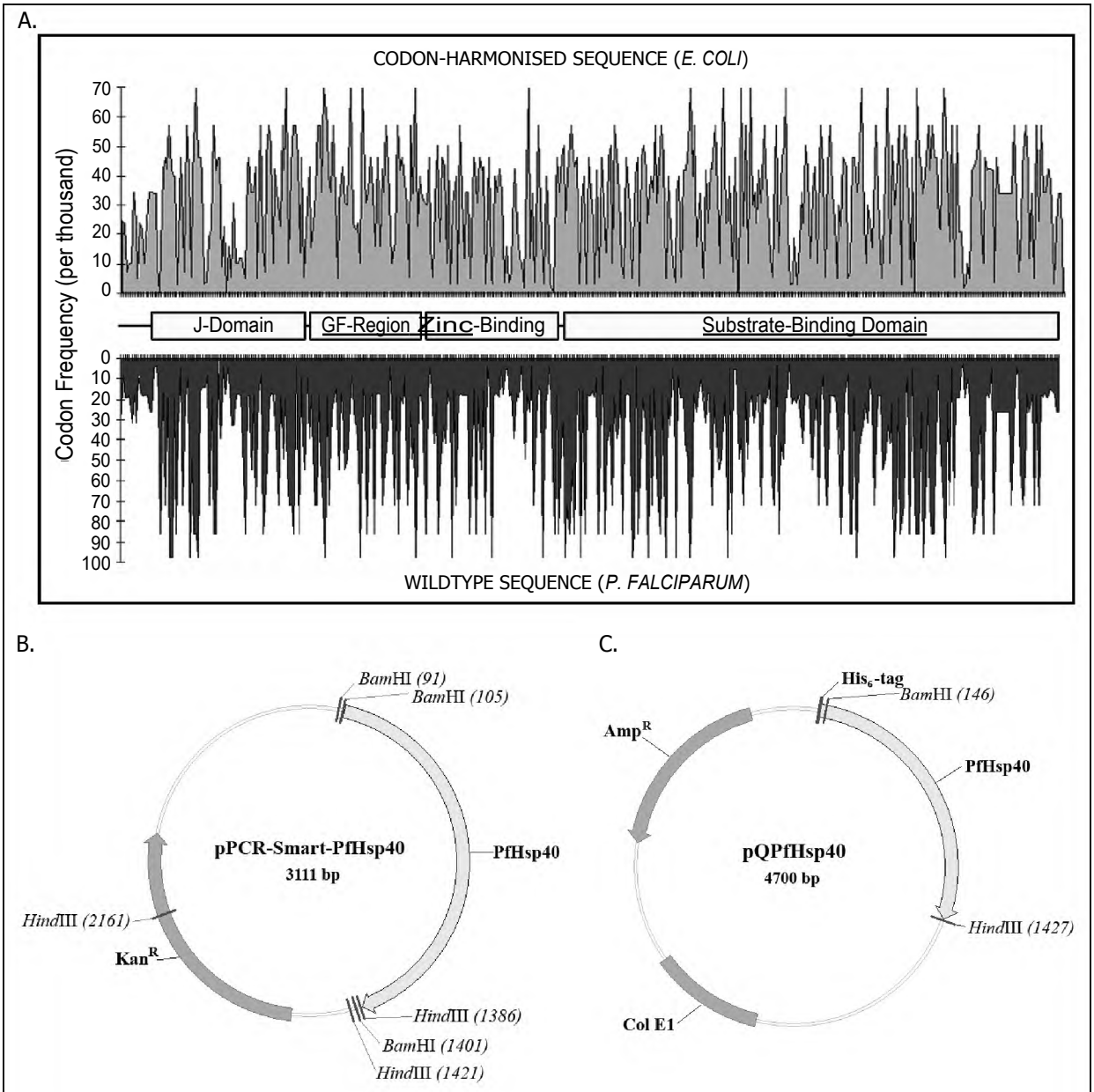

FIGURE 3.1 Construction and cloning of the codon-harmonised PfHsp40 synthetic gene. (A) Graphical representation of the codon-harmonisation of the PfHsp40 coding sequence for heterologous expression in *E. coli*. The *E. coli* K12 codon frequency of the codon-harmonised PfHsp40 sequence is shown in grey relative to the *P. falciparum* codon frequency of the wildtype sequence shown in black. The codons corresponding to each amino acid residue of the PfHsp40 protein sequence are aligned in order on the x-axis, with the corresponding codon frequency (per thousand) indicated on the y-axis. The rhythm of codon frequency of the codon-harmonised sequence demonstrates the preservation of translational pause sites as encountered in the wildtype sequence in the source organism. This contrasts the use of higher frequency codons for each amino acid residue as is encountered in the approach of codon-optimisation. The codon-harmonised PfHsp40 coding sequence was synthesised and inserted into the PCR-Smart vector (Lucigen) to produce (B) plasmid pPCR-Smart-PfHsp40 (3111 bp). The PfHsp40 insert was excised from the pPCR-Smart-PfHsp40 plasmid with *BamHI* and *HindIII* restriction enzymes and ligated into the pQE30 expression vector (Qiagen) to produce (C) plasmid pQPfHsp40 (4700 bp) encoding hexahistidine (His_6)-tagged PfHsp40 (49 kDa). Construction of the pQPfHsp40 plasmid was confirmed by restriction digestion analysis as indicated in *FIGURE 3.3* and subsequent DNA sequencing. Plasmids pPCR-Smart-PfHsp40 and pQPfHsp40 confer kanamycin (Kan^R) and ampicillin (Amp^R) resistance respectively as indicated. The plasmid maps were generated with the Vector NTI Advance™ software package (version 10.3; Invitrogen).

3.2.1.2 Codon-Optimisation, Synthesis and Cloning of the Pfj1 Synthetic Gene

3.2.1.2.1 Synthesis of the Pfj1 Coding Sequence by Polymerase Chain Reaction Assembly

The protocol for polymerase chain reaction (PCR) assembly was adapted from that described by STEMMER *et al*. (1995), comprised of the assembly of overlapping oligonucleotide primers constituting the synthetic gene in an initial round of amplification, and subsequent amplification of the assembled gene product. Overlapping primers constituting the complete Pfj1 coding sequence were designed and codon-optimised for heterologous expression from the assembled product in *E. coli* K12, using DNAWorks (version 2.0; HOOVER and LUBKOWSKI, 2002). The primer sequences were adjusted by hand to include a flanking 5'-*BamHI* restriction site for cloning purposes, a central *SmaI* site for delineation of the front and back halves of the Pfj1 coding sequence, and a *BstBI* site between the encoded J-domain and GF-region for subsequent J-domain swapping experiments (detailed in *CHAPTER 5*). Moreover, internal *BamHI* and *PstI* sites were removed for subsequent cloning purposes. The assembled codon-optimised sequence encoding the complete Pfj1 protein (residues 1-672) is detailed in *APPENDIX C1*, and the corresponding PCR assembly primer sequences are detailed in *APPENDIX F1*. Due to the size of the Pfj1 coding sequence, the front and back halves of the Pfj1 synthetic gene (Pfj1-Front and Pfj1-Back) were assembled independently. The synthesis of Pfj1-Front was achieved with forward primers 1-21 (Pfj1Fwd_1 to Pfj1Fwd_21), and reverse primers 29-50 (Pfj1Rev_29 to Pfj1Rev_50), and was performed by Dr. William S. Nicoll (Rhodes University). The synthesis of Pfj1-Back was achieved with forward primers 21-50 (Pfj1Fwd_21 to Pfj1Fwd_50) and reverse primers 1-29 (Pfj1Rev_1 to Pfj1Rev_29).

The initial assembly of the respective halves of the Pfj1 coding sequence was achieved in a reaction comprised of 10 µl of 20 nM forward primer mix, 10 µl of 20 nM reverse primer mix, 10 µl of 5x reaction buffer (6 mM MgSO4, 0.1% (v/v) Triton X-100, 0.1 $mg.ml^{-1}$ BSA, 10 mM $(NH_4)_2SO_4$, 10 mM KCl, 20 mM Tris-Cl, pH 8.0), 2 µl of 10 mM dNTP mix (Roche Applied Sciences) and sterile distilled water to a final volume of 49 µl. After incubation at 95°C for 4 minutes, 1 µl of 3 $U.µl^{-1}$ Expand High Fidelity *Taq* Polymerase (Roche Applied Sciences) was added to the reaction. Temperature cycling was allowed to proceed as follows in a GeneAmp PCR System 9700 (version 3.05; Applied Biosystems): one cycle of denaturation (95°C for 1 minute), 25 cycles of denaturation, annealing and extension (95°C for 30 seconds, 60°C for 30 seconds, 72°C for 90 seconds) and a final 4°C hold. Subsequent amplification of the assembly reaction products was achieved in a reaction comprised of 1 µl of the initial PCR assembly reaction product, 2 µl of 10 µM 5'-Forward Primer (Pfj1Fwd_1 and Pfj1Fwd_21 for Pfj1-Front and -Back respectively; *APPENDIX F1*), 2 µl of 10 µM 5'-Reverse Primer (Pfj1Rev_29 and Pfj1Rev_1 for Pfj1-Front and -Back respectively; *APPENDIX F1*), 10 µl of 5x reaction

buffer (described above), 2 µl of 10 mM dNTP mix, 1 µl of 3 U.µl^{-1} Expand High Fidelity *Taq* Polymerase and sterile distilled water to a final volume of 50 µl. Temperature cycling was allowed to proceed as detailed for the first phase of amplification. Assembly and amplification of the Pfj1 sequence was verified by 0.8% agarose gel electrophoresis as per *APPENDIX D3*.

3.2.1.2.2 Cloning of the pQPfj1 Expression Plasmid

The strategy for the cloning of plasmid pQPfj1 is summarised in *FIGURE 3.2*. The amplified front and back halves of the Pfj1 coding sequence were purified subsequent to agarose gel electrophoresis and ligated into the pGEM-T Easy® cloning vector (Promega) as per the manufacturer's instructions, producing plasmids pGPfj1-Front and pGPfj1-Back respectively (*FIGURE 3.2A* and *3.2C*). The Pfj1-Front sequence was excised from plasmid pGPfj1-Front with *Bam*HI (Fermentas) and *Sma*I (Roche Applied Sciences) restriction enzymes, purified subsequent to agarose gel electrophoresis, and ligated into the *Bam*HI/*Sma*I-digested pQE30 expression vector (Qiagen) to produce plasmid pQPfj1-Front (*FIGURE 3.2B*). The Pfj1-Back coding sequence was ligated in the reverse orientation in plasmid pGPfj1-Back, therefore requiring re-amplification from the plasmid for the insertion of a 3'-*Pst*I restriction site for subsequent cloning into the pQE30 expression vector. The Pfj1-Back sequence was re-amplified as per the specifications of the second PCR assembly amplification phase described in *SECTION 3.2.1.2.1*, using 100 ng of plasmid pGPfj1-Back as template DNA and the primers detailed in *APPENDIX F2*. The amplification product was gel purified subsequent to agarose gel electrophoresis, and ligated into the pGEM-T Easy® vector to produce pGPfj1-Back-*Pst*I (*FIGURE 3.2C*). The Pfj1-Back sequence was excised from plasmid pGPfj1-Back-*Pst*I with *Sma*I and *Pst*I (Fermentas) restriction enzymes, purified subsequent to agarose gel electrophoresis and ligated into the *Sma*I/PstI-digested pQPfj1-Front plasmid to produce pQPfj1 encoding full length Pfj1 (*FIGURE 3.2E*). The protocols for restriction enzyme digestion, agarose gel electrophoresis, purification and subsequent ligation of the plasmid DNA and Pfj1-Front and -Back inserts is provided in *APPENDICES D2, D3, D4* and *D5* respectively. Ligation products were transformed into *E. coli* JM109 (Promega) as per *APPENDIX D8*. Plasmid DNA was isolated from the resulting colonies as per *APPENDIX D1* and verified by restriction digestion analysis as detailed in *FIGURE 3.3.* Subsequent DNA sequencing was employed as per *APPENDIX D6* using the sequencing primers detailed in *APPENDIX F3*, to determine the presence of mutations introduced during the amplification procedures. In particular, the integrity of the re-amplified Pfj1-Back coding sequence was verified with the use of internal sequencing primers (*APPENDIX F3*).

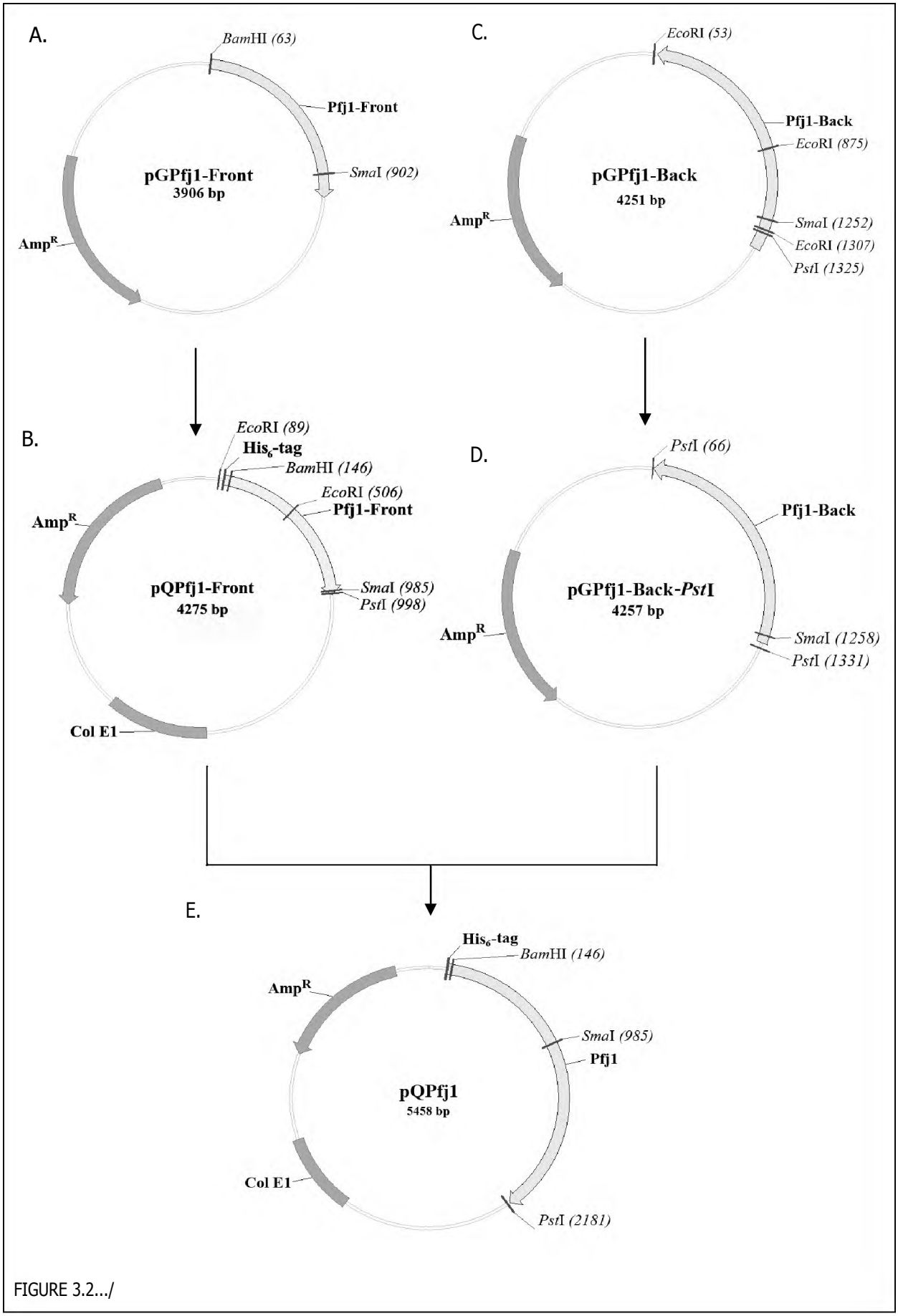
A.
BamHI (63)
Pfj1-Front
SmaI (902)
pGPfj1-Front
3906 bp
AmpR
C.
EcoRI (53)
Pfj1-Back
EcoRI (875)
pGPfj1-Back
4251 bp
AmpR
SmaI (1252)
EcoRI (1307)
PstI (1325)
B.
EcoRI (89)
His6-tag
BamHI (146)
EcoRI (506)
Pfj1-Front
AmpR
pQPfj1-Front
4275 bp
SmaI (985)
PstI (998)
Col E1
D.
PstI (66)
Pfj1-Back
pGPfj1-Back-PstI
4257 bp
AmpR
SmaI (1258)
PstI (1331)
E.
His6-tag
BamHI (146)
AmpR
SmaI (985)
Pfj1
pQPfj1
5458 bp
Col E1
PstI (2181)

FIGURE 3.2.../

.../FIGURE 3.2 Cloning strategy for the construction of the pQPfj1 plasmid encoding full-length Pfj1. The front half of the Pfj1 coding sequence was assembled by PCR assembly with engineered 5'-*Bam*HI and 3'-*Sma*I restriction enzyme recognition sites. Subsequent ligation into the pGEM-T Easy® cloning vector (Promega) produced (A) plasmid pGPfj1-Front (3906 bp). The Pfj1-Front insert was excised from this plasmid with *Bam*HI and *Sma*I restriction enzymes, and subsequently inserted into the multiple cloning site of the pQE30 expression vector (Qiagen) to produce (B) plasmid pQPfj1-Front (4275 bp). The back half of the Pfj1 coding sequence was assembled by PCR assembly with an engineered 5'-*Sma*I restriction enzyme recognition site. Subsequent ligation into the pGEM-T Easy® vector produced (C) plasmid pGPfj1-Back (4251 bp). The Pfj1-Back insert was ligated into the pGEM-T Easy® vector in the reverse orientation, therefore subsequent reamplification was performed to insert a *Pst*I site on the 3' end of the coding sequence for subsequent cloning into plasmid pQPfj1-Front. The amplification product was re-inserted into the pGEM-T Easy® plasmid to produce (D) plasmid pGPfj1-Back-*Pst*I. The Pfj1-Back insert was excised from plasmid pGPfj1Back-*Pst*I with *Sma*I and *Pst*I restriction enzymes and inserted into plasmid pQPfj1-Front to produce (E) plasmid pQPfj1 (5458 bp) encoding hexahistidine (His_6)-tagged full length Pfj1 (76 kDa). Construction of the plasmids in stages (A) - (E) was confirmed by restriction digestion analysis as indicated in *FIGURE 3.3* and subsequent DNA sequencing. All of the plasmids depicted confer resistance to ampicillin as indicated (Amp^R). The plasmid maps were generated with the Vector NTI Advance™ software package (version 10.3; Invitrogen).

3.2.1.2.3 Mutagenesis of the Pfj1 Coding Sequence

Site-directed mutagenesis was performed by non-PCR based whole plasmid amplification (PAPWORTH *et al*., 1996) to correct a Gly^{248} to Ser^{248} mutation (G248S) erroneously introduced into the Pfj1-Front coding sequence during PCR assembly and detected by DNA sequencing analysis. Complementary mutagenesis primers were designed for the introduction of an S248G mutation into the Pfj1 coding sequence (refer to *APPENDIX F4*). The primers were synthesised by Integrated DNA Technologies (IDT, USA). Each mutagenesis reaction was comprised of 100 ng of pQPfj1 parental plasmid template, 2.5 µl of Dimethyl sulfoxide (DMSO; Sigma-Aldrich), 10 µl of 25 mM $MgCl_2$, 1 µl of 10 mM dNTP mix (Roche Applied Sciences), 125 ng of the forward primer, 125 ng of the reverse primer, 5 µl of 10x *Pfu* DNA polymerase buffer (100 mM KCl, 100 mM $(NH_4)_2SO_4$, 20 mM $MgSO_4$, 1% (v/v) Triton X-100, 1 $mg.ml^{-1}$ BSA, 200 mM Tris-Cl, pH 8.8; Promega), 1 U of *Pfu* DNA Polymerase (Promega) and sterile distilled water to a final volume of 50 µl. Thermal cycling was allowed to proceed as follows: one cycle of denaturation (95°C for 30 seconds), 18 cycles of denaturation, annealing and extension (95°C for 30 seconds, 52°C for 60 seconds, 68°C for 5 minutes), one cycle of final extension (68°C for 7 minutes) and a 4°C hold. Digestion of the parental pQPfj1 plasmid in the amplification product was achieved by the addition of 5 U of *Dpn*I restriction endonuclease (Stratagene) to the reaction mixture and subsequent incubation at 37°C for 2 hours. Pre- and post-*Dpn*I samples were retained and analysed by 0.8% agarose gel electrophoresis (as per *APPENDIX D3*). Supercompetent *E. coli* JM109 cells (Promega) were transformed with the *Dpn*I-treated mutagenesis product (as per *APPENDIX D8*) for subsequent screening purposes. Plasmid DNA was isolated from the resulting colonies (*APPENDIX D1*) and screened for the desired S248G mutation by DNA

PROTEIN EXPRESSION VARIABLES [1]	
Media	2x YT
	LB
	LB-Lysine (0.1 mg.ml^{-1})
Growth Temperature [2]	26"C (Room Temperature)
	30"C
	37"C
Selection Pressure (Ampicillin)	50 µg.ml^{-1}
	50 µg.ml^{-1} (supplemented every hour post-induction)
	100 µg.ml^{-1}
	200 µg.ml
E. coli Strain [3]	BL21
	DH5α
	JM109
	OD259™
	Rosetta 2
	RR1
	XL1-Blue
	XL10-Gold
Induction [4]	Selection absent
	IPTG (1 mM)
	A_{600} = 0.6-0.8
	A_{600} < 0.6
	A_{600} > 0.8
	Length of induction time

PROTEIN PURIFICATION VARIABLES	
Denaturing Conditions	Non-denaturing
	4 M urea
	8 M urea
Protein Solubilisation	PEI (0.1%)
	N-Sarcosyl (7.5%)
Column: Culture volume Ratio	1:2000
	1:4000
	1:8000
Columns Utilised	Ni-NTA
	Q-Sepharsose Fast Flow™
Column Washes	Imidazole (50-150 mM)
	HEPES (5 mM)
	ATP (10 mM)
	Triton X-100 (1%)
	NaCl (100 mM – 1 M)
Protein Concentration	Polyethylene Glycol (PEG)
	Centricon® centrifugal units (Millipore)

[1] reviewed by BIRKHOLTZ *et al.* (2008); SØRENSEN and MORTENSEN (2005); GRÄSLUND *et al.* (2008); [2] BERWAL *et al.* (2008); [3] sourced as per *APPENDIX E*; [4] FLICK *et al.* (2004).

Purification strategies included the use of both non-denaturing and denaturing conditions in the absence and presence of urea respectively, solubilisation of the target proteins with polyethyleneimine (PEI; Sigma-Aldrich) and N-Sarcosyl (Sigma-Aldrich), and use of a Q-Sepharose Fast Flow™ anion exchange column (Sigma-Aldrich; 100 mM - 1 M NaCl gradient) subsequent to Nickel affinity chromatography (*TABLE 3.1*). The binding of non-target proteins to the Nickel affinity columns was overcome with incremented volumes of induced culture relative to the utilised column, in addition to washes with varied concentrations of imidazole, HEPES, ATP, Triton X-100 and NaCl as indicated. The combination of strategies found to yield optimum quantities of PfHsp40 and Pfj1 is further detailed in *SECTION 3.2.2.1* and *3.2.2.2*.

3.2.2.1 Expression and Purification of Recombinant PfHsp40

In brief, recombinant hexahistidine-tagged PfHsp40 (His_6-PfHsp40) was expressed from the pQE30-based pQPfHsp40 plasmid (*FIGURE 3.1C*) in *E. coli* XL1-Blue at 26°C in Luria-Bertani media (LB; 1% (w/v) tryptone, 0.5% (w/v) yeast extract, 1% (w/v) NaCl) supplemented with 200 $\mu g.ml^{-1}$ ampicillin. Protein expression was induced with 1 mM IPTG in early log phase (A_{600} < 0.6) in the presence of selection pressure, and the cells were harvested 16 hours post-induction. Protein purification was performed in batch, under denaturing conditions (4 M urea) in the presence of 0.1 % (v/v) PEI for protein solubilisation, 10 mM imidazole, 300 mM NaCl and 10 mM Tris-Cl (pH 8.0). Cell lysis was achieved by sonication and treatment with 1 mM lysozyme (freeze-thaw at -20 °C) in the presence of proteinase inhibitors (1 mM phenyl methyl sulfonyl fluoride (PMSF), 0.5 $\mu g.ml^{-1}$ Pepstatin A and 1 $\mu g.ml^{-1}$ Leupeptin). The cell lysate was cleared by centrifugation (16 000xg, 20 minutes, 4°C). Protein in the soluble fraction was allowed to bind a 50% Nickel-nitrilotriacetic acid slurry (Ni-NTA; Qiagen) in a ratio of 1:4000 column to culture volume for 4 hours at 4°C with gentle agitation. The beads were subsequently washed consecutively with incremented concentrations of imidazole (50, 100 and 150 mM), 50 mM HEPES, 10 mM ATP and 1% (v/v) Triton X-100 respectively in 300 mM NaCl and 10 mM Tris-Cl (pH 8.0). Washes were performed in the absence of urea to permit protein refolding. Bound protein was eluted from the beads with 1 M imidazole. The imidazole in the eluted fraction was removed by dialysis (5% (v/v) glycerol, 2 mM $MgCl_2$, 0.8 mM DTT, 50 mM NaCl, 50 mM Tris-HCl, pH 7.4), and the protein was concentrated with Polyethylene Glycol (PEG-3000; Sigma-Aldrich). Purification of the recombinant protein was verified by SDS-PAGE analysis as per *APPENDIX D10* and Western analysis using a mouse monoclonal anti-His (1:5000; GE Healthcare) or mouse anti-penta-His (1:5000; Qiagen) primary antibody and a horse-radish peroxidase (HRP)-conjugated sheep anti-mouse secondary antibody (1:5000; GE Healthcare) as per *APPENDIX D11*. The concentration of the purification product was determined by Bradford's Assay as per *APPENDIX D9*.

3.2.2.2 Expression and Purification of Recombinant Pfj1

In brief, recombinant hexahistidine-tagged Pfj1 (His_6-Pfj1) was expressed from the pQE30-based pQPfj1 plasmid (*FIGURE 3.2E*) in *E. coli* XL1-Blue at 37°C in 2x Yeast Tryptone media (2x YT; 1.6% (w/v) tryptone, 1% (w/v) yeast extract, 0.5% (w/v) NaCl) supplemented with 200 $\mu g.ml^{-1}$ ampicillin. Protein expression was induced with 1 mM IPTG in mid log phase ($_{(A600}$ of 0.6 - 0.8) in the presence of selection pressure, and the cells were harvested 16 hours post-induction. Protein purification was performed in batch, under non-denaturing conditions in the presence of 0.1% (v/v) PEI for protein solubilisation, 10 mM imidazole, 300 mM NaCl and 10 mM Tris-Cl (pH 8.0). Cell lysis was achieved by sonication and treatment with 1 mM lysozyme (freeze-thaw at -20 °C) in the presence of 1 mM PMSF. The cell lysate was cleared by centrifugation (16 000xg, 20 minutes, 4°C). Protein in the soluble fraction was allowed to bind a 50% Nickel-charged Chelating Sepharose Fast Flow™ slurry (GE Healthcare) in a ratio of 1:4000 column to culture volume for 4 hours at 4°C with gentle agitation. The beads were subsequently washed consecutively with incremented concentrations of imidazole (50, 100 and 150 mM) in 300 mM NaCl and 10 mM Tris-Cl (pH 8.0). Bound protein was eluted from the beads with 1 M imidazole. Purification of the recombinant protein was verified by SDS-PAGE analysis as per *APPENDIX D10* and Western analysis using a mouse monoclonal anti-His primary antibody (1:5000 dilution; GE Healthcare) and an HRP-conjugated sheep anti-mouse secondary antibody (1:5000 dilution; GE Healthcare) as per *APPENDIX D11*.

3.3 RESULTS AND DISCUSSION

3.3.1 Construction of the pQPfHsp40 and pQPfj1 Expression Constructs

Synthesis of the PfHsp40 and Pfj1 synthetic genes and subsequent cloning into the pQE30 expression vector was verified by restriction digestion analysis as detailed in *FIGURE 3.3* below. Subsequent DNA sequencing was employed to confirmed the integrity of the amplified coding regions and assembled constructs as previously detailed. An undesired Gly^{248} to Ser^{248} mutation was identified in the zinc-binding domain of the Pfj1-Front coding sequence and subsequently corrected by site-directed mutagenesis as discussed in *SECTION 3.2.1.2.3*. Correction of the mutation was verified by DNA sequencing analysis.

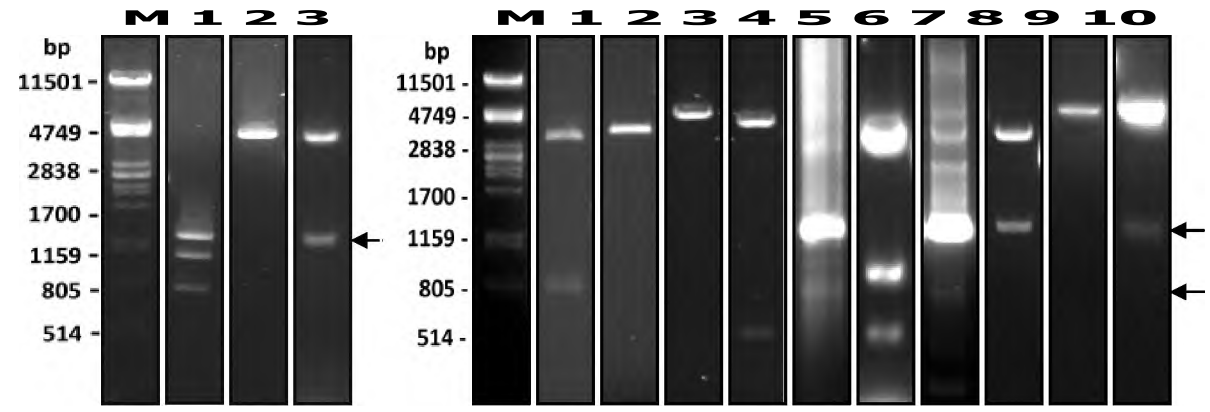

FIGURE 3.3 Confirmation of the cloning **of the pQPfHsp40 and pQ**Pfj1 **plasmid**s **by agarose gel electrophoresis. (A) Construction of the pQPfHsp40 plasmid. The PfHsp40 coding sequence (1281 bp) was excised from the pPCR**-Smart-**PfHsp40 plasmid with** *Bam*H**I and** *Hind***III restriction enzymes (1281 bp, 1041 bp, 740 bp, 20 bp, 15 bp and 14 bp;** ***lane 1***) **and ligated into the Bam**HI/Hind**III-digested pQE30 vector (3419 bp;** *lane 2*) **to produce plasmid pQPfHsp40. The latter plasmid was verified by digestion with** *Bam*H**I and** *Hind***III, releasing the 1281 bp PfHsp40 insert (3419 bp and 1281 bp;** *lane 3*). **The arrow indicates the position of the PfHsp40** coding **sequence (1281 bp). (B) Construction of the pQ**Pfj1 **plasmid. The** Pfj1-**Front coding sequence (839 bp) was excised from the pG Pfj1-Front plasmid with** ***Bam***H**I** and ***Sma*I restriction enzymes (3067 bp and** 839 bp; ***lane 1***) **and inserted into the** *Bam*H**I/*****Sma*****I-digested pQE30 plasmid (3436 bp;** *lane 2*). **This produced plasmid pQ**Pfj1-**Front, which was verified by digestion with** ***Bam***H**I (4275 bp;** *lane 3*) **and** *Eco*R**I (3858 bp and** 417 bp; ***lane 4***). The **Pfj1-Back coding sequence was amplified by PCR assembly (1236 bp;** *lane 5*) **and inserted in reverse orientation into the pGEM-T Easy® vector to produce pG**Pfj1-**Back, which was verified by digestion** with *Eco***RI (2997 bp, 822 bp and 432 bp;** *lane 6*). **The** Pfj1-**Back coding sequence was re-**amplified **for insertion** of a 3'-***Pst*I **restriction site (1242 bp;** *lane 7*) **and re-inserted into the pGEM-T Easy® vector to produce pG**Pfj1-Back-*Pst*I. The Pfj1-**Back coding sequence (1192 bp) was excised from plasmid pG**Pfj1-**Back-***Pst*I **with** *Sma*I and *Pst*I **(2292 bp, 1192 bp and 73 bp;** ***lane 8***) **and inserted into the** *Sma*I/*Pst*I**-digested pQPfj1-Front plasmid (4262** bp; ***lane 9***) **to produce pQ**Pfj1. **Insertion of the Pfj1-Back coding sequence into the latter plasmid was verified with digestion with** ***Sma*I** and *Pst*I **(4262 bp and 1196** bp; ***lane 10***). **The upper and lower arrows indicate the position of the** Pfj1-**Back (1196 bp)** and Pfj1-**Front (839 bp) sequences respectively. The corresponding plasmid maps for the restriction digestions indicated in the figure are presented in** *FIGURES* ***3.1*** and *3.2*. **The digested fragments were resolved by 0.8% agarose gel electrophoresis. Restriction enzymes used were sourced commercially as listed in** ***APPENDIX E***. **In both panels** *lane M* **represents a** ***Pst*I-digested λDNA Marker with the corresponding base pair (bp) size markers indicated on the left. All stages of the cloning of the pQPfHsp40 and** pQPfj1 **plasmids were verified by DNA sequencing**.

3.3.2 ***Expression and Purification of Recombinant PfHsp40 and Pfj1***

3.3.2.1 ***Isolation of Recombinant PfHsp40***

The production and isolation of recombinant hexahistidine-tagged PfHsp40 proved successful, albeit at low levels as represented in *FIGURE 3.4*. **The expression of the protein could be driven from the pQPfHsp40 plasmid in** *E. coli* **XL1-**Blue **with enhanced selection pressure of 200 µg.ml^{-1} ampicillin** (***FIGURE 3.4A***). **Significant variation was observed in independent** *E. coli* XL 1-**Blue [pQPfHsp40] colonies in terms of recombinant protein expression levels and time points relative to induction, therefore rigorous colony scr eening was employed prior to the isolation procedure described** to **identify colonies successfully producing the protein.**

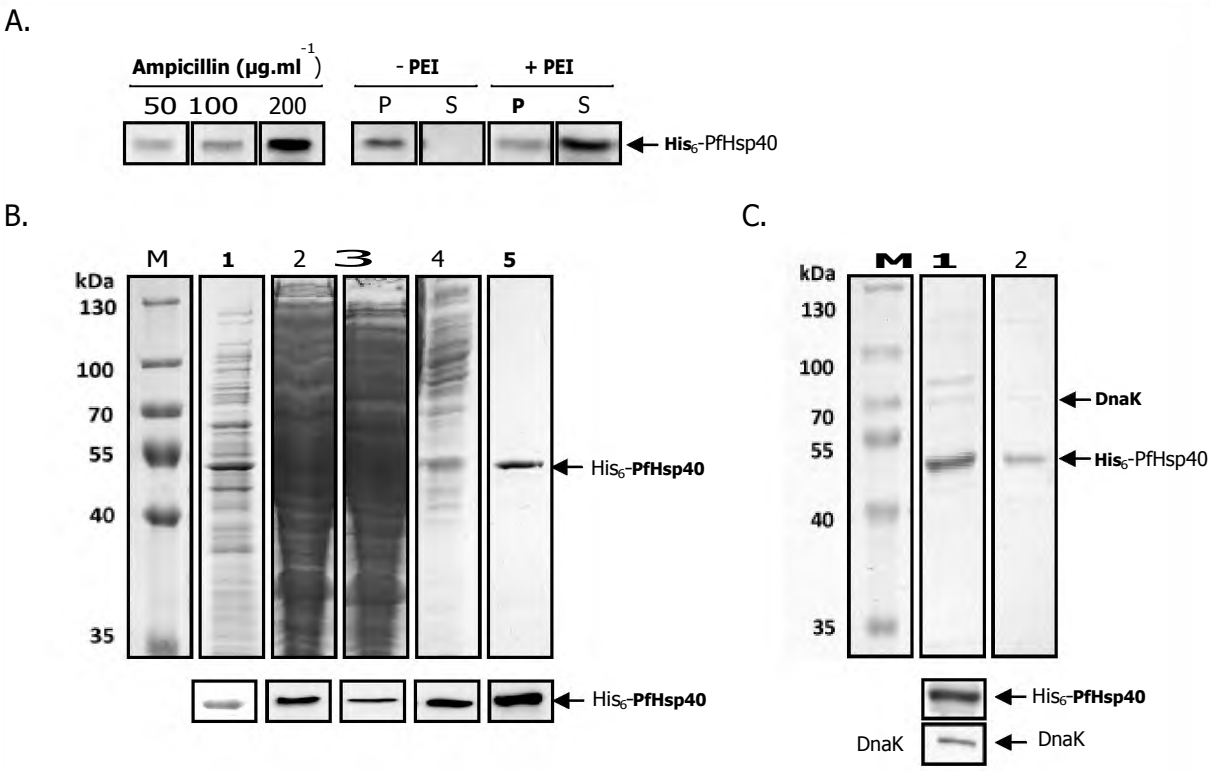

FIGURE 3.4 Heterologous production and isolation of recombinant hexahistidine-tagged PfHsp40. **Recombinant His_6-PfHsp40 expression was driven from the pQE30-based pQPfHsp40 plasmid in *E. coli* XL1-Blue at 26°C with 1 mM IPTG in LB media supplemented with 200 µg.ml^{-1} ampicillin for plasmid selection.** (A) **Expression of the recombinant protein was significantly enhanced with increased selection pressure of 200** µg.ml^{-1} **ampicillin, contrasted to 50** µg.ml^{-1} **and 100** µg.ml^{-1} **ampicillin in the growth media as indicated**. The **protein was detected in the insoluble pellet fraction (P) following sonication. The protein could be detected in the soluble fraction (supernatant; S) following the addition of 0.1% (v/v) polyethyleneimine (PEI) to the cell lysate prior to sonication. The presence or absence of PEI treatment is indicated by the symbols '+' and '-' respectively.** The His_6-PfHsp40 **protein was detected by Western analysis using a mouse monoclonal** anti-His **(GE Healthcare) or mouse anti-penta-His (Qiagen) primary antibody, and an HRP-conjugated sheep anti-**mouse **secondary antibody (GE Healthcare).** (B) **The protein was successfully purified by Nickel** affinity **chromatography on a Ni-NTA column (Qiagen) under denaturing conditions in the presence of 4 M urea** and **with protein solubilisation with 0.1%** (v/v) PEI. ***Upper panel* – Stages of the purification process were verified** by **10% SDS**-PAGE. ***Lanes*: *1* – *E. coli*** XL1-**Blue [pQPfHsp40] whole cell lysate fraction 16 hours post-induction,** *2* **–** *E. coli* XL1-**Blue [pQPfHsp40] supernatant fraction post-sonication and treatment with 4M urea and** 0.1% (v/v) **PEI,** *3* – Post-**sonication supernatant fraction unbound to the Ni-NTA column,** *4* – Non-**target** proteins were **removed from the column with** 50 - **150 mM imidazole, 50 mM HEPES, 10 mM ATP and 1% (v/v)** Triton X-100, *5* – **recombinant His_6-PfHsp40** (49 kDa) **eluted from the column with 1 M imidazole. The concentration of the purified protein was in the range of 0.1 µg.µl^{-1}** as **determined by Bradford's Assay**. ***Lower panel*** - The **purification of recombinant His_6-PfHsp40 protein was verified by Western analysis as detailed above.** (C) **Endogenous** Hsp70, **DnaK, was co-purified with recombinant His_6-PfHsp40 from the Ni-NTA column under non-denaturing purification conditions in the absence of urea. DnaK contamination could not be eliminated by subsequent anion exchange chromatography on a Q-Sepharose Fast Flow™ (Sigma-**Aldrich**) column** and elution **with a 0.1 - 1 M NaCl gradient. *Upper panel* – 10% SDS-PAGE analysis of recombinant His_6-PfHsp40 purification by Nickel affinity chromatography under non-denaturing conditions and anion exchange.** *Lanes*: ***1*** **–** Recombinant His_6-**PfHsp40 (49 kDa) purified on a Ni-NTA column under non-denaturing conditions,** *2* **– Purified recombinant His_6-**PfHsp40 (49 kDa) **and contaminating DnaK (69 kDa) eluted from a Q-Sepharose Fast Flow™ column with 0.**1 - 1 **M NaCl. *Lower panel*** – Western **analysis was employed for the detection of His_6-PfHsp40 as described above.** DnaK **was detected with rabbit polyclonal anti-**Hsp72/73 **(Upstate Biotechnology)** and HRP-**conjugated goat anti-rabbit secondary antibody (GE Healthcare).** In (B) and (C) *lane M* **represents a Fermentas Pageruler™ Protein Ladder, with corresponding size markers indicated in kDa on the left.**

Notably, the use of non-denaturing conditions for the purification of recombinant hexahistidine-tagged PfHsp40 was found to yield significant contaminating amounts of the endogenous prokaryotic Hsp70, DnaK. The contaminant could not be eliminated from the protein preparation by subsequent anion exchange chromatography on a Q-Sepharose column with an elution gradient of 100 mM - 1 M NaCl (*FIGURE 3.4C*). Consequently, PfHsp40 was purified under denaturing conditions in the presence of 4 M urea (*FIGURE 3.4B*). It is likely that the co-purification of DnaK under non-denaturing conditions represented the association of the chaperone protein with PfHsp40 in a chaperone-substrate interaction. The recognition of excess amounts of the prokaryotic Hsp40, DnaJ, as a substrate by DnaK has previously been described (LAUFEN *et al.*, 1999). It could therefore be argued that PfHsp40 was not appropriately folded despite the use of the approach of codon-harmonisation. In favour of this argument, expression from the codon-harmonised PfHsp40 synthetic gene resulted in the production of an insoluble protein product (*FIGURE 3.4A*). This contrasts the described use of codon-harmonisation for the enhanced production and solubility of the MSP-1_{42} protein by ANGOV *et al.* (2008). Despite this, the observed expression of PfHsp40 from the codon-harmonised gene is a marked improvement on the previously reported lack of expression of the protein from the wildtype gene in *E. coli* BL21 (MEHLIN *et al.*, 2006). Notably, expression of the codon-harmonised PfHsp40 gene was observed in the *E. coli* BL21 strain in this study (data not shown).

It could equally be argued that the recombinant PfHsp40 protein was rendered insoluble as a result of its potential toxicity to the bacterial expression host. Consistent with this, over-expression of the recombinant protein could not be achieved in the prokaryotic system (*lane 1*, *FIGURE 3.4B*), suggesting the degradation of the protein product or the suppression of translation. Moreover, the growth of the *E. coli* XL1-Blue [pQPfHsp40] culture was observed to be significantly reduced in contrast to that of the vector control *E. coli* XL1-Blue [pQE30] culture, potentially indicating a reduction in cell viability in the presence of recombinant PfHsp40. Notably, only low levels of PfHsp40 expression could be detected in approximately 5% of *E. coli* XL1-Blue [pQPfHsp40] colonies screened for expression. Despite the posed complications, the solubilisation of the recombinant PfHsp40 protein could be promoted by treatment with the ionic reagent, PEI (0.1%; *FIGURE 3.4A*). PEI promotes protein solubilisation during cell lysis by precipitating nucleic acids that would otherwise bind to the target protein and promote aggregation. Importantly, the reagent does not disrupt the structural or functional integrity of the target protein as previously demonstrated (NUNN *et al.*, 2002; SHONHAI *et al.*, 2008; TRABBIC-CARLSON *et al.*, 2004). Following purification under non-denaturing conditions in the presence of PEI (*FIGURE 3.4B*), recombinant PfHsp40 was shown to be active in *in vitro* characterisation assays as detailed in *CHAPTER 6.*

3.3.2.2 Partial **Isolation of Recombinant Pfj1**

Attempts to produce and isolate the recombinant Pfj1 **protein remained largely unsuccessful** (*FIGURE 3.5*) **despite the use of varied approaches to the enhancement of recombinant protein expression** in **a prokaryotic system, including the employment of codon-optimisation and the** range of **strategies summarised in *TABLE 3.1*. Recombinant hexahistidine-tagged** Pfj1 **remained recalcitrant to expression from the engineered pQ**Pfj1 **plasmid in all tested *E. coli* strains,** with **production of the protein undetectable even by Western analysis. Significantly low levels of Pfj1 expression** were **detected** by **Western analysis in a single colony of** *E. coli* XL1-**Blue [pQ**Pfj1] **in the presence of enhanced selection pressure (200 µg.ml^{-1}) following** rigorous **colony screening (***lane 1***, *FIGURE 3.5*). The recombinant** Pfj1 protein could only **be isolated partially in very low concentrations from the heterologous system** by **Nickel affinity chromatography**, with **insufficient expression of the protein resulting in** the **undesired** co-**purification of numerous contaminating proteins** (*lane 5*, ***FIGURE 3.5***). **Notably, the partial isolation of recombinant** Pfj1 **could only be achieved subsequent to** protein **solubilisation with** 0.1% PEI**. This** suggests that the **protein was predominantly insoluble following expression** in the **heterologous system and may have posed toxic**ity **problems** to the **bacterial host**.

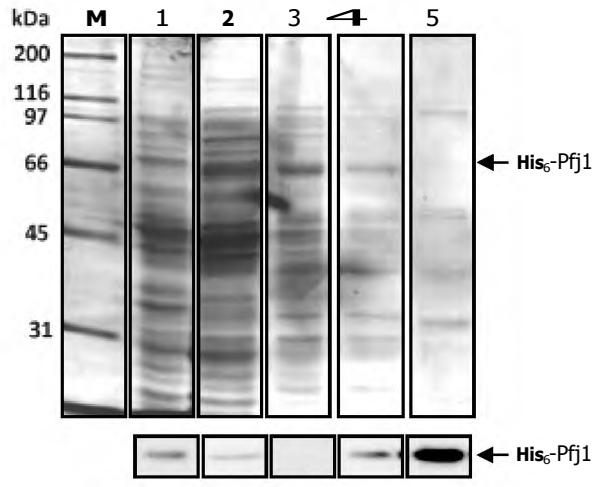

FIGURE 3.5 Heterologous production and partial isolation of recombinant hexahistidine-tagged Pfj1. **Recombinant** His_6-**Pfj1 expression was driven from the pQE30-based pQPfj1** plasmid in ***E. coli*** XL1-**Blue at** 37°C **with 1 mM IPTG in 2x YT media supplemented with 200 µg.ml^{-1} ampicillin for plasmid selection. The protein could only be** partially **purified by Nickel affinity chromatography on a Nickel-charged Chelating Sepharose Fast Flow**™ **column (GE Healthcare) under** non-**denaturing conditions and with protein solubilisation with 0.1% (v/v) PEI. *Upper panel* –** 10% SDS-**PAGE analysis of the stages of the purification process.** *Lanes*: ***M* – SDS-**PAGE **Molecular Mass Marker (Bio-**Rad**) with corresponding size markers in kDa indicated on the left, *1* – *E. coli* XL1-Blue [pQ**Pfj1**] whole cell lysate fraction 16 hours post-induction,** *2* **– *E. coli* XL1-Blue [pQ**Pfj1**] supernatant fraction post-sonication and treatment with 0.1% (v/v) PEI, *3* –** Post-**sonication supernatant fraction unbound** to the **column,** *4* **– Non-target proteins were** eluted **from the column with** 50 - **150 mM imidazole,** *5* **– recombinant His_6-Pfj1** (76 kDa) **and** non-**target proteins eluted from the column with 1 M imidazole**. *Lower panel* – **The His_6-**Pfj1 **protein was detected by Western analysis using a mouse monoclonal** anti-**His primary antibody (GE Healthcare) and an HRP-conjugated sheep anti-mouse secondary antibody (GE Healthcare)**.

Attempts to reproduce and optimise the partial isolation of recombinant Pfj1 depicted in *FIGURE 3.5* were unsuccessful. The protein could therefore not be isolated in sufficient quantity or purity for subsequent *in vitro* characterisation studies. Unfortunately, the utilisation of a eukaryotic expression system for the production of Pfj1 was not feasible owing to the codon usage selected for the synthetic gene encoding the protein. Due to the lack of purified recombinant Pfj1, alternative approaches were employed in the characterisation of the co-chaperone properties of the protein as further described in *CHAPTER 5*.

3.4 CONCLUSIONS

As a result of the differences that exist between PfHsp40 and Pfj1, and the multitude of factors influencing the success of the heterologous production of *P. falciparum* and Hsp40 proteins, the approaches of codon-harmonisation and -optimisation could not be compared unequivocally in this study. In hindsight, it would have been more meaningful to evaluate the effects of these two approaches on the production of the same protein product, however, this was beyond the scope of this study and remains to be performed in future work. Nevertheless, the approach of codon-harmonisation was shown to promote the successful heterologous expression of PfHsp40 in a prokaryotic expression system. Albeit at low levels, this was previously not attainable from the wildtype PfHsp40 gene (MEHLIN *et al.*, 2006). In contrast, the expression of Pfj1 remained a challenge despite the employment of codon-optimisation in the design of the corresponding synthetic gene, hindering subsequent *in vitro* characterisation studies.

The heterologous production of recombinant PfHsp40 and Pfj1 appeared to be complicated by the potential toxicity of the proteins to the bacterial host. This has been shown consistently for the expression of Hsp40 proteins in heterologous systems (AL-HERRAN and ASHRAF, 1998; NICOLL *et al.*, 2006). It is also suggested that *P. falciparum* proteins of a higher isoelectric point (pI; greater than 6.0), higher molecular weight (greater than 56 kDa), greater protein disorder or those that lack homology to proteins of the heterologous expression system are predisposed to insolubility or lack of expression in *E. coli* prokaryotic expression systems (MEHLIN *et al.* 2006). These factors are suggested to be more strongly correlated to the lack of expression of certain target proteins than codon-bias (MEHLIN *et al.* 2006). Notably, Pfj1 represents an atypically large Hsp40 protein (76 kDa in size in the hexahistidine-tagged recombinant form) that is considerably different to the homologous *E. coli* Hsp40 protein, DnaJ, and exhibits a comparatively high isoelectric point of 9.25. Furthermore, Pfj1 exhibits Lys-, Pro- and Asn-rich regions of low complexity that could pose complications to the integrity with which the protein is expressed heterologously. In contrast, PfHsp40 represents a smaller protein (49 kDa in size in the hexahistidine-tagged recombinant form) that is significantly

homologous to *E. coli* DnaJ, bears fewer regions of lower-complexity and exhibits a comparatively lower isoelectric point of 7.05. These differences potentially account for the successful production of PfHsp40, and not Pfj1, in the employed expression system. It has also been suggested that mRNA levels and stability may be of greater importance in the efficient heterologous expression of certain proteins, than the abundance of tRNA species corresponding to the target gene (WU *et al*., 2004). Notably, mRNA stability is of consideration in the approach of codon-harmonisation, but is not accounted for in the approach of codon-optimisation.

A domain approach to the isolation of recombinant Pfj1 may prove more successful than the attempts described in this study to express and purify the complete Pfj1 protein. Importantly, the J-domain of Pfj1 was shown to be expressed from the corresponding codon-optimised coding region engineered in this study, in a chimeric protein produced in *E. coli* as further detailed in *CHAPTER 5*. It is possible that the production of Pfj1 in the heterologous bacterial host may be promoted by the trimming of the lower complexity regions of the protein, including the N-terminal leader sequence preceding the J-domain and the C-terminal extension following the substrate-binding domain.

Furthermore, it remains to be determined whether the use of an alternative expression system may better promote the production and isolation of recombinant PfHsp40 and Pfj1. In particular, yeast, mammalian or baculovirus/insect cell line expression systems may satisfy post-translational modification requirements, if any, of the target proteins (as reviewed by BIRKHOLTZ *et al.,* 2008). This would require re-synthesis of the genes of interest to complement the codon usage preferences of the heterologous systems, and the re-cloning of these genes into suitable expression vectors. The use of alternative fusion-tag vector systems, such as those encoding maltose binding protein (MBP)- or glutathione S-transferase (GST)-fusion proteins, may be more efficient at promoting the solubility and expression of the Hsp40 proteins of interest in future studies, and remains to be assessed.

CHAPTER 4:

LOCALISATION STUDIES:

Elucidation of the Presence and Localisation of PfHsp40 and Pfj1 in Intraerythrocytic-Stage P. falciparum Parasites

4.1 INTRODUCTION

The transcriptional upregulation of PfHsp40 and Pfj1 in erythrocytic stage *P. falciparum* parasites has previously been described (BOZDECH *et al*., 2003; LE ROCH *et al*., 2003; WATANABE *et al*., 1997) however it has not been determined whether this upregulation translates into the production of these respective Hsp40 proteins. This study describes the use of immunofluorescence assays to determine the presence and localisation of PfHsp40 and Pfj1 in the asexual intraerythrocytic stages of cultured *P. falciparum*-infected erythrocytes, to provide insight into the roles of these type I Hsp40 proteins in the parasite's biology. Peptide-directed antibodies specific to PfHsp40 and Pfj1 were designed and raised for this purpose. In particular, this work was aimed at substantiating the potential for interactions of PfHsp40 and Pfj1 with PfHsp70-I. The upregulation and distribution of PfHsp70-I in the intraerythrocytic phase of the parasite's lifecycle has been documented (BISWAS and SHARMA, 1994; JOSHI *et al*., 1992; PESCE *et al*., 2008); this abundant protein has been implicated in protein folding and processing tasks in the parasite cytoplasm, nucleus (KUMAR *et al*., 1991) and parasitophorous vacuole (NYALWIDHE and LINGELBACH, 2006) as previously detailed. The possibility that PfHsp40 and Pfj1 co-chaperone compartment- or stage-specific tasks of PfHsp70-I was investigated as further discussed.

Similarly, the proposed association of PfHsp40 with the stage-specific Merozoite Surface Protein-7 (MSP-7; encoded by PF13_0197) was explored in this study. The proposed interaction between these two proteins was detected by yeast two-hybrid analysis (LACOUNT *et al*., 2005; refer to *SECTION 2.5.3*; *CHAPTER 2*) but has not been validated. For this purpose, the distribution of PfHsp40 was assessed relative to that of MSP-7 in the developing merozoite stage of the parasite to substantiate the potential interaction between these proteins.

Specifically, the objectives of this study were to (*i-vi*):

i. Confirm the presence and distribution of PfHsp70-I in the intraerythrocytic stages of *P. falciparum* development
ii. Engineer and raise peptide-directed antibodies specific to PfHsp40 and Pfj1
iii. Confirm the presence of PfHsp40 and Pfj1 in the intraerythrocytic stages of *P. falciparum* development
iv. Determine the localisation of PfHsp40 and Pfj1 in these stages relative to PfHsp70-I
v. Assess the effect of induced heat shock on the localisation of PfHsp40 and Pfj1
vi. Determine the localisation of the putative PfHsp40 interactor protein, MSP-7 relative to PfHsp40

4.2 MATERIALS AND METHODS

4.2.1 Parasite Culture

P. falciparum parasites (strain 3D7) were continually cultured in RPMI 1640 media supplemented with 50 mM glucose, 25 mM HEPES, 0.65 mM hypoxanthine, 0.2% (w/v) $NaHCO_3$, 48 $\mu g.ml^{-1}$ gentamicin, 0.5% (w/v) Albumax II and 2-4% (v/v) human type 0^+ erythrocytes, at 37°C under N_2 containing 3% (v/v) CO_2 and 4% (v/v) O_2. Cultures were synchronised during the ring stage of parasite development with sorbitol as previously described (LAMBROS and VANDERBERG, 1979). For heat shock experiments, subcultures were incubated at 37°C (control) and 43°C (heat shock) respectively for 2 hours prior to use.

4.2.2 Production of P. falciparum and Erythrocyte Lysates

Production of the *P. falciparum*-infected erythrocyte lysate fractions is schematically represented in *FIGURE 4.1A*. *P. falciparum*-infected erythrocytes were separated from a culture containing uninfected erythrocytes by centrifugation with a step-wise Percoll gradient containing 3% (w/v) alanine as previously described (GINSBURG *et al*., 1998). Subsequent to washes in phosphate-buffered saline (PBS; 137 mM NaCl, 2.7 mM KCl, 10.3 mM Na_2HPO_4, 1.8 mM KH_2PO_4, pH 7.4), the parasite-infected erythrocytes were optionally treated with 0.1 % (w/v) saponin in PBS to enable lysis of the erythrocyte membranes. Subsequently, intact parasites were sedimented by centrifugation (2300 *x*g, 3 minutes) and excess saponin was removed by washing with PBS. The supernatant of the centrifugation step containing the infected erythrocyte cytoplasm was retained. Lysates of uninfected erythrocytes and whole *P. falciparum*-infected erythrocytes were similarly prepared, without treatment with saponin. Samples were frozen in liquid nitrogen and lyophilised until further use.

4.2.3 Specifications for Peptide-Directed Antibody Design and Synthesis

Peptide-directed antibodies specific to PfHsp40 and Pfj1 were designed based on regions on high antigenicity in the C-termini of the two proteins. Epitopic regions of the two proteins were selected using algorithms determined for peptide antigenicity (HOPP and WOODS, 1981; JAMES and WOLFE, 1998), surface probability (EMINI *et al*., 1985), hydropathy (KYTE and DOOLITTLE, 1982) and chain flexibility (KARPLUS and SCHULTZ, 1988) as provided in GeneRunner software (version 3.05; Hastings Software Inc.). Cross-reactivity of the antibodies was avoided by confirmation of the specificity of the selected peptide regions to the target proteins by a BLAST search (ALTSCHUL *et al*., 1997). Synthesis of the antibodies to the predicted epitopes was kindly performed in the laboratory of

Professor Richard Zimmerman (Universität des Saarlandes, Germany). The peptides (*TABLE 4.1*) were synthesised with a preceding cysteine residue [C] and subsequently conjugated to haemocyanin.

TABLE 4.1 Designed Anti-PfHsp40 and Anti-Pfj1 Peptide-Directed Antibody Specifications

Antibody	Target Protein	Recognition Region	Peptide (N- to C- terminus)	Source
Anti-PfHsp40	PfHsp40	Residues 381-395	[C]SPVDKEYIKVRVTK	Rabbit
Anti-Pfj1	Pfj1	Residues 505-520	[C]NKNEENMSDDEKKKI	Rabbit

Antibodies were raised in individual rabbits immunised with the respective conjugated peptides. A pre-immunisation serum sample was collected and weekly post-immunisation serum samples were drawn for 8 weeks subsequent to immunisation. Serum samples were tested for reactivity against the target proteins by Western analysis as detailed in *SECTION 4.2.4*.

4.2.4 Detection of Proteins in P. falciparum Lysates by Western Analysis

P. falciparum-infected erythrocyte lysate samples were reconstituted in PBS containing 0.1% (v/v) Triton X-100. The protein concentration of the samples was determined by Bradford's Assay (as per *APPENDIX D9*) to allow for comparable detection of the proteins of interest in the respective fractions. The proteins of interest were detected in the reconstituted lysates by Western analysis (*APPENDIX D11*) as follows: PfHsp40 and Pfj1 were detected with the engineered rabbit anti-PfHsp40 and rabbit anti-Pfj1 polyclonal antibodies (pAb) respectively (1:5000 dilution; *SECTION 4.2.3*) and PfHsp70-▮was detected with rabbit anti-PfHsp70-▮pAb (1:5000 dilution). HRP-conjugated goat anti-rabbit pAb (1:5000 dilution; GE Healthcare) served as the secondary antibody for this detection. Negative controls were prepared using the pre-immunisation sera of the respective antibodies in place of primary antibody (1:5000 dilution). Whole cell lysates of *E. coli* XL1-Blue producing recombinant hexahistidine-tagged versions of PfHsp40, Pfj1 and PfHsp70-▮from plasmids pQPfHsp40, pQPfj1 (*CHAPTER 3*) and pQPfHsp70-▮respectively, served as positive controls. PfHsp70-▮production was driven in *E. coli* XL1-Blue following a previously described method (SHONHAI *et al*., 2008). Plasmid pQPfHsp70-▮(originally termed pQE30/PfHsp70; MATAMBO *et al*., 2004) and the anti-PfHsp70-▮antibody were kind gifts from Dr. Addmore Shonhai, Rhodes University (SHONHAI, 2007).

4.2.5 Detection of Proteins by Immunofluorescence Assays

Immunofluorescence localisation studies were employed to detect the proteins of interest (PfHsp40, Pfj1, PfHsp70-▮, MSP-7 and a Maurer's cleft marker protein, PfSBP-1) in trophozoite- and mixed-stage *P. falciparum*-infected erythrocytes, under non-heat shock and heat shock conditions respectively. Glass cover-slips were incubated in 1 $mg.ml^{-1}$ poly-L-lysine for 15 minutes and subsequently washed in PBS. A culture of *P. falciparum* infected erythrocytes was resuspended in PBS (1:10; pH 7.4) and 30

µl aliquots bound to individual poly-L-lysine coated cover-slips by centrifugation (700 rpm, 2 minutes) in 1 ml of PBS in 24-well plates. Unbound erythrocytes were removed by subsequent washes with PBS. Optional lysis of the erythrocyte membranes was achieved by incubation in 0.25% (w/v) saponin for 15 seconds, followed by the removal of excess saponin by repeated rinses with PBS. The bound erythrocytes were fixed and permeabilized with ice-cold methanol (-20 °C) for 2 minutes, and subsequently washed with PBS. Fixed erythrocytes were incubated in blocking solution (1 mM $MgCl_2$, 1 mM $CaCl_2$, 50% (v/v) Fetal Calf Serum (FCS), 20 $mg.ml^{-1}$ Bovine Serum Albumin (BSA) and 0.1% (v/v) Tween-20 in PBS) for 30 minutes. Subsequently, samples were incubated for 1 hour in the appropriate primary antibody diluted in blocking solution (1:200 rabbit anti-PfHsp40 pAb, 1:200 rabbit anti-Pfj1 pAb, 1:500 rabbit anti-PfHsp70-I pAb; 1:500 rabbit anti-MSP-7 pAb or 1:250 mouse anti-PfSBP-1 pAb). The anti-MSP-7 antibody (KAUTH *et al*., 2006; WOEHLBIER *et al*., 2006) and the anti-PfSBP-1 antibody (BLISNICK *et al*., 2000) were kind gifts from Professor Herman Bujard (University of Heidelberg, Germany) and Dr Jude Przyborski (Philipps University, Germany) respectively. Subsequent to several washes in PBS, the samples were incubated in the dark in the appropriate secondary antibody, including 1:250 TRITC-conjugated goat anti-rabbit (Invitrogen) or 1:1000 Alexa Fluor 488 goat anti-mouse monoclonal antibody (mAb; Invitrogen) diluted in blocking solution. Subsequent to several washes of the samples in PBS, the parasite nuclei were stained by brief incubation (10 seconds) in 1 $\mu g.ml^{-1}$ 4'6-diamidino-2-phenylindole (DAPI; Invitrogen) in PBS. The samples were rinsed with distilled water and mounted in Permafluor (Beckman Coulter) or Faramount (Dako) aqueous mounting media. The cells were viewed by fluorescence microscopy on a Nikon Eclipse E600 fluorescence microscope (100x Apochromat objective) and images were captured using a Media Cybernetics CoolSNAP-Pro monochrome cooled charged coupled device (CCD) camera. In this instance, pseudo-colouring and merging of the captured images was achieved with Adobe® Photoshop CS software (version 8.0). Alternatively, the cells were viewed by confocal fluorescence microscopy on a Zeiss Meta Laser Scanning Microscopy (LSM) 510 Microscope (62.5x objective) and images were captured using the accompanying Zeiss LSM 519 software. Background and non-specific fluorescence signal was monitored in control experiments with (i) rabbit pre-immunisation serum used in place of primary antibody, and (ii) in the absence of primary antibody.

4.2.6 Detection of Pfj1 by Immuno-Electron Microscopy

Pfj1 was detected in cultured *P. falciparum* erythrocytes by immuno-electron microscopy as further described. Cultured *P. falciparum*-infected erythrocytes were washed in cacodylate buffer (0.1 M sodium cacodylate, 0.1 M sucrose, 2 mM $CaCl_2$, 2 mM $MgCl_2$, pH 7.4) and subsequently fixed for 1 hour in fixative solution (cacodylate buffer containing 4% (w/v) paraformaldehyde and 0.25% (w/v)

gluteraldehyde). The fixed erythrocytes were incubated for 1 hour in fixative containing 1% (w/v) tannic acid and subsequent incubation for an additional hour in fixative containing 1% (w/v) osmium tetroxide. This was followed by subsequent washes in fixative and immobilisation in 2% (w/v) low melting-point agarose. The sample was dehydrated in incremented concentrations of ethanol and embedded in LR White resin (Electron Microscopy Sciences). Ultrathin sections were cut and mounted onto nickel grids. Prior to use, sections were rehydrated in PBS for 10 minutes, and blocked for 20 minutes in PBS containing 50 mM glycine. The sections were blocked for an additional 20 minutes in PBS containing 1% (w/v) BSA and 5% (v/v) goat serum. This was followed by incubation with primary antibody (1:1000 rabbit anti-Pfj1 pAb) in PBS supplemented with 0.2% (v/v) goat serum and 0.2% (w/v) Aurion BSA (Electron Microscopy Sciences) for 1 hour at room temperature. Subsequently the sections were washed with PBS containing 0.2% (v/v) goat serum, 0.2% (w/v) BSA and 0.1% (v/v) Tween-20. Incubation with gold-labelled secondary antibody was achieved for 1 hour at room temperature (1:25 colloidal gold-conjugated anti-rabbit antibody (GE Healthcare, UK) in PBS containing 0.2% (v/v) goat serum and 0.2% (w/v) Aurion BSA). The sections were washed as before (0.2% (w/v) BSA, 0.2% (v/v) goat serum, 0.1% (v/v) Tween-20 in PBS) and fixed in 2% (w/v) gluteraldehyde in PBS for 10 minutes. Subsequent to repeated washes with distilled water, counterstaining of the sections was achieved with uranyl acetate and lead citrate. Samples were prepared in duplicate. Non-specific gold labelling was monitored in control sections incubated with 1:25 gold-labelled secondary antibody in the absence of primary antibody, or with 1:1000 pre-immunisation serum used in place of primary antibody. Immuno-gold labelling was visualised and captured with a JEOL 1200 EX2 Transmission Electron Microscope.

4.3 RESULTS AND DISCUSSION

4.3.1 Detection of Chaperone Proteins in P. falciparum-Infected Erythrocyte Lysate

PfHsp70-▮ and PfHsp40 were detected in mixed-stage *P. falciparum*-infected erythrocyte lysate fractions by Western analysis as depicted in *FIGURE 4.1*. PfHsp70-▮was detected as a 75 kDa protein in the parasite fraction and appeared absent from the erythrocyte cytoplasm fraction of the lysate (*lanes P* and *S* respectively*; FIGURE 4.1*). This is consistent with the lack of an identifiable PEXEL/HT motif in PfHsp70-▮ for export to extra-parasitic locations in the infected erythrocyte, and the previously described absence of the protein in the erythrocyte cytoplasm (BANUMATHY *et al*., 2002; SARGEANT *et al*., 2006). Notably, the engineered anti-PfHsp40 antibody detected a specific protein of expected size (49 kDa) in the parasite fraction, corresponding to the detection of heterologously-produced recombinant PfHsp40 in *E. coli* XL1-Blue [pQPfHsp40] (*lanes P* and *R* respectively, *FIGURE 4.1*). This identified protein is suggested to represent PfHsp40 specifically detected by the anti-

PfHsp40 antibody, as it was not detected in the erythrocyte cytoplasm fraction (*lane S; FIGURE 4.1*) and was not recognised by the pre-immunisation rabbit serum of the engineered antibody. The **identification of PfHsp40 in cultured *P. falciparum*-infected erythrocytes serves to validate the predicted gene expression profile of the protein in the intraerythrocytic stages of the parasite's development (LE ROCH *et al*., 2003; detailed in *FIGURE 2.6, CHAPTER 2*). Moreover, the apparent absence of PfHsp40 in the infected erythrocyte cytoplasm is consistent with the lack of a recognisable PEXEL/HT motif in the protein (SARGEANT *et al*., 2006). The presence of PfHsp70-I and PfHsp40 in the parasite in the intraerythrocytic stages of development supports the notion of the proposed interaction between these two proteins. This was further supported by an overlap in the localisation patterns of the two proteins , as described in *SECTION 4.3.2*.**

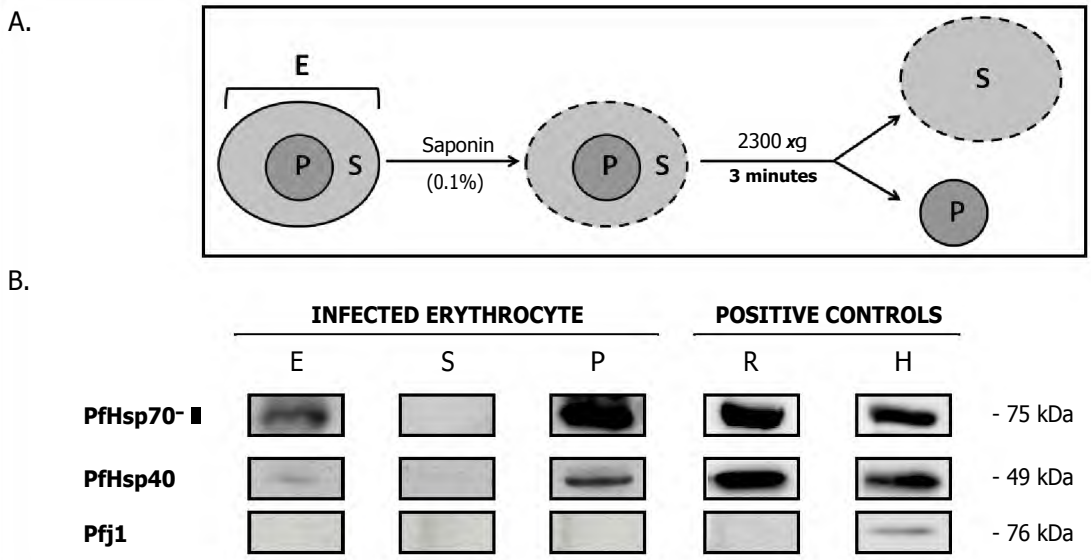

FIGURE 4.1 Detection of PfHsp70-I, PfHsp40 and Pfj1 in mixed-stage *P. falciparum*-infected erythrocyte lysate fractions by Western analysis. (A) Schematic representation of the production of parasite and erythrocyte lysate fractions from cultured *P. falciparum*-infected erythrocytes. Parasite-infected erythrocytes (E) were enriched from the culture and treated with 0.1% (w/v) saponin to enable lysis of the erythrocyte membranes. Intact parasites (P; pellet) were isolated from the infected erythrocyte cytoplasm (S; supernatant) by subsequent centrifugation (2300 *x*g, 3 minutes). (B) **Detection of PfHsp70-I, PfHsp40** and Pfj1 in ***P. falciparum*-infected erythrocyte lysate** (***lane E***) by **Western analysis with the anti-PfHsp70-I, anti-**PfHsp40 **and anti-**Pfj1 **antibodies. PfHsp70-I and PfHsp40 were detect**able **in the parasite fraction** (***lane P***), and **appeared absent from the erythrocyte cytoplasm fraction (*lane S*) consistent with the lack of a recognisable PEXEL/HT export motif. The antibodies were presumed to be specific, based on the detection of corresponding heterologously produced hexahistidine-tagged recombinant PfHsp70-I and PfHsp40 in** *E. coli* XL1-Blu**e [pQPfHsp70-I or pQPfHsp40]** (*lane R*)**. The recognition of the recombinant proteins was verified by additional detection with a mouse anti-**His **antibody (*lane H*). The detection of Pfj1 in the infected erythrocyte lysate fractions or in** *E. coli* **XL1Blue** [pQPfj1] **lysate was not achieved with use of the engineered anti-**Pfj1 **antibody as further discussed in the text. The detection of PfHsp70-I and PfHsp40 in *lanes E*, *S*, *P* and** *R* was **achieved with rabbit anti-PfHsp70-I and rabbit anti-PfHsp40 primary antibody respectively, and HRP-conjugated goat anti-rabbit secondary antibody. In** *lane H* **the corresponding proteins were detected with mouse anti-His primary antibody and HRP-conjugated sheep** anti-**mouse secondary antibody (GE Healthcare). The approximate sizes of the detected PfHsp70-I** (75 kDa), **PfHsp40 (49 kDa) and Pfj1 (75 kDa) proteins are indicated. The pre-immunisation sera of the anti-**PfHsp70-I **and** anti-**PfHsp40 antibodies did not react with components of the infected erythrocyte** or ***E. coli*** XL1-**Blue fractions in the** appropriate **negative controls**.

Independent studies have suggested the transcriptional upregulation of Pfj1 in intraerythrocytic stage *P. falciparum* parasites, providing evidence for the potential production of the protein during these stages (BOZDECH *et al*., 2003; WATANABE, 1997). However, the engineered rabbit anti-Pfj1 polyclonal antibody (detailed in *SECTION 4.2.3*) failed to detect an appropriate protein corresponding to the anticipated size of Pfj1 (76 kDa) in the *P. falciparum*-infected erythrocyte lysate (*FIGURE 4.1*). Instead, the anti-Pfj1 antibody detected numerous non-specific proteins in the erythrocyte fraction and in the uninfected erythrocyte negative control (data not shown). The detection of these proteins was attributed to the reactivity of the pre-immunisation serum of the anti-Pfj1 antibody, as determined in the appropriate pre-immunisation negative control. All post-immunisation serum samples produced in the engineering of the anti-Pfj1 antibody were tested for reactivity against recombinant Pfj1, and yielded similar non-specific results in Western analysis. The open reading frame of the Pfj1 gene (PFD0462w) is assumed to be correct based on transcriptional data reported by WATANABE (1997). However, Pfj1 represents a significantly large type I Hsp40, raising the possibility that this protein undergoes post-translational splicing in the parasite. This is unlikely to account for the inability of the engineered anti-Pfj1 antibody to recognise Pfj1 in parasite-infected erythrocyte lysate as the antibody similarly failed to recognise full-length recombinant hexahistidine-tagged Pfj1 in *E. coli* XL1-Blue (positive control *lane R*, *FIGURE 4.1*). The recombinant protein could be detected with an anti-His antibody in the positive control as indicated (*lane H*, *FIGURE 4.1*). Despite these findings, the anti-Pfj1 pre-immunisation serum did not react with elements of the erythrocyte cytoplasm or of the parasite in subsequent immunofluorescence studies, while the antibody in the post-immunisation sera proved specific to the parasite as further discussed in *SECTION 4.3.2.3*. This highlights the important consideration of the existence of differences in the detection of non-native and native proteins in Western analysis and immunofluorescence assays respectively.

4.3.2 Localisation Studies: Immunofluorescence Assays and Immuno-Electron Microscopy

4.3.2.1 Confirmation of the Localisation of PfHsp70-I in Erythrocytic Stage P. falciparum Parasites

Previously, PfHsp70-I was shown to localise to the parasite cytoplasm and nucleus in intraerythrocytic stage *P. falciparum* parasites (KUMAR *et al*., 1991). In agreement with this, PfHsp70-I was identified in the parasite cytoplasm in more than 90% of trophozoite- and schizont-stage parasites, in addition to the parasite nucleus in approximately 50% of trophozoite-stage parasites in the immunofluorescence assays performed in this study (*FIGURE 4.2*). Notably, KUMAR *et al.* (1991) described the cytoplasmic distribution of PfHsp70-I as the minor localisation pattern. Interestingly, the protein exhibited an apparent cytoplasmic distribution distinct from the nucleus in the developing merozoites of the schizont phase (*FIGURE 4.2*). Consistent with this apparent shift in

localisation, PfHsp70-I was first identified as a 75 kDa protein present on the merozoite surface (ARDESHIR *et al*., 1987). This merozoite surface localisation was potentially evident in the enlarged schizont images presented in *FIGURE 4.2B* and *4.2C*. The localisation of PfHsp70-I to distinct sites in the trophozoite and schizont stages of development highlights the numerous possible stage-specific roles of this protein in the parasite. Adding to this, FOTH *et al.* (2008) recently provided evidence for the post-translational modification of PfHsp70-I in schizont-stage *P. falciparum* parasites.

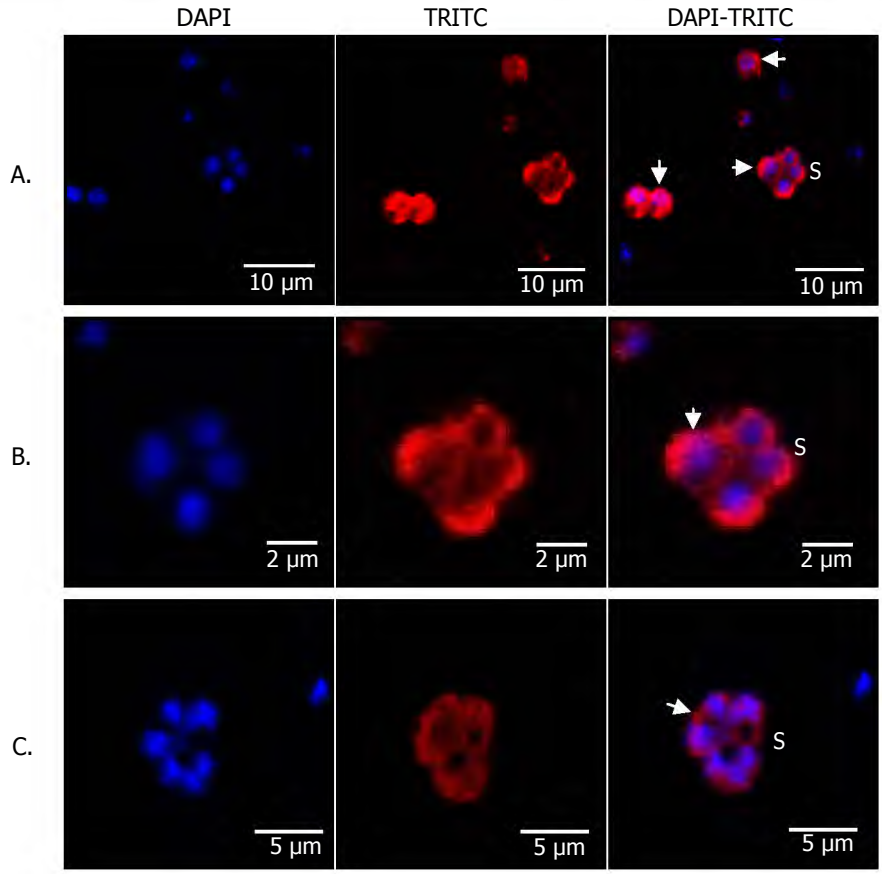

FIGURE 4.2 Detection of PfHsp70-I in ***P. falciparum***-infected erythrocytes by immunofluorescence staining. The distribution of PfHsp70-I is shown for cultured (A) mixed trophozoite- and schizont-stage and (B and C) schizont-stage parasite-infected erythrocytes[1] respectively. PfHsp70-I appeared to localise to the parasite cytoplasm in all stages of development in addition to the parasite nucleus in certain trophozoite-stage parasites (with an approximate incidence of 50%). The detection of PfHsp70-I was achieved with rabbit anti-PfHsp70-I pAb and TRITC-conjugated goat anti-rabbit secondary pAb (indicated in red; visualised with a TRITC filter) using intact parasite-infected erythrocytes maintained at 37°C prior to immunofluorescence staining (non-heat shock). Signal was not detected in the negative controls, with the use of secondary antibody only or with the use of pre-immunisation serum as primary antibody. Columns: *DAPI* – parasite nuclei detected with a UV filter (indicated in blue; notably the erythrocytes are anucleate); *TRITC* - PfHsp70-I localisation; *DAPI-TRITC* – merged image of parasite nuclear staining and PfHsp70-I localisation. Schizonts are indicated by the presence of multiple nuclei of the developing merozoites and are denoted with the letter 'S'. White arrows indicate the parasite boundaries in the absence of corresponding phase-contrast images. Immunofluorescence samples were viewed on a Zeiss Meta Laser Scanning Microscopy (LSM) 510 Microscope (62.5x objective) and the images were captured using the accompanying Zeiss LSM 519 software. Size-bars are indicated in µm in the bottom right corner of each frame.

[1] Intraerythrocytic stages of *P. falciparum* development are represented in *FIGURE 1.4*, *CHAPTER 1*

Cautiously, it must be noted that in the absence of accompanying phase-contrast images for the fluorescence images captured on the Zeiss Meta LSM 510 Microscope, the schizont-stage infections illustrated in *FIGURE 4.2* may equally be interpreted as multiple trophozoite-stage infections. Similarly, the apparent nuclear localisation of PfHsp70-▮in the trophozoite-stage parasites remains to be confirmed, as the nuclear boundaries are poorly-defined by the DAPI staining in the absence of corresponding phase-contrast images.

PfHsp70-▮was previously identified in the parasitophorous vacuole (NYALWIDHE and LINGELBACH, 2006) however this could not be confirmed in the immunofluorescence assays employed in this study. Notably, the size of the vacuolar compartment renders it in indistinguishable from the boundaries of the parasite plasma membrane. This putative PfHsp70-▮localisation remains to be assessed with the use of an appropriate marker protein such as the *P. falciparum* parasitophorous vacuolar protein-1 (PfPV-1; NYALWIDHE and LINGELBACH, 2006) or serine-rich protein (PfSERP; ANSORGE *et al*., 1996; NYALWIDHE *et al*., 2002). An independent proteomic study proposed the localisation of PfHsp70-▮to the Maurer's clefts developed by the parasite in the infected erythrocyte, consistent with the proposed role of these secretory organelles in the sorting and processing of exportome proteins (VINCENSINI *et al*., 2005). Contrary to this, PfHsp70-▮was not identified in extra-parasitic locations in this study (*FIGURE 4.2*). Moreover, PfHsp70-▮lacks a recognisable PEXEL/HT export motif (SARGEANT *et al*., 2006) and could previously not be identified in the infected erythrocyte cytoplasm with an alternative anti-PfHsp70-▮antibody (BANUMATHY *et al*., 2002). Although this does not exclude the possibility of the condition-specific export of this protein beyond the confines of the parasitophorous vacuole membrane, the proteomic findings of VINCENSINI *et al.* (2005) are questionable. It is most likely that PfHsp70-▮serves fundamental chaperone roles within the parasite, including the folding of newly translated proteins, the mediation of the appropriate stress response of the organism, and the maturation of particular client proteins in co-operation with PfHsp90 and numerous associated co-chaperone proteins. Moreover, it is likely that PfHsp70-▮resides in the parasitophorous vacuole to facilitate the sorting and export of proteins destined for extra-parasitic locations.

The absence of PfHsp70-▮from the infected erythrocyte cytoplasm is consistent with the proposed recruitment and utilisation of human Hsp70 for the assembly of parasite protein complexes in the host cell (BANUMATHY *et al*., 2002). Curiously, immunostaining with a mouse anti-human Hsp72/73 antibody (Stressgen) detected a protein in the parasite cytoplasm of trophozoite- and schizont-stage parasites and did not recognise human Hsp70 in the erythrocyte (not shown). The cross-reactivity of this antibody with Hsp70 proteins from organisms other than the human has been described, suggesting that the observed distribution pattern may represent the detection of an additional

cytoplasmic Hsp70 homolog of the parasite, such as PfHsp70-x or PfHsp70-z (*TABLE 2.4*, *CHAPTER 2*). The protein was not detected in the parasite nucleus and was therefore assumed to represent a protein other than PfHsp70-▮ The localisation of other Hsp70 homologs of the parasite remains to be validated (reviewed by SHONHAI *et al.*, 2007).

4.3.2.2 Detection of PfHsp40 in P. falciparum-Infected Erythrocytes

The immunofluorescence assays performed in this study revealed the localisation of PfHsp40 to the parasite cytoplasm in trophozoite- and schizont-stage parasites in heat shock and non-heat shock conditions, with an incidence of greater than 90% (*FIGURE 4.3*). This is in keeping with the cytoplasmic distribution of analogous type ▮Hsp40 proteins in eukaryotic organisms, as discussed in *CHAPTER 2*. Moreover, this is consistent with the observed cytoplasmic distribution of PfHsp70-▮ in this study (*FIGURE 4.2*), suggesting the potential co-localisation of PfHsp40 and PfHsp70-▮ and contributing additional rationale to the proposed interaction of PfHsp70-▮ and PfHsp40 in the intraerythrocytic stages of *P. falciparum* development.

In addition to the major distribution pattern of PfHsp40 in the parasite cytoplasm, the apparent detection of the protein in distinct punctate sites in the infected erythrocyte cytoplasm was observed (*FIGURE 4.3*). These sites were potentially indicative of the Maurer's clefts as they appeared immediately beneath the erythrocyte plasma membrane (fourth column, *FIGURE 4.3*) and were less evident in the emerging trophozoites. In dispute of this putative extra-parasitic localisation, PfHsp40 does not bear an identifiable export motif for secretion into the erythrocyte cytoplasm. Moreover, PfHsp40 was not detected in the erythrocyte cytoplasm in the prior Western analysis study (*FIGURE 4.1*), although the identified structures may have been disrupted upon treatment with saponin during preparation of the lysate (SPIELMANN *et al.*, 2006). The apparent distribution pattern observed in the Maurer's clefts was determined to be specific to the engineered anti-PfHsp40 antibody, as the corresponding pre-immunisation serum did not elicit an immunofluorescence signal in the parasite or the infected erythrocyte cytoplasm. The proposed presence of a non-PEXEL/HT Hsp40 protein of the parasite, Pfj4, in the Maurer's clefts of certain parasitized erythrocytes has been reported (PESCE *et al.*, 2008). It is therefore possible that the extra-parasitic distribution observed in this study represents the true localisation of PfHsp40 to sites in the erythrocyte cytoplasm, but it may just as likely denote the non-specific binding of the anti-PfHsp40 antibody itself to these sites. Notably, the anti-PfHsp40 antibody is unlikely to cross-react with exportome Hsp40 proteins such as PFE0055c (*TABLE 2.1, CHAPTER 2*) in the Maurer's clefts, as the antibody was designed against a highly specific portion of the PfHsp40 C-terminus (*TABLE 4.1*). Despite this, the tendency of antibodies to bind non-specifically to the Maurer's clefts has been reported (MAIER *et al.*, 2007; SPIELMANN *et al.*, 2006).

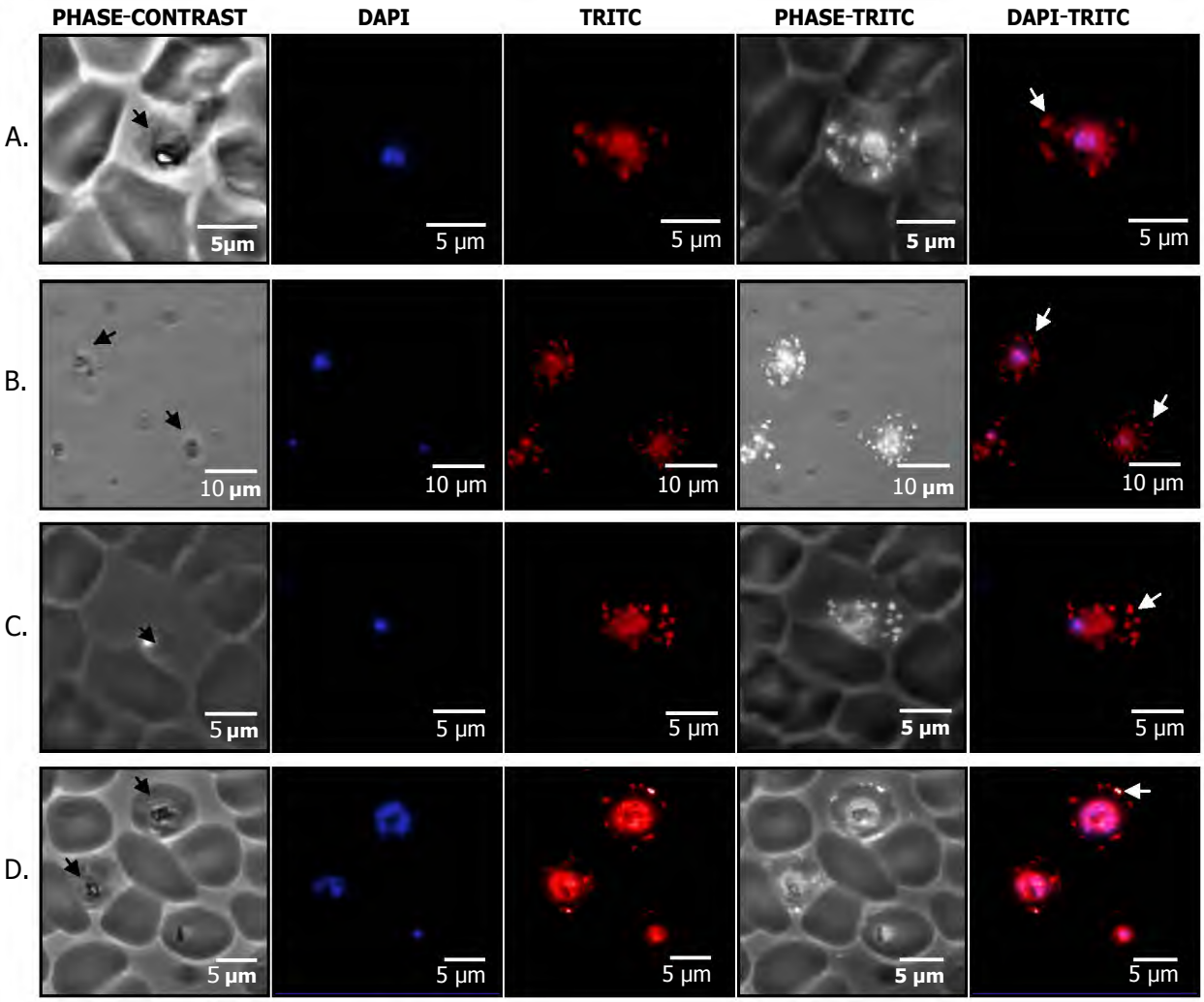

E.

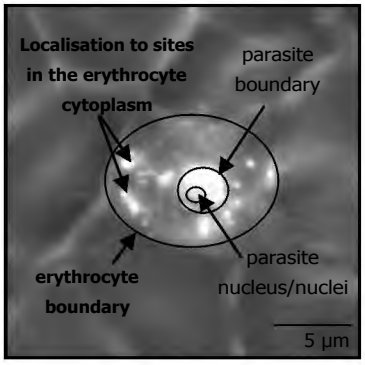

FIGURE 4.3 Detection of PfHsp40 in mixed-stage *P. falciparum*-infected erythrocytes by immunofluorescence staining. Staining in the parasite cytoplasm was observed for (A) intact trophozoite-stage parasite-infected erythrocytes, (B) saponin-treated trophozoite-stage parasite-infected erythrocytes, (C) intact trophozoite-stage parasite-infected erythrocytes incubated at 43°C for 2 hours prior to immunofluorescence staining (heat shock) and (D) schizont-stage parasite-infected erythrocytes. The infected cells were maintained at 37°C prior to immunofluorescence staining (non-heat shock) with the exception of (B). White arrows indicate the apparent detection of PfHsp40 in extra-parasitic locations immediately beneath the erythrocyte membrane, potentially indicative of the Maurer's clefts. A schematic interpretation of the apparent distribution of PfHsp40 is provided in (E). Notably, the presence of multiple nuclei may represent the infection of the erythrocyte with more than one parasite in culture, or the schizont stage of parasite development as indicated in (A) and (D) respectively. PfHsp40 was detected using rabbit anti-PfHsp40 pAb and TRITC-conjugated goat anti-rabbit secondary pAb (indicated in red; visualised with a TRITC filter). Parasite nuclei were detected with DAPI staining visualised with UV light (indicated in blue). Columns: *PHASE* – phase-contrast image with black arrows indicating the position of the parasites; *DAPI* – parasite nuclei; *TRITC* – PfHsp40 localisation; ***PHASE**-TRITC* – merged image indicating PfHsp40 localisation relative to the phase-contrast image; ***DAPI**-TRITC* – merged image indicating PfHsp40 localisation relative to the parasite nuclear staining. Fluorescence signal was not detected in the negative controls with the use of pre-immunisation serum as primary antibody or the use of secondary antibody only. Samples were visualised on a Nikon Eclipse E600 fluorescence microscope (100x Apochromat objective). Images were recorded with a coupled Media Cybernetics coolSNAP-Pro monochrome CCD camera, and pseudo-coloured using Adobe® Photoshop CS (version 8.0). Size bars are indicated in µm for each frame.

4.3.2.2.1 Assessment of the Apparent Extra-Parasitic Localisation of PfHsp40

Subsequent experiments were performed to validate the apparent Maurer's cleft localisation of PfHsp40, using an antibody raised against an appropriate marker protein, the *P. falciparum* Skeleton Binding Protein-1 (PfSBP-1; BLISNICK *et al*., 2000). The 48 kDa PfSBP-1 protein is known to span the membrane of the Maurer's clefts, with partial exposure on the erythrocyte cytoplasmic face where it interacts with a skeleton protein of the erythrocyte plasma membrane (BLISNICK *et al*., 2000). PfSBP-1 has also been reported in the parasitophorous vacuole membrane where it is required for the trafficking of the *P. falciparum* erythrocyte membrane protein 1 (PfEMP1) to the infected erythrocyte surface (MAIER *et al*., 2007). In this study, PfSBP-1 was detected in Maurer's cleft-like structures and potentially also in the parasitophorous vacuole of all trophozoite- and schizont-stage parasites as depicted in *FIGURE 4.4.* The distribution pattern of the protein appeared to be similar to the apparent extra-parasitic localisation of PfHsp40 observed in the initial immunofluorescence assays (*FIGURE 4.3*), although the latter appeared to be more punctate and less abundant (*FIGURE 4.4*).

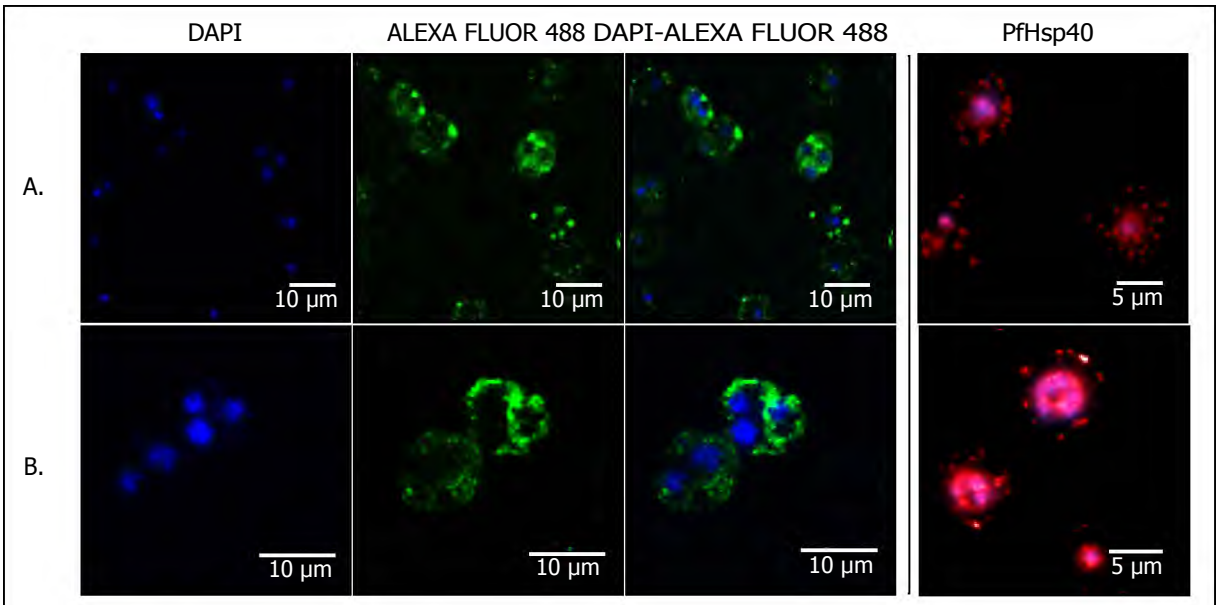

FIGURE 4.4 Detection of ***P. falciparum*** Skeleton-Binding Protein-1 (PfSBP-1) in ***P. falciparum***-infected erythrocytes by immunofluorescence staining. PfSBP-1 was shown to localise to Maurer's cleft-like structures in trophozoite- and schizont-stage parasite-infected erythrocytes (BLISNICK *et al*., 2000) as illustrated in (A) and (B) respectively. The position of these structures was verified by Z-stack analysis. This distribution pattern may also indicate the localisation of PfSBP-1 to the parasitophorous vacuole membrane (MAIER *et al*., 2007). The corresponding distribution of PfHsp40 in trophozoite- and schizont-stage parasites from prior immunofluorescence studies is provided in the right-hand column (extracted from *FIGURE 4.3*). Detection of PfSBP-1 was achieved with mouse anti-PfSBP-1 pAb and Alexa Fluor 488 goat anti-mouse mAb. The infected cells were maintained at 37°C prior to immunofluorescence staining (non-heat shock) and kept intact. Signal was not detected in the appropriate negative controls, with the use of secondary antibody only or with the use of pre-immunisation serum as primary antibody. Columns: *DAPI* – parasite nuclei detected with a UV filter (indicated in blue); *ALEXA FLUOR 488* – PfSBP-1 localisation; *DAPI-ALEXA FLUOR 488* – merged image of parasite nuclear staining and PfSBP-1 localisation; *PfHsp40* - corresponding PfHsp40 localisation (extracted from *FIGURE 4.3*). Immunofluorescence samples were viewed on a Zeiss Meta Laser Scanning Microscopy (LSM) 510 Microscope (62.5x objective) and the images were captured using the accompanying Zeiss LSM 519 software. Size-bars are indicated in µm in each frame.

Notably, the apparent distribution of PfHsp40 in the erythrocyte cytoplasm was of high incidence, observed in all infected erythrocytes exhibiting a cytoplasmic distribution of the protein in the initial triplicate immunofluorescence assays performed (*FIGURE 4.3*). Confounding to this, the distribution of PfHsp40 appeared to be restricted to the parasite cytoplasm and the apparent extra-parasitic localisation of the protein was not observed in independent repeat experiments (data not shown). Consequently, it may be considered that PfHsp40 was distributed to the Maurer's clefts under specific cellular conditions present in the cultured parasite-infected erythrocytes used in the initial immunofluorescence studies. Consistent with this argument, the only notable difference between the independent immunofluorescence studies was the use of different parasitized erythrocyte subcultures. In the prior studies, the cultured parasites exhibited slightly accelerated growth rates, completing the intraerythrocytic lifecycle in less than 48 hours at 37°C. This accelerated growth could have posed significant stress to the parasite, and may account for the possible distribution of PfHsp40 and other stress response proteins to the Maurer's clefts. It may even be argued that the 'Maurer's cleft' distribution of PfHsp40 appeared to be slightly enhanced under conditions of induced heat shock (*FIGURE 4.3C*). This is highly speculative however, and the only tangible conclusion from this study is that the cytoplasmic distribution of PfHsp40 in the parasite represented the major localisation pattern of the protein in the intraerythrocytic stages of development.

4.3.2.2.2 Localisation of the PfHsp40-Interactor Protein, Merozoite Surface Protein-7

The *P. falciparum* Merozoite Surface Protein-7 (MSP-7) was identified as a potential interactor protein of PfHsp40 in a yeast two-hybrid analysis of the protein interaction network of the parasite (LACOUNT *et al*., 2005; *SECTION 2.5.3*, *CHAPTER 2*). MSP-7 is targeted to the membrane of developing merozoite-stage parasites following synthesis and proteolytic splicing of the precursor form of the protein in the schizont stage (PACHEBAT *et al*., 2007). Importantly, MSP-7 has been implicated in the invasion of the human erythrocyte by the merozoite stage of *P. falciparum* (KADEKOPPALA *et al*., 2008) through co-operation with Merozoite Surface Proteins-1 and -6 (MSP-1 and MSP-6) in a multiprotein complex (KAUTH *et al*., 2006). This highlights a crucial role for MSP-7 in the pathogenesis of the parasite (PACHEBAT *et al*., 2007) and emphasises the importance of elucidating associated protein interactions. In this study, the localisation of MSP-7 was assessed in the intra-erythrocytic stages of *P. falciparum* development by immunofluorescence staining as detailed in *FIGURE 4.5*. The protein was consistently detected in the emerging merozoites of the schizont-stage in a predominant surface and cytoplasmic distribution consistent with the literature (*FIGURE 4.5*). This distribution is in line with the presence and cytoplasmic distribution of PfHsp40 in the merozoites of the schizont stage as presented in *FIGURE 4.3.* Weak or no immunostaining was observed for MSP-7 in trophozoite-stage parasites, consistent with the protein's gene expression profile predicted by LE ROCH *et al*. (2003).

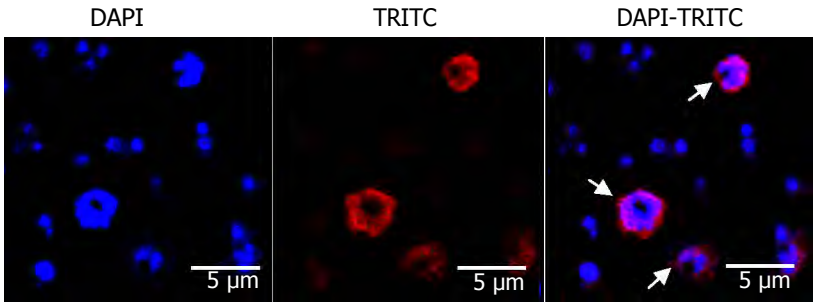

FIGURE 4.5 Detection of Merozoite Surface Protein-7 (MSP-7) in mixed-stage ***P. falciparum***-infected erythrocytes by immunofluorescence staining. MSP-7 was detected in an apparent surface localisation in developing merozoites of the schizont-stage (as indicated by the white arrows) in addition to the merozoite cytoplasm. The protein was not strongly detected in trophozoite-stage parasites suggesting that the protein was upregulated in the schizont stage. Detection of the protein was achieved with rabbit anti-MSP-7 pAb and TRITC-conjugated goat anti-rabbit secondary pAb (indicated in red). The infected cells were maintained at 37°C prior to immunofluorescence staining (non-heat shock) and kept intact. Signal was not detected in the appropriate negative controls, with the use of secondary antibody only or with the use of pre-immunisation serum as primary antibody. Columns: *DAPI* – parasite nuclei detected with a UV filter (indicated in blue); *TRITC* - MSP-7 localisation; *DAPI-TRITC* – merged image of parasite nuclear staining and MSP-7 localisation. Immunofluorescence samples were viewed on a Zeiss Meta Laser Scanning Microscopy (LSM) 510 Microscope (62.5x objective) and the images were captured using the accompanying Zeiss LSM 519 software. Size-bars are indicated in µm in each frame.

The potential overlap in localisation of MSP-7 and PfHsp40 lends itself to the notion that these proteins may exhibit interactions in the intraerythrocytic stages of development. The purpose of the proposed association of PfHsp40 with MSP-7 in the parasite is speculative, as discussed in *SECTION 2.5.3*, *CHAPTER 2*. It is possible that PfHsp40 recognises MSP-7 as a client protein, and subsequently co-operates with PfHsp70-I in the targeting of the protein to the merozoite surface, or in the assembly of the MSP-1-MSP-6-MSP-7 multiprotein merozoite surface complex. Consistent with this notion, PfHsp70-I has been identified on the merozoite surface as previously described (ARDESHIR *et al*., 1997) and alluded to in the findings presented in *FIGURE 4.2*. Notably, the existence and nature of the proposed association of PfHsp40 with MSP-7 remains to be validated by protein binding assays.

4.3.2.3 Detection of Pfj1 in P. falciparum-Infected Erythrocytes

Pfj1 appeared to localise predominantly to the parasite nucleus in more than 90% of trophozoite-stage parasites under all conditions investigated in the immunofluorescence assays, evident from the overlapping of the immuno- and DAPI staining (fifth column, *FIGURE 4.6*). This distribution is consistent with the predicted nuclear localisation of Pfj1 described in *CHAPTER 2* (PSortII prediction; NAKAI and HORTON, 1999). In addition, immunofluorescence signal was detected in the cytoplasm of all parasites exhibiting the anti-Pfj1 nuclear immunostaining (*FIGURE 4.6*). It would appear that the engineered anti-Pfj1 antibody was more efficient at detecting native Pfj1 in the immunofluorescence assays presented in *FIGURE 4.6*, than denatured Pfj1 in the prior Western analysis described in *SECTION 4.3.1*. The anti-Pfj1 pre-immunisation serum did not elicit an immunofluorescence response

in the uninfected or infected erythrocyte cells in the negative controls in this study, attributing the immunostaining observed in the parasite to the specific binding of the antibody in the post-immunisation serum in the test samples.

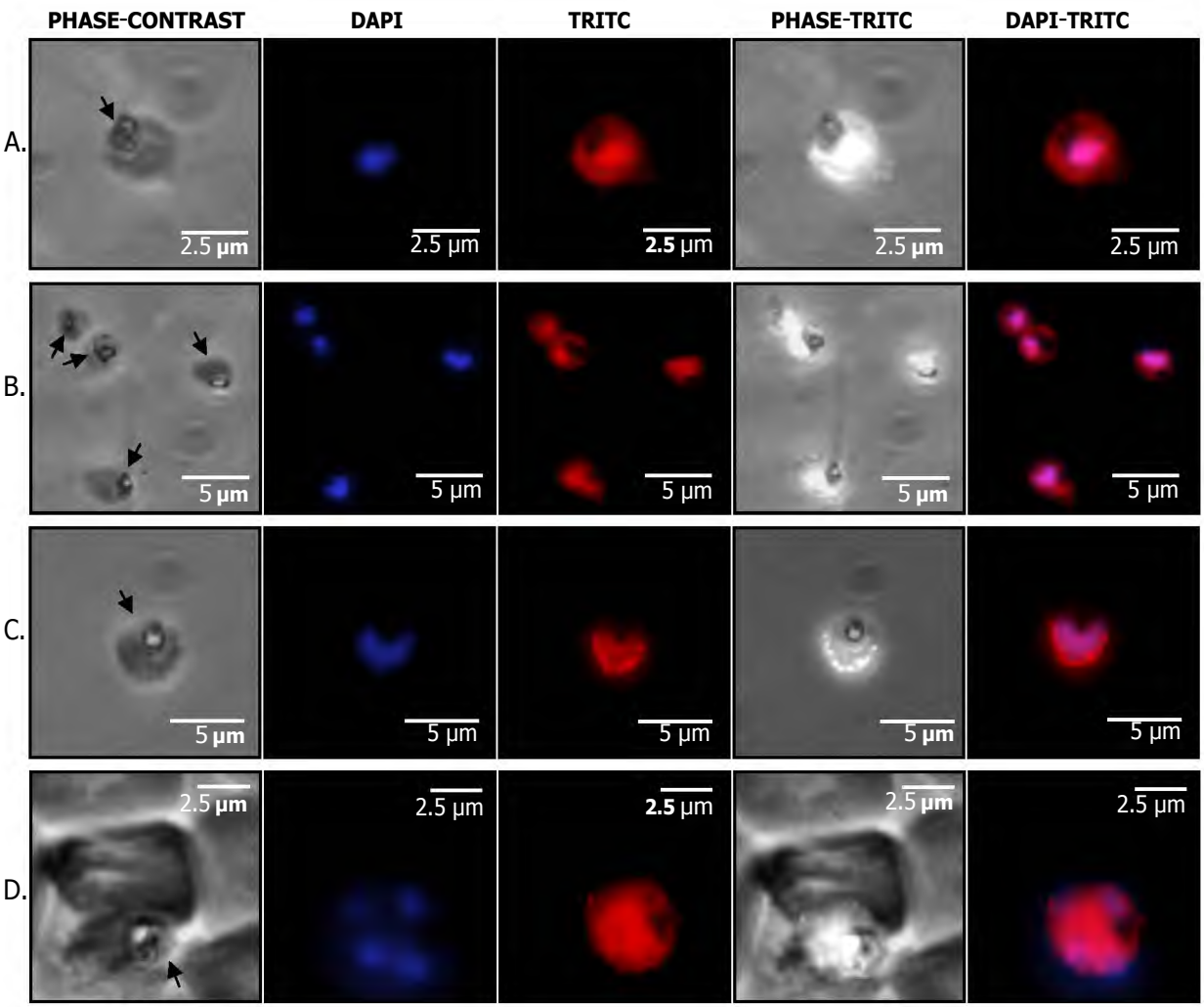

FIGURE 4.6 **Putative detection of Pfj1 in** mixed-**stage** ***P. falciparum*****-infected erythrocytes by** immuno**fluorescence staining. Staining was observed for (A) saponin-treated trophozoite-stage parasite-infected erythrocytes, (B)** saponin-**treated trophozoite-stage parasite-infected erythrocytes incubated at 43°C for 2 hours prior to staining (heat shock), (C) saponin-treated developing** schizont-**stage parasite**-infected **erythrocytes and (D) intact mature schizont**-stage **parasite-infected erythrocytes. Infected cells were maintained at 37°C prior to immuno-fluorescence staining with the exception of (B). Fluorescence staining was detected in the parasite cytoplasm and nucleus in the trophozoite-stage parasites represented in (A) and (B). Immunostaining of the nucleus was diminish**ed **with an increase in parasite cytoplasmic staining** in **the schizont-**stages **represented in (C) and (D). Pfj1 was detected using rabbit anti-**Pfj1 **pAb and TRITC-conjugated goat anti-rabbit secondary pAb (indicated in red; visualised with a TRITC filter). Parasite nuclei were detected** with DAPI **staining visualised with UV light (indicated in blue). Signal was not detected in the negative controls, with the use of secondary antibody only or with the use of pre-immuni**sation **serum as primary antibody.** Columns: *PHASE* – phase-**contrast image with black arrows indicating the position of the parasites;** *DAPI* – **parasite nuclei;** *TRITC* – **Pfj1 localisation;** *PHASE-**TRITC*** – **merged image indicating Pfj1 localisation relative to the phase**-contrast image; ***DAPI***-*TRITC* – **merged image indicating Pfj1 localisation relative to the parasite nuclear staining.** Images **were visualised on a Nikon Eclipse E600 fluorescence microscope (100x Apochromat objective) couple**d to a **Media Cybernetics coo**lSNAP-**Pro monochrome CCD camera, and** pseudo-**coloured using** Adobe® **Photoshop CS (version 8.0). Size bars are indicated in** µm in **each frame.**

Apparent Pfj1 levels in the nucleus appeared to lessen in the schizont stage, with localisation to the periphery of the parasite cytoplasm in immature developing schizonts (*FIGURE 4.6C* and *4.6D*). Notably, the evident shift of the protein from the nucleus in the schizont stage was similarly observed for PfHsp70-I (*FIGURE 4.2*) as described in *SECTION 4.3.2.1*. The detection of Pfj1 in the intraerythrocytic stages of development is consistent with the previously predicted expression profile of the protein based on transcriptomic data (BOZDECH *et al.*, 2003; WATANABE, 1997). Moreover, the overlap in the PfHsp70-I and Pfj1 localisation patterns in the parasite cytoplasm and nucleus, and the apparent shift of both proteins out of the nucleus in the developing intraerythrocytic parasites highlights the potential co-localisation of these proteins, and supports the notion that these proteins may exhibit interactions.

The apparent localisation of Pfj1 to the parasite nucleus was further explored with immuno-electron microscopy (EM) as depicted in *FIGURE 4.7* below.

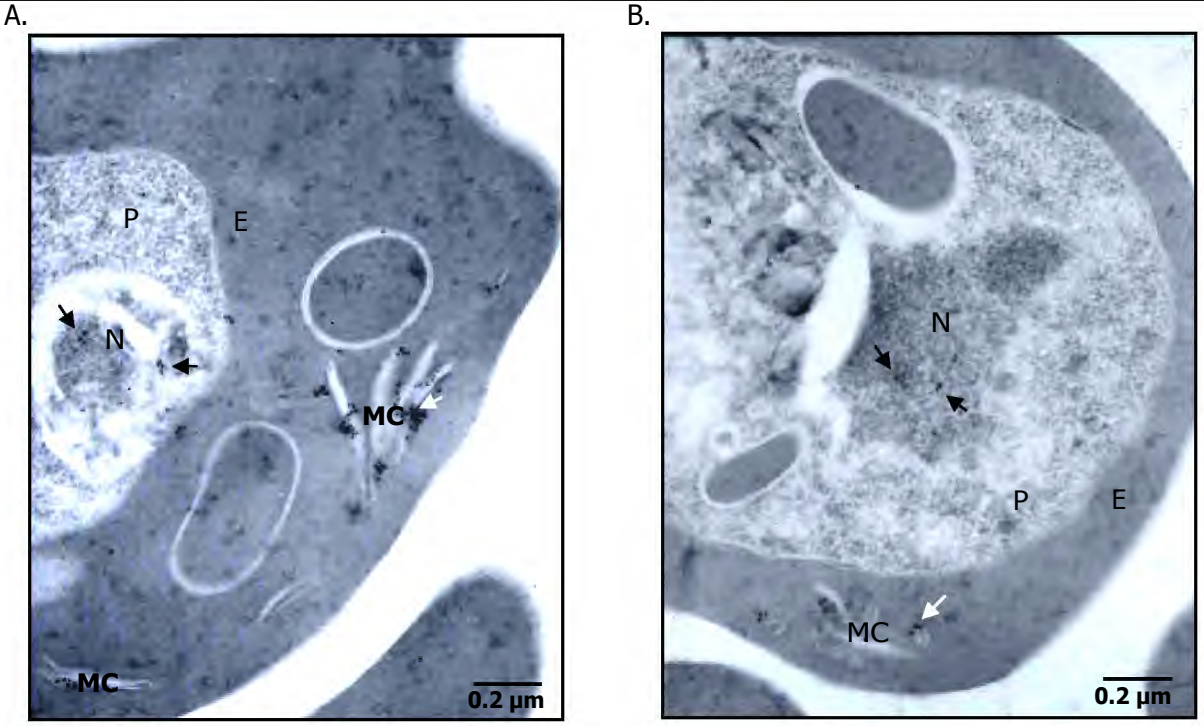

FIGURE 4.7 Putative detection of Pfj1 in trophozoite-stage *P. falciparum*-infected human erythrocytes by immuno-electron microscopy (EM). Pfj1 was detected with (A) 1:500 and (B) 1:1000 rabbit anti-Pfj1 primary antibody and gold-conjugated anti-rabbit secondary antibody. Immunostaining in the parasite nucleus is indicated with black arrows. Apparent non-specific staining of the Maurer's clefts by the antibody or a component of the rabbit serum is indicated with white arrows. The secondary antibody did not display non-specific gold labelling. Abbreviations used: *P* – parasite cytoplasm; *N* – parasite nucleus; *E* – erythrocyte cytoplasm; *MC* – Maurer's clefts. Size bars are indicated in µm in each frame.

An apparent nuclear and cytoplasmic labelling trend was observed in the test samples in certain trophozoite-stage parasite sections when probed with the anti-Pfj1 antibody (*FIGURE 4.7*). This staining was potentially specific as it was not observed in the pre-immunisation negative control, and

is in keeping with the distribution of Pfj1 determined by the prior immuno-fluorescence studies. Unfortunately, the results from immuno-EM were rendered inconclusive as a result of apparent non-specific labelling in the Maurer's clefts. This labelling was attributed to the non-specific binding of elements of the rabbit serum as determined in the pre-immunisation negative control, however attempts to lessen inconsistent labelling in the test samples with lowered primary antibody concentrations yielded the same results (*FIGURE 4.7B*).

4.4 CONCLUSIONS

In summary, this study has confirmed the presence of PfHsp40 and Pfj1 in the *P. falciparum* parasite in the intraerythrocytic stages of development using specific peptide-directed antibodies raised to detect these proteins. The identification of these type ▮Hsp40 proteins in the asexual blood-stages is consistent with previously predicted gene expression profiles derived from transcriptional data (BOZDECH *et al*., 2003; LE ROCH *et al*., 2003) and is in keeping with the importance of chaperone proteins in general in this phase of the parasite's lifecycle.

PfHsp40 was observed to localise predominantly to the parasite cytoplasm in trophozoite- and schizont-stage parasites. This distribution pattern overlaps with that reported for PfHsp70-▮in this study and prior work (KUMAR *et al*., 1991). This is potentially indicative of co-localisation, contributing rationale to the proposed interaction of PfHsp70-▮with PfHsp40 in the parasite cytoplasm. The cytoplasmic distribution of PfHsp40 further supports the general 'house-keeping' co-chaperone role envisaged for the protein and the parallels drawn between PfHsp40 and analogous cytoplasmic type ▮Hsp40 proteins of eukaryotic origin (discussed in *CHAPTER 2*). More specifically, it is probable that PfHsp40 undergoes farnesylation at the C-terminal CAAX box motif and subsequently associates with the cytoplasmic face of the intracellular organellar membranes to facilitate protein translocation. It is also likely that PfHsp40 associates with the PfHsp90/PfHsp70-▮multi-chaperone complex in the parasite cytoplasm to participate in the processing and activation of mature client proteins, as previously described for the corresponding *S. cerevisiae* cytoplasmic CAAX-box type ▮Hsp40 protein, Ydj1 (FLOM *et al*., 2008). PfHsp40 may also serve stage-specific roles in the *P. falciparum* parasite, as alluded to by the proposed interaction of the co-chaperone protein with MSP-7 (LACOUNT *et al*., 2005). In this study, MSP-7 was shown to exhibit an apparent merozoite surface and cytoplasmic localisation. This is consistent with the detection of PfHsp40 in the merozoite cytoplasm. The identification of PfHsp70-▮in the vicinity of the merozoite surface (ARDESHIR *et al*., 1987) suggests that PfHsp70-▮and PfHsp40 may co-operate in the processing of MSP-7 for targeting to the merozoite surface, or in the assembly of the MSP-1-MSP-6-MSP-7 multiprotein merozoite surface complex. It remains to be determined whether these chaperones can recognise MSP-7 in a chaperone-substrate

dependent manner, and whether the PfHsp40-MSP-7 interaction detected by yeast two-hybrid analysis represents a true association *in vivo*.

In addition to the major cytoplasmic localisation pattern of PfHsp40, it cannot be excluded that the protein may be distributed beyond the confines of the vacuolar membrane to sites in the erythrocyte cytoplasm. The apparent stage-specific progression of the PfHsp40 distribution pattern observed in the infected erythrocyte cytoplasm in this study suggests that the protein may localise to the Maurer's clefts. What is more, the observed extra-parasitic distribution pattern of PfHsp40 appeared similar to that of the Maurer's cleft marker protein, PfSBP-1 in this study, and that of the exportome Hsp40 protein PFE0055c, as determined by others (BHATTACHARJEE *et al*., 2008; HILLER *et al*., 2004). Interestingly, PfSBP-1 lacks an identifiable export motif, highlighting the possible localisation of additional PEXEL/HT-negative proteins to these sites. Notably, an apparent extra-parasitic distribution has similarly been described for the PEXEL/HT-negative type II Hsp40 protein, Pfj4. Cautiously however, it cannot be excluded that the anti-PfHsp40 antibody may be predisposed under certain conditions to non-specific binding to the Maurer's clefts, as previously suggested for other antibodies (SPIELMANN *et al*., 2006).

Similarly, the localisation patterns of PfHsp70-I and Pfj1 were shown to overlap in this study, with distribution to the parasite cytoplasm and nucleus in intraerythrocytic-stage parasites. Both of these chaperone proteins were observed to shift out of the nucleus of the developing merozoites, alluding to stage-specific roles. The apparent co-localisation of PfHsp70-I and Pfj1 and shift in distribution patterns during the progression of the intraerythrocytic stages lends itself to the potential of these two proteins to co-operate in an Hsp70-Hsp40 partnership. Cautiously, the results pertaining to the localisation of Pfj1 could not be confirmed by Western analysis and remain to be validated in this manner. Notably the design of a new, specific peptide-directed anti-Pfj1 antibody was hampered by the significant domain and residue conservation of Hsp40 proteins in general, and the identification of unique antigenic regions of the Pfj1 protein that are not of low complexity. The transfection of *P. falciparum* parasites with green fluorescent protein (GFP)-fusion constructs may be considered for future localisation studies, to complement the immunochemical-based localisation strategies described here. Considerations for the use of this technique in future experiments are further detailed in *CHAPTER 7.*

Interestingly, the localisation patterns of PfHsp40 and Pfj1 appeared to remain constant under induced conditions of heat shock. In critique of this, a heat-shock temperature of 43°C is significantly higher that the temperature fluctuation range of the febrile incidences of malaria illness (37-41°C) and may therefore have reduced the viability of the cultured parasites. Although the exposure of

parasite-infected erythrocytes to a temperature of 43°C may not have appropriately simulated heat shock as it is encountered *in vivo*, this temperature was selected based on the upregulation of Pfj1 mRNA at this temperature (WATANABE, 1997). Moreover, the upregulation of PfHsp70-▮and a type ▮▮ Hsp40 protein, Pfj4, have been reported at this temperature (PESCE *et al*., 2008). The upregulation of *P. falciparum* type ▮▮▮ and ▮V Hsp40 proteins at the more appropriate induced temperature of 41°C in the intraerythrocytic stages of the parasite has also been described (OAKLEY *et al.* 2007). It remains to be determined whether PfHsp40 or Pfj1 expression is constitutive or upregulated in response to heat shock in *P. falciparum*-infected erythrocytes, as described for PfHsp70-▮

The findings of this study have supported the notion that PfHsp70-▮ may forge Hsp70-Hsp40 partnerships with PfHsp40 and Pfj1 in the trophozoite, schizont and merozoite stages of intraerythrocytic *P. falciparum* development. Immunoprecipitation experiments were employed to validate the proposed association of PfHsp70-▮ and PfHsp40, but proved inconclusive (data not shown). PfHsp70-▮appeared to co-precipitate with PfHsp40 bound to the anti-PfHsp40 antibody in the parasite-infected erythrocyte lysate, however co-precipitation of the protein was similarly observed in the pre-immunisation serum negative control. Moreover, PfHsp70-▮was observed to bind non-specifically to the Protein G Sepharose (Sigma-Aldrich) or Protein A/G PLUS Agarose beads (Santa-Cruz Biotechnology) in the absence of bound antibody in the experiment. Irrespective of this, a true Hsp70-Hsp40 association may be too transient to capture by immunoprecipitation, and this is further complicated by the potential recognition of Hsp40 as a substrate by Hsp70 in this system.

Further substantiation of the potential for Hsp70-Hsp40 partnerships between PfHsp70-▮ and PfHsp40 and Pfj1 in the *P. falciparum* parasite was achieved by investigation of the proposed co-chaperone properties of the type ▮Hsp40 proteins, as described in *CHAPTERS 5* and *6.*

CHAPTER 5:

IN VIVO CHARACTERISATION:

Assessment of the Functionality of PfHsp40 and Pfj1 in an In Vivo Prokaryotic Complementation System

5.1 INTRODUCTION

It is known that Hsp40 proteins are not entirely interchangeable with respect to their interaction with distinct Hsp70 proteins (KELLEY and GEORGEOPOULOS, 1997; KLUCK *et al*., 2002; MINAMI *et al*., 1996; PRÖLS *et al*., 2001; SCHLENSTEDT *et al*., 1995; SULLIVAN *et al*., 2000). Interchangeability is thought to be reliant on the interaction of the Hsp40 proteins of interest with homologous or functionally equivalent Hsp70 proteins, or their involvement in analogous chaperone processes in the cell (DELOCHE *et al*., 1997; GENEVAUX *et al*., 2001). Prior work has demonstrated the functional interchangeability of diverse Hsp40 proteins in prokaryotic and eukaryotic complementation systems, in *E. coli* (DELOCHE *et al*., 1997; GENEVAUX *et al*., 2002; HENNESSY *et al*., 2005a; KELLEY and GEORGOPOULOS, 1997; NICOLL *et al*., 2007) and *S. cerevisiae* respectively (EDKINS *et al*., 2004; FEWELL *et al*., 2002; SCHLENSTEDT *et al*., 1995; YAN *et al*., 2002). The interchangeability of the Hsp40 proteins in these studies was assessed in terms of the ability of an exogenously produced Hsp40 protein of interest to replace functionally compromised or deficient endogenous Hsp40 proteins *in vivo*, through interaction with the appropriate endogenous Hsp70 proteins or involvement in distinct chaperone processes.

Hsp40 proteins are thought to mediate the specificity of interaction with their more promiscuous Hsp70 partner proteins, suggested by the generally larger ratio of Hsp40 proteins relative to Hsp70 proteins encoded on the genomes of numerous diverse organisms as previously discussed (BOTHA *et al*., 2007; HENNESSY *et al*., 2000; VOS *et al*., 2008). In particular, the J-domain appears to be a major determinant of this specificity, as investigated by numerous J-domain swapping experiments (reviewed in HENNESSY *et al*., 2005b). Coupled to rational mutagenesis, these experiments have provided insight into the established sequence-specific and structural elements of the J-domain that govern the specificity of interaction with partner Hsp70 proteins (GENEVAUX *et al*., 2002; HENNESSY *et al*., 2005a).

This study was aimed at the characterisation of the *in vivo* functionality of recombinant PfHsp40 and Pfj1 in a heterologous system. The approaches of J-domain swapping, rational mutagenesis and Hsp40 interchange in a prokaryotic complementation system were employed to identify common factors of J-domain based Hsp70-Hsp40 interaction in the prokaryotic and parasitic systems. Specifically, the objectives of this study were to (*i-iv*):

i. Assess the ability of exogenously produced PfHsp40 and Pfj1 to functionally replace endogenous prokaryotic Hsp40 in the *E. coli* OD259 *in vivo* complementation system (DELOCHE *et al*., 1997)

ii. Conduct domain swapping of the J-domain of a prokaryotic DnaJ protein with the atypical J-domain of Pfj1 to produce a Pfj1 J-domain DnaJ chimera protein

iii. Assess the functionality of the Pfj1 J-domain chimera in the *E. coli* OD259 complementation system to identify common mechanisms of J-domain based interaction with Hsp70

iv. Perform rational mutagenesis on the Pfj1 J-domain to identify important residues and motifs governing the functionality of the domain

5.2 MATERIALS AND METHODS

5.2.1 In Vivo Complementation Assays

Functional *in vivo* complementation assays were performed in the thermosensitive *E. coli* OD259 strain (MC4100 *dnaJ*::Tn*10* Δ*cbpA*::Kan^{r} Δ*ara714 araD139*) as previously described (DELOCHE *et al.*, 1997; KELLEY and GEORGOPOULOS, 1997). Prior work has demonstrated the ability of the *A. tumefaciens* DnaJ protein (*Agt* DnaJ; accession AAR84666.1) to functionally replace wildtype *E. coli* CbpA (curved DNA binding protein A; CbpA) and DnaJ in the *E. coli* OD259 strain at 40°C (HENNESSY *et al*., 2005a). *E. coli* OD259 cells exogenously producing *Agt* DnaJ from plasmid pRJ30 therefore served as a positive control for the complementation assays (HENNESSY *et al*., 2005a). Substitution of residue His^{33} of the highly conserved HPD motif in the loop region between helices II and III of the J-domain is known to abolish interactions with Hsp70 (HENNESSY *et al*., 2005a; TSAI and DOUGLAS, 1996) therefore *E. coli* OD259 cells exogenously producing mutant *Agt* DnaJ-H33Q from plasmid pRJ30-H33Q served as the negative control. Moreover, untransformed *E. coli* OD259 served as an additional negative control to demonstrate the thermosensitivity of the strain in the absence of DnaJ and CbpA complementation.

Competent *E. coli* OD259 cells were transformed with the appropriate plasmids (as per *APPENDIX D8*) for exogenous production of the recombinant proteins of interest, and grown overnight at 30°C. Single colonies were used to inoculate 5 ml of 2x yeast-tryptone media (2x YT; 1.6% tryptone; 1% yeast extract, 0.5% NaCl) containing 100 µg.ml^{-1} ampicillin for plasmid selection and 50 µg.ml^{-1} kanamycin for strain selection. The cultures were grown overnight at 30 °C (200 rpm), subsequently diluted 1:100 with 2x YT media (100 µg.ml^{-1} ampicillin, 50 µg.ml^{-1} kanamycin) and grown further at 30°C until an approximate $_{A600}$ of 2.0 was obtained. Cultures were diluted to an $_{A600}$ of 0.3 with 2x YT media and subsequent 10-fold serial dilutions were performed to a final dilution of 1×10^{-8}. Aliquots of 3 µl of each dilution were spotted onto three separate 2x YT-agar plates (1.5% agar in 2x YT media) containing 50 µM IPTG. These plates were incubated at 30°C, 40°C and 42°C respectively for 12 - 16 hours to determine the ability of the exogenously produced recombinant proteins (*Agt* DnaJ, *Agt*

DnaJ-H33Q, PfHsp40 and Pfj1) to functionally replace wild-type DnaJ and CbpA in *E. coli* OD259, by the reversal of the strain's thermosensitivity. Complementation assays were performed in triplicate.

5.2.2 Western Analysis for the Detection of Recombinant Proteins in E. coli OD259

Western analysis was performed on whole cell lysates of transformed *E. coli* OD259 exogenously producing the recombinant proteins of interest. Proteins extracts were resolved by 12% (w/v) SDS-PAGE and detected by Western analysis (*APPENDICES D10* and *D11)*. The hexahistidine-tagged recombinant proteins produced from the pQE30-based plasmids were detected with mouse monoclonal anti-His primary antibody (GE Healthcare) and horseradish-peroxidase conjugated anti-mouse secondary antibody (GE Healthcare) using chemiluminescence-based detection (ECL Western blotting kit, GE Healthcare). Detection was captured with a Chemidoc chemiluminescence imaging system (Bio-Rad).

5.2.3 Functionality of the Pfj1 J-domain and Identification of Functionally Important Residues

5.2.3.1 Construction of the Pfj1-J-Agt-DnaJ Chimeric Derivative

The region encoding the J-domain of the *Agt* DnaJ protein encoded on plasmid pRJ30 is flanked by endonuclease restriction sites, *Bam*HI and *Bst*BI. During the construction of the pQPfj1 plasmid, *Bam*HI and *Bst*BI restriction sites were similarly engineered into positions flanking the encoded J-domain of Pfj1 (detailed in *CHAPTER 3;* refer to *APPENDIX C1*). The J-domain of *Agt* DnaJ encoded on the pRJ30 plasmid was thus interchanged with the region encoding the Pfj1 J-domain from plasmid pQPfj1, to give rise to plasmid pQJ1Ag (*FIGURE 5.1A*) encoding the chimeric derivative protein Pfj1-J-*Agt*-DnaJ. The chimera comprises residues 60-125 of Pfj1 (the J-domain) fused to residues 71-380 of *Agt* DnaJ (the GF-region, cysteine-rich zinc-binding domain, and C-terminal substrate binding domain) as detailed in *APPENDIX C2*.

5.2.3.2 Site-directed Mutagenesis of Select Residues of the Pfj1 J-Domain

Site-directed mutagenesis was performed on selected residues of the Pfj1 J-domain using the Pfj1-J-*Agt*-DnaJ chimera encoded on plasmid pQJ1Ag as a platform. Residues of the Pfj1 J-domain that were targeted for mutagenesis are depicted in the homology model and schematic diagram of the J-domain in *FIGURE 5.1A* and *5.1B* respectively. The rationale behind each performed mutation is summarised in *TABLE 5.1* provided in *SECTION 5.3.2.2*.

Complementary mutagenesis primers were designed for (i) introduction of the desired mutation into the Pfj1-J-*Agt*-DnaJ coding sequence in the pQJ1Ag plasmid by non-PCR based whole plasmid amplification (PAPWORTH *et al.*, 1996), and (ii) the simultaneous introduction or elimination of a

restriction endonuclease site for the identification of successful mutant plasmids by restriction digestion analysis (as detailed in *FIGURE 5.2*). The designed mutagenesis primers (detailed in *APPENDIX F4*) were synthesised by Integrated DNA Technologies(IDT, USA).

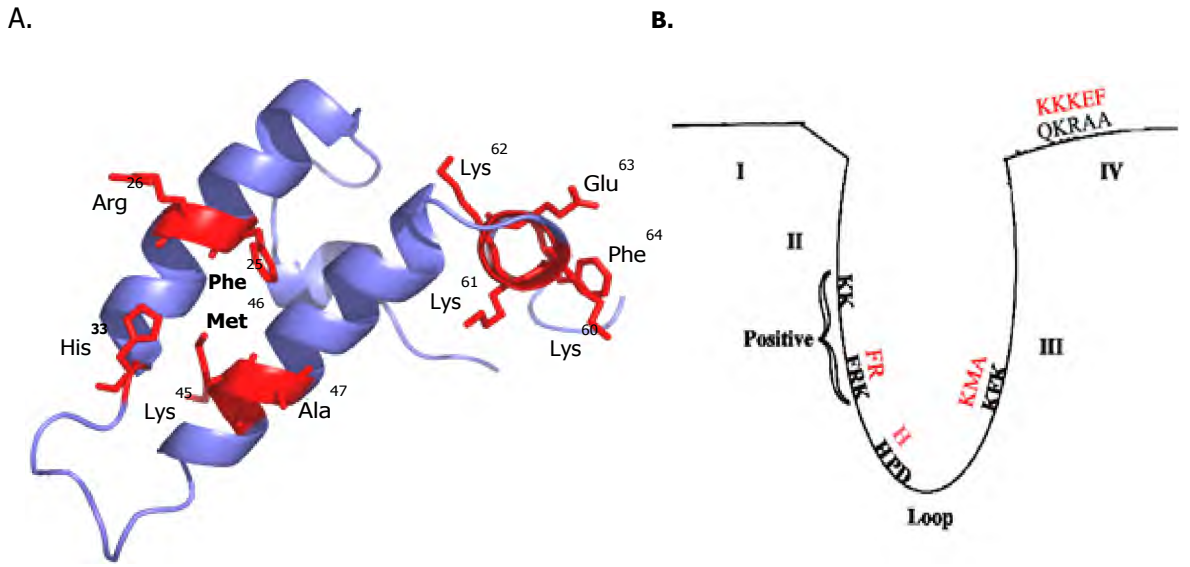

FIGURE 5.1 Residues of the J-domain of Pfj1 targeted for site-directed mutagenesis. (A) **Homology model of the Pfj1 J-domain of Pfj1 with the residues targeted for site-directed mutagenesis indicated in red. Residues are numbered according to position in the Pfj1-J-*Agt*-DnaJ chimeric protein. The homology model was rendered using Modeller (version 8.2; FISER *et al.*, 2000; MARTI-RENOM *et al.*, 2000; SALI and BLUNDELL, 1993) as previously detailed (*FIGURE 2.3*, *CHAPTER 2*). The image of the model was rendered using PyMol (version 0.95; DELANO, 2005). (B) Stylised diagram of the Hsp40 J-domain (in black) showing the positions of helices I - IV and the highly conserved residues and motifs of the domain (adapted from HENNESSY *et al.*, 2005*a*). Residues indicated in red are the corresponding residues of the J-domain of Pfj1 targeted for mutagenesis in the Pfj1-J-*Agt*-DnaJ chimeric protein.**

Each mutagenesis reaction was comprised of 100 ng of pQJ1Ag parental plasmid template, 2.5 µl of DMSO **(Sigma-Aldrich), 10 µl of 25 mM $MgCl_2$ (Roche Applied Sciences)**, 1 µl **of 10 mM dNTP mix** (Roche **Applied Sciences), 125 ng of the appropriate forward primer, 125 ng of the appropriate reverse primer, 5 µl** of 10x *Pfu* **DNA polymerase buffer** (**100 mM KCl, 100 mM $(NH_4)_2SO_4$**, 20 mM $MgSO_4$**, 1% Triton X**-100, 1 **mg.ml^{-1} BSA, 200 mM Tris-Cl, pH 8.8; Promega),** 1 U of *Pfu* DNA **Polymerase** (**Promega) and distilled water to a final volume of 50 µl. Temperature cycling was allowed to proceed as follows: one cycle of denaturation (95°C for 30 seconds), 18 cycles of denaturation, annealing and extension (95°C for 30 seconds, 52°C for 60 seconds, 68°C for 5 minutes), one cycle of final extension (68°C for 7 minutes) and a 4°C hold. Digestion of the parental pQJ1Ag plasmid in the amplification product was achieved by the addition of 5 U of *Dpn* I restriction endonuclease (Stratagene) to the reaction mixture and subsequent incubation at 37°C for 2 hours.** Pre- **and post-*Dpn* I samples were retained and analysed by 0.8% agarose gel electrophoresis** (as per *APPENDIX D3*). **Supercompetent** *E. coli* **JM109 cells (Promega) were transformed with *Dpn* I** treated

mutagenesis product (*APPENDIX D8*) for subsequent screening purposes. Plasmid DNA was isolated from the resulting colonies (*APPENDIX D1*) and analysed by restriction digestion analysis (*APPENDIX D2*) as detailed in *FIGURE 5.2.* Mutant pQJ1Ag plasmids were verified by DNA sequencing (*APPENDIX D6*).

A.

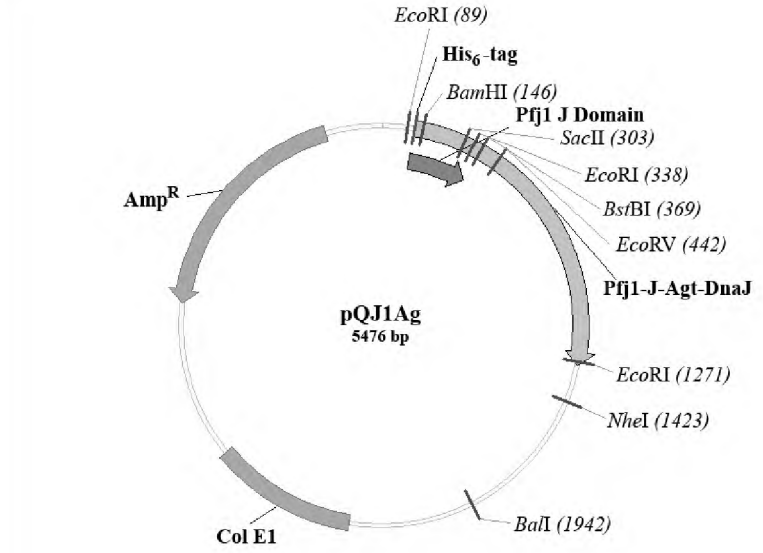

B.

```
PROTEIN   M  A  K  Q  D  P  Y  T  V  L  G  L  S  R  N  A  T-  T  N.
  5'      ATG GCG AAA CAG GAC CCG TAC ACC GTT CTG GGT CTG TCT CGT AAC GCG ACC ACC AAC
  3'      TAC CGC TTT GTC CTG GGC ATG TGG CAA GAC CCA GAC AGA GCA TTG CGC TGG TGG TTG

                          F25A R26A                                  H33Q
PROTEIN   D  I  K  K  Q  [F 25] [R 26] L  L  A  K  K  Y  [H 33] P- -D  I  N  P.
                                      29                                35
  5'      GAC ATC AAG AAA CAG TTC CGT CTG CTG GCG AAG AAA TAC CAC CCG GAC ATC AAC CCG
  3'      CTG TAG TTC TTT GTC AAG GCA GAC GAC CGC TTC TTT ATG GTG GGC CTG TAG TTG GGC
          EcoRV(211)                 BalI(236)                  EcoRV(256)

                          KFA, KMK, KFK                                  50
PROTEIN   S  P  D  A  K  Q  [K  M 46] [A 47] S 48  ,  T  A- -A  Y  E  L  L  S.
  5'      TCT CCG GAC GCG AAA CAG AAA ATG GCG TCT ATC ACC GCG GCG TAC GAA CTG CTG TCT
  3'      AGA GGC CTG CGC TTT GTC TTT TAC CGC AGA TAG TGG CGC CGC TAG CTT GAC GAC AGA
                                      NheI(290)   SacII(303)

                          QKRAA, K62A
PROTEIN   D  P.  [K  K  K  E  F]  Y  D  K  T- G-
  5'      GAC CCG AAG AAG AAA GAA TTC TAC GAC AAA ACC GGG 3'
  3'      CTG GGC TTC TTC TTT CTT AAG ATG CTG TTT TGG CCC 5'
                          EcoRI(388)
```

FIGURE 5.2 Strategy for confirmation of the site-directed mutagenesis of the Pfj1 J-domain by restriction digestion analysis. (A) Plasmid map of the parental pQJ1Ag construct (4576 bp in size) indicating the restriction sites used for differentiation between mutant and parental pQJ1Ag plasmids in screening subsequent to site-directed mutagenesis. The position of the Pfj1 J-domain in the Pfj1-J-*Agt*-DnaJ chimera between the *Bam*HI and *Bst*BI restriction sites is indicated; restriction sites were inserted or removed in this region during mutagenesis for screening as further detailed. The parental and mutant pQJ1Ag plasmids confer ampicillin resistance to transformed *E. coli*-cells as indicated (Amp^R; β-lactamase gene). The plasmid map was generated with the Vector NTI Advance™ software package (version 10.3; Invitrogen). (B) The codon-optimised nucleotide sequence of the Pfj1 J-domain with the translated protein sequence highlighted in grey. Residues and motifs targeted for site-directed mutagenesis are indicated and labelled in boxes. Restriction .../

.../FIGURE 5.2
sites introduced or removed for mutagenesis screening by restriction digestion analysis are underlined in the nucleotide sequence and labelled by position relative to the pQJ1Ag plasmid. With mutation F25A an *Eco*RV restriction site (sequence 5'-GATATC-3'; position 211) was engineered into the pQJ1Ag plasmid by silent mutation of residue Asp[20]. A *Bal* I restriction site (sequence 5'-TGGCCA-3'; position 236) was introduced with mutation R26A by silent mutation of residue Ala[23]. With mutation H33Q an *Eco*RV restriction site (sequence 5'-GATATC-3'; position 256) was engineered into pQJ1Ag by silent mutation of the Asp[33] residue. Mutation of the KMA motif to KFA, enabled introduction of an *Nhe* I restriction site (sequence 5'-GCTAGC-3'; position 290) by silent mutation of residues Ala[47] and Ser[48]. With mutations KMK and KFK of the KMA motif, the *Sac* II restriction site (sequence 5'-CCGCGG-3'; position 303) was eliminated by silent mutation of Thr[50]. Finally, mutation K62A and mutation of the KKKEF motif to QKRAA, enabled removal of the *Eco*RI restriction site (sequence ' GAATTC'; position 388) by the introduction of Ala[62].

5.2.3.3 Assessment of the functionality of the Pfj1 J-domain in E. coli OD259

The functionality of the Pfj1 J-domain chimera and associated mutant proteins was assessed using complementation assays in the *E. coli* DnaJ deletion strain (*dnaJ cbpA* OD259), as detailed in *SECTION 5.2.1*.

5.3 RESULTS AND DISCUSSION

5.3.1 PfHsp40 and Pfj1 were unable to reverse the thermosensitivity of E. coli OD259

The *dnaJ cbpA* deficient *E. coli* OD259 strain is reported to be thermosensitive above temperatures of 37°C in the absence of functional complementation of DnaJ or CbpA (DELOCHE *et al*., 1997). This was evident in the absence of growth at temperatures of 40°C and 42°C in the *in vivo* complementation assays employed in this study (control panels; *FIGURE 5.3*). The exogenous production of a complementary Hsp40 protein such as *Agt* DnaJ may reverse the thermosensitivity of this strain, as previously reported (HENNESSY *et al*., 2005a) and indicated in the positive control of the complementation assay presented in *FIGURE 5.3.* The substitution of residue His[33] (mutation H33Q) of the HPD motif appeared to abolish the functionality of the *Agt* DnaJ protein in the *in vivo* system (negative control; *FIGURE 5.3*), suggesting that the protein exerted its functionality through specific interaction with *E. coli* DnaK.

Recombinant PfHsp40 and Pfj1 were unable to suppress the thermosensitivity of the *dnaJ cbpA* deficient *E. coli* OD259 strain in the *in vivo* complementation assay, indicated by the lack of growth following exogenous production of these recombinant proteins at temperatures of 40°C and above (*FIGURE 5.3*). Importantly, growth was observed at 30°C indicating that the lack of complementation at higher temperatures was not attributed to toxicity of the *P. falciparum* Hsp40 proteins in the *E. coli* strain.

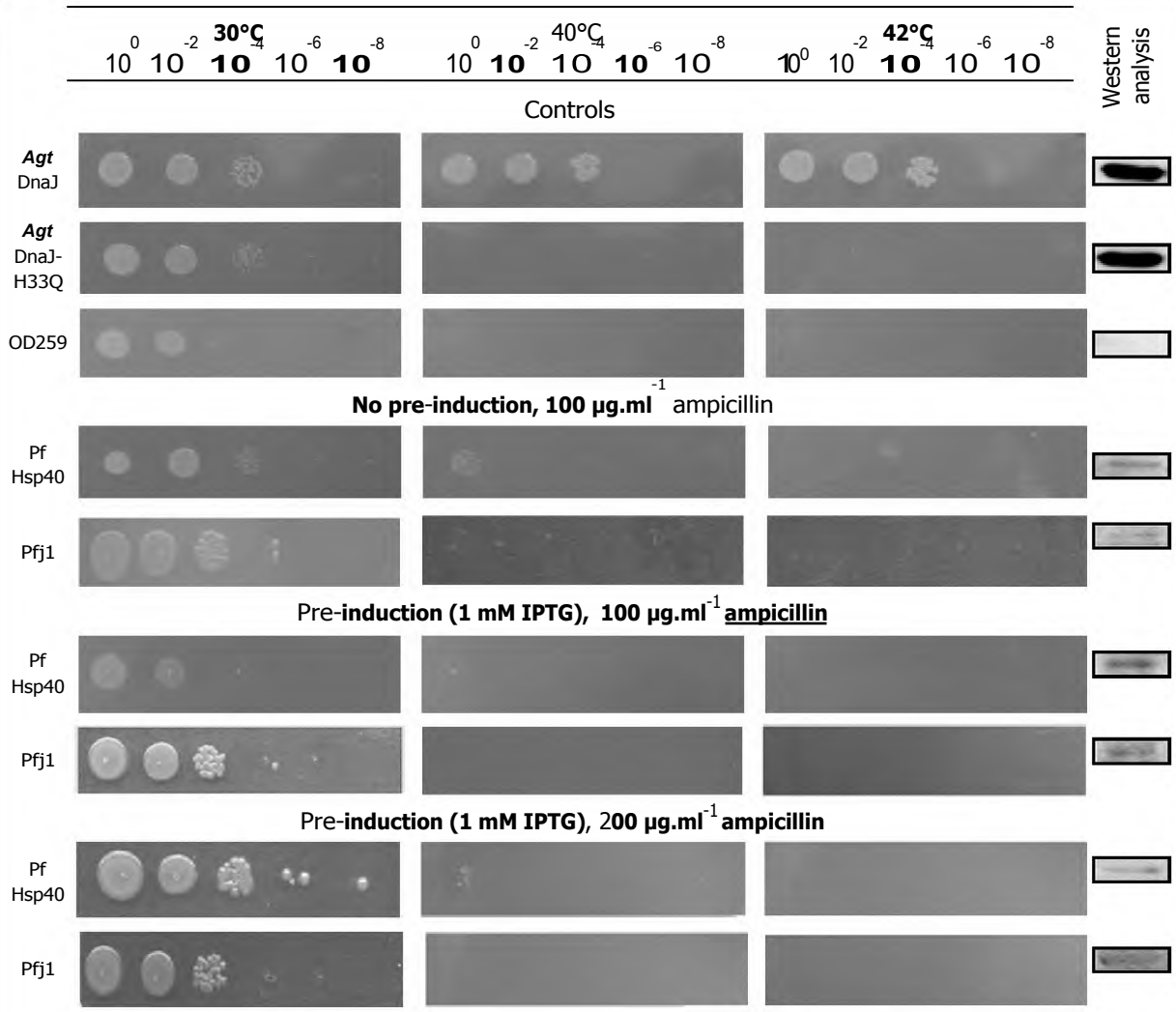

FIGURE 5.3 Assessment of the ability of PfHsp40 and Pfj1 to reverse the thermosensitivity of *E. coli* OD259. The ability of recombinant PfHsp40 and Pfj1 to reverse the thermosensitivity of the *dnaJ cbpA* deficient *E. coli* OD259 strain was determined by the presence or absence of growth of cells heterologously producing these proteins at temperatures of 30°C, 40°C and 42°C respectively. PfHsp40 and Pfj1 were unable to reverse the thermosensitivity of the *E. coli* strain indicated by the lack of growth at 40°C and 42°C shown in the appropriate panels. Recombinant PfHsp40 and Pfj1 expression was driven using 1mM IPTG pre-induction in the culture and with an added selection pressure of 100 µg.ml^{-1} and 200 µg.ml^{-1} ampicillin as indicated. Dilutions of 10^{0}, 10^{-2}, 10^{-4}, 10^{-6} and 10^{-8} of a culture of A_{600} = 0.3 (diluted from a culture of A_{600}=1.8-2.0) were spotted onto 2x YT-agar plates containing 50 µg.ml^{-1} kanamycin (strain selection), 100 µg.ml^{-1} ampicillin (plasmid selection) and 50 µM IPTG (for induction of heterologous protein expression). The positive control included *E. coli* OD259 cells exogenously producing *Agt* DnaJ while the negative controls included untransformed *E. coli* OD259 (spotted onto kanamycin-IPTG plates without ampicillin) and *E. coli* OD259 producing *Agt* DnaJ-H33Q. Western analysis of total protein extracts from the respective *E. coli* OD259 transformants is shown in the right hand panel. Recombinant proteins were detected by chemiluminescence with mouse monoclonal anti-His primary antibody, and horseradish peroxidase (HRP)-conjugated rabbit anti-mouse secondary antibody. The detected proteins are N-terminally hexahistidine (His_6)-tagged fusion proteins resulting from expression from the pQE30 plasmid. The predicted molecular masses of the hexahistidine-tagged proteins are as follows: PfHsp40 - 49.9 kDa; Pfj1 - 77.3kDa; *Agt* DnaJ and *Agt* DnaJ-H33Q - approximately 42.4 kDa.

The detection of PfHsp40 and Pfj1 in whole cell lysates of *E. coli* OD259 exogenously producing the respective recombinant proteins was achieved following significant over-exposure of the probed

Western blots. Contrasted to the detection of *Agt* DnaJ and *Agt* DnaJ-H33Q in the positive and negative controls respectively, PfHsp40 and Pfj1 were expressed at considerably lower levels (*FIGURE 5.3*). This remained unchanged with enhanced selection pressure with antibiotic (200 µg.ml^{-1} ampicillin) and pre-induction of protein expression from the pQE30-based plasmids in the culture (1 mM IPTG). The possibility must be considered that the suppression of the thermosensitivity of the *E. coli* OD259 strain was hindered by insufficient levels of PfHsp40 and Pfj1 protein production in the heterologous system for functional replacement of wildtype *E. coli* DnaJ and CbpA. The heterologous expression of comparable amounts of the parasitic Hsp40 proteins in *E. coli* OD259 remains a challenge. Importantly, the functionality of PfHsp40 and Pfj1 could be dependent on their appropriate folding in the heterologous system, which may require DnaJ and CbpA.

Conversely it may be argued that PfHsp40 and Pfj1 exerted their functionality via a different mechanism to the prokaryotic prototypes of Hsp40 in the *in vivo* system, attributed to significant differences in functional residues or subtle differences governing specificity for peptide substrate. Considering that the highest region of dissimilarity between the parasitic Hsp40 proteins and those of prokaryotic origin (*E. coli* DnaJ and *Agt* DnaJ) appears to be in the region of the C-terminus (evident in the alignment in *FIGURE 2.2*, *CHAPTER 2*), it may be considered that the substrate binding domains of PfHsp40 and Pfj1 were unable to recognise the protein substrates of *E. coli* DnaJ and successfully transfer them to *E. coli* DnaK for folding in the prokaryotic system. Subtle differences in the other Hsp40 domains may equally be sufficient to account for the lack of functional interchangeability of the respective Hsp40 proteins. Such differences may govern the specificity or affinity of interaction with partner Hsp70s or represent a divergence in chaperone function. Both PfHsp40 and Pfj1 bear N-terminal leader sequences which may target the proteins to subcellular compartments in the parasite and provide insight into potential specialised chaperone functions of these proteins. Furthermore, it is uncertain as to whether post-translational modification of PfHsp40 and Pfj1 are required for their functionality. The CAAX-box motif of PfHsp40 may implicate the protein in membrane interactions following post-translational farnesylation. Farnesylation of the CAAX-box motif of the *S. cerevisiae* type I Hsp40, Ydj1, was previously shown to be a prerequisite for the growth of *S. cerevisiae* at elevated temperatures (CAPLAN *et al*., 1992b). This farnesylation has also been shown to mediate the role of Ydj1 in protein translocation across intracellular membranes (CAPLAN *et al*., 1992a) and recently, the interaction of Ydj1 with Hsp90 client proteins through association with the Hsp90/Hsp70 multi-chaperone complex (FLOM *et al*., 2008). It is therefore possible that the absence of appropriate post-translational farnesylation of PfHsp40 in the *E. coli* OD259 strain may have contributed to the inability of the protein to functionally replace wildtype DnaJ and CbpA. Previously, a CAAX-box motif-bearing Hsp40 protein from *Trypanosoma cruzi*, Tcj2,

was shown to functionally replace Ydj1 (EDKINS *et al*., 2004) in the thermosensitive *S. cerevisiae* strain *ydj1* JJ160 (JOHNSON and CRAIG, 2000). It would be of interest to assess the ability of PfHsp40 (and Pfj1) to functionally replace Ydj1 in this eukaryotic strain. This would require re-synthesis of the PfHsp40 and Pfj1 coding regions, which have been tailored for expression in a prokaryotic system in this work as detailed in *CHAPTER 3*.

5.3.2 Functionality of the J-domain of Pfj1 in a Prokaryotic System

5.3.2.1 The Pfj1-J-Agt-DnaJ Chimera is Functional in E. coli OD259

As observed for *Agt* DnaJ in the positive control of the *in vivo* complementation system, exogenous expression of the Pfj1-J-*Agt*-DnaJ chimeric protein was able to suppress the thermosensitivity of *E. coli* OD259 (*FIGURE 5.4*). The functionality of the chimera may have been attributed to the potential protein aggregation suppression activity of the protein in the *E. coli* strain, and/or the ability of the chimera to functionally replace DnaJ and CbpA through specific interaction with *E. coli* DnaK. In favour of the latter argument, subsequent substitution of residue His[33] of the HPD motif of the Pfj1 J-domain was shown to abolish functionality of the Pfj1-J-*Agt*-DnaJ chimeric protein in the *in vivo* system (discussed in *SECTION 5.3.2.3*). Importantly, this confirmed the functionality of the Pfj1 J-domain in *E. coli* OD259 and the ability of this domain to mediate interactions of the Pfj1-J-*Agt*-DnaJ chimera with DnaK.

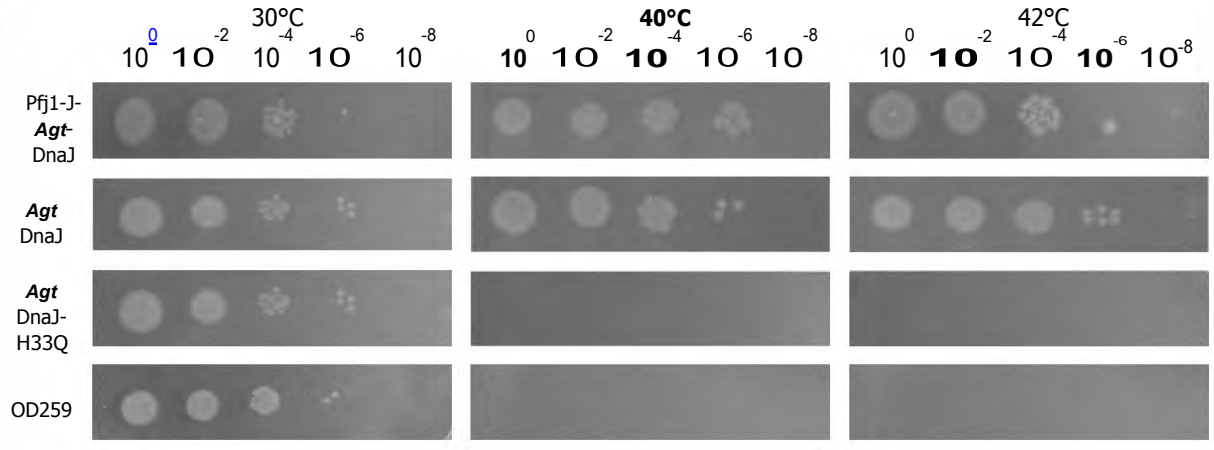

FIGURE 5.4 Assessment of the ability of the Pfj1-J-*Agt*-DnaJ chimera to reverse the thermosensitivity of *E. coli* OD259. The Pfj1-J-*Agt*-DnaJ chimera was able to suppress the thermosensitivity of *E. coli* OD259, as indicated by growth at the elevated temperatures of 40°C and 42°C (upper panel). Dilutions of 10^{0}, 10^{-2}, 10^{-4}, 10^{-6} and 10^{-8} of a culture of A_{600} = 0.3 (diluted from a culture of A_{600} = 1.8 - 2.0) were spotted onto 2x YT-agar plates containing 100 µg.ml^{-1} ampicillin (plasmid selection), 50 µg.ml^{-1} kanamycin (strain selection) and 50 µM IPTG (for the induction of heterologous recombinant protein expression). The positive control included *E. coli* OD259 cells producing *Agt* DnaJ. Negative controls included untransformed *E. coli* OD259 and *E. coli* OD259 producing *Agt* DnaJ-H33Q.

Notably, the atypical Pfj1 J-domain proved functional in the *in vivo* complementation system despite exhibiting only 17% protein sequence conservation relative to the J-domains of *E. coli* and *Agt* DnaJ (evident in *FIGURE 2.2, CHAPTER 2*). The interchangeability of the J-domain of *Agt* DnaJ with that of Pfj1 highlights the possibility that J-domains of prokaryotic and parasitic origin are able to interact with Hsp70 partners using a common, conserved mechanism as further discussed.

5.3.2.2 Site-Directed Mutagenesis of the Pfj1 J-domain of the Pfj1-J-Agt-DnaJ Chimera

Rationale for the substitutions of the selected residues and motifs of the Pfj1 J-domain of the Pfj1-J-*Agt*-DnaJ chimera is summarised in *TABLE 5.1*.

TABLE 5.1 Mutagenesis of the J-domain of the Pfj1-J-**Agt**-DnaJ Chimera: Rationale for Mutations

Mutation				Rationale for Mutation
Site	Name	Residues Targeted	Mutation	
Helix II	F25A	Phe^{25}	Ala^{25}	The partially solvent-exposed side chain of this residue potentially constitutes part of the contact surface with ATPase domain of Hsp70. Mutation of the corresponding residue in *E. coli* DnaJ abolishes J-domain function (BERJANSKII *et al*., 2000; GENEVAUX *et al*., 2002).
	R26A	Arg^{26}	Ala^{26}	The solvent-exposed side chain of this residue potentially constitutes part of the contact surface with the ATPase domain of Hsp70. Mutation of the corresponding residues in *E. coli* and *A. tumefaciens* DnaJ abolishes J-domain function (BERJANSKII *et al*., 2000; GENEVAUX *et al*., 1997; HENNESSY *et al*., 2005a).
HPD motif in loop between helices II and III	H33Q	His^{33}	Gln^{33}	Negative Control. The conserved HPD motif is crucial to interactions with Hsp70; mutation of these residues is known to abolish interaction with Hsp70 (TSAI and DOUGLAS, 1996).
KMA motif (Helix III)	KFA	Met^{46}	Phe^{46}	The KFK motif of helix III is highly conserved, including Phe^{47} flanked by positive residues, Lys^{46} and Lys^{48} in *E. coli* DnaJ. Phe^{47} is crucial to J-domain function and is proposed to interact with His^{33} of the HPD motif to stabilise helices II and III. The flanking solvent-exposed Lys residues potentially interact with Hsp70 or other regions of DnaJ (GENEVAUX *et al*., 1997; HENNESSY *et al*., 2000).
	KMK	Ala^{47}	Lys^{47}	
	KFK	Met^{46} Ala^{47}	Phe^{46} Lys^{47}	
KKKEF motif (Helix IV)	K62A	Lys^{62}	Ala^{62}	The QKRAA motif of helix IV in *E. coli* DnaJ is proposed to mediate binding to DnaK (AUGER and ROUDIER, 1997) and to control the specificity of interaction with partner Hsp70 proteins (GARIMELLA *et al*., 2006; HENNESSY *et al*., 2005a). HENNESSY *et al.* (2005a) suggest both a structural and functional role for helix IV in the J-domain. Significant conservation of residues corresponding to residue Lys^{62} in DnaJ-like proteins may implicate the residue in this position in general binding to Hsp70 (HENNESSY *et al*., 2000).
	QKRAA	Lys^{60} Lys_{61} Lys_{62} Lys_{63} Glu_{64} Phe	Gln^{60} Lys_{61} Arg_{62} Ala_{63} Ala_{64} Ala	

Confirmation of the Pfj1 J-**domain mutations was achieved by restriction digestion analysis** of the **pQJ1Ag plasmid** (***FIGURE*** *5.5*) **as detailed in** ***SECTION 5.2.3.2*** and with **subsequent DNA sequencing.**

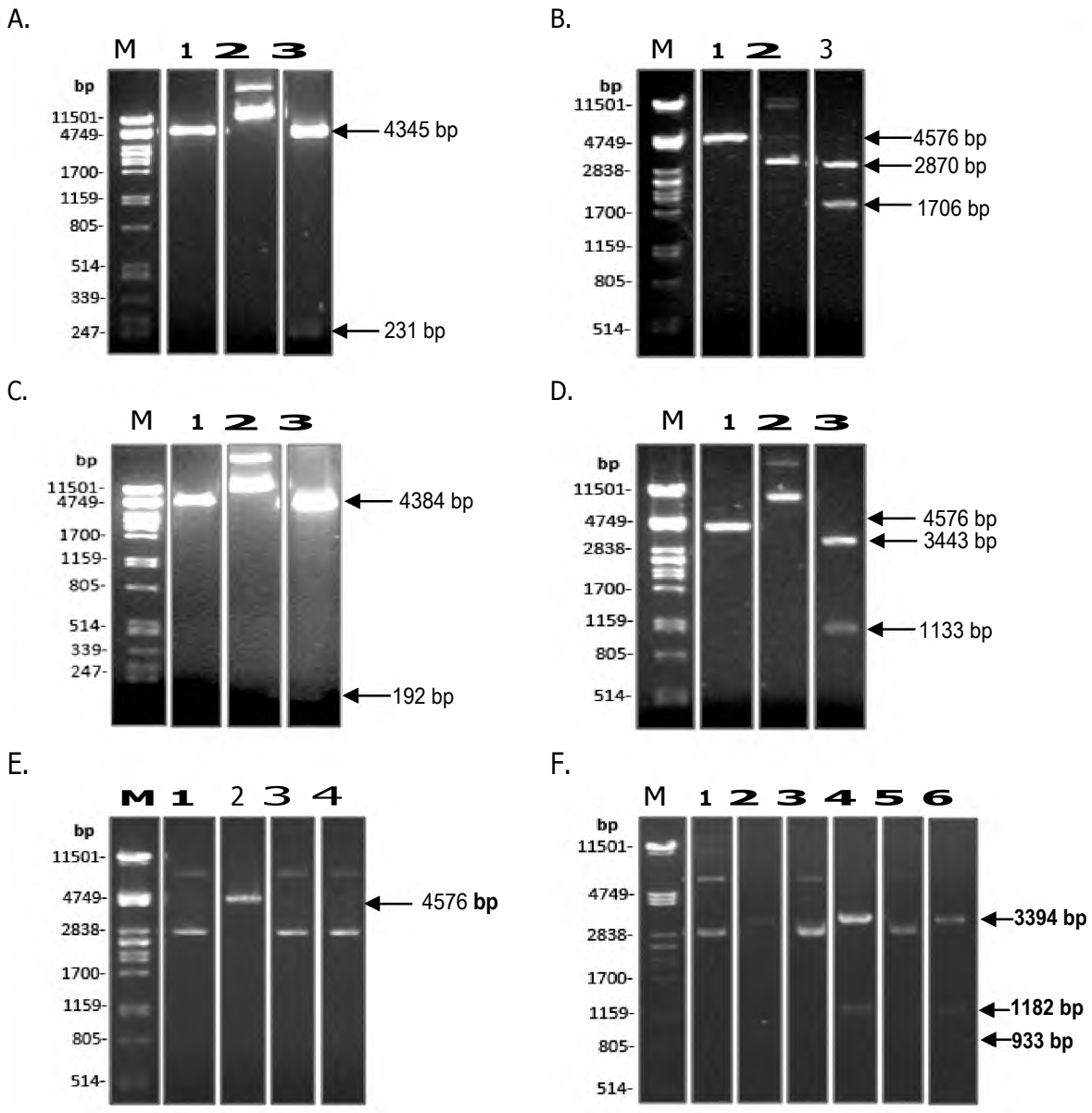

FIGURE 5.5 **Confirmation of the mutagenesis of the pQJ1Ag plasmid by restriction digestion analysis. Restriction digestion products were resolved by 0.8 % (B, D, E, and F) and 1.5 % (A and C) agarose gel electrophoresis. (A) Mutant plasmid pQJ1Ag-F25A bears an additional** ***Eco****RV* **site to the parental plasmid pQJ1Ag.** *Lane 1* **–** ***Eco****RV*-**digested parental pQJ1Ag yielded a linear plasmid of 4576 bp resulting from digestion at the single** *Eco*RV **restriction site on the plasmid;** *Lane 2* **– Undigested pQJ1Ag-F25A (uncut plasmid control) represented by supercoiled, nicked and double nicked plasmid DNA;** *Lane 3* **–** *Eco*RV-**digested pQJ1Ag-F25A yielded fragments of 3435 bp and 231 bp respectively resulting from digestion at two** *Eco*RV **restriction sites, including the additional** *Eco*RV **site introduced by site-directed mutagenesis. (B) Mutant plasmid pQJ1Ag-R26A bears an additional** *Bal*I **site to the parental plasmid pQJ1Ag.** ***Lane 1*** **–** *Bal*I-**digested parental pQJ1Ag yielded a linear plasmid of 4576 bp attributed to digestion at the single** *Bal*I **restriction site on the plasmid;** ***Lane 2*** **- Undigested pQJ1Ag-**R26A; ***Lane 3*** **–** *Bal*I**-digested pQJ1Ag-**R26A **yielded fragments of 2870 bp and 1706 bp respectively resulting from additional digestion at the** *Bal*I **restriction site introduced by mutagenesis. (C) Mutant plasmid pQJ1Ag-H33Q bears an additional** *Eco*RV **restriction site to parental plasmid pQJ1Ag.** ***Lane 1*** **–** *Eco*RV**- digested pQJ1Ag yielded a linear plasmid of**

.../

/...FIGURE 5.5
4576 bp resulting from digestion at the single *Eco*RV site on the plasmid; *Lane 2* – Undigested pQJ1Ag-H33Q; Lane 3 – *Eco*RV-digested pQJ1Ag-H33Q yielded fragments of 3483 bp and 192 bp resulting from digestion at the introduced *Eco*RV restriction site by mutagenesis. (D) Mutant plasmid pQJ1Ag-KFA exhibits an additional *Nhe*I site to parental plasmid pQJ1Ag. *Lane 1 – Nhe*I-digested pQJ1Ag yielded a linear plasmid of 4576 bp resulting from digestion at the single *Nhe*I site on the plasmid; *Lane 2* – Undigested pQJ1Ag-KFA; *Lane 3 – Nhe*I-digested pQJ1Ag-KFA yielded two fragments of 3443 bp and 1133 bp respectively resulting from additional digestion at the introduced *Nhe*I restriction site. (E) Mutant plasmids pQJ1Ag-KMK and pQJ1Ag-KFK lack the single *Sac*II restriction site exhibited on the parental plasmid pQJ1Ag. *Lane 1* – Undigested parental pQJ1Ag control; *Lane 2 – Sac*II-digested pQJ1Ag yielded a linear plasmid of 4576 bp resulting from digestion at the single *Sac*II restriction site on the plasmid; *Lanes 3 and 4 – Sac*II-digested plasmids pQJ1Ag-KMK and pQJ1Ag-KFK yielded undigested plasmids resulting from the loss of the *Sac*II restriction site during mutagenesis. (F) In contrast to the three *Eco*RI sites exhibited on the parental pQJ1Ag, plasmids pQJ1Ag-K62A and pQJ1Ag-QKRAA bear only two *Eco*RI sites resulting from loss of a single *Eco*RI site during mutagenesis. *Lane 1* – Undigested parental pQJ1Ag; *Lane 2 – Eco*RI digested pQJ1Ag at three *Eco*RI restriction sites resulting in three fragments of 3394 bp, 933 bp and 248 bp respectively; *Lanes 3 and 5* - Undigested mutant pQJ1Ag-K62A and pQJ1Ag-QKRAA respectively; *Lanes 4 and 6 – Eco*RI-digested pQJ1Ag-K62A and pQJ1Ag-QKRAA respectively yielded two fragments of 3394 bp and 1182 bp resulting from loss of an *Eco*RI restriction site. In all panels, *lane M* represents a *Pst*I-digested λDNA Marker as indicated by the size markers. All mutant plasmid constructs detected by restriction digestion analysis were verified by subsequent DNA Sequencing. Restriction enzymes were sourced commercially as listed in *APPENDIX E*.

5.3.2.3 Functionality of the Pfj1 J-domain Mutants in E. coli OD259

The functionality of the Pfj1-J-*Agt*-DnaJ mutant derivatives was assessed using the *in vivo* functional complementation system in *E. coli* OD259 as previously described (*FIGURE 5.6*). *E. coli* OD259 exogenously producing the parental Pfj1-J-*Agt*-DnaJ chimeric protein served as the positive control (*FIGURE 5.6*) based on the previously determined functionality of the protein in the *in vivo* complementation system (*SECTION 5.3.2.1*). In this study, mutation of residues Phe^{25} and Arg^{26} of helix II of the J-domain, and mutation of residue His^{33} of the HPD motif abolished Pfj1 J-domain function in the prokaryotic system. Production of the Pfj1-J-*Agt*-DnaJ-F25A, Pfj1-J-*Agt*-DnaJ-R26A or Pfj1-J-*Agt*-DnaJ-H33Q mutant proteins failed to suppress the thermosensitivity of *E. coli* OD259 at 40°C or 42°C, indicated by the lack of growth of the strain at these temperatures (*FIGURE 5.6*). *E. coli* OD259 producing the HPD-mutated Pfj1-J-Agt-DnaJ-H33Q chimera thus served as an appropriate negative control for the functional complementation assay. Exogenous production of the Pfj1-J-*Agt*-KFA mutant chimera resulted in partial suppression of the thermosensitivity of *E. coli* OD259 such that growth was recovered at 40°C but not at 42°C. This indicated that replacement of residue Met^{46} with Phe^{46} in the KMA motif of helix III of the Pfj1 J-domain resulted in partial preservation of the functionality of the Pfj1-J-*Agt*-DnaJ chimera. Interestingly, the thermosensitivity of the strain was suppressed at 40°C and 42°C on the production of mutant Pfj1-J-*Agt*-DnaJ proteins bearing KMK and KFK replacements of the KMA motif respectively. Partial suppression of the thermosensitivity of *E. coli* OD259 was observed following production of the Pfj1-J-*Agt*-DnaJ mutant bearing a K62A mutation; residue Lys^{62} of the K^{60}KKEF^{65} motif of helix IV of the Pfj1 J-domain, corresponds to the

QKRAA **motif encountered in prokaryotic DnaJ** proteins. Notably, **functionality of the Pfj1 J**-domain **in the prokaryotic system was maintained following the replacement** of the **KKKEF** motif **with** that of QKRAA; **production of the Pfj1**-J-*Agt*-DnaJ-QKRAA **mutant protein suppressed** *E. coli* **OD259** the **thermosensitivity at temperatures of** 40°**C and 42°C. Further discussion of the results of the functionality of the Pfj1**-J-*Agt*-**DnaJ mutants is provided in *SECTION 5.3.2.5***.

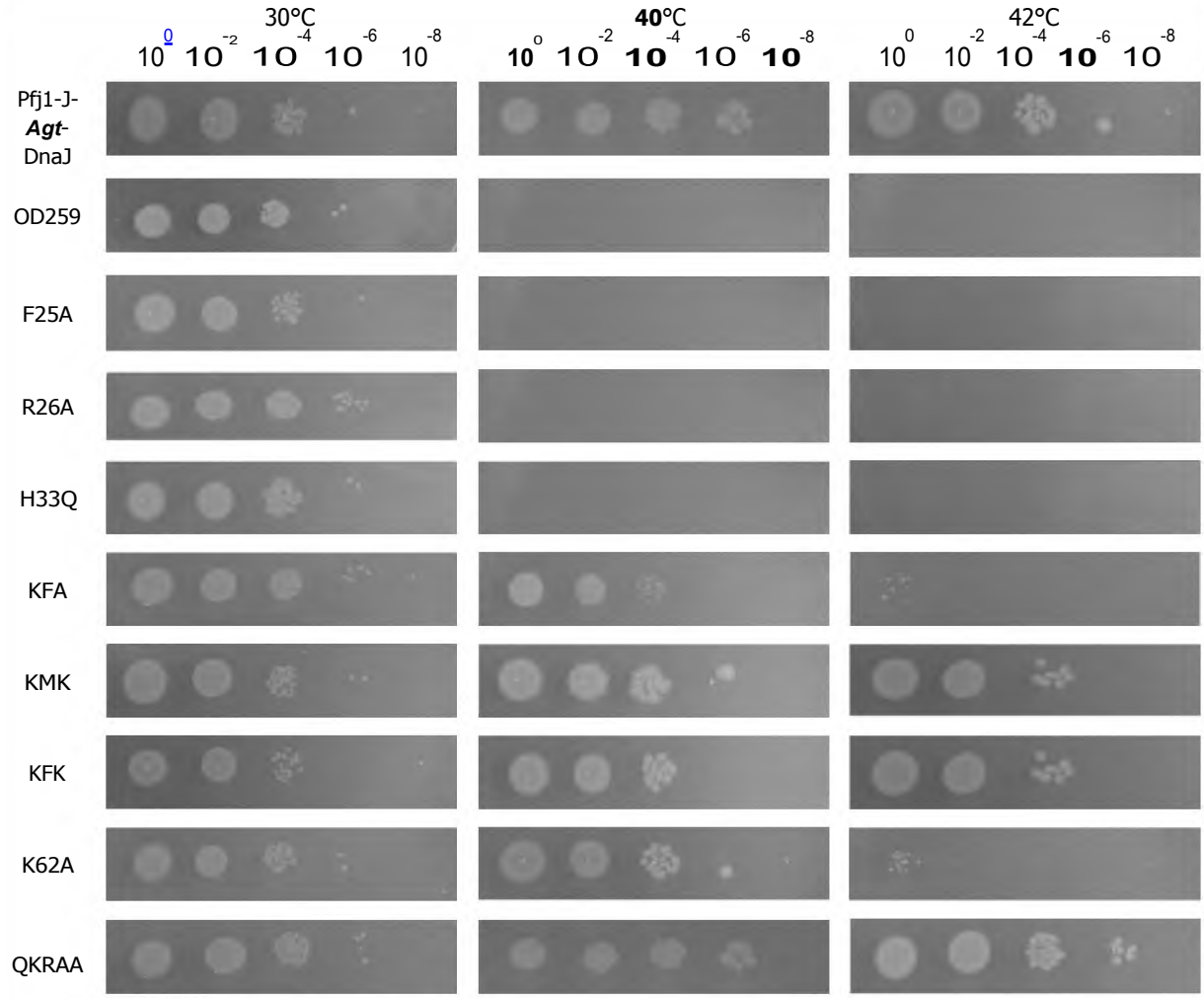

FIGURE 5.6 Assessment of the functionality of mutant derivatives of the Pfj1-J-***Agt*-DnaJ chimera in *E. coli*** OD259. **The ability of the mutant chimeras** (**F25A, R26A, H33Q, KFA, KMK, KFK, K62A and QKRAA) to suppress the thermosensitivity of** the ***dnaJ cbpA*** *E. coli* **OD259 strain was determined from the presence or absence of growth at temperatures of 30°C, 40**°C and 42°**C respectively. Dilutions of 10**^{0}, 10^{-2}, 10^{-4}**, 10**$^{-6}$ and 10^{-8} of a culture of A_{600} **= 0.3 (diluted from a culture of** A_{600}**= 1.8 - 2.0) were spotted onto 2x** YT-**agar plates containing 100 µg.ml**$^{-1}$ **ampicillin (plasmid selection), 50 µg.ml**$^{-1}$ **kanamycin (plasmid selection) and** 50 **µM IPTG** (for the **induction of heterologous recombinant protein** expression). **Growth was observed in** the **positive control** of ***E. coli*** OD259 **producing wildtype** (unmutated) Pfj1-J-*Agt*-**DnaJ chimeric protein**, at **the elevated temperatures of 40°C and 42°C. Growth was not observed in the negative controls of untransformed** *E. coli* **OD259 and *E. coli*** OD259 **producing** Pfj1-J-*Agt*-DnaJ-**H33Q; H33Q mutation of J-domain of the Pfj1**-J-*Agt*-**DnaJ abolished interaction with DnaK as observed for the same mutation of *Agt*** DnaJ.

5.3.2.4 Expression of the Pfj1-J-Agt-DnaJ Chimera and Mutants in E. coli OD259

Confirmation of the heterologous expression of the Pfj1-J-*Agt*-DnaJ chimera and mutant proteins, and *Agt* DnaJ control proteins in the *E. coli* OD259 strain was achieved by Western analysis, as depicted in *FIGURE 5.7*.

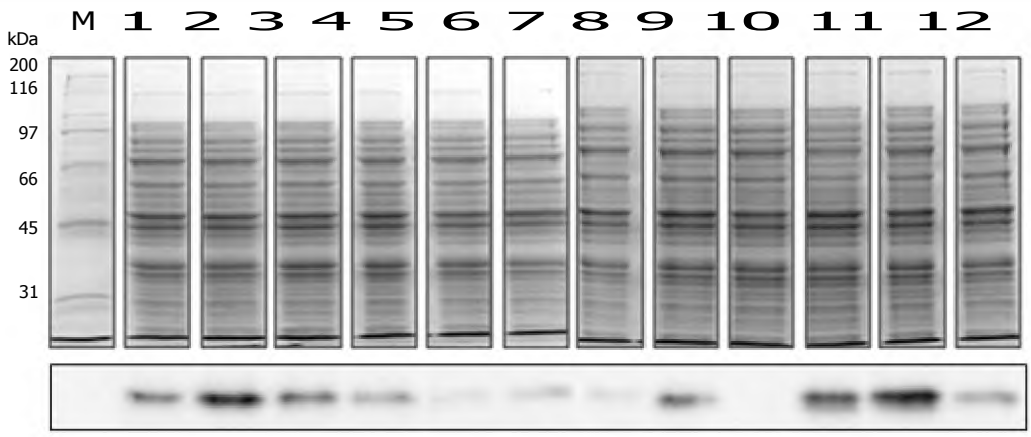

FIGURE 5.7 Confirmation of the heterologous production of the Pfj1-J-***Agt***-DnaJ mutant chimera proteins in ***E. coli*** OD259. SDS-PAGE (upper panels) and Western analysis (lower panel) of total protein extracts from *E. coli* OD259 [pQJ1Ag] transformants. Proteins were detected by chemiluminescence with mouse monoclonal anti-His primary antibody, and horseradish peroxidase (HRP)-conjugated rabbit anti-mouse secondary antibody. Detected proteins were N-terminally hexahistidine (His_6)-tagged fusion proteins resulting from expression from the pQE30 plasmid. The predicted molecular mass of the His_6-tagged Pfj1-J-*Agt*-DnaJ chimera and associated mutants is approximately 42.2 kDa in size, while that of *Agt* DnaJ and *Agt* DnaJ-H33Q is approximately 42.4 kDa. *Lanes: M* – SDS-PAGE Molecular Mass Marker (Bio-Rad), ***1*** – extract containing Pfj1-J-*Agt*-DnaJ-F25A, *2* – extract containing Pfj1-J-*Agt*-DnaJ-R26A, *3* – extract containing Pfj1-J-*Agt*-DnaJ-H33Q, *4* – extract containing Pfj1-J-*Agt*-DnaJ-KFA, *5* – extract containing Pfj1-J-*Agt*-DnaJ-KMK, *6* – extract containing Pfj1-J-*Agt*-DnaJ-KFK, *7* - extract containing Pfj1-J-*Agt*-DnaJ-K62A, *8* – extract containing Pfj1-J-*Agt*-DnaJ-QKRAA, *9* – extract containing no recombinant protein, *10* – extract containing *Agt* DnaJ, *11* – extract containing *Agt* DnaJ-H33Q, *12* – extract containing parental (unmutated) Pfj1- J-*Agt*-DnaJ chimera.

Due to low levels of protein production in *E. coli* OD259, the exogenously expressed proteins of interest could not be visualized as overproduced proteins by SDS-PAGE analysis (*FIGURE 5.7*, upper panels) but were detected by subsequent Western analysis (*FIGURE 5.7*, lower panels). This indicated that the inability of the Pfj1-J-*Agt*-DnaJ F25A, R26A, H33Q, K62A and KFA mutants to suppress the thermosensitivity of *E. coli* OD259 was not attributed to a lack of protein production in the heterologous system (*FIGURE 5.7, lower panel, lanes 2-5 and lane 7*). As anticipated, hexahistidine-tagged protein was not detected in the negative control, *E. coli* OD259 (*FIGURE 5.7*, lower panel, lane 9). Notably, in Western analysis of independent complementation experiments that gave the identical complementation phenotypes, the levels of protein production were observed to differ to those presented in *FIGURE 5.7* (data not shown). This indicated that the observed complementation was not correlated to the degree of recombinant protein production in the *E. coli OD259* strain.

Further emphasising this, the KMK and KFK mutants of the Pfj1-J-Agt-DnaJ chimera appeared to suppress the thermosensitivity of *E. coli* OD259 despite low levels of protein production. It could be argued that this indicates the enhanced functionality of these mutant proteins.

The variable protein levels detected for those recombinant proteins that were able to suppress the thermosensitivity of *E. coli* OD259 were in the equivalent range of the variable protein levels detected for the recombinant proteins unable to suppress thermosensitivity. Importantly, the Pfj1-J-*Agt*-DnaJ chimera and mutant proteins were detectable in the range of the *Agt* DnaJ and *Agt* DnaJ-H33Q proteins in the *E. coli* OD259 lysates (*FIGURE 5.7, lower panel, lanes 10 and 11*). This contrasts to what was observed for the expression of full length Pfj1 and PfHsp40 relative to *Agt* DnaJ expression in the thermosensitive strain (*FIGURE 5.3, SECTION 5.3.1*) further emphasising that insufficient protein production of full length Pfj1 and PfHsp40 in the *E. coli* OD259 strain rendered the corresponding complementation results inconclusive.

5.3.2.5 The Importance of the Mutated Residues and Motifs of the Pfj1 J-domain

Mutagenesis studies on Hsp40 proteins typically enable the identification of residues that (i) serve structural roles, (ii) are involved in interaction with Hsp70 partners or (iii) increase the specificity of the Hsp40/Hsp70 partnership (HENNESSY *et al*., 2000; TSAI and DOUGLAS, 1996). Mutation of the HPD tripeptide motif in the loop region between helices II and III of the J-domain has consistently been shown to abolish functional interaction of Hsp40 proteins with partner Hsp70s as previously discussed (GENEVAUX *et al*., 2001, 2002; HENNESSY *et al*., 2005a,b; LAUFEN *et al*., 1999; TSAI and DOUGLAS, 1996). Moreover, residues of the HPD motif of the J-domain of bovine auxilin have been shown to exhibit hydrophobic interactions and side-chain contacts with bovine Hsc70 in complex (JIANG *et al.*, 2007). Substitution of residue His^{33} (mutation H33Q) appeared to abolish functionality of the Pfj1 J-domain in the *in vivo* complementation assays employed, suggesting that the J-domain exerted its functionality through specific interaction with *E. coli* DnaK. Moreover, this suggests the existence of a conserved mechanism of HPD-mediated Hsp70 interaction in *P. falciparum*, despite the significant divergence in conservation of the atypical J-domain of Pfj1.

Residues Tyr^{25} and Lys^{26} of the J-domain of *E. coli* DnaJ and *Agt* DnaJ have been implicated as candidate catalytic residues potentially comprising the interaction surface with DnaK (GENEVAUX *et al*., 2002; HENNESSY *et al*., 2005a,b). Structural data from the J-domain of the polyomavirus T antigen similarly revealed that residues Tyr^{25} and Lys^{26} of the positively charged helix II potentially interact with the ATPase domain of DnaK (BERJANSKII *et al*., 2000). Consistent with these data, mutation of the corresponding residues Phe^{25} and Arg^{26} of the Pfj1 J-domain disrupted functionality of the Pfj1-J-*Agt*-

DnaJ chimera. This suggests a structural or functional role of these residues in the interaction of the Pfj1 J-domain with Hsp70. In particular, substitution of the conserved basic residue at position 26 of helix II was found to compromise the functionality of the J-domains of human (Hsj1a), parasitic (*P. falciparum* Pfj1 and Pfj4) and bacterial (*E. coli* and *Agt* DnaJ) origin (GENEVAUX *et al*., 2002; HENNESSY *et al*., 2005A,B; NICOLL *et al*., 2007). It is possible that this basic residue together with the HPD motif comprises the conserved fundamental interaction surface required for J-domain-based interaction of Hsp40 with Hsp70 as previously implied (LU and CYR, 1998). Interestingly, the structure of the J-domain of bovine auxilin complexed to bovine Hsc70 revealed that J-domain residues comprising the interaction interface were derived from the loop region and from helix III; no residues of helix I, II or IV were flagged for Hsc70 interaction (JIANG *et al*., 2007). Nevertheless, this represents the only available structural data of J-domain interaction with a eukaryotic Hsc70 thus far. Moreover, auxilin is a type III Hsp40 and bears a relatively atypical, non-conserved J-domain relative to the type I and II Hsp40 proteins discussed here.

Previously, mutation of the conserved residue Phe^{47} of the KFK motif of Helix III of the J-domain was shown to abolish the functionality of *E. coli* DnaJ and *S. cerevisiae* Ydj1 (GENEVAUX *et al*., 2002; JOHNSON and CRAIG, 2000). The side-chain of residue Phe^{47} protrudes into the inter-helical space between helices II and III and exhibits proximity to His^{33} of the highly conserved HPD motif. The corresponding residue Phe^{47} of the *Agt* DnaJ protein has been proposed to interact with residue His^{33} of the HPD motif (HENNESSY *et al*., 2000) highlighting a potential mechanistic role of this residue in the interaction of the J-domain with Hsp70 (LANDRY, 2003). In contrast, it is has been proposed that this residue serves a structural role through steric maintenance of the orientation of the J-domain or of the loop region comprising the main interaction surface with Hsp70 (GENEVAUX *et al*., 2002). This argument is supported by the results obtained for the KFA substitution (M46F mutation) of the 'KMA' motif of the Pfj1-J-*Agt*-DnaJ chimera; functionality of the mutant protein was preserved, albeit at reduced levels. It is possible that structural disruption of the Pfj1 J-domain may have resulted from insertion of the larger aromatic side-chain of Phe^{46} into the hydrophobic pocket between helices II and III, resulting in compromised functionality of the mutant chimera and the partial complementation result observed. This disruption may have been counteracted by the addition of Lys^{47} in the KFK-mutation (double mutation M47F/A48K), as improved suppression of thermosensitivity was observed for *E. coli* OD259 producing the mutant Pfj1-J-*Agt*-DnaJ-KFK protein (*FIGURE 5.6*). Alternatively, the insertion of residue Phe^{46} may have generated a substantially hydrophobic region (Phe^{46}, Ala^{47}) in helix III of the J-domain, resulting in localized disruption of the helical structure. Subsequent insertion of Lys^{47} (KFK-mutation) may have alleviated this hydrophobicity, thereby producing a more stabilised helical structure and hence, maintaining

functionality of the J-domain. Interestingly, single substitution A48K of the Pfj1 J-domain (rendering a KMK motif) and substitution F47L of the J-domain of *Agt* DnaJ (rendering a KLK motif; HENNESSY *et al*., 2005a,b) had no adverse effect on the *in vivo* functionality of either protein. These observations placed together with the demonstrated functionality of the 'KMA' motif in the unmutated Pfj1-J-*Agt*-DnaJ chimera (*SECTION 5.3.2.1*), suggest that the minimum requirement for functionality of this helix III motif is the conservation of a hydrophobic residue at position 47 (Met^{47}, Phe^{47} or Leu^{47}).

Interestingly, the KFK motif is not conserved in helix III of the type III Hsp40 J-domain of bovine auxilin. However, alignment of the sequence of this J-domain with that of *E. coli* DnaJ (not shown) reveals the conservation of residue Phe^{891} of auxilin, corresponding to the position of the KFK motif. This residue of the auxilin J-domain was proposed to exhibit hydrophobic interactions with bovine Hsc70 in complex as discussed in *SECTION 2.3.2*, *CHAPTER 2* (JIANG *et al*., 2007). Closer observation of the orientation of this residue in the crystal structure of auxilin (PDB: 1NZ6) similarly reveals proximity to the HPD motif in the loop region of the J-domain. This highlights the importance of this conserved Phe (or hydrophobic) residue in the J-domain and supports the proposed mechanistic and structural roles predicted for this residue in interaction with partner Hsp70s.

Published structures of J-domains of diverse origin (summarised in *TABLE 1.1*, *CHAPTER 1*) have revealed the relative mobility of helix IV. Residues of this helix are proposed to serve a primary structural or indirect functional role in mediating the specificity of interaction with Hsp70. In particular, the conserved QKRAA motif of helix IV in prokaryotic J-domains is proposed to enhance the affinity or specificity of interactions with DnaK, and mutation of the conserved residue Arg^{63} of this motif has been shown to result in partial or complete loss of J-domain functionality (GARIMELLA *et al*., 2006; HENNESSY *et al*., 2005a,b). The findings of AUGER and ROUIDER (1997) suggest that the QKRAA motif mediates binding to DnaK by serving as a substrate mimic. In this study, mutation of the residue Lys^{62} (K62A) in the Pfj1 J-domain corresponding to Arg^{63} t of the prokaryotic QKRAA motif, resulted in partial loss of function of the Pfj1-J-*Agt*-DnaJ chimera in the employed *in vivo* complementation system (*FIGURE 5.6*). This suggests that the K62A mutation abolished weak or indirect interactions with *E. coli* DnaK. While a basic residue at this position may not be critical for J-domain-based interactions with Hsp70, it may be important for mediating the affinity or specificity of the interaction. Interestingly, functionality of the Pfj1 J-domain in the prokaryotic system was maintained on mutation of the KKKEF motif to that of QKRAA encountered in prokaryotic DnaJ. Notably, the KKKEF motif of the unmutated Pfj1-J-*Agt*-DnaJ chimera appeared sufficient for interaction with DnaK in the prokaryotic system. It is possible that the QKRAA motif may enhance the specificity of interaction with DnaK in the prokaryotic system, while the KKKEF motif of Pfj1 may

mediate specificity of binding to partner Hsp70s in *P. falciparum.* Consistent with this, the conserved QKRAA motif of prokaryotic DnaJ proteins differs in human, *S. cerevisiae* and *P. falciparum* type ▮ Hsp40s (*FIGURE 2.2*, *CHAPTER 2*), with the minimum requirement of basic conserved residues in the second and third positions of the pentapeptide motif.

5.4 CONCLUSIONS

The data from this study suggests that a common mode of J-domain based Hsp70-Hsp40 interaction may be conserved in *P. falciparum*, as has previously been identified for Hsp40 proteins of prokaryotic and eukaryotic origin. This was implied by the functionality of the Pfj1 J-domain in substitution of the J-domain of *Agt* DnaJ in the prokaryotic *in vivo* complementation system, and was further substantiated by the indication that Pfj1 may exert its functionality via a conserved HPD-motif mediated interaction with partner Hsp70s. This *in vivo* assay system has provided a platform from which to explore the co-chaperone properties of Pfj1, which was otherwise not possible due to difficulties experienced with the isolation of the full length protein from a heterologous source (detailed in *CHAPTER 3*).

As previously discussed, J-domains of diverse origin appear to be interchangeable with respect to their ability to interact with homologous Hsp70 proteins, or their involvement in similar cellular processes. It is therefore possible that the J-domains of Pfj1 and *E. coli* DnaJ and/or CbpA are involved in analogous chaperone processes or interact with homologous Hsp70 proteins. It is known that *E. coli* DnaJ and CbpA interact with DnaK in the prokaryotic system (LIBEREK *et al*., 1991; UEGECHI *et al*., 1995). Previously, PfHsp70-▮was shown to functionally replace DnaK in a thermosensitive *E. coli* DnaK mutant strain (*E. coli dnaK756*) indicating the potential functional equivalence of these Hsp70 homologs (SHONHAI *et al*., 2005). The proposed interaction of the Pfj1 J-domain with DnaK in the *E. coli* OD259 strain in this study may thus serve to substantiate similar interactions of the Pfj1 J-domain with PfHsp70-▮in *P. falciparum*. Importantly, identified Hsp40 interaction residues in DnaK appear to be conserved in PfHsp70-▮as detailed in *CHAPTER 2*. Cautiously, it must be noted that this study was based on the assumption that the employed *in vivo* complementation assays were designed to probe an interaction between the Pfj1-J-*Agt*-DnaJ chimera protein and *E. coli* DnaK. This interaction remains to be verified with *in vitro* protein binding assays, protein refolding and/or ATPase assays with purified recombinant forms of the proteins of interest.

Intriguingly, the Pfj1 J-domain exhibited functionality in the prokaryotic system despite its low level of amino acid sequence conservation relative to the J-domains of *E. coli* DnaJ and *Agt* DnaJ. Placed in context with other J-domain swapping experiments, this suggests the presence of key conserved features of the Pfj1 J-domain that are fundamental to the functioning of J-domains in general. The

importance of these key features, including specific residues and motifs, was addressed by single and multiple amino acid substitution analysis as described. The results suggested that residues of helix II (Phe^{25}, Arg^{26}) placed with the invariant HPD motif may comprise the interaction surface with partner Hsp70s. Moreover, the KMK motif of helix III may maintain the structural or functional integrity of the Pfj1 J-domain, through potential interactions with the loop region housing the HPD motif of this domain. Residue Met^{47} was identified as an integral hydrophobic component of the KMK motif, analogous to Phe^{47} of the corresponding KFK motif of more typical Hsp40 proteins. While the data suggests that this residue primarily serves a structural role, the possibility cannot be excluded that it may serve an indirect functional role ensuring that the J-domain is orientated correctly for interactions with Hsp70. Mutation of the KKKEF motif of helix IV of the Pfj1 J-domain suggested that these residues may be crucial to governing the specificity or affinity of interaction with Hsp70. Residue Lys^{62} of this motif was suggested to exhibit weak or indirect interactions with Hsp70, or maintain the structural integrity of helix IV. It is possible that subtle identified differences in the Pfj1 J-domain may reflect slight differences in affinity or specificity for Hsp70 that were not sufficient to exhibit effect in the *in vivo* complementation assay. Such differences may be explored more extensively using quantitative *in vitro* binding assays. Moreover, the results of the rational mutagenesis of the Pfj1 J-domain must be interpreted cautiously as they may represent system-specific results derived from the prokaryotic *in vivo* complementation system.

Functional replacement of *E. coli* DnaJ and CbpA was not shown for full length PfHsp40 and Pfj1 in the *in vivo* complementation system, potentially attributed to insufficient exogenous protein production or lack of functional interchangeability. Use of a eukaryotic complementation system may be a more appropriate means of assessing the *in vivo* functionality of PfHsp40 and Pfj1, envisaging that such a system may meet the appropriate post-translational modification and subcellular compartmentalisation requirements required for functionality. The proposed use of an *S. cerevisiae* complementation system for these purposes is further described in *SECTION 7.2.3*, *CHAPTER 7*. Domain swapping experiments and rational mutagenesis of the more conserved J-domain of PfHsp40 may also be valuable in substantiating the mechanism of J-domain based Hsp70-Hsp40 interaction in *P. falciparum*.

CHAPTER 6:

IN VITRO CHARACTERISATION:

Comparison of Hsp70-Hsp40 Interactions of

P. falciparum and the Human Host

6.1 INTRODUCTION

A functional *P. falciparum* Hsp70-Hsp40 partnership has previously not been demonstrated experimentally. This study describes the use of *in vitro* assays to assess the ability of purified recombinant PfHsp40 to stimulate the chaperone activity of PfHsp70-1. Radioactive single turnover and steady state Adenosine triphosphatase (ATPase) assays were performed to demonstrate the effect of PfHsp40 on ATP hydrolysis by PfHsp70-1, indicative of the Hsp70 protein folding cycle. Similarly, aggregation suppression assays were used to demonstrate the ability of PfHsp40 to function independently and in combination with PfHsp70-1 to diminish the protein aggregation of a model thermolabile substrate. These activities were gauged against an established human Hsp70-Hsp40 partnership, involving cytosolic Hsp70 and the type II Hsp40 protein, Hsj1a (CHEETHAM *et al*., 1994). In addition, the co-chaperone activity of PfHsp40 was contrasted to that of human Hsj1a and a 'promiscuous' type III Hsp40 protein from *S. cerevisiae* termed Hlj1 (YOUKER *et al*., 2004).

The utilisation of host chaperones by the *P. falciparum* chaperone machinery in intra-erythrocytic stage parasites has been suggested (BANUMATHY *et al*., 2002). In particular, the proposed exploitation of human Hsp70 and the export of numerous members of the parasite's Hsp40 chaperone machinery into the erythrocyte cytosol (SARGEANT *et al*., 2006) suggests that heterologous interactions may exist between the host Hsp70 and parasite Hsp40 molecular chaperones. This has been discussed at length in *CHAPTER 2*. Such interactions have previously not been substantiated experimentally. In this study the aforementioned *in vitro* assays were used to explore the potential for heterologous partnerships between the *P. falciparum* and human Hsp70 and Hsp40 proteins; in particular, the association of HsHsp70 with PfHsp40 and PfHsp70-1 with Hsj1a respectively. Moreover, this was aimed at substantiating the conservation of the mechanism of Hsp70-Hsp40 interaction in *P. falciparum*, proposed in *CHAPTER 5*.

Previous work has described established techniques for the assessment of the effect of a range of small molecule modulators on the activity of molecular chaperones with implications for prospective drug targets (BRODSKY and CHIOSIS, 2006; FEWELL *et al.,* 2004; WRIGHT *et al.,* 2008). This has encompassed research on the effect of modulators on the chaperone activity of PfHsp70-1 in the absence of co-chaperone stimulation. Using this platform, the effect of select compounds on the identified human and malaria Hsp70-Hsp40 partnerships was assessed.

Specifically, the objectives of this study were to (*i-v*):

i. Assess the ability of PfHsp40 to serve as a co-chaperone partner of PfHsp70-1
ii. Gauge the co-chaperone activity of PfHsp40 relative to characterised co-chaperone proteins

iii. Draw parallels between the Hsp70-Hsp40 partnerships of *P. falciparum* and human origin

iv. Substantiate the potential for heterologous human and *P. falciparum* Hsp70-Hsp40 partnerships

v. Establish a model system for the screening and identification of small molecule modulators specific to the homologous and heterologous Hsp70-Hsp40 partnerships of the parasite chaperones

6.2 MATERIALS AND METHODS

6.2.1 Description and Isolation of Recombinant Proteins

The recombinant proteins utilised and referred to in this study, are summarised in *TABLE 6.1*. Protein sequences of the respective proteins are provided in fasta format in *APPENDIX C2*. Heterologous production and purification of the proteins is further detailed.

TABLE 6.1 Description and Classification of the Recombinant Proteins Used for ***In Vitro*** Characterisation

Protein	Classification	Gene ID	Protein Accession	Source Organism
PfHsp40	Hsp40 (Type I)	PF14_0359	NP_702248	*P. falciparum*
Pfj1	Hsp40 (Type II)	PFD0462w	NP_702750	*P. falciparum*
Hsj1a	Hsp40 (Type II)	DNAJB2	X63368	*H. Sapiens*
Hlj1	Hsp40 (Type III)	P48353	NP_013884	*S. cerevisiae*
HsHsp70	Hsp70	HSPA1A	NP_005336	*H. Sapiens*
PfHsp70-I	Hsp70	PF08_0054	AAA29626	*P. falciparum*

6.2.1.1 Expression and Purification of the P. falciparum Type I Hsp40 protein, PfHsp40

The heterologous expression and purification of recombinant PfHsp40 is detailed in *SECTION 3.3.2.1*, *CHAPTER 3*.

6.2.1.2 Expression and Purification of the Human Type II Hsp40, Hsj1a

Enhancement of the ATPase and substrate binding activity of HsHsp70 by Hsj1a has been described (CHEETHAM *et al*., 1994). Recombinant hexahistidine-tagged Hsj1a, or His_6-Hsj1a, was expressed from the pQE30-derived pQHsj1a plasmid (MCNAMARA, 2006) in *E. coli* XL1-Blue at 37°C in LB media (1% tryptone, 0.5% yeast extract, 1% NaCl) supplemented with 100 µg.ml^{-1} ampicillin. Protein expression was induced with 1 mM IPTG ($_{(A600}$ of 0.6-0.8) and the cells were harvested 5 hours post-induction. Protein purification was performed under batch and non-denaturing conditions in the presence of 0.1% PEI, 10 mM imidazole, 300 mM NaCl and 10 mM Tris-Cl (pH 8.0). Cell lysis was achieved by sonication and treatment with 1 mM lysozyme (freeze-thaw at -20 °C) in the presence of proteinase inhibitors (1 mM PMSF, 0.5 µg.ml^{-1} Pepstatin A and 1 µg.ml^{-1} Leupeptin). The cell lysate was cleared

by centrifugation (16 000xg, 20 minutes, 4°C). Protein in the soluble fraction was allowed to bind a Ni-NTA slurry (1:500 column to culture volume; Qiagen) for 4 hours at 4°C with gentle agitation. The beads were subsequently washed with 50, 100 and 150 mM imidazole respectively, followed by the elution of bound protein with 1 M imidazole. The imidazole in the eluted fraction was removed by dialysis (5% (v/v) glycerol, 2 mM $MgCl_2$, 0.8 mM DTT, 50 mM NaCl, 50 mM Tris-Cl, pH 7.4), and the protein was concentrated with Polyethylene Glycol (PEG-3000; Sigma-Aldrich).

6.2.1.3 Expression and Purification of the S. cerevisiae Type III Hsp40, Hlj1

The J-domain of the *S. cerevisiae* transmembrane endoplasmic reticulum type III Hsp40 protein, Hlj1, was used as a control for the assessment of co-chaperone activity in the assays detailed in this study. Stimulation of Hsp70 ATPase activity by the Hlj1 J-domain has been published; the protocol for the purification of recombinant Hlj1 was adapted accordingly (YOUKER *et al*., 2004). Plasmid pGEX-KG-Hlj1 encodes an N-terminally tagged glutathione-S-transferase (GST) fusion protein bearing the first 86 amino acids of the Hlj1 sequence (259 base pairs) comprising the J-domain (*APPENDIX C2*). The fusion protein bears an additional C-terminal hexahistidine tag resulting from subcloning of the Hlj1 coding sequence from the pQE60 plasmid. In brief, a culture of *E. coli* M15 cells transformed with the pGEX-KG-Hlj1 plasmid was grown to $_{A600}$ —0.5 at 37°C in LB media containing 50 µg.ml^{-1} ampicillin. Following back dilution (1:1000), the culture was grown at 30°C to $_{A600}$ —0.15 and induced with 0.2 mM IPTG. The cells were harvested 7 hours post-induction, and resuspended in Buffer 88 (150 mM KOAc, 5mM MgOAc, 250 mM sorbitol, 20 mM HEPES, pH 6.8) containing 1 mM EDTA, 0.1% (v/v) Triton X-100 and proteinase inhibitors (1 mM PMSF, 1 µg.ml^{-1} Leupeptin, 0.5 µg.ml^{-1} Pepstatin A). Post freeze-thaw (-80°C), cell lysis was achieved by sonication and the lysate was cleared by centrifugation (16 000xg, 20 minutes, 4°C). The soluble fraction was loaded onto a column of glutathione-agarose (Sigma-Aldrich; 3:2000 column to culture volume ratio). Bound protein was washed with consecutive washes of Buffer 88 supplemented with 1 mM EDTA and proteinase inhibitors, 1 M KCl, and 7 mM ATP respectively. The bound Hlj1 was eluted with 10 mM reduced glutathione in the presence of 50 mM Tris-Cl, pH 8.0, and subsequently dialysed (5% glycerol, 2 mM $MgCl_2$, 0.8 mM DTT, 50 mM NaCl, 50 mM Tris-Cl, pH 7.4). The dialysed fraction was passed over a Q-Sepharose Fast Flow^{TM} anion exchange column (Sigma-Aldrich; 1:500 column to culture volume) equilibrated in dialysis buffer. The unbound fraction containing recombinant Hlj1 was concentrated by centrifugation (5000 xg; 30 minutes) with Centricon® centrifugal filter units (Millipore).

6.2.1.4 Expression and Purification of the P. falciparum Hsp70, PfHsp70-I

Recombinant hexahistidine-tagged PfHsp70-I or His_6-PfHsp70-I was expressed from the pQE30-derived pQPfHsp70-I plasmid (originally termed pQE30/PfHsp70; MATAMBO *et al*., 2004) in *E. coli*

Rosetta™ 2(DE3) (Novagen) at 26°C in LB media supplemented with 50 µg.ml^{-1} ampicillin and 34 µg.ml^{-1} chloramphenicol for plasmid and strain selection respectively. Protein expression was induced with 1 mM IPTG ($_{(A600}$ of 0.6 - 0.8), and cells were harvested 5 hours post-induction. PfHsp70-I purification was performed under denaturing (8M urea) and non-denaturing (0.1% (v/v) PEI) conditions respectively in the presence of 10 mM imidazole, 300 mM NaCl and 10 mM Tris-Cl (pH 8.0). Cell lysis was achieved by sonication and treatment with 1 mM lysozyme in the presence of proteinase inhibitors (1 mM PMSF, 0.5 µg.ml^{-1} Pepstatin A and 1 µg.ml^{-1} Leupeptin). The cell lysate was cleared by centrifugation (16 000xg, 20 minutes, 4°C). Protein in the soluble fraction was allowed to bind a Ni-NTA column (1:500 column to culture volume), subsequently washed with 10 and 20 mM imidazole respectively, and eluted with a 25 - 500 mM imidazole gradient. Washes were performed in the absence of urea in the denaturing purification to permit protein refolding. The imidazole in the eluted fractions was removed by dialysis (5% (v/v) glycerol, 2 mM $MgCl_2$, 0.8 mM DTT, 50 mM NaCl, 50 mM Tris-Cl, pH 7.4), and the protein in the dialysed fraction was allowed to bind a Q-Sepharose Fast Flow™ anion exchange column (Sigma-Aldrich; 1:500 column to culture volume) equilibrated in dialysis buffer. Bound protein was washed with dialysis buffer and eluted from the column with 200 mM NaCl. The eluted protein was dialysed as before to eliminate excess NaCl, and concentrated by centrifugation as previously detailed. PfHsp70-I purified under non-denaturing and denaturing conditions is further denoted as N/PfHsp70-I and D/PfHsp70-I respectively.

6.2.1.5 Recombinant Human Hsp70, HsHsp70

Recombinant hexahistidine-tagged human Hsp70, His_6-HsHsp70, purified under non-denaturing conditions was a kind gift from Dr Michael Klein and Professor Xiaojeng Chen of the Department of Molecular and Computational Biology, University of Southern California, United States.

6.2.2 SDS-PAGE and Western Analysis of the Purified Recombinant Proteins

Confirmation of the isolation of the recombinant protein products was achieved by 10% (w/v) SDS-PAGE and subsequent Western analysis as detailed in *APPENDIX D11.* The SDS-PAGE gels were prepared in duplicate and stained with Coomassie Blue and Silver nitrate respectively. The recombinant protein preparations were tested for contaminating DnaK and DnaJ from the heterologous expression systems used by Western analysis. Protein concentrations of the preparations were determined by Bradford's Assay (*APPENDIX D9*).

6.2.3 Single Turnover and Steady State ATPase Assays

Single turnover and steady state radioactive ATPase assays were employed to assess the basal and co-chaperone stimulated ATPase activity of recombinant HsHsp70 and PfHsp70-I, as schematically

represented in *FIGURE* 6.1. The protocols for the ATPase assays were adapted from those previously described (FEWELL ***et al*****., 2004; WRIGHT** *et al*****., 2008**).

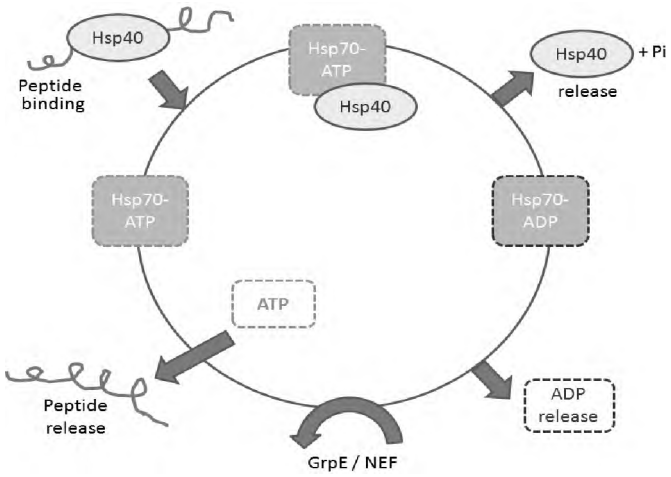

FIGURE **6.1** The **Hsp40-stimulated ATPase cycle of Hsp70: single turnover vs. steady state ATPase assays. Protein substrate** is **recruited to Hsp70 by the co-chaperone** Hsp40 **promoting the ATPase activity of** Hsp70**. ATP hydrolysis represents the rate-limiting step of the ATPase cycle. In the** ATP-**bound state, Hsp70 exhibits low affinity for protein substrate and high exchange rates. In an ADP-bound state, Hsp70 adopts a conformation with increased affinity for protein substrate** and **slower exchange rates, thereby facilitating folding of the substrate. The exchange of** Hsp70-**bound ADP for ATP is facilitated by a nucleotide – exchange factor (NEF), thereby decreasing Hsp70 affinity for substrate and allowing the release of the protein folding intermediate. Further processing of the su**bstrate **may follow, entailing additional cycles of binding and release. Single turnover ATPase assays were used to gauge ATP hydrolysis in the ATP hydrolysis step of the Hsp70 ATPase cycle only. In contrast,** steady state **ATPase assays were employed to gauge ATP hydrolysis through repetitions of the entire ATPase cycle. Notably, ATPase assays were performed in the absence of protein substrate. The figure was adapted from** SZABO ***et al.*** (1994).

6.2.3.1 *Single Turnover ATPase Assays*

Hsp70-**[α^{32}P]ATP complex was prepared through the incubation of 25 µg of purified Hsp70 protein (purified** N/PfHsp70- **or HsHsp70) with 25 µM ATP (Sigma Scientific) and 100µCi of [α^{32}P]ATP (Perkin-Elmer Life Sciences) in** single t**urnover Complex Buffer (STCB; 110 mM Mg OAc, 100 mM KCl, 25 mM HEPES, pH 7.5) at 4°C for 30 minutes. Free unbound [α^{32}P]ATP was eliminated by purification at 4°C on an illustra^{TM} NICK Sephadex G-50 column (GE Healthcare) equilibrated in STCB. Eluted fractions of** Hsp70-**[α^{32}P]ATP complex were dete cted with a Geiger Counter. The fractions were pooled, treated with glycerol to a final concentration of 10 % and frozen in aliquots using liquid nitrogen. The complex was stored at -80°C for a period of no longer than 2 weeks prior to use in ATPase assays.**

For each reaction in which the basal or co**-chaperone stimulated ATPase activity was determined, a 25 µL aliquot of Hsp70-[α^{32}P]ATP complex was rapidly thawed at 30°C and added to 2.5 µL STCB in a 50 µL reaction. In the co-chaperone stimulated reactions, purified Hlj1 (0.55 µM), Hsj1a (0.3 µM)** or **PfHsp40 (0.4 µM) w**as **added to the specified final concentrations respectively 60 seconds after the start of the reaction. The reaction was allowed to proceed at 30°C and aliquots of 6 µL were removed at selected time points throughout a 10 minute time course. ATP hydrolysis was interrupted in these aliquots by treatment with 2 µL of Stop Solution (2 M LiCl, 4 M Formic Acid, 36 mM ATP) and** the

reduction of the reaction temperature to 4°C. Aliquots of the stopped reactions (2 µL) were spotted in duplicate on thin layer chromatography plates and allowed to develop in TLC Buffer (0.5 M LiCl, 1 M Formic Acid). The [α^{32}P]ATP isotope was diluted 1:100 and similarly spotted and developed to determine spontaneous hydrolysis. Phosphorimager analysis (Fujifilm Phosphorimager BAS 2500 coupled to Image Gauge software, version 4.0) was employed in the determination of the percentage of ATP hydrolysed to ADP and P_i in each reaction. Curve fits and kinetic analyses were performed on the obtained data in KaleidaGraph (version 3.0.4, Synergy Software) and Sigmaplot (version 10.0, Systat Software Inc.). Kinetic analyses for the co-chaperone stimulated reactions were performed with the 60 second time point corrected to zero.

6.2.3.2 Steady State ATPase Assays

Purified recombinant Hsp70 protein (2 µM PfHsp70-I and 2.125 µM HsHsp70 respectively) was preincubated in reaction buffer (50 mM NaCl, 2 mM $MgCl_2$, 10 mM DTT, 50 mM HEPES, pH 7.4) for 15 minutes at 4°C. The reaction was started by the simultaneous addition of 50 µM ATP and 0.01 µCi [α^{32}P]ATP and allowed to proceed at 30°C over a 30 minute time course. At selected time points, 4 µL aliquots of each reaction were removed and added to 2 µL of Stop Solution (2 M LiCl, 4 M Formic Acid, 36 mM ATP) at 4°C. The aliquots representing each time point were subjected to thin layer chromatography (in duplicate) and analysed for ATP hydrolysis by Phosphorimager analysis as previously detailed in the protocol for the single turnover ATPase assays. The data from each time point was corrected for spontaneous ATP hydrolysis as observed in a control experiment in the absence of chaperone proteins. Co-chaperone stimulation of the basal Hsp70 activity was similarly assessed by the addition of 1 µM of the co-chaperone protein of interest (purified recombinant Hlj1, Hsj1a and PfHsp40) to the preincubated reaction mixture prior to the addition of ATP. Background ATP hydrolysis of the co-chaperone protein preparations was assessed and subtracted accordingly.

6.2.4 Malate Dehydrogenase Aggregation Suppression Assays

Aggregation suppression assays were employed to assess the ability of the investigated chaperone proteins (recombinant PfHsp70-I, HsHsp70, Hlj1, Hsj1a and PfHsp40) and associated Hsp70-Hsp40 partnerships to suppress the heat-induced aggregation of L-Malate Dehydrogenase (MDH) at 48°C over time. The MDH (0.72 µM; Roche Applied Sciences, Germany) and chaperone protein(s) of interest (0.3 µM respectively) were suspended in assay buffer (100 mM NaCl, 50 mM Tris-Cl, pH 7.4) pre-equilibrated to 48°C. The accumulation of protein aggregates was monitored by changes in Absorbance at 360 nm in a thermo-controlled spectrophotometer (Model 14NT-UV-VIS, Aviv Instruments Inc, Lakewood, N.J., USA). As a reference, MDH aggregation was monitored in the

absence of chaperone proteins at 48°C over time. Similarly in the absence of MDH, the thermal stability of the chaperone proteins under investigation was assessed to ensure accurate monitoring of the MDH aggregation in the test experiments. Furthermore, BSA (0.3 µM) was used in a control experiment in the absence of chaperone proteins to ensure that the observed MDH aggregation suppression was specific to chaperone protein activity, and to further demonstrate the thermal instability of MDH in the absence of chaperone protein intervention. Protein concentrations were calculated assuming the monomeric form of the relevant proteins.

6.2.5 Assessment of the Effect of Small Molecule Modulators on Hsp70-Hsp40 Activity

The homologous and heterologous Hsp70-Hsp40 partnerships established in the ATPase assays (*SECTION 6.2.3*) represented a model system for the identification of small molecule modulators specific to interactions of the parasite chaperone proteins. In demonstration of this, two previously-characterised small molecule modulators of Hsp70, MAL3-39 (FEWELL *et al*., 2004) and DMT002264 (WRIGHT *et al*., 2008) illustrated in *FIGURE 6.2*, were assessed for their ability to modulate the basal and co-chaperone stimulated ATPase activity of HsHsp70 and PfHsp70-I *in vitro*, using the single turnover and steady state assays previously described.

A.

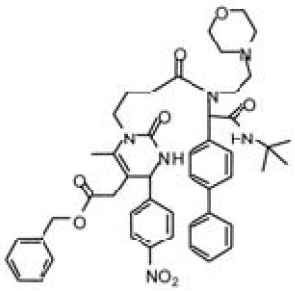

B.

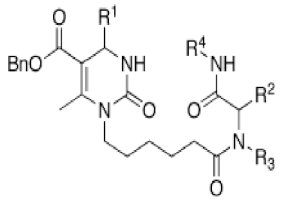

R1	R2	R3	R4
p-Biphenyl	C-Hexyl	*n*-Hexyl	*n*-Butyl

FIGURE 6.2 Chemical structures of the small molecule modulators, MAL3-39 and DMT002264. The ability of compounds (A) MAL3-39 and (B) DMT002264 to modulate the co-chaperone stimulated and basal ATPase activity of HsHsp70 and PfHsp70-I was assessed in single turnover and steady state ATPase assays. MAL3-39 represents a 15-Deoxyspergualin (DSG) derivative, previously shown to inhibit the stimulation of the ATPase activity of Hsp70 by the J-domain containing large T antigen of the simian virus 40 *in vitro* (FEWELL *et al.*, 2004). DMT002264 represents a pyrimidinone-peptoid hybrid, or cyclohexylcarboxyaldehyde, derived from an additional DSG derivative, MAL3-101. DMT002264 was shown to stimulate the ATPase activity of the yeast Hsp70, Ssa1p, 3.2-fold *in vitro* (WRIGHT *et al*., 2008).

Single turnover and steady state ATPase assays were conducted as previously detailed with the following exceptions. In single turnover assays, the compounds MAL3-39 and DMT002264 were prepared in Dimethyl sulfoxide (DMSO) and added to a final concentration of 300 µM respectively at the start of each reaction. In steady state assays, preincubation of the assay components prior to the

addition of ATP was achieved in the presence of 300 µM of each respective compound prepared in DMSO. In all assays, an equal volume of DMSO was added to the reactions not treated with compounds.

6.3 RESULTS AND DISCUSSION

6.3.1 Purification of Recombinant Proteins

SDS-PAGE and Western analysis of the purified recombinant proteins used in this study is provided in *FIGURE 6.3*.

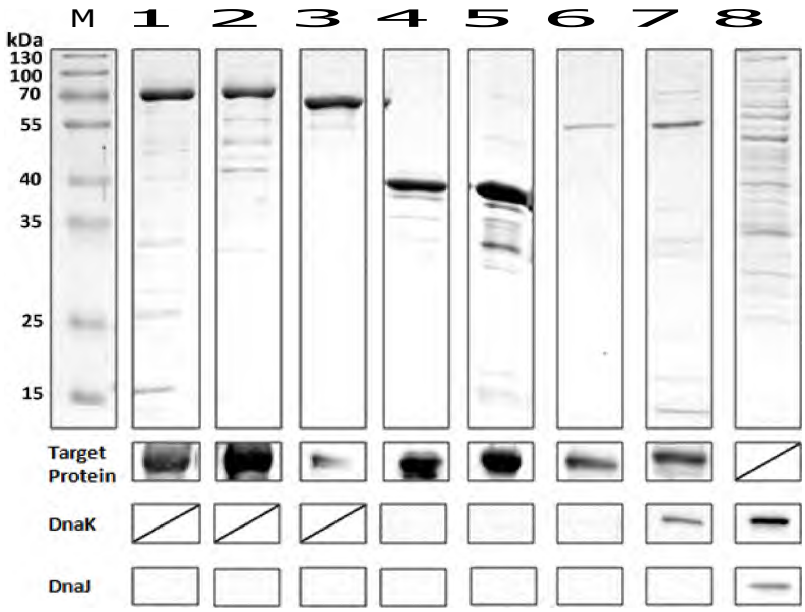

FIGURE 6.3 SDS-PAGE and Western analysis of purified recombinant proteins used for ***in vitro*** characterisation studies. *Lanes*: *M* – Marker (Fermentas Pageruler™ Protein Ladder), *1* – D/His_6-PfHsp70-▮(76 kDa), *2* – N/His_6-PfHsp70-▮(76 kDa), *3* – His_6-HsHsp70 (72 kDa), *4* – GST-Hlj1-His_6 (36 kDa), *5* – His_6-Hsj1a (32 kDa), *6* – D/His_6-PfHsp40 (49 kDa), *7* – N/His_6-PfHsp40 (49 kDa), *8* – *E. coli* XL1-Blue cell lysate (positive control). D/ and /N denote proteins purified under denaturing and non-denaturing conditions respectively. Each lane contains 2 µg of purified protein, with the exception of His_6–PfHsp40 in *lanes 6* and *7*. Concentrations of the purified recombinant proteins were determined by Bradford's assay: D/His_6-PfHsp70-▮ - 0.67 µg.µl^{-1} ; N/His_6-PfHsp70-▮ - 0.71 µg.µl^{-1} ; His_6-HsHsp70 - 1.8 µg.µl^{-1} ; GST-Hlj1-His_6 - 0.45 µg.µl^{-1} ; His_6-Hsj1a - 0.50 µg.µl^{-1} ; His_6-PfHsp40 - 0.11 µg.µl^{-1} . *Upper panel* – Coomassie-Blue stain of 10% (w/v) SDS-PAGE analysis. Silver staining was also employed (not shown) to assess the presence of co-purified proteins and truncation products as further discussed in the text. *Panel 2* – Detection of target proteins by Western analysis. His_6-PfHsp70-▮(*lanes 1* and *2*) was detected with rabbit polyclonal anti-PfHsp70-▮ His_6-HsHsp70 (*lane 3*) was detected with rabbit polyclonal anti-Hsp72/73 (Upstate Biotechnology), GST-Hlj1-His_6 (*lane 4*) was detected with goat polyclonal anti-GST (GE Healthcare), His_6-Hsj1a (*lane 5*) was detected with mouse monoclonal anti-penta-His (Qiagen) and His_6-PfHsp40 (6 and 7) was detected with rabbit polyclonal anti-PfHsp40 (engineered in this research). Secondary antibodies used: HRP-conjugated goat anti-rabbit and goat anti-mouse (GE Healthcare) and HRP-conjugated anti-sheep/goat (Exalpha Biologicals). *Panels 3 and 4* – Detection of DnaK and DnaJ contamination in the protein purification products by Western analysis: DnaK was detected with rabbit polyclonal anti-Hsp72/73 (Upstate Biotechnology) and DnaJ was detected with rabbit polyclonal anti-DnaJ (Stressgen), with HRP-conjugated goat anti-rabbit secondary antibody. Contaminating DnaK is evident in the D/His_6-PfHsp40 preparation (*lane 7*).

The presence of contaminating DnaK and DnaJ in the protein preparations from the prokaryotic heterologous expression systems was ruled out by Western analysis as indicated. Notably, the DnaK-free denaturing preparation of PfHsp40 (*lane 6*, *FIGURE 6.3*) was used in subsequent *in vitro* ATPase assays, and not the DnaK-contaminated non-denaturing preparation of the recombinant protein (*lane 7*, *FIGURE 6.3*).

6.3.2 ATPase Assays

6.3.2.1 Co-chaperone Enhancement of ATP Hydrolysis in Single Turnover

ATP Hydrolysis typically constitutes the rate-limiting step of the ATPase cycle of Hsp70 proteins (BURKHOLDER *et al.,* 1994; RUSSELL *et al.,* 1999). Consequently, enhancement of the Hsp70 ATPase activity is achieved by co-chaperone regulation by Hsp40. In single turnover assays this enhancement was gauged in the ATP hydrolysis step of the Hsp70 ATPase cycle only. The reaction was initiated by the addition of co-chaperone protein to Hsp70-ATP complex, with negligible susceptibility to ATP rebinding in the absence of ATP regeneration. In this context, stimulation of the ATPase activity of HsHsp70 and PfHsp70-▮ by Hlj1, Hsj1a and PfHsp40 was demonstrated as detailed in *FIGURE 6.4* overleaf. The fold change in ATP hydrolysis relative to basal activity was derived from the curve fits of the illustrated reactions, and is summarised in *TABLE 6.2*.

TABLE 6.2 Single Turnover ATP Hydrolysis of Basal and Co-chaperone Stimulated HsHsp70 and PfHsp70-▮ATPase Activity

Co-chaperone stimulation	µM	Fold change in ATP hydrolysis	
		HsHsp70	PfHsp70-▮
None *(basal)*	-	[1]	[1]
Hlj1	0.55 µM	8.13	17.02
Hsj1a	0.3 µM	12.95	34.51
PfHsp40	0.4 µM	4.40*	9.47

* ATP Hydrolysis by HsHsp70 has been corrected with the loss in the corresponding PfHsp70-▮activity as a reference, refer to *FIGURE 6.4C*; *Basal* refers to Hsp70 activity in the absence of co-chaperone stimulation; A fold change of [1] in ATP hydrolysis indicates that activity has been adjusted to serve as a reference for co-chaperone stimulated activity.

The basal ATPase activity of PfHsp70-▮(in the absence of co-chaperone) was gauged to be 2.27 fold higher than that of HsHsp70 for the ATP hydrolysis stage of the ATPase cycle (*TABLE 6.2*). Moreover, PfHsp70-▮ exhibited significantly higher sensitivity to co-chaperone stimulation with more than double the fold increase in ATP hydrolysis relative to HsHsp70 for each respective co-chaperone protein.

A.

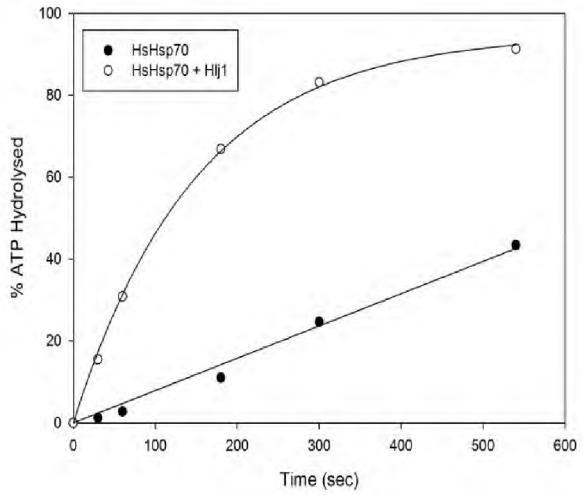

D.

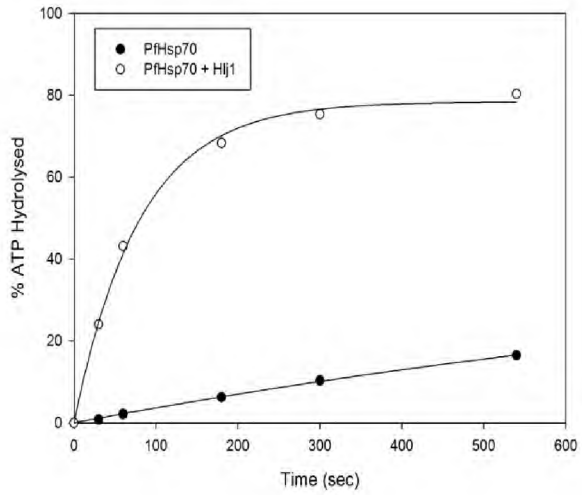

B.

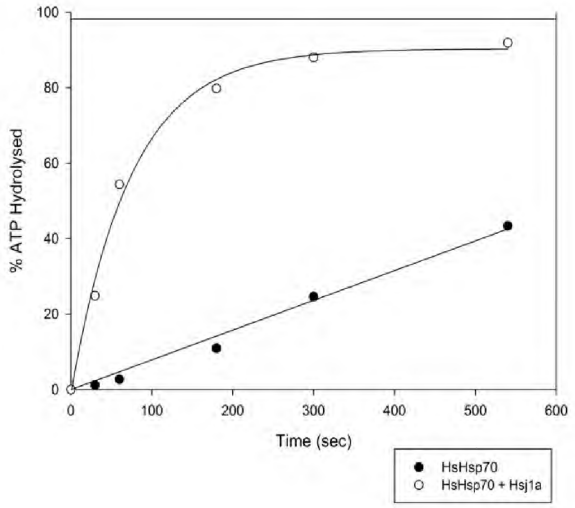

E.

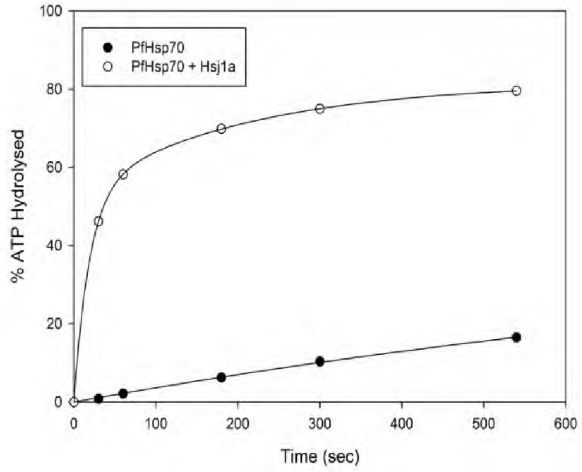

C.

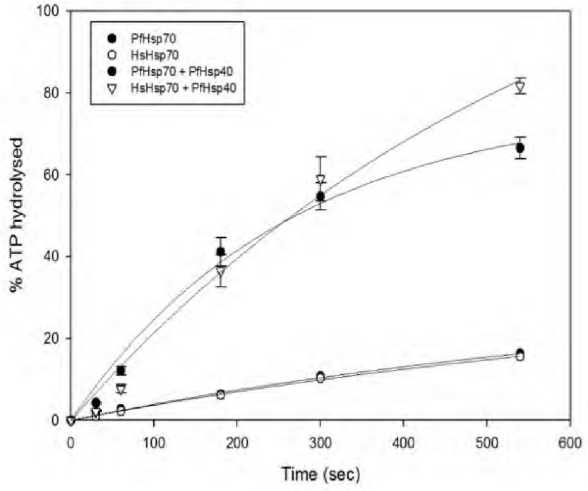

F.

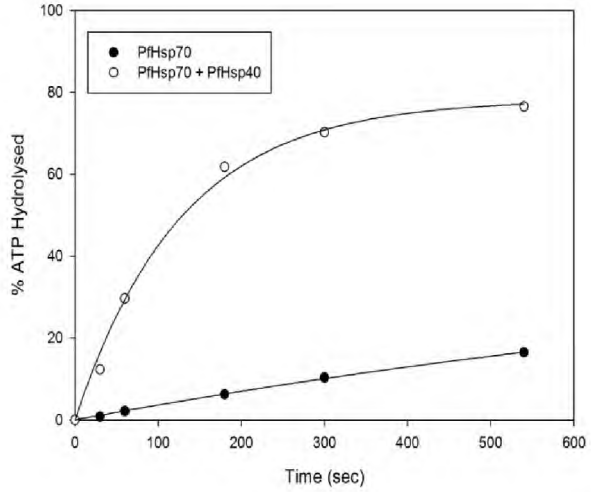

FIGURE 6.4.../

.../FIGURE 6.4 Co-chaperone stimulation of the ^{32}ATPase activity of HsHsp70 and PfHsp70-1 in single turnover assays. Stimulation of the ATPase activity of [α^{32}P]ATP-bound HsHsp70 (A-C) and PfHsp70-1 (D-F) was observed by the addition of 0.55µM Hlj1, 0.3 µM Hsj1a, and 0.4 µM PfHsp40 respectively 60 seconds into the start of the reaction. In (C) PfHsp40 stimulation of PfHsp70-1 is included as a reference to illustrate the loss of ATPase activity and co-chaperone stimulation observed with use of ageing Hsp70-[α^{32}P]ATP complex; repetition of this experiment is required. The 60 second time points were corrected to zero, and curve fits applied using the single exponential equation $[ADP_t] = [ADP_{max}](1-e^{-kt})$, where *k* represents the rate of ATP hydrolysis per second and the amplitude of the reaction is represented as $[ADP_{max}]$. The Hsj1a stimulation of HsHsp70 (B) and PfHsp70-1 ATPase activity (E) was best represented as a two-step exponential process $[ADP_t] = [ADP_{max1}](1-e^{-k_1 t}) + [ADP_{max2}](1-e^{-k_2 t})$. Representative curve fits were generated in Sigmaplot (version 10.0, Systat Software Inc.) and verified in KaleidaGraph (version 3.0.4, Synergy Software).

Interestingly, the stimulation of the ATPase activity of HsHsp70 and PfHsp70-1 by Hsj1a was best expressed as a two-step exponential process (*FIGURE 6.4*) potentially highlighting a different mechanism of co-chaperone stimulation. Moreover, Hsj1a proved the most efficient co-chaperone at stimulating the ATPase activity of both Hsp70 proteins, and this remained unaffected at a lowered concentration of 0.3 µM (in relation to 0.4 µM PfHsp40 and 0.55 µM Hlj1). It is possible that this high degree of co-chaperone stimulation may not inevitably signify appropriate stimulation of chaperone activity *in vivo*. Consistent with this, the homologous PfHsp70-1/PfHsp40 partnership exhibited the least enhancement of PfHsp70-1 ATPase activity (*TABLE 6.2*) and most likely represents appropriate stimulation. The enhancement of PfHsp70-1 basal ATPase activity in the presence of PfHsp40 represents the first report of biochemical evidence for a functional interaction between a *P. falciparum* Hsp70 and Hsp40 protein.

As previously discussed, PfHsp70-1 and PfHsp40 are predicted to be parasite-resident proteins, as they do not bear an export motif for transport to the cytoplasm of the parasitized erythrocyte (HILLER *et al.*, 2004; MARTI *et al.*, 2004). Moreover, Hsj1a may not constitute a part of the erythrocyte proteome (PASINI *et al.*, 2006). The host-parasite heterologous Hsp70-Hsp40 partnerships demonstrated in this study (PfHsp70-1/Hsj1a and HsHsp70-PfHsp40) are therefore unlikely to prevail *in vivo* in the *P. falciparum*-infected erythrocyte. Nevertheless, these partnerships have demonstrated the potential for heterologous interactions between chaperone proteins of human and parasite origin, and in particular between the exported HPD-bearing *P. falciparum* Hsp40 proteins and HsHsp70 in the parasitized erythrocyte. Such partnerships remain to be validated with parasite Hsp40 proteins that are known to be exported to the host cell cytosol. Importantly, the demonstrated heterologous partnerships have highlighted similarities in the activities of the respective chaperone proteins, implying a conserved mechanism in both the human host and the parasite. This could have implications for future approaches to the use of the parasite molecular chaperone proteins as candidate drug targets.

6.3.2.2 Co-chaperone Enhancement of ATP Hydrolysis in Steady State

In the steady state ATPase assays employed, ATP hydrolysis was gauged for repetitions of the complete ATPase cycle of Hsp70. Enhancement of the ATPase activity of HsHsp70 and PfHsp70-I was achieved with co-chaperone stimulation by Hlj1, Hsj1a and PfHsp40 in this context as illustrated in *FIGURE 6.5*.

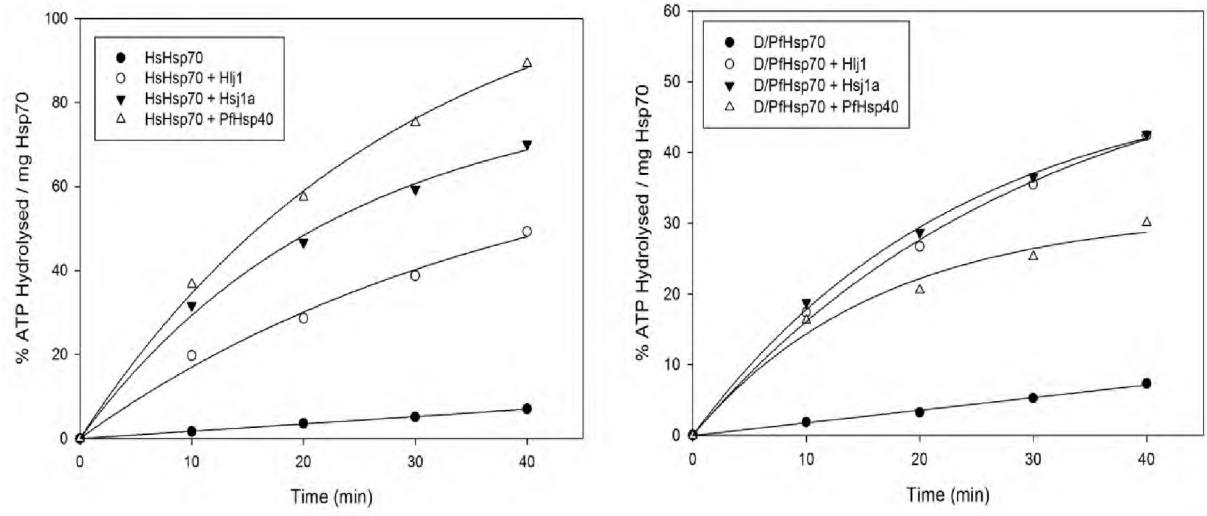

FIGURE 6.5 Co-chaperone stimulation of the ATPase activity of PfHsp70-I and HsHsp70 in steady state assays. The ATPase activity of (A) 2.125 µM HsHsp70, (B) 2 µM D/PfHsp70-I purified under denaturing conditions and (C) 2 µM N/PfHsp70-I purified under non-denaturing conditions was assessed *in vitro*. Stimulation of the activity was achieved in the presence of 1 µM co-chaperone protein (Hlj1, Hsj1a, or PfHsp40 respectively) as indicated. The reactions were corrected for spontaneous ATP hydrolysis as observed in the ATP only control, and the co-chaperone stimulated reactions were corrected for background hydrolysis posed by the introduction of the respective co-chaperones. The reactions were illustrated with representative single exponential curve fits generated in Sigmaplot (version 10.0, Systat Software Inc.).

TABLE 6.3 summarises the ATPase activity approximated from the 10 minute time points of each reaction presented in *FIGURE 6.5.* Activity was expressed in terms of ATP turnover, indicative of the number of ATP molecules hydrolysed per number of Hsp70 molecules per minute.

TABLE 6.3 Steady State Turnover of Basal and Co-chaperone Stimulated HsHsp70 and PfHsp70-Δ ATPase Activity

Hsp70 Protein	Co-chaperone stimulation (1 µM)	% ATP hydrolysed . mg Hsp70^{-1} ± S.D.	Turnover number* ± S.D. (ATP molecules converted . Hsp70 molecules^{-1} . min^{-1})	Turnover (mean fold change)
HsHsp70 (2.125 µM)	None *(basal)*	1.45 (± 0.405)	0.010 (± 0.003)	[1]
	Hlj1	19.74 (N.D.)	0.138 (N.D.)	13.58
	Hsj1a	31.70 (N.D.)	0.222 (N.D.)	21.81
	PfHsp40	34.03 (± 1.266)	0.238 (± 0.009)	23.41
D/PfHsp70-Δ (2 µM)	None *(basal)*	2.00 (± 0.426)	0.014 (± 0.003)	[1]
	Hlj1	17.42 (± 4.059)	0.122 (± 0.028)	8.71
	Hsj1a	18.80 (± 1.032)	0.132 (± 0.007)	9.40
	PfHsp40	14.29 (± 2.821)	0.100 (± 0.020)	6.78
N/PfHsp70-Δ (2 µM)	None *(basal)*	7.75 (± 0.768)	0.099 (± 0.006)	[1]
	Hlj1	35.78 (± 4.846)	0.244 (± 0.034)	2.46
	Hsj1a	34.95 (± 4.057)	0.253 (± 0.032)	2.56
	PfHsp40	36.50 (± 2.513)	0.256 (± 0.018)	2.58

*Turnover values are expressed assuming the monomeric form of the proteins; [1] The fold change in turnover in the presence of co-chaperone stimulation is expressed relative to basal Hsp70 activity; *Basal* refers to basal chaperone activity in the absence of co-chaperone stimulation.

The basal ATPase activity of N/PfHsp70-Δ was observed to be 3.85 fold higher than the corresponding activity of D/PfHsp70-Δ in the *in vitro* steady state assays. Moreover, a higher ATP turnover was achieved for the co-chaperone stimulated N/PfHsp70-Δ ATPase activity (*TABLE 6.3*). This potentially implies a loss in PfHsp70-Δ activity during purification under denaturing conditions, possibly attributed to insufficient refolding of the protein following denaturation with urea as previously suggested (SHONHAI, 2007). Equally it may be argued that the higher ATPase activity of PfHsp70-Δ purified under non-denaturing conditions was a consequence of pre-stimulation by a contaminant in the protein preparation. Silver staining of the non-denaturing and denaturing preparations of PfHsp70-Δ did not reveal significant differences in the co-purification of proteins and truncation products in the respective purifications, and the presence of contaminating prokaryotic Hsp40, DnaJ, was ruled out by Western analysis (*FIGURE 6.3*). However the possibility of stimulation by co-purified peptide fragments cannot be excluded. Such fragments would be released upon the binding of ATP in Hsp70-ATP complex formation, explaining the lower relative N/PfHsp70-Δ basal ATPase activity observed in single turnover (*TABLE 6.2*). Consistent with this, the activity of N/PfHsp70-Δ was shown to be 5.34 fold higher than that of HsHsp70 in steady state; considerably higher than what was observed in single turnover. Moreover, a lower fold change in N/PfHsp70-Δ activity was observed in the co-chaperone stimulated reactions in steady state, although stimulation was achieved to the same order as HsHsp70 with respect to ATP turnover (*TABLE 6.3*). In this context, the importance of comparing non-denaturing preparations of both recombinant HsHsp70 and PfHsp70-Δ becomes apparent.

The ability of PfHsp40 to serve as a co-chaperone of PfHsp70-I was further demonstrated in the steady state ATPase assays described in this study. In general, co-chaperone stimulation was shown for a 2:1 molar ratio of Hsp70 to Hsp40 in the assays, assuming the monomeric form of the respective proteins. The ratio of Hsp70 to Hsp40 *in vivo* in the *P. falciparum* parasite and parasitized human erythrocyte is as yet unknown, however it has been reported that Hsp40 functions in substoichiometric levels to Hsp70 in the prokaryotic system (in a 10:1 ratio of Hsp70 to Hsp40 respectively; BARDWELL *et al*., 1986; PIERPAOLI *et al*., 1998).

Interestingly, the 'background' activity of a DnaK-contaminated non-denaturing preparation of PfHsp40 (*lane 6*, *FIGURE 6.3*) appeared to be roughly equivalent to the steady state co-chaperone stimulated HsHsp70 ATPase activities detailed above in *TABLE 6.3* (corresponding data not shown). This might be indicative of potential stimulation of the ATPase activity of DnaK by PfHsp40 in the steady state reaction. Consistent with this, the observed DnaK-contaminated PfHsp40 activity was significantly higher than the background activity of PfHsp40 alone (denaturing preparation) and the basal ATPase activity of the Hsp70 proteins described in this study. Based on the assumption that PfHsp40 is able to stimulate the chaperone activity of DnaK, the lack of functional interaction between these two proteins in the prokaryotic *E. coli* OD259 complementation system previously described, may have been attributed to insufficient production of PfHsp40 in the heterologous system (refer to *SECTION 5.3.1, CHAPTER 5*). Cautiously though, the stimulation of Hsp70 activity has been described in the presence of excess amounts of Hsp40 following the recognition of the co-chaperone protein as a potential substrate (LAUFEN *et al*., 1999).

6.3.3 Protein Aggregation Suppression Activity Assays

Protein aggregation suppression is achieved by the holdase and refoldase activity of molecular chaperone proteins in the cell. More specifically, chaperone proteins recognise and bind to unfolded polypeptide substrates in a manner that prevents aggregation, and subsequently facilitates protein refolding into the native state. This chaperone activity has been shown *in vitro* with the use of model thermolabile protein substrates (BASHA *et al.,* 2004; GOLOUBINOFF *et al.*, 1999; MOGK *et al.*, 1999). In particular, the aggregation suppression activity of PfHsp70-I has been demonstrated in the absence of a co-chaperone partner (RAMYA *et al.*, 2006; SHONHAI *et al*., 2008). This study explored the ability of PfHsp40 to enhance the aggregation suppression activity of PfHsp70-I and to exert such activity in its own right as a chaperone protein, consistent with its classification as a type I Hsp40 (LU and CYR, 1998b; WALSH et al., 2004).

MDH aggregation suppression was observed in the presence of all of the respective chaperone proteins and partnerships investigated in this study, to varying degrees as illustrated in *FIGURE 6.6*.

A.

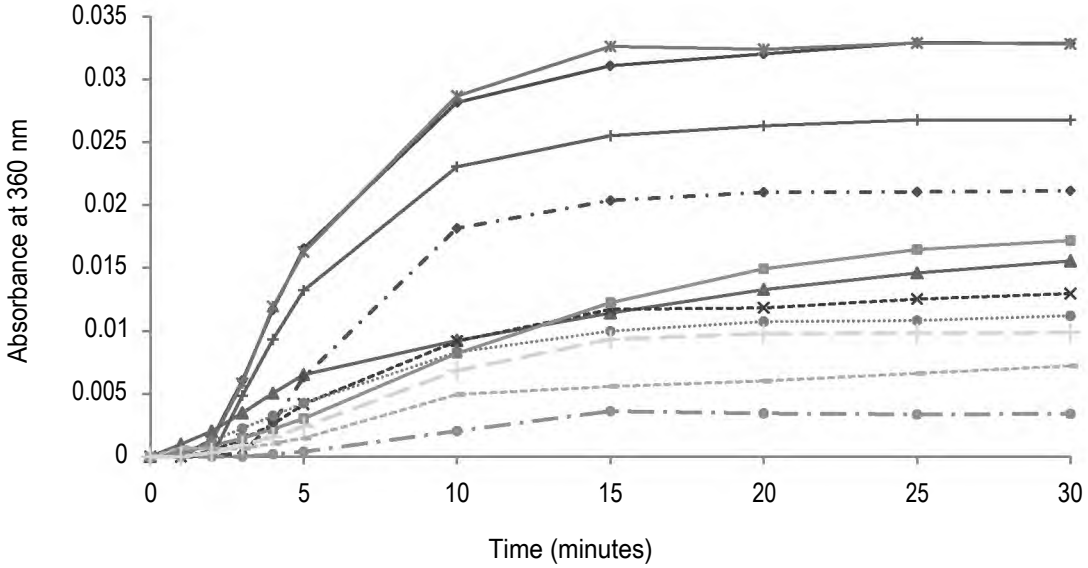

B.

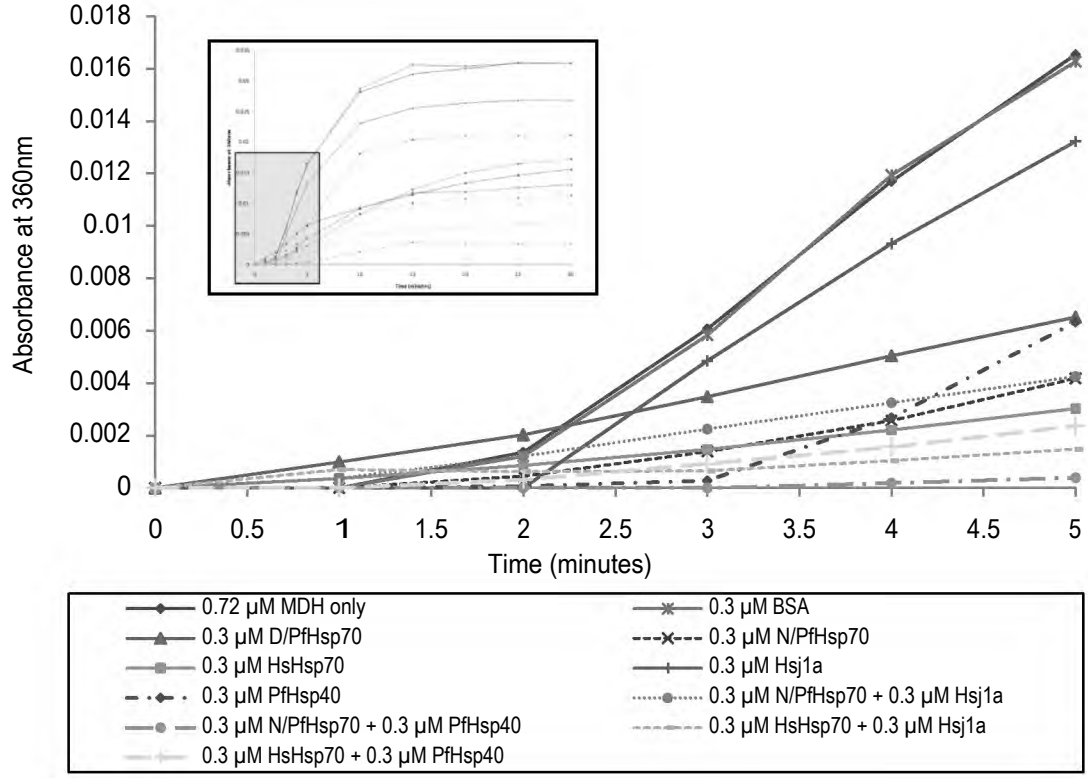

FIGURE 6.6 Suppression of the heat-induced aggregation of MDH by the chaperone activity of recombinant PfHsp70-▮ HsHsp70, Hsj1a and PfHsp40, acting in Hsp70-Hsp40 combination and independently. The heat-induced aggregation of 0.72 µM MDH was monitored at 48°C and 360 nm over time. Suppression of MDH aggregation was observed in the presence of 0.3 µM Hsp40 (Hsj1a and PfHsp40) and 0.3 µM Hsp70 (HsHsp70 and PfHsp70-▮), independently and in varied Hsp70-Hsp40 partnerships as represented for (A) the full reaction time course and (B) the initial reaction lag phase (0-5 minutes) relative to the full time course (inset). PfHsp70-▮purified under non-denaturing and denaturing conditions is denoted as N/PfHsp70-▮ and D/PfHsp70-▮ respectively. Percentage of initial total MDH aggregation observed in the presence of chaperone proteins: BSA control – negligible, D/PfHsp70-▮– 44.6%, N/PfHsp70-▮– 38.2%, HsHsp70 – 44.6%, Hsj1a – 81.6% , PfHsp40 – 64.6%, HsHsp70 + Hsj1a – 20.3% , HsHsp70 + PfHsp40 – 33.5%, N/PfHsp70-▮+ Hsj1a – 33.5%, N/PfHsp70-▮+ PfHsp40 – 10.4%. No aggregation was observed for the chaperone proteins or BSA at 48°C in the absence of MDH (data not shown) indicating thermal stability at this temperature.

FIGURE 6.7 illustrates the percentage of MDH aggregation observed in the presence of the respective chaperone proteins relative to total aggregation observed with MDH alone.

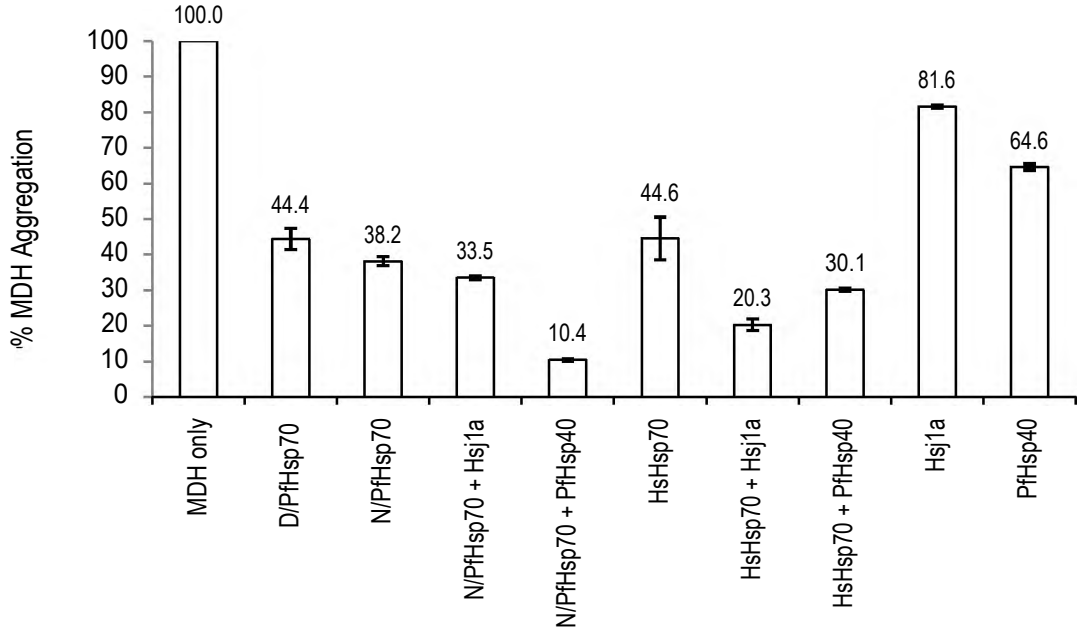

FIGURE 6.7 The percentage of the initial heat-induced MDH aggregation observed in the presence of the recombinant purified chaperone proteins. Percentage aggregation was calculated assuming 100% aggregation of 0.72 µM MDH in the absence of chaperone proteins at saturation (20-30 minutes into the reaction). Chaperone proteins were added to the test experiments at a concentration of 0.3 µM respectively. The presence of 0.3 µM BSA had no effect on MDH aggregation (data not shown) attributing the suppression of MDH aggregation in the test experiments to chaperone protein activity.

PfHsp70-▮purified under non-denaturing conditions was shown to be significantly more efficient at suppressing the thermal aggregation of MDH than PfHsp70-▮purified under denaturing conditions and HsHsp70 at sub-stoichiometric amounts relative to MDH *in vitro* (*FIGURE 6.7*). This is consistent with the argument that PfHsp70-▮exhibited enhanced ATPase activity in the single turnover and steady state ATPase assays (*SECTION 6.3.2.2*). Here, a 61.8% decrease in MDH aggregation has been shown in the presence of a 2.4-fold molar excess of PfHsp70-▮relative to MDH. Previously a 1:2 molar ratio of MDH to PfHsp70-▮was shown to reduce total MDH aggregation by 20% (SHONHAI *et al.*, 2008).

Interestingly, both Hsj1a and PfHsp40 were effective at preventing the thermal aggregation of MDH, albeit to a lesser degree than observed in the presence of Hsp70 protein (*FIGURE 6.7*). This emphasises the ability of Hsp40 proteins to function independently as chaperone proteins in substrate binding (ROSSER and CYR, 2006) but contrasts previous suggestions that type ▮▮ Hsp40 proteins are unable to function independently of Hsp70 in preventing protein aggregation (FAN *et al.*, 2003). PfHsp40 proved more effective than Hsj1a at preventing the thermal aggregation of MDH,

consistent with its classification as a type I Hsp40; the presence of the zinc-binding domain is suggested to enhance chaperone activity through stabilisation of the neighbouring substrate binding domain and its interactions with protein substrate (BANECKI *et al.*, 1996; LINKE *et al.*, 2003; SZABO *et al.*, 1996). It is also possible that differences in certain type I and II Hsp40 substrate binding domains govern different affinities or specificities for protein substrate. In line with this, the *E. coli* type I Hsp40, DnaJ, has been shown to suppress the aggregation of denatured rhodanese independently and in co-operation with DnaK, while the *E. coli* type II Hsp40, CbpA, has been shown to function with DnaK to this effect, but not independently (CHAE *et al.*, 2004). Interestingly, the ability of CbpA to functionally replace DnaJ *in vivo* has been demonstrated despite these differences (UEGUCHI *et al.*, 2005). Similarly, the *S. cerevisiae* type I Hsp40, Ydj1, has been shown to suppress protein aggregation (CYR, 1995) while the *S. cerevisiae* type II Hsp40, Sis1, is thought to lack this ability (LU and CYR, 1998b). Moreover, the human type II Hsp40, DnajB1 (Hdj1), may co-operate with Hsp70 but cannot act independently to prevent protein aggregation (FREEMAN and MORIMOTO, 1996). Importantly, SCHNAIDER *et al.* (2000) have demonstrated the ability of the Hsj1a-related human type II Hsp40, Hsj1b (DnaJB2 isoform b) to prevent the aggregation of rhodanese. This serves to support the MDH aggregation suppression observed in the presence of Hsj1a in this study (*FIGURE 6.7*).

As previously detailed, the Hsp70 peptide binding pocket is proposed to bind the backbones and side-chains of exposed hydrophobic residues of peptide substrates in a manner that is conducive to folding. In contrast, Hsp40 is suggested to bind only the exposed hydrophobic side-chains of substrates in a manner that facilitates substrate selection and transfer to Hsp70 (RÜDIGER *et al.*, 1997, 2001). From the lag phase of the reactions in this study, the Hsp40 proteins appear to exert their aggregation suppression activity via a different mechanism to Hsp70, with rapid suppression and apparent release of MDH after 2 and 3 minutes into the start of the reaction (*FIGURE 6.6B*). In contrast, the Hsp70 proteins appeared to demonstrate gradual and improved overall MDH aggregation suppression. This is consistent with the notion that Hsp40 proteins function as holdases with the ability of delivering client protein to Hsp70 for refolding while Hsp70 proteins bind client protein with the ability to exert both holdase and refoldase activity.

Interestingly, the presence of 0.3 µM Hlj1 appeared to enhance protein aggregation (data not shown). The recombinant Hlj1 protein was not observed to aggregate in the absence of MDH however, implying that co-aggregation was promoted by illegitimate binding to MDH. Certain type III Hsp40s exhibit an inability to bind protein substrate in a legitimate manner, attributed to the lack of a conserved Hsp40 substrate binding domain (WALSH *et al.*, 2004). Recombinant Hlj1 thus served as a negative control in this experiment, attributing the observed holdase activity of PfHsp40 and Hsj1a to action exerted by their substrate binding domains.

Notably, PfHsp70-1 and HsHsp70 were able to associate with protein substrate independently of co-chaperone protein, although the presence of equimolar amounts of the latter appeared to enhance MDH aggregation suppression. The investigated homologous Hsp70-Hsp40 partnerships were able to suppress the aggregation of MDH more effectively than the corresponding heterologous partnerships (*FIGURES 6.6* and *6.7*). More specifically, Hsj1a was shown to function more efficiently in combination with HsHsp70 in the prevention of MDH aggregation, and by the same token PfHsp40 was shown to function more effectively in combination with PfHsp70-1. These differences suggest that the Hsp70 and Hsp40 proteins co-operated in partnership to reduce MDH aggregation, as opposed to acting collectively as independent chaperones. This is envisaged to have involved the capture of unfolded protein substrate by Hsp40 and subsequent delivery to Hsp70 for aggregation prevention and refolding as discussed. Hsp40 proteins may only function with select Hsp70 proteins in protein aggregation prevention, as implied by the co-operation of Ydj1 with Ssa but not Ssb Hsp70 proteins to this effect in *S. cerevisiae* (CYR, 1995). Importantly, the co-operation of PfHsp70-1 and PfHsp40 in the suppression of protein aggregation lends itself as additional evidence for the interaction of these proteins *in vivo* in the *P. falciparum* parasite.

The lower efficiency of the demonstrated heterologous partnerships at preventing the thermal aggregation of MDH contrasts to what was observed in the ATPase assays. It has been proposed that efficient co-chaperone regulation and productive interaction with Hsp70 involves the appropriate coupling of ATP hydrolysis stimulation and client protein presentation and transfer (HENNESSY *et al*., 2005). It is therefore possible that the high degree of stimulation of PfHsp70-1 by Hlj1 and Hsj1a observed in single turnover represents inappropriate stimulation of chaperone activity not efficiently coupled to substrate capture. Based on this assumption, the *in vitro* enhancement of Hsp70 interaction with protein substrate better signifies appropriate co-chaperone regulation. Importantly, the treatment of the two processes of co-chaperone regulation as isolated and independent processes represents a drawback of the employed *in vitro* assays. Recently, a more suitable fluorescence polarization assay was developed and used in the simultaneous assessment of the ATP hydrolysis and substrate binding activity of human Hsp70 (KANG *et al*., 2008).

Substrate specificity is of importance in the selection of model thermolabile substrates for the characterisation of aggregation suppression activity. BOSHOFF *et al.* (2008) reported that *A. tumefaciens* DnaJ had no effect on MDH aggregation or on the ability of the corresponding prokaryotic Hsp70, DnaK, to bind MDH. In contrast to this, the corresponding *E. coli* DnaJ has been shown to suppress the aggregation of denatured rhodanese (CHAE *et al*., 2004). This highlights the need for an assessment of the detailed heterologous and homologous human and malaria Hsp70-Hsp40 partnerships with alternative thermolabile substrates, to demonstrate true differences in

aggregation suppression activity independent of substrate specificity. With this, the considerable diversity in the substrate binding domains of the Hsp40 proteins of *P. falciparum* becomes an important consideration (*CHAPTER 2*). The potential ability of the exported *P. falciparum* Hsp40 proteins to bind and transfer parasite protein substrate to HsHsp70 is of interest and remains to be assessed.

It must also be noted that the aggregation suppression assays described in this study were conducted without the removal of endogenous ATP. This may have affected the activity of the respective chaperone proteins and partnerships investigated. For unequivocal comparison of the ability of these proteins to suppress the thermal aggregation of MDH, the *in vitro* assays remain to be conducted in an ATP-independent manner and in the presence of a known concentration of ATP.

6.3.4 The Effect of Small Molecule Modulators on Hsp70 ATPase Activity

The effect of the small molecule modulators DMT002264 and MAL3-39 on the ATPase activity of HsHsp70 and PfHsp70-I in single turnover and steady state ATPase assays as illustrated in *FIGURE 6.8* overleaf. From the curve fits for the single turnover assays and the ATP turnover numbers calculated from the steady state assays, the fold change in the basal and co-chaperone stimulated ATPase activity of HsHsp70 and PfHsp70-I was calculated relative to that observed in the absence of compound. The fold change in ATPase activity for each reaction performed in single turnover and steady state is presented in *TABLE 6.4*.

TABLE 6.4 Effect of Small Molecule Modulators MAL3-39 and DMT002264 on the Basal and Co-chaperone-Stimulated ATPase Activity of HsHsp70 and PfHsp70-I in Steady State and Single Turnover

Small molecule modulator	Co-chaperone stimulation	HsHsp70			PfHsp70-I		
		Steady state		Single turnover	Steady state		Single turnover
		Turnover[1]	Fold Change[2]	Fold Change[3]	Turnover[1]	Fold Change[2]	Fold Change[3]
None	*Basal*	0.011	[1]	-	0.084	[1]	-
	Hlj1	0.138	[1]	[1]	0.284	[1]	[1]
	Hsj1a	0.222	[1]	[1]	0.232	[1]	[1]
MAL3-39	*Basal*	0.008	0.722	-	0.058	0.691	-
	Hlj1	0.092	0.667	1.198	0.183	0.644	0.940
	Hsj1a	0.152	0.685	1.146	0.163	0.703	1.071
DMT002264	*Basal*	0.018	1.637	-	0.100	1.187	-
	Hlj1	0.167	1.210	1.238	0.255	0.898	0.999
	Hsj1a	0.229	1.030	1.199	0.241	1.039	1.048

[1] Turnover is defined as the number of ATP molecules hydrolysed per enzyme molecules per minute ($_{-1}$). [2] (ATP molecules hydrolysed . Hsp70 molecules^{-1} . min^{-1}) derived from the 10 minute time point of each reaction. [3] Fold change in turnover in steady state; Fold change in single turnover represents the change in the rate of ATP hydrolysis, derived from the slope of curve fit of each reaction; A fold change of [1] indicates that ATPase activity has been adjusted to a value of 1.0 to serve as a reference; *Basal* refers to chaperone activity in the absence of co-chaperone stimulation.

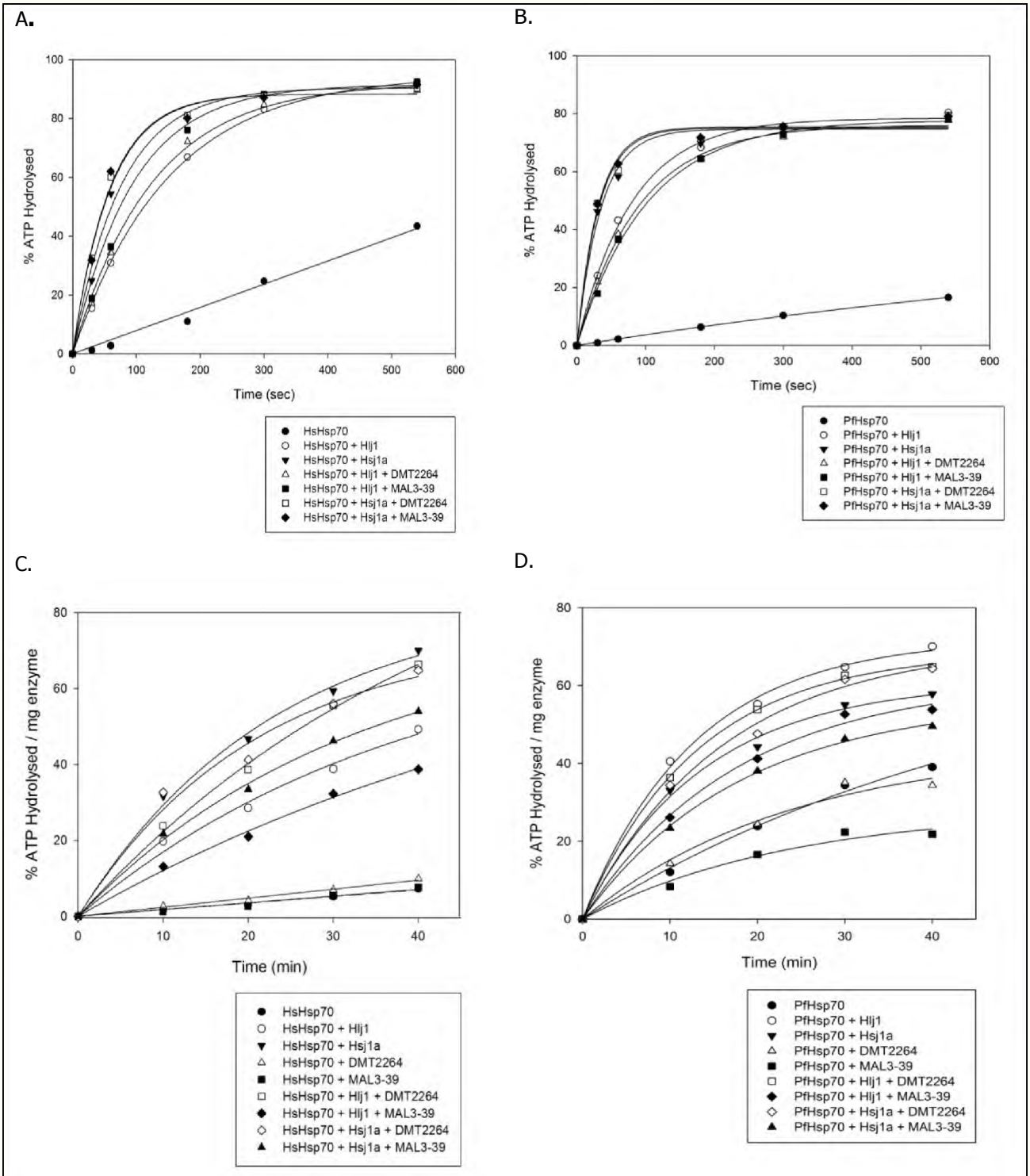

FIGURE 6.8 Assessment of the ability of MAL3-39 and DMT002264 to modulate the basal and co-chaperone stimulated ATPase activity of HsHsp70 and PfHsp70-I. The effects of the compounds on Hsp70 activity was assessed in (A-B) single turnover and (C-D) steady state. In single turnover, co-chaperone stimulation was achieved with 0.55 µM Hlj1 and 0.3 µM Hsj1a respectively in the presence of 300 µM of each respective compound. The reactions were represented as single exponential curve fits $[ADP_t] = [ADP_{max}](1-e^{-k1t})$, except for the Hsj1a-stimulated Hsp70-ATPase activity which was best represented by the exponential process $[ADP_t] = [ADP_{max1}](1-e^{-k1t}) + [ADP_{max2}](1-e^{-k2t})$. In steady state assays, the stimulation of 2.125 µM HsHsp70 and 2 µM PfHsp70-I was achieved with 1 µM of Hlj1 or Hsj1a in the presence of 300 µM of each respective compound. The reactions were represented as single exponential processes. Representative curve fits were generated in Sigmaplot (version 10.0, Systat Software Inc.) and verified using KaleidaGraph (version 3.0.4, Synergy Software). In the figure keys "DMT2264" denotes compound DMT002264 and "PfHsp70" denotes N/PfHsp70-I

MAL3-39 induced an apparent inhibition of the ATPase activity of both HsHsp70 and PfHsp70-1, independently of co-chaperone stimulation in steady state. In line with this, the compound had no effect on the co-chaperone stimulation of the ATP hydrolysis step of either Hsp70 protein in single turnover. This implies that the compound acted on another stage of the ATPase cycle or interacted with HsHsp70 and PfHsp70-1 in a manner that did not impact on the ability of either protein to hydrolyse ATP or interact with Hsp40. MAL3-39 did not act as a specific modulator of PfHsp70-1 activity, due to its failure to differentiate between the parasite and human Hsp70 proteins or co-chaperone stimulation of these proteins. Interestingly, MAL3-39 was previously shown to inhibit Hsp70 stimulation by the J-domain containing large T antigen (TAg) of the simian virus 40 (SV40), but not of the yeast Hsp40, Ydj1p (FEWELL *et al*., 2004). This highlights the potential for exploiting varied mechanisms of Hsp40 stimulation of Hsp70 for the discovery of more specific small molecule modulators. This is of importance considering the proposed conserved mechanism of Hsp70-Hsp40 interaction in *P. falciparum* as is encountered in the human host. Importantly, the effect of MAL3-39 on PfHsp40 stimulation of PfHsp70-1 activity remains to be assessed; this study was hindered by problems relating to the production and purification of sufficient quantities of PfHsp40. It remains to be established whether PfHsp40 exhibits a different mechanism of Hsp70 stimulation to that of its human counterparts. Hsj1a appeared to exert its chaperone activity via a different mechanism in the single turnover ATPase assays (*FIGURE 6.4; SECTION 6.3.2.1*) although it would be more valuable to compare the activity of PfHsp40 to that of a human type I Hsp40 such as DnaJA1.

In contrast, DMT002264 showed distinction between HsHsp70 and PfHsp70-1 through mild enhancement of the ATPase activity of HsHsp70 in steady state. This enhancement was reduced in the presence of co-chaperone regulation; however the compound showed no significant effect in single turnover. Enhancement of the ATPase activity of the yeast Hsp70, Ssa1p, by DMT002264 has been described (WRIGHT *et al*., 2008). The distinction between Hsp70 proteins highlights the potential for discovering small molecule modulators specific to diminishing the activity of PfHsp70-1 only.

Notably, significantly high concentrations of the test compounds were utilised in this study (300 µM); while this serves the purpose of high-throughput screening for the identification of 'hit' compounds that may subsequently be modified for more effective inhibition, this concentration is not as appropriate for the purposes of initial chaperone protein kinetic analyses. In further critique of this work, it is questionable as to whether the presence of 50 µM ATP was sufficient to represent saturating concentrations in the steady state ATPase assays employed. This concentration was utilised for consistency with that previously reported for steady state ATPase assays performed in the presence of small molecule modulators (WRIGHT *et al*., 2008; refer to SECTION 6.3.4). It would be of

value to repeat the steady state ATPase assays performed in the absence of test compounds (*SECTION 6.3.2.2*) with increased concentrations of the unlabelled ATP in the reactions to verify the determined ATP turnover for PfHsp70-▮in particular.

6.4 CONCLUSIONS

In this study, evidence for a functional Hsp70-Hsp40 interaction of the *P. falciparum* parasite has been demonstrated, with the interaction between PfHsp70-▮ and PfHsp40. The effect of this partnership on the stimulation of the activity of PfHsp70-▮was established in the context of ATP hydrolysis and interaction with heterologous protein substrate. Placed in context with results from the prior localisation studies in *CHAPTER 4*, the interaction between PfHsp70-▮ and PfHsp40 demonstrated *in vitro* lends itself as evidence for the existence of this chaperone partnership *in vivo*. This established interaction, together with the established human Hsp70-Hsp40 partnership between human Hsp70 and Hsj1a, constitutes a platform for the further screening and discovery of small molecule modulators specific to the parasite chaperone proteins and interactions. Moreover, the potential for heterologous partnerships between the human and parasite chaperone proteins has been substantiated, and similarly remains to be assessed in depth. In particular, future work includes further substantiation of the partnership between PfHsp70-▮ and PfHsp40 in the *P. falciparum* parasite, as discussed further in *CHAPTER 7*.

It is well known that *P. falciparum* undergoes significant exposure to heat shock in the intraerythrocytic or fever stages associated with malaria, consequently resulting in the upregulation of heat shock protein expression (BISWAS and SHARMA, 1994; OAKLEY *et al.*, 2007). The efficient chaperone activity of PfHsp70-▮ contrasted to the HsHsp70 activity *in vitro*, could represent an adaptation to the requirements of a parasitic lifestyle. High protein folding and processing turnover could be consistent with the numerous structural and functional changes necessitated by such intracellular parasitism as described by NYALWIDHE *et al.* (2003) and others, underlining the appropriateness of the use of the parasite's heat shock proteins as candidate drug targets. This study has demonstrated the potential to screen for small molecule modulators capable of differentiating between human and parasite Hsp70 proteins and their co-chaperone regulation by homologous Hsp40 partners. This has been demonstrated in the context of two small molecule modulators sourced from a library of compounds that remain to be screened in the established model parasite and host comparative chaperone systems described here. Importantly, the apparent conservation of the Hsp70-Hsp40 mechanism of interaction in *P. falciparum* raises implications for the future screening of small molecule modulators specific to the interactions and activities of the parasite chaperone systems. The established PfHsp70-▮PfHsp40 partnership serves as a good basis

for such screening, as it has the potential to promote the identification of inhibitors specific to *P. falciparum* substrate binding and substrate transfer. Previously the effect of 15-deoxyspergualin (DSG) on the binding of PfHsp70-I to a model substrate was assessed in the absence of co-chaperone stimulation (RAMYA *et al*., 2006).

As previously discussed in *CHAPTER 3*, the heterologous expression of many *P. falciparum* proteins has proved challenging for numerous reasons. Approaches to the enhanced heterologous expression and folding of target proteins by the co-expression of chaperone proteins have been described (BANEYX and PALUMBO, 2003; DE MARCO and DE MARCO, 2004; THOMAS *et al*., 1997). BOSHOFF *et al.* (2004) have proposed the appropriateness of using homologous chaperone systems for such purposes, given that chaperones are evolutionarily paired to their client substrate proteins. The established PfHsp70-I-PfHsp40 partnership may thus be exploited for the enhancement of the heterologous expression and subsequent purification of *P. falciparum* proteins. This may serve to aid the characterisation of malarial proteins flagged as potential vaccine or drug target candidates.

CHAPTER 7:

CONCLUSIONS AND FUTURE PERSPECTIVES

7.1 CONCLUDING REMARKS

7.1.1 Insight into the Co-chaperone Regulation of the P. falciparum Hsp70, PfHsp70-

The research detailed in this dissertation has attempted to address the lack of knowledge pertaining to the co-chaperone regulation of the highly abundant and potentially cytoprotective *P. falciparum* Hsp70 protein, PfHsp70-. The characteristic Hsp40 protein, PfHsp40, and the larger, atypical Hsp40 protein, Pfj1, represent the only two type Hsp40 proteins of the parasite, and are thus the most likely candidates for the accomplishment of this co-chaperone regulation. To motivate for this, the co-chaperone properties of PfHsp40 and Pfj1 were elucidated as further discussed.

7.1.1.1 The Co-chaperone Properties of the Prototypical Type Hsp40, PfHsp40

Recombinant PfHsp40 was successfully isolated following production from a codon-harmonized synthetic gene in a prokaryotic heterologous expression system. The ability of the protein to co-chaperone the activity of PfHsp70- was demonstrated in *in vitro* assays including single turnover and steady state ATPase assays, and protein aggregation suppression assays with a model thermolabile substrate. PfHsp40 was able to enhance the ATPase and aggregation suppression activity of PfHsp70- *in vitro*, supporting the potential for interaction between these proteins *in vivo*. Moreover, PfHsp40 was shown to demonstrate thermal stability and exhibit aggregation suppression activity in its own right, suggesting that this protein may contribute to the cytoprotection of the *P. falciparum* parasite independently and through specific co-operation with PfHsp70-. In particular, this cytoprotective role may be pertinent to the intraerythrocytic stages of *P. falciparum* development, as suggested for other chaperone proteins such as PfHsp90 and PfHsp70- (BANUMATHY *et al*., 2003; PAVITHRA *et al*., 2004, 2007). Consistent with this, PfHsp40 was detected in the parasite cytoplasm in cultured *P. falciparum*-infected erythrocytes by immunofluorescence staining, validating the gene expression profile predicted for the protein from transcriptomic analyses (LE ROCH *et al*., 2003). This distribution was shown to overlap with that of PfHsp70- in heat shock and non-heat shock conditions, contributing additional rationale to the notion that PfHsp70- and PfHsp40 may co-operate in constitutive, stress-related and/or stage-specific protein folding and assembly tasks *in vivo*. Moreover, the cytoplasmic distribution of PfHsp40 is consistent with the parallels drawn between this protein and analogous cytoplasmic type Hsp40 proteins of eukaryotic origin. More specifically, PfHsp40 may undergo post-translational farnesylation at the C-terminal CAAX-box motif, allowing the protein to associate with the cytosolic face of organellar membranes to facilitate protein translocation. This modification may also serve to connect PfHsp40 to the PfHsp90/PfHsp70- complex identified in the parasite (BANUMATHY *et al*., 2003) as recently described for the analogous type Hsp40, Ydj1 in *S. cerevisiae* (FLOM *et al*., 2008). Placed together with *in silico* bioinformatics

analyses, the findings presented in this work support the notion that PfHsp40 most likely facilitates standard 'house-keeping' processes in the *P. falciparum* parasite as a chaperone in its own right and as a presumed co-chaperone partner of PfHsp70-I. Importantly, the proposed interaction between PfHsp70-I and PfHsp40 represents the most apparent 'house-keeping' Hsp70-Hsp40 partnership in the *P. falciparum* parasite, as typified by DnaK-DnaJ in *E. coli*, Ssa1-Ydj1 in *S. cerevisiae*, and HspA1A-DnaJB2 in *H. sapiens*.

7.1.1.2 The Co-chaperone Properties of the Atypical Type I Hsp40, Pfj1

The co-chaperone abilities of the atypical type I Hsp40 protein, Pfj1, were investigated using an *in vivo* prokaryotic complementation system. The functionality of the lesser-conserved J-domain of Pfj1 was demonstrated by its ability to replace the equivalent domain of *A. tumefaciens* DnaJ, in interactions with DnaK in the thermosensitive *dnaJ cbpA E. coli* OD259 strain. Considering that the J-domain defines the Hsp40 protein class and represents the minimum requirement for interaction with Hsp70, the functionality of the Pfj1 J-domain in the prokaryotic system served to substantiate the co-chaperone abilities of this protein. Importantly, this *in vivo* assay system provided a platform from which to explore the co-chaperone properties of Pfj1, which was otherwise not possible due to the recalcitrance of the recombinant Pfj1 protein to heterologous production and isolation. Placed together with the previously demonstrated functional equivalence of PfHsp70-I and *E. coli* DnaK in a prokaryotic system (SHONHAI *et al*., 2005), the ability of the Pfj1 J-domain to exhibit specific interactions with DnaK may suggest its ability to interact with PfHsp70-I by the same token. In line with this, rational site-directed mutagenesis studies alluded to the conservation of key elements in the Pfj1 J-domain for interaction with Hsp70 partner proteins. More specifically, elements of helix II and the invariant HPD-motif appeared to constitute the Hsp70 interaction interface of the J-domain, while residues of helix III appeared to uphold the functional or structural integrity of the domain. Residues of helix IV of the Pfj1 J-domain appeared to mediate the specificity or affinity of interaction with Hsp70. These findings are consistent with analogous studies performed on classical J-domains (GENEVAUX *et al*., 2002; HENNESSY *et al*., 2005a). Likewise, multiple protein sequence alignments and homology modelling revealed the conservation of Hsp40-interaction residues in PfHsp70-I. The preservation of Hsp70-Hsp40 interaction residues in PfHsp70-I and Pfj1 motivates for a functional chaperone partnership between these proteins in the *P. falciparum* parasite. In further support of this proposed partnership, the localisation patterns of PfHsp70-I and Pfj1 were shown to overlap in this work, with distribution to the parasite cytoplasm and nucleus in intraerythrocytic-stage parasites in heat shock and non-heat shock conditions. The distribution of both proteins was shown to shift from the nucleus of the developing merozoite-stage during the intraerythrocytic progression of the

parasite's lifecycle, alluding to more divergent or specialised stage-specific protein folding and assembly roles for this prospective Hsp70-Hsp40 partnership.

7.1.2 Consequences for the Conserved Mechanism of Hsp70-Hsp40 Interaction in P. falciparum

The findings detailed in this work have provided evidence for the conservation of the prototypical mode of J-domain based Hsp40 interaction with Hsp70 in *P. falciparum*, as previously elucidated for characterised Hsp70-Hsp40 associations in other organisms. This was deduced from the functionality of the Pfj1 J-domain in substitution of the J-domain of *Agt* DnaJ in the prokaryotic *in vivo* complementation system described above, and by the observation that Pfj1 exerted its functionality by a conserved HPD-motif mediated interaction in this system. The conservation of the mode of Hsp70-Hsp40 interaction in the *P. falciparum* parasite was further alluded to by the functional interchangeability of human and parasite Hsp70 and Hsp40 proteins in the *in vitro* ATPase and protein aggregation suppression assays detailed in this work. Specifically, the functional heterologous partnerships demonstrated *in vitro* between PfHsp70-I and the human Hsp40, Hsj1a, and between the human Hsp70, HspA1A, and PfHsp40, implied the existence of a common mode of interaction. While this deduction substantiates the potential for heterologous partnerships between human Hsp70 and the HPD-bearing exportome Hsp40 proteins of the parasite in the infected erythrocyte cytoplasm, it also questions the appropriateness of the use of the parasite's Hsp70-Hsp40 partnerships as specific anti-malarial targets. Nevertheless, small molecule modulators capable of distinguishing between Hsp70 homologs have been identified in this study and others (BRODKY and CHIOSIS, 2006; FEWELL *et al.*, 2004). Moreover, the model homologous and heterologous human and parasite Hsp70-Hsp40 partnerships established in this study serve as a foundation from which to identify small molecule modulators specific to parasite chaperone activity and co-chaperone regulation. Notably, PfHsp40 represents the only typical type I Hsp40 protein of *P. falciparum*, making it possible to surmise that the specific inhibition or knockout of this protein would have severe consequences for the viability of the parasite.

On a different note, the significant divergence of the complete Hsp70-Hsp40 network of *P. falciparum* leaves much to be explored in terms of drug discovery. In particular, the parasite appears to have evolved a highly diverse and specialised Hsp40 complement of forty-three member proteins, which may be sub-divided into the more conserved, parasite-resident proteins and the lesser-conserved, exportome proteins. The non-HPD bearing exportome Hsp40 proteins appear to be unique to *P. falciparum*, with an apparent absence of homologs in the human host and related apicomplexan parasites. Intriguingly, the absence of a conserved HPD motif in these newly categorised type IV Hsp40 proteins suggests that they exert their functionality via an alternative

mechanism to that of the prototypical J-domain based interaction with Hsp70. This, placed together with the proposed participation of these proteins in erythrocyte remodelling, places these proteins as prime candidates to serve as novel anti-malarial targets.

7.2 APPROACHES TO FUTURE WORK

7.2.1 Hsp70-Hsp40 Protein Interaction Studies

7.2.1.1 In Vitro Protein-Protein Binding Assays

Future work is aimed at further substantiating the association of PfHsp70-I with PfHsp40 and Pfj1 with binding experiments. Attempts to authenticate these partnerships *in vivo* in *P. falciparum* with immunoprecipitation experiments were unsuccessful in this work as a result of the non-specific binding of PfHsp70-I in the appropriate negative controls. This problem was recurrent in *in vitro* pull-down assays using recombinant purified PfHsp70-I and PfHsp40. Further complicating to this, the non-specific binding of the target proteins in the appropriate negative controls of these assays appeared to be unaffected by the presence of absence of ATP. The efforts to detect an association between PfHsp70-I and the Hsp40 proteins of interest thus remain to be optimised, and may only prove effective if the proposed interactions are not too transient for detection, and are not plagued by the recognition of Hsp40 as a substrate by Hsp70 in these systems. Transient 'on-off' Hsp70-Hsp40 associations may be detected more effectively in *in vitro* protein-protein binding studies using available biosensor technology, such as Quartz Crystal Microbalance with Dissipation (QCMD). In this manner, the binding kinetics of the proposed Hsp70-Hsp40 associations may be investigated simultaneously, for insight into the nature of these proposed partnerships and the manner in which they differ to analogous partnerships in other organisms.

7.2.1.2 In Vivo Protein Interaction Systems

An alternative approach to the assessment of the ability of PfHsp70-I to interact with PfHsp40 or Pfj1 involves the use of an *in vivo* Green Fluorescent Protein (GFP) Fragment Reassembly Trap system, developed by MAGLIERY *et al*. (2005). In this system, the proteins of interest are expressed in *E. coli* as fusion proteins fused to the two respective halves of GFP, which are brought together upon the successful interaction of the target proteins to elicit a fluorescent signal. The cloning of the coding regions of the PfHsp70-I, PfHsp40 and Pfj1 into the appropriate vectors for this system has been initiated. The similar employment of a fluorescence-based protein-protein interaction system in a mammalian cell line may also be considered. Alternatively, yeast two-hybrid analyses may be employed as described by LACOUNT *et al.* (2005) to explore the proposed Hsp70-Hsp40 partnerships.

7.2.2 Studies in the Homologous System

7.2.2.1 Assessment of Protein Expression Upregulation in P. falciparum in Response to Heat Shock

For further substantiation of the potential of PfHsp70-1 and the type II Hsp40 proteins of interest to interact, it remains to be confirmed whether their corresponding patterns of transcriptional upregulation in prior transcriptomic studies (BOZDECH *et al*., 2003; LE ROCH *et al*., 2003) translate into similar patterns of expression upregulation in synchronised *P. falciparum*-infected erythrocyte cultures and particularly, in response to heat shock.

7.2.2.2 Alternative Approaches to Localisation Studies

This work has described the use of immunochemical techniques to assess the presence and localisation of PfHsp40 and Pfj1 relative to PfHsp70-1 in the intraerythrocytic stages of *P. falciparum* development. Notably, the anti-PfHsp40 and anti-Pfj1 peptide-directed antibodies developed in this work were raised in the same organism as that of the anti-PfHsp70-1 antibody, therefore it was not possible to perform Hsp70-Hsp40 co-localisation studies. Future efforts therefore include the design, synthesis and use of alternative antibodies for such co-localisation experiments. Antibodies directed against the full length target proteins or the Hsp40 domains downstream of the highly conserved J-domain may be considered for future experiments. However, this carries the risk of antibody cross-reactivity considering the high degree of conservation among Hsp40 proteins. This accounts for the initial approach of peptide-directed antibody design and synthesis detailed in this work.

An assessment of the localisation of PfHsp70-1, PfHsp40 and Pfj1 relative to additional established Maurer's cleft and/or parasitophorous vacuole marker proteins also remains to be performed. These marker proteins may include the *P. falciparum* membrane-associated histidine-rich protein-1 (MAHRP-1; SPYCHER *et al*., 2003) or members of the *P. falciparum* two transmembrane Maurer's cleft protein family (PfMC-2TM; SAM-YELLOWE *et al*., 2004) in the Maurer's clefts, and *P. falciparum* serine-rich protein (PfSERP-1; ANSORGE *et al*., 1996; NYALWIDHE *et al*., 2002) or *P. falciparum* parasitophorous vacuole protein (PfPV-1; NYALWIDHE and LINGELBACH, 2006) in the parasitophorous vacuole.

The transfection of *P. falciparum* parasites with GFP-fusion constructs encoding the Hsp40 proteins of interest represents an independent means of assessing the localisation of the target proteins in the malaria parasite. The choice of promoter control for this system may be of critical importance as revealed by RUG *et al*. (2004) for the RESA protein. With this in mind, efforts may be focussed on identifying the endogenous promoters of PfHsp40 and Pfj1 from the *P. falciparum* genome, to drive the appropriate expression of these proteins in transfected cells. In critique of this approach to localisation studies, GFP represents a relatively large fusion-tag that may inadvertently alter the

distribution of the target proteins. Nevertheless, this strategy represents a highly appropriate means of validating the localisation results obtained from immunochemical techniques. Moreover, this approach may be applied to live cell imaging studies, to provide insight into the potentially dynamic roles and distribution patterns of the heat shock proteins of interest in the *P. falciparum* parasite in response to heat shock or other stage- or condition-specific variables.

7.2.3 In Vivo Complementation Assays in a Thermosensitive S. cerevisiae Strain

The functionality of PfHsp40 and Pfj1 remain to be assessed in *in vivo* complementation assays in the thermosensitive *S. cerevisiae* strain *ydj1* JJ160 (JOHNSON and CRAIG, 2000). Of particular interest is the potential of the CAAX-box bearing PfHsp40 protein to functionally replace the equivalent type I Hsp40, Ydj1, in this complementation system. Rational site-directed mutagenesis may be employed to explore the functionality of select PfHsp40 and Pfj1 residues if the proteins are found to be functional in this eukaryotic system. A domain approach to the assessment of the functionality of the Hsp40 proteins in this system may also be considered. Notably, these experiments rely on the re-design and -synthesis of the coding regions of PfHsp40 and Pfj1 to account for the codon usage preference of *S. cerevisiae*.

7.2.4 Additional Approaches to the Production and Isolation of Recombinant PfHsp40 and Pfj1

Future work also includes the use of alternative approaches to the isolation of the recombinant Hsp40 proteins of interest, such as: (i) the use of an alternative expression system such as yeast, mammalian or baculovirus/insect cell lines, which may satisfy post-translational modification requirements if any, (ii) the use of alternative fusion-tag vector systems, such as those encoding maltose binding protein (MBP)- or glutathione S-transferase (GST)-fusion proteins, (iii) a domain approach to the isolation and characterisation of PfHsp40 and Pfj1. Notably, these approaches may rely on the re-design and -synthesis of the coding regions of these proteins to cater for the codon usage preference of the heterologous system of choice. In particular, the isolation of recombinant Pfj1 is crucial to the elucidation of a partnership with PfHsp70-I in *in vitro* characterisation assays.

7.2.5 Applications of the Established PfHsp70-I-PfHsp40 Partnership

7.2.5.1 Screening of Small Molecule Modulators

Future prospects include the high throughput screening of a library of small molecule modulators for the identification of 'hit' compounds capable of specifically modulating the established partnership between PfHsp70-I and PfHsp40. In addition to assessing the effect of these modulators on the activity of this partnership in *in vitro* ATPase assays, the effect of these compounds on the

aggregation prevention activity of PfHsp70-I and PfHsp40 remains to be determined in *in vitro* protein aggregation suppression assays.

7.2.5.2 Protein Expression Enhancement in Co-expression Systems

The established partnership between PfHsp70-I and PfHsp40 may also be exploited in future efforts to promote the successful expression and isolation of other *P. falciparum* proteins in heterologous co-expression systems. The design and establishment of an appropriate system for these purposes is currently under consideration.

7.2.6 The Possibility of Other Hsp70-Hsp40 Combinations?

Notably, the *P. falciparum* genome encodes only two type I Hsp40 proteins relative to six Hsp70 homologs. In this work, the focus has been placed on elucidating partnerships between these type I Hsp40 proteins and the most abundant and well characterised Hsp70 homolog of the parasite, PfHsp70-I However, it is of importance to establish whether PfHsp40 or Pfj1 may co-operate with other Hsp70 homologs such as PfHsp70-x in protein-folding and translocation tasks in the parasite. Moreover, Hsp70 partners and roles remain to be established for the remaining 41 members of the *P. falciparum* Hsp40 complement described in this work. In particular, the roles of the putative parasite-resident type II Hsp40 protein encoded by PFB0595w (termed PfSis1 in this work) may prove crucial to the regulation of Hsp70 activity in the parasite, as predicted for PfHsp40.

ABRAHAMSEN, M.S., TEMPLETON, T.J., ENOMOTO, S., ABRAHANTE, J.E., ZHU, G., LANCTO, C.A., DENG, M., LIU.C, WIDMER, G., TZIPORI, S., BUCK, G.A., XU, P., BANKIER, A.T., DEAR, P.H., KONFORTOV, B.A., SPRIGGS, H.F., IYER, L., ANANTHARAMAN, V., ARAVIND, L. and KAPUR, V. (2004). Complete genome sequence of the apicomplexan, *Cryptosporidium parvum*. *Science*, 304, 441-445.

ABRAVAYA, K., MYERS, M.P., MURPHY, S.P. and MORIMOTO, R.I. (1992). The human heat shock protein hsp70 interacts with HSF, the transcription factor that regulates heat shock gene expression. *Genes and Development*, 6, 1153-1164.

ADAMS, S., BROWN, H. and TURNER, G. (2002). Breaking down the blood-brain barrier: signalling a path to cerebral malaria? *Trends in Parasitology*, 18, 360-366.

ADISA, A., RUG, M., KLONIS, N., FOLEY, M., COWMAN, A.F. and TILLEY, L. (2003). The Signal Sequence of Exported Protein-1 Directs the Green Fluorescent Protein to the Parasitophorous Vacuole of Transfected Malaria Parasites. *The Journal of Biochemistry*, 278, 6532-6542.

AGARRABERES, F.A. and DICE, J.F. (2001). A molecular chaperone complex at the lysosomal membrane is required for protein translocation. *Journal of Cell Science*, 114, 2491-2499.

AL-HERRAN, S. and ASHRAF, W. (1998). Physiological consequences of the over-production of *E. coli* truncated molecular chaperone DnaJ. *FEMS Microbiology Letters*, 162, 117-122.

ALI, M.M., ROE, S.M., VAUGHAN, C.K., MEYER, P., PANARETOU, B., PIPER, P.W., PRODROMOU, C. and PEARL, L.H. (2006). Crystal structure of an Hsp90-nucleotide-p23/Sba1 closed chaperone complex. *Nature*, 440, 1013-1017.

ALIGUE, R., AKHAVAN-NIAK, H. and RUSSELL, P. (1994). A role for Hsp90 in cell cycle control: Wee1 tyrosine kinase activity requires interaction with Hsp90. *The EMBO Journal*, 13, 6099-6106.

ALTSCHUL, S.F., MADDEN, T.L., SCHÄFFER, A.A., ZHANG, J., ZHANG, Z., MILLER, W. and LIPMAN, D.J. (1997). Gapped BLAST and PSI-BLAST: a new generation of protein database search programs. *Nucleic Acids Research*, 25, 3389-3402.

ANCEVSKA-TANEVA, N., ONOPRISHVILI, I., ANDRIA, M.L., HILLER, J.M. and SIMON, E.J. (2006). A member of the heat shock protein 40 family, hlj1, binds to the carboxyl tail of the human my opioid receptor. *Brain Research*, 1081, 28 33.

ANFINSEN, C.B. (1973). Principles that govern the folding of protein chains. *Science*, 181, 223-230.

ANGOV, E., HILLIER, C.J., KINCAID, R.L. and LYON, J.A. (2008). Heterologous Protein Expression is Enhanced by Harmonizing the Codon Usage Frequencies of the Target Gene with those of the Expression Host. *PLoS ONE*, 3, e2189.

ANSORGE, I., BENTING, J,. BHAKDI, S. and LINGELBACH, K. (1996). Protein sorting in *Plasmodium falciparum*-infected red blood cells permeabilized with the pore-forming protein streptolysin O. *Biochemistry Journal*, 315, 307-315.

APETRI, A.C. and HORWICH, A.L. (2008). Chaperonin chamber accelerates protein folding through passive action of preventing aggregation. *Proceedings of the National Academy of Sciences*, 105, 17351-17355.

ARDESHIR, F., FLINT, J.E., RICHMAN, S.J. and REESE, R.T. (1987). A 75 kd merozoite surface protein of *Plasmodium falciparum* which is related to the 70 kd heat-shock proteins. *The EMBO Journal*, 6, 493-499.

ARON, R.; LOPEZ, N.; WALTER, W.; CRAIG, E. A. and JOHNSON, J. (2005). *In vivo* bipartite interaction between the Hsp40 Sis1 and Hsp70 in *Saccharomyces cerevisiae*. *Genetics,* 169, 1873–1882.

AUGER, I. and ROUDIER, J. (1997). A function for the QKRAA motif: mediating binding of DnaJ to DnaK. Implications for the association of rheumatoid arthritis with HLA-DR4. *The Journal of Clinical Investigation*, 99, 1818-1822.

BACA, A.M. and HOL, W.G.J. (2000). Overcoming codon bias: a method for high-level overexpression of *Plasmodium falciparum* and other AT-rich parasite genes in *Escherichia coli*. *International Journal of Parasitology*, 30, 113-118.

BAHL, A., BRUNK, B., CRABTREE, J., FRAUNHOLZ, M.J., GAJRIA, B., GRANT, G.R., GINSBURY, H., GUPTA, D., KISSINGER, J.C., LABO, P., LI, L., MAILMAN, M.D., MILGRAM, A.J., PEARSON, D.S., ROOS, D.S., SCHUG, J., STOECKERT, C.J. and WHETZEL, P. (2003). PlasmoDB: the *Plasmodium* genome resource. A database integrating experimental and computational data. *Nucleic Acids Research*, 31, 212-215.

BALER, R., WELCH, W.J. and VOELLMY, R. (1992). Heat shock gene regulation by nascent polypeptides and denatured proteins: hsp70 as a potential autoregulatory factor. *The Journal of Cell Biology*, 117, 1151-1159.

BALLINGER, C.A., CONNELL, P., WU, Y., HU, Z., THOMPSON, L.J., YIN, L.-Y. and PATTERSON, C. (1999). Identification of CHIP, a Novel Tetratricopeptide Repeat-Containing Protein That Interacts with Heat Shock Proteins and Negatively Regulates Chaperone Functions. *Molecular and Cellular Biology*, 19, 4535-4545.

BANECKI, B., LIBEREK, K., WALLS, D., WAWRZYNÓW, A.,GEORGOPOULOS, C., BERTOLI, E., TANFANI, F. and ZYLICZ, M. (1996). Structure-Function Analysis of the Zinc Finger Region of the DnaJ Molecular Chaperone. *The Journal of Biological Chemistry*, 271, 14840-14848.

BANEYX, F. and PALUMBO, J.L. (2003). Improving heterologous protein folding via molecular chaperones and foldase co-expression. *Methods in Molecular Biology*, 205, 171-197.

BANNISTER, L.H., HOPKINS, J.M., MARGOS, G., DLUZEWSKI, A.R. and MITCHELL, G.H. (2004). Three-dimensional ultrastructure of the ring stage of Plasmodium falciparum: evidence for export pathways. *Microscopy and Microanalysis*, 10, 551-562.

BANUMATHY, G., SINGH, V. and TATU, U. (2002). Host Chaperones Are Recruited in Membrane-bound Complexes by *Plasmodium falciparum*. *The Journal of Biological Chemistry*, 277, 3902-3912.

BANUMATHY, G., SINGH, V., PAVITHRA, S.R. and TATU, U. (2003). Heat Shock Protein 90 Function is Essential for *Plasmodium falciparum* Growth in Human Erythrocytes. *The Journal of Biological Chemistry*, 278, 18336-18345.

BARDWELL, J.C.A., TILLY, K., CRAIG, E., KING, J., ZYLICZ, M., and GEORGOPOULOS, C. (1986). The nucleotide sequence of the *Escherichia coli* K12 dnaJ+ gene. *The Journal of Biological Chemistry*, 261, 1782-1785.

BARENT, R.L., NAIR, S.C., CARR, D.C., RUAN, Y., RIMERMAN, R.A., FULTON, J., ZHANG, Y. and SMITH, D.F. (1998). Analysis of FKBP51/FKBP52 Chimeras and Mutants for Hsp90 Binding and Association with Progesterone Receptor Complexes. *Molecular Endocrinology*, 12, 342-354.

BARNWELL, J. W. (1990). Vesicle-mediated transport of membrane and proteins in malaria-infected erythrocytes. *Blood Cells*, 16, 379-395.

BARRAL, J.M., BROADLEY, S.A., SCHAFFAR, G., and HARTL, F.U. (2004). Roles of molecular chaperones in proteins misfolding diseases. *Seminars in Cell and Developmental Biology*, 15, 17-29.

BASHA, E., LEE, G.J., DEMELER, B. and VIERLING, E. (2004). Chaperone activity of cytosolic small heat shock proteins from wheat. *European Journal of Biochemistry*, 271, 1426-1436.

BECKER, J. and CRAIG, E.A. (1994). Review: Heat shock proteins as molecular chaperones. *European Journal of Biochemistry*, 219, 11-23.

BECKER, J., WALTER, W., YAN, W. and CRAIG, E.A. (1996). Functional Interaction of Cytosolic hsp70 and a DnaJ-Related Protein, Ydj1p, in Protein Translocation In Vivo. *Molecular and Cellular Biology*, 16, 4378-4386

BENDER, A., VAN DOOREN, G.G., RALPH, S.A., MCFADDEN, G.I. and SCHNEIDER, G. (2003). Properties and prediction of mitochondrial transit peptides from *Plasmodium falciparum*. *Molecular and Biochemical Parasitology*, 132, 59-66.

BENSON, D.A., KARSCH-MIZRACHI, I., LIPMAN, D.J., OSTELL, J. and WHEELER, D.L. (2008). GenBank. *Nucleic Acids Research*, 36, D25-D30.

BERCOVICH, B., STANCOVSKI, I., MAYER, A., BLUMENFELD, N., LASZLO, A., SCHWARTZ, A.L. and CIECHANOVER, A. (1997). Ubiquitin-dependent degradation of certain proteins substrates *in vitro* requires the molecular chaperone Hsc70. *The Journal of Biological Chemistry*, 272, 9002-9010.

BERJANSKII, M.V., RILEY, M.I., XIE, A., SEMENCHENKI, C., FOLKS, W.R. and VAN DOREN, S.R. (2000). NMR structure of the N-terminal J domain of murine polyomavirus T antigens. Implications for the DnaJ-like domains and for mutations of the T antigens. *The Journal of Biological Chemistry*, 275, 36094-36103.

BERMAN, H.M., HENRICK, K. and NAKAMURA, H. (2003). Announcing the worldwide Protein Data Bank. *Nature Structural Biology*, 10, 980.

BERWAL, R., GOPLAN, N., CHANDEL, K., PRASAD, G.B.K.S. and PRAKASH, S. (2008). *Plasmodium falciparum*: Enhanced soluble expression, purification and biochemical characterization of lactate dehydrogenase. *Experimental Parasitology*, 120, 135-141.

BHATTACHARJEE, S., VAN OOIJ, C., BALU, B., ADAMS, J.H. and HALDAR, K. (2008). Maurer's clefts of *Plasmodium falciparum* are secretory organelles that concentrate virulence protein reporters for delivery to the host erythrocyte. *Blood*, 111, 2418-2426.

BIENZ, M. and PELHAM, H.R. (1987). Mechanisms of heat shock gene activation in higher eukaryotes. *Advances in Genetics*, 24, 31-72.

BIRKHOLTZ, L.-M., BLATCH, G., COETZER, T.L., HOPPE, H.C., HUMAN, E., MORRIS, E.J., NGCETE, Z., OLDFIELD, L., ROTH, R., SHONHAI, A., STEPHENS, L. and LOUW, A.I. (2008). Heterologous expression of plasmodial proteins for structural studies and functional annotation. *Malaria Journal*, 7: 197.

BISCHOFBERGER, P., HAN, W., FEIFEL, B., SCHÖNFELD, H.J. and CHRISTEN, P. (2003). D-peptides as inhibitors of the DnaK/DnaJ/GrpE chaperone system. *The Journal of Biological Chemistry*, 278, 19044-19047.

BISWAS, S. and SHARMA, Y.D. (1994). Enhanced expression of *Plasmodium falciparum* heat shock protein PFHSP70-I at higher temperatures and parasite survival. *Microbiology Letters*, 124, 425-430.

BLANC, L., DE GASSART, A., GERMINARD, C., BETTE-BOBILLO, P. and VIDAL, M. (2005). Exosome release by reticulocytes – An integral part of the red blood cell differentiation system. *Blood Cells, Molecules, and Diseases*, 35, 21-26.

BLATCH, G.L. (2006). Networking of Chaperones by Co-Chaperones. Georgetown, Texas, U.S.A.: Landes Bioscience.

BLISNICK, T., MORALES BETOULLE, M.E., BARALE, J.C., UZUREAU, P., BERRY, L., DESROSES, S., FUJIOKA, H., MATTEI, D. and BRAUN BETON, C. (2000). Pfsbp1, a Maurer's cleft *Plasmodium falciparum* protein, is associated with the erythrocyte skeleton. *Molecular and Biochemical Parasitology*, 111, 107-121.

BODDEY, J.A., MORITZ, J.L., SIMPSON, R.J. and COWMAN, A.F. (2008). Role of the Plasmodium Export Element in trafficking parasite proteins to the infected erythrocyte. *Traffic, In Press*, DOI: 10.1111/j.1600-0854.2008.00864.x.

BORGES, J.C., FISCHER, H., CRAIEVICH, A.F., and RAMOS, C.H.I. (2005). Low Resolution Structural Study of Two Human Hsp40 Chaperones in Solution. *The Journal of Biological Chemistry*, 280, 13671-13681.

BORK, P., SANDER, C. and VALENCIA, A. (1992). An ATPase domain common to prokaryotic cell cycle proteins, sugar kinases, actin, and hsp70 heat shock proteins. *Proceedings of the National Academy of Sciences,* 89, 7290-7294.

BOSHOFF, A., NICOLL, W.S., HENNESSY, F., LUDEWIG, M., DANIEL, S., MODISAKENG, K.W., SHONHAI, A., MCNAMARA, C., BRADLEY, G. and BLATCH, G.L. (2004). Molecular chaperones in biology, medicine and protein biotechnology. *South African Journal of Science*, 100, 665-677.

BOTHA, M., PESCE, E.-R. and BLATCH, G.L. (2007). The Hsp40 Proteins of Plasmodium falciparum: Regulating Chaperone Power in the Parasite and the Host. *International Journal of Biochemistry and Molecular Biology*, 39, 1781-1803.

BOZDECH, Z., LLINÁS, M., PULLIAM, B.L., WONG, E.D., ZHU, J. and DERISI, J.L. (2003). The transcriptome of the intraerythrocytic developmental cycle of *Plasmodium falciparum*. *PLoS Biology*, 1, 85-100.

BREHMER, D., RÜDIGER, S., GÄSSLER, C.S., KLOSTERMEIER, D., PACKSCHIES, L., REINSTEIN, J., MAYER, M.P. and BUKAU, B. (2001). Tuning of chaperone activity of Hsp70 proteins by modulation of nucleotide exchange. *Nature Structural Biology*, 8, 427-432.

BRINKER, A., SCHEUFLER, C., VON DER MÜLBE, F., FLECKENSTEIN, B., HERRMANN, C., JUNG, G., MOAREFI, I. And HARTL, F.U. (2002). Ligand Discrimination by TPR Domains: Relevance and Selectivity of EEVD-Recognition in Hsp70.Hop.Hsp90 Complexes. *The Journal of Biological Chemistry*, 277, 19265-19275.

BRODSKY, J.L. (1996). Post-translational translocation: not all hsc70s are created equal. *Trends in Biochemical Sciences*, 21, 122-126.

BRODSKY, J.L. and BRACHER, A. (2006). Nucleotide Exchange Factors for Hsp70 Molecular Chaperones. *In* Blatch, G.L. (ed), *Networking of Chaperones by Co-Chaperones*. Georgetown, Texas, U.S.A.: Landes Bioscience, p. 1-12.

BRODSKY, J.L. and CHIOSIS, G. (2006). Hsp70 molecular chaperones: emerging roles in human disease and identification of small molecule modulators. *Current Topics in Medicinal Chemistry*, 6, 1215-1225.

BROWN, G.V., CULVENOR, J.G., CREWTHER, P.E., BIANCO, A.E., COPPEL, R.L., SAINT, R.B., STAHL, H.-D., KEMP, D.J. and ANDERS, R.F. (1985). Localization of the ring-infected erythrocyte surface antigen (RESA) of *Plasmodium falciparum* in merozoites and ring-infected erythrocytes. *The Journal of Experimental Medicine*, 162, 774-779.

BROWN, H., HIEN, T.T., DAY, N., MAI, N.T.H., CHUONG, L.V., CHAU, T.T.H., LOC, P.P., PHU, N.H., BETHELL, D., FARRAR, J., GATTER, K., WHITE, N. and TURNER, G. (1999). Evidence of blood-brain barrier dysfunction in human cerebral malaria. *Neuropathy and Applied Neurobiology*, 25, 331-340.

BRUCE, B.D. and CHURCHICH, J. (1997) Characterization of the molecular-chaperone function of the heat-shock-cognate-70-interacting protein. *European Journal of Biochemistry,* 245, 738–744.

BUCHBERGER, A., THEYSSEN, H., SCHRODER, H., MCCARTY, J.S., VIRGALLITA, G., MILKEREIT, P., REINSTEIN, J and BUKAU, B. (1995). Nucleotide-induced conformational changes in the ATPase and substrate binding domains of the DnaK chaperone provide evidence for interdomain communication. *The Journal of Biological Chemistry*, 270, 16903-16910.

BUCHBERGER, A., SCHRÖDER, H., HESTERKAMP, T., SCHÖNFELD, H.-J. and BUKAU, B. (1996). Substrate Shuttling Between the DnaK and GroEL Systems Indicates a Chaperone Network Promoting Protein Folding. *Journal of Molecular Biology*, 261, 328-333.

BUCHNER, J. (1999). Hsp90 & Co. – a holding for folding. *Trends in Biochemical Sciences*, 24, 136-141.

BUKAU, B. and HORWICH, A.L. (1998). The Hsp70 and Hsp60 chaperone machines. *Cell*, 92, 351-366.

BUKAU, B., DEUERLING, E.E., PFUND, C., and CRAIG, E. (2000). Getting newly synthesized proteins into shape. *Cell*, 101, 119-122.

BURKHOLDER, W.F., PANAGIOTIDIS, C.A., SILVERSTEIN, S.J., CEGEIELSKA, A., GOTTESMAN, M.E. and GAITANARIS, G.A. (1994). Isolation and characterization of an *Escherichia coli* DnaK mutant with impaired ATPase activity. *Journal of Molecular Biology*, 242, 364-377.

CAJO, G.C., HORNE, B.E., KELLEY, W.L., SCHWAGER, F., GEORGOPOULOS, C. and GENEVAUX, P. (2006). The role of the DIF motif in the DnaJ (Hsp40) co-chaperone regulation of the DnaK (Hsp70) chaperone cycle. *The Journal of Biological Chemistry*, 281, 12436-12444.

CALLAHAN, M.K., CAILLOT, D., JACQUIN, C., CLARK, P.R. and MÉNORET, A. (2002). Differential Acquisition of Antigenic Peptides by Hsp70 and Hsc70 under Oxidative Conditions. *The Journal of Biological Chemistry*, 277, 33604-33609.

CANNATA, N., MERELLI, E. and ALTMAN, R.B. (2005). Time to Organize the Bioinformatics Resourceome. *PLoS Biology*, 1, e76.

CAPLAN, A.J., CYR, D.M. and DOUGLAS, M.G. (1992a). YDJ1p facilitates polypeptide translocation across different intracellular membranes by a conserved mechanism. *Cell*, 71, 1143-1155.

CAPLAN, A.J., TSAI, J., CASEY, P.J. and DOUGLAS, M.G. (1992b). Farnesylation of YDJ1p is required for function at elevated growth temperatures in *Saccharomyces cerevisiae*. *The Journal of Biological Chemistry*, 267, 18890-18895.

CAPLAN, A.J. (2003). What is a co-chaperone? *Cell Stress and Chaperones*, 8, 105-107.

CARLTON, J. M., ANGIUOLI, S.V., SUH, B.B., KOOIJ, T.W., PERTEA. M., SILVA, J.C., ERMOLAEVA, M.D., ALLEN, J.E., SELENGUT, J.D., KOO, H.L., PETERSON, J.D., POP, M., KOSACK, D.S., SHUMWAY, M.F., BIDWELL, S.L., SHALLOM, S.J., VAN AKEN, S.E., RIEDMULLER, S.B., FELDBLYUM, T.V., CHO, J.K., SEDEGAH, M., SHOAIBI, A., CUMMINGS, L.M., FLORENS, L., YATES, J.R., RAINE, J.D., SINDEN, R.E., HARRIS, M.A., CUMMINGHAM, D.A., PREISER, P.R., BERGMAN, L.W., VAIDYA, A.B., VAN LIN, L.H., JANSE, C.J., WATERS, A.P., SMITH, H.O., WHITE, O.R., SALZBERG, S.L., VENTER, J.C., FRASER, C.M., HOFFMAN, S.L., GARDNER, M.J. and CARUCCI, D.J. (2002). Genome sequence and comparative analysis of the model rodent malaria parasite *Plasmodium yoelii yoelii*. *Nature*, 419, 512–519.

CARLTON, J.M. (2003). The *Plasmodium vivax* genome sequencing project. *Trends in Parasitology,* 19, 227–231.

CHAE, C., SHARMA, S., HOSKINS, J.R. and WICKNER, S. (2004). CbpA, a DnaJ Homolog, Is A DnaK Co-chaperone, and Its Activity Is Modulated By CbpM. *The Journal of Biological Chemistry*, 279, 33147-33153.

CHAMBERLAIN, L.H. and BURGOYNE, R.D. (1997). Activation of the ATPase activity of heat-shock proteins Hsc70/Hsp70 by cysteine-string protein. *Biochemistry Journal*, 322, 853-858.

CHANG, H.H., FALICK, A.M., CARLTON, P.M., SEDAT, J.W., DERISI, J.L. and MARLETTA, M.A. (2008). N-terminal processing of proteins exported by malaria parasites. *Molecular and Biochemical Parasitology*, 160, 107-115.

CHAPPELL, T.G., WELCH, W.J., SCHLOSSMAN, D.M., PALTER, K.B., SCHLESIGNER, M.J. and ROTHMAN, J.E. (1986). Uncoating ATPase is a member of the 70 kilodalton family of stress proteins. *Cell*, 45, 3–13.

CHEETHAM, M. E., JACKSON, A. P. and ANDERTON, B. H. (1994). Regulation of 70-kDa heat-shock-protein ATPase activity and substrate binding by human DnaJ-like proteins, HSJ1a and HSJ1b. *European Journal of Biochemistry*, 226, 99–107.

CHEETHAM, M.E. and CAPLAN, A.J. (1998). Structure, function and evolution of DnaJ: Conservation and adaptation of chaperone function. *Cell Stress and Chaperones*, 3, 28-36.

CHEN, M.S., SILVERSTEIN, A.M., PRATT, W.B. and CHINKERS, M. (1996). The tetratricopeptide repeat domain of protein phosphatise 5 mediates binding to glucocorticoid receptor heterocomplexes and acts as a dominant negative mutant. *The Journal of Biological Chemistry*, 271, 32315-32320.

CHEN, S. and SMITH, D.F. (1998). Hop as an adaptor in the heat shock protein 70 (Hsp70) and hsp90 chaperone machinery. *The Journal of Biological Chemistry*, 273, 35194-35200.

CHENNA, R., SUGAWARA, H., KOIKE,T., LOPEZ, R., GIBSON, T.J., HIGGINS, D.G. and THOMPSON, J.D. (2003). Multiple sequence alignment with the Clustal series of programs. *Nucleic Acids Research*, 31, 3497-3500.

CHOGLAY, A.A., CHAPPLE, J.P., BLATCH, G.L. and CHEETHAM, M.E. (2001). Identification and characterisation of a human mitochondrial homologue of the bacterial co-chaperone GrpE. *Gene*, 267, 125-134.

CHOU, P.Y. and FASMAN, G.D. (1974). Prediction of protein conformation. *Biochemistry*, 13, 222-245.

CHROMY, L.R., PIPAS, J.M. and GARCEA, R.L. (2003). Chaperone-mediated in vitro assembly of Polyomavirus capsids. *Proceedings of the National Academy of Sciences*, 100, 10477-10482.

CHUNG, K.T., SHEN, Y. and HENDERSHOT, L.M. (2002). BAP, a mammalian BiP-associated protein, is a nucleotide exchange factor that regulates the ATPase activity of BiP. *The Journal of Biological Chemistry*, 277, 47557-47564.

CINTRON, N.S. and TOFT, D. (2006). Defining the requirements for Hsp40 and Hsp70 in the Hsp90 chaperone pathway. *The Journal of Biological Chemistry*, 281, 26235-26244.

CLARKE, S. (1992). Protein isoprenylation and methylation at carboxyl-terminal cysteine residues. *Annual Review of Biochemistry*, 61, 355-386.

CONNELL, P., BALLINGER, C.A., JIANG, J., WU, Y., THOMPSON, L.J., HÖHFELD, J. and PATTERSON, C. (2001). The co-chaperone CHIP mediates protein triage decisions by heat-sock proteins. *Nature Cell Biology*, 3, 93-96.

COOKE, B.M., LINGELBACH, K., BANNISTER, L.H. and TILLEY, L. (2004). Protein trafficking in *Plasmodium falciparum*-infected red blood cells. T*rends in Parasitology*, 20, 581-589.

COPPEL, R.L., LUSTIGMAN, S., MURRAY, L. and ANDERS, R.F. (1988). MESA is a *Plasmodium falciparum* phosphoprotein associated with the erythrocyte membrane skeleton. *Molecular and Biochemical Parasitology*, 31, 223-231.

CRAIG, A. and SCHERF, A. (2001). Molecules on the surface of the Plasmodium falciparum infected erythrocyte and their role in malaria pathogenesis and immune invasion. *Molecular and Biochemical Parasitology*, 115, 129-143.

CRAIG, E.A., WEISSMAN, J.S. and HORWICH, A.L. (1994) Heat shock proteins and molecular chaperones: mediators of protein conformation and turnover in the cell. *Cell*, 78, 365-372.

CUNNEA, P.M., MIRANDA-VIZUETE, A., BERTOLI, G., SIMMEN, T., DAMDIMOPOULOS, A.E., HERMANN, S., LEINONEN, S., HUIKKO, M.P., GUSTAFSSON, J.A., SITIA, R. and SPYROU, G. (2003). ERdj5, an endoplasmic reticulum (ER)-resident protein containing DnaJ and thioredoxin domains, is expressed in secretory cells or following ER stress. *The Journal of Biological Chemistry*, 278, 1059-1066.

CUPP-VICKERY, J.R. and VICKERY, L.E. (1997). Crystallization and preliminary X-ray crystallographic properties of Hsc20, a J-motif co-chaperone protein from *Escherichia coli*. *Protein Science*, 6, 2028-2030.

CUPP-VICKERY, J.R. and VICKERY, L.E. (2000). Crystal structure of Hsc20, a J-type Co-chaperone from *Escherichia coli*. *Journal of Molecular Biology*, 304, 835-845.

CYR, D.M. (1995). Co-operation of the molecular chaperone Ydj1 with specific Hsp70 homologs to suppress protein aggregation. *FEBS Letters*, 259, 129-132.

DA SILVA, E., FOLEY, M., DLUZEWSKI, A. R., MURRAY, L. J. , ANDERS, R. F. and TILLEY, L. (1994). The *Plasmodium falciparum* protein RESA interacts with the erythrocyte cytoskeleton and modifies erythrocyte thermal stability. *Molecular and Biochemical Parasitology*, 66, 59-69.

DAS, A., SYIN, C., FUJIOKA, H., ZHENG, H., GOLDMAN, N., AIKAWA, M. and KUMAR, N. (1997). Molecular characterization and ultrastructural localisation of *Plasmodium falciparum* Hsp60. *Molecular and Biochemical Parasitology*, 88, 95-104.

DATE, S.V. and STOECKERT, C.J. (2006). Computational modeling of the *Plasmodium falciparum* interactome reveals novel protein function on a genome-wide scale. *Genome Research*, 16, 542-549.

DE JONG, W.W., LEUNISSEN, J.A.M. and VOORTER, C.E.M. (1993). Evolution of the α-Crystallin / Small Heat Shock Protein Family. *Molecular Biology and Evolution*, 10, 103-126.

DE MARCO, A. and DE MARCO, V. (2004). Bacteria co-transformed with recombinant proteins and chaperones cloned in independent plasmids are suitable for expression tuning. *Journal of Biotechnology*, 109, 45-52.

DE OLIVEIRA-FERREIRA, J., BANIC, D.M., SANTOS, F., FERREIRA-DA-CRUZ, M.F., DUBOIS, P. and DANIEL-RIBIERO, C.T. (1999). Cellular and antibody responses to the *Plasmodium falciparum* heat shock protein Pf72/HSP70 during and after acute malaria in individuals from an endemic area of Brazil. *Acta Tropica*, 73, 1-10.

DELANO, W.L. (2005). The PyMOL Molecular Graphics System. DeLano Scientific LLC, South San Francisco, CA, USA. http://www.pymol.org.

DELOCHE, O., KELLEY, W.L. and GEORGOPOULOS, C. (1997). Structure-function analyses of Ssc1p, Mdj1p and Mge1p *Saccharomyces cerevisiae* mitochondrial proteins in *Escherichia coli*. *Journal of Bacteriology*, 179, 6066-6075.

DEMAND, J., LÜDERS, J and HÖHFELD, J. (1998). The carboxy-terminal domain of Hsc70 provides binding sites for a distinct set of chaperone cofactors. *Molecular and Cellular Biology*, 18, 2023-2028.

DEUERLING, E., SCHULTZE-SPECKING, A., TOMOYASU, T., MOGK, A. and BUKAU, B. (1999). Trigger factor and DnaK cooperate in the folding of newly synthesised proteins. *Nature*, 400, 693-696.

DEUERLING, E. and BUKAU, B. (2004). Chaperone-Assisted Folding of Newly Synthesized Proteins in the Cytosol. *Critical Reviews in Biochemistry and Molecular Biology*, 39, 261-277.

DITTMARR, K.D., BANACH, M., GALIGNIANA, M.D. and PRATT, W.B. (1996). The Role of DnaJ-like Proteins in Glucocorticoid Receptor.Hsp90 Heterocomplex Assembly by the Reconstituted hsp90.p60.hsp70 Foldosome Complex. *The Journal of Biological Chemistry*, 273, 7358-7366.

DIXON, M.W., HAWTHORNE, P.L., SPIELMANN, T., ANDERSON, K.L., TRENHOLME, K.R., GARDINER, D.L. (2008). Targeting of the ring exported protein 1 to the Maurer's clefts is mediated by a two-phase process. *Traffic*, 9, 1316-1326.

DOBSON, C.M. (2003). Protein folding and misfolding. *Nature*, 426, 884-890.

DOBSON, S., KAR, B., KUMAR, R., ADAMS, B. and BARIK, S. (2001). A novel tetratricopeptide repeat (TPR) containing PP5 serine/threonine protein phosphatase in the malaria parasite, *Plasmodium falciparum*. *BMC Microbiology*, 1, 31.

EDKINS, A.L., LUDEWIG, M.H., and BLATCH G.L. (2004). A *Trypanosoma cruzi* heat shock protein 40 is able to stimulate the adenosine triphosphate hydrolysis activity of heat shock protein 70 and can substitute for a yeast heat shock protein 40. *International Journal of Biochemistry and Cell Biology*, 36, 1585-1598.

ELLIS, R.J. (1987). Proteins as molecular chaperones. *Nature*, 328, 378-379.

ELLIS, R.J. (1990). The molecular chaperone concept. *Seminars in Cell Biology*, 1, 1-9.

ELLIS, R.J. (2001). Macromolecular crowding: obvious but underappreciated. *Trends in Biochemical Sciences*, 26, 597-604.

ELMENDORF, H.G. and HALDAR, K. (1994). *Plasmodium falciparum* exports the Golgi marker sphingomyelin synthase into a tubulovesicular network in the cytoplasm of mature erythrocytes. *The Journal of Cell Biology*, 124, 449-462.

EMINI, E.A., HUGHES, J.C., PERLOW, D.S. and BOGER, J. (1985). Induction of hepatitis A virus-neutralizing antibody by a virus-specific synthetic peptide. *The Journal of Virology*, 55, 836-839.

FADER, C.M., SAVINA, A., SANCHEZ, D. and COLOMBO, M.I. (2005). Exosome secretion and red cell maturation: Exploring components involved in the docking and fusion of multivesicular bodies in K562 cells. *Blood Cells, Molecules, and Diseases*, 35, 153-157.

FAN, C.Y., LEE, S. and CYR, D.M. (2003). Mechanisms for regulation of Hsp70 function by Hsp40. *Cell Stress and Chaperones*, 8, 309-316.

FAN, C.Y., LEE, S., REN, H.Y. and CYR, D.M. (2004). Exchangeable Chaperone Modules Contribute to Specification of Type ▮and Type ▮▮Hsp40 Cellular Function. *Molecular Biology of the Cell*, 15, 761-773.

FAN, C.Y., REN, H.Y., LEE, P., CAPLAN, A.J. and CYR, D.M. (2005). The Type ▮Hsp40 Zinc Finger-Like Region Is Required for Hsp70 to Capture Non-native polypeptides from Ydj1. *The Journal of Biochemistry*, 280, 695-702.

FARH, L. MITCHELL, D.A. and DESCHENES, R.J. (1995). Farnesylation and proteolysis are sequential, but distinct steps in the CaaX box modification pathway. *Archives of Biochemistry and Biophysics*, 318, 113-121.

FAYAZI, Z., GHOSH, S., MARION, S., BAO, X., SHERO, M. and KAZEMI-ESFARJANI, P. (2006). A *Drosophila* orthologs of the human MRJ modulates polyglutamine toxicity and aggregation. *Neurobiology of Disease*, 24, 226-244.

FAYET, O., ZIEGELHOFFER, T. and GEORGOPOULOS, C. (1989). The groES and groEL heat shock gene products of *Escherichia coli* are essential for bacterial growth at all temperatures. *Journal of Bacteriology*, 171, 1379-1385.

FELDHEIM, D., ROTHBLATT, J. and SCHEKMAN, R. (1992). Topology and functional domains of Sec63p, an endoplasmic reticulum membrane protein required for secretory protein translocation. *Molecular and Cellular Biology*, 12, 3288-3296.

FELDMAN, D.E. and FRYDMAN, J. (2000). Protein folding *in vivo*: the importance of molecular chaperones. *Current Opinion in Structural Biology*, 10, 26-33.

FERNANDEZ-SÁIZ, V., MORO, F., ARIZMENDI, J.M., ACERBRÓN, S.P. and MUGA, A. (2006). Ionic contacts at DnaK substrate binding domain involved in the allosteric regulation of lid dynamics. *The Journal of Biological Chemistry*, 281, 7479-7488.

FEWELL, S.W., PIPAS, J.M. and BRODSKY, J.L. (2002). Mutagenesis of a functional chimeric gene in yeast identified mutations in the simian virus 40 large T antigen J domain. *Proceedings of the National Academy of Sciences*, 99, 2002-2007.

FEWELL, S. W., WRIGHT, C.M., LYON, M.A., DUMITRESCU, T.P., WIPF, P. and BRODSKY, J.L. (2004). Small Molecule Modulators of Endogenous and Co-chaperone-stimulated Hsp70 ATPase Activity. *The Journal of Biological Chemistry*, 279, 51131-51140.

FINK, A.L. (1999). Chaperone-mediated protein folding. *Physiological Reviews*, 79, 425-449.

FISER, A., DO, R.K. and SALI, A. (2000). Modeling of loops in protein structures. *Protein Science*, 9, 1753-1773.

FLAHERTY, K.M., WILBANKS, S.M., DE LUCA-FLAHERTY, C. and MCKAY, D.B. (1990). Three-dimensional structure of the ATPase fragment of the 70 kDa heat shock cognate protein. *Nature*, 346, 623-628.

FLAHERTY, K.M., MCKAY, D.B., KABSCH, W. and HOLMES, K.C. (1991). Similarity of the three-dimensional structures of actin and the ATPase fragment of a 70-kDa heat shock cognate protein. *Proceedings of the National Academy of Sciences*, 88, 5041-5045.

FLICEK, P., AKEN, B.L., BEAL, K., BALLESTER, B., CACCAMO, M., CHEN, Y., CLARKE, L., COATES, G., CUNNINGHAM, F., CUTTS, T., DOWN, T., DYER, S.C., EYRE, T., FITZGERALD, S., FERNANDEZ-BANET, J., GRÄF, S., HAIDER, S., HAMMOND, M., HOLLAND, R., HOWE, K.L., HOWE, K., JOHNSON, N., JENKINSON, A., KÄHÄRI, A., KEEFE, D., KOKOCINSKI, F., KULESHA, E., LAWSON, D., LONGDEN, I., MEGY, K., MEIDL, P., OVERDUIN, B., PARKER, A., PRITCHARD, B., PRLIC, A., RICE, S., RIOS, D., SCHUSTER, M., SEALY, I., SLATER, G., SMEDLEY, D., SPUDICH, G., TREVANION, S., VILELLA, A.J., VOGEL, J., WHITE, S., WOOD, M., BIRNEY, E., COX, T., CURWEN, V., DURBIN, R., FERNANDEZ-SUAREZ, X.M., HERRERO, J., HUBBARD, T.J., KASPRZYK, A., PROCTOR, G., SMITH, J., URETA-VIDAL, A. and SEARLE, S. (2008). Ensembl 2008. *Nucleic Acids Research*, 36, D707-D714.

FLICK, K., AHUJA, S., CHENE, A., BEJARANO, M.T. and CHEN, Q. (2004). Optimized expression of *Plasmodium falciparum* erythrocyte membrane protein 1 domains in *Escherichia coli*. *Malarial Journal*, 15: 50.

FLISS, A.E., RAO, J., MELVILLE, M.W., CHEETHAM, M.E. and CAPLAN, A.J. (1999). Domain Requirements of DnaJ-like (Hsp40) Molecular Chaperones in the Activation of a Steroid Hormone Receptor. *The Journal of Biological Chemistry*, 274, 34045-34052.

FLOM, G.A., LEMIESZEK, M., FORTUNATO, E.A. and JOHNSON, J.L. (2008). Farnesylation of Ydj1 is Required for In Vivo Interaction with Hsp90 Client Proteins. *Molecular Biology of the Cell*, 19, 5249-5258.

FLORENS, L., WASHBURN, M.P., RAINE, J.D., ANTHONY, R.M., GRAINGERK, M., HAYNES, J.D., MOCH, J.K., MUSTER, N., SACCI, J.B., TABB, D.L., WITNEY, A.A., WOLTERS, D., WU, Y., GARDNER, M.J., HOLDERK, A.A., SINDEN, R.E., YATES, J.R. and CARUCCI, D.J. (2002). A proteomic view of the *Plasmodium falciparum* life cycle. *Nature*, 419, 520-526.

FLYNN, G.C., CHAPPELL, T.G. and ROTHMAN, J.E. (1989). Peptide binding and release by proteins implicated as catalysts of protein assembly. *Science*, 245, 385-390.

FLYNN, G.C., POHL, J., FLOCCO, M.T. and ROTHMAN, J.E. (1991). Peptide-binding specificity of the molecular chaperone BiP. *Nature*, 353, 726-730.

FOLEY, M. TILLEY, L., SAWYER, W. H. and ANDERS, R. F. (1991). The ring-infected erythrocyte surface antigen of *Plasmodium falciparum* associates with spectrin in the erythrocyte membrane. *Molecular and Biochemical Parasitology*, 46, 137-147.

FOTH, B.J., RALPH, S.A., TONKIN, C.J., STRUCK, N.S., FRAUNHOLZ, M., ROOS, D.S., COWMAN, A.F. and MCFADDEN, G.I. (2003). Dissecting Apicoplast Targeting in the Malaria Parasite *Plasmodium falciparum*. *Science*, 299, 705-708.

FOTH, B.J., ZHANG, N., MOK, S., PREISER, P.R. and BOZDECH, Z. (2008). Quantitative protein expression profiling reveals extensive post-transcriptional regulation and post-translational modifications in schizont-stage malaria parasites. *Genome Biology*, 9: R177.

FREEMAN, B.C., MYERS, M.P., SCHUMACHER, R. and MORIMOTO, R.I (1995). Identification of a regulatory motif in Hsp70 that affects ATPase activity, substrate binding and interaction with HDJ-1. *The EMBO Journal*, 14, 2281-2292.

FREEMAN, B.C. and MORIMOTO, R.I. (1996). The human cytosolic molecular chaperones hsp90, hsp70 (hsc70) and hdj-1 have distinct roles in recognition of a non-native protein and protein folding. *The EMBO Journal*, 15, 2969-2979.

FRYDMAN, J., NIMMESGEM, E., OHTSUKA, K. and HARTL, F.U. (1994). Folding of nascent polypeptide chains in a high molecular mass assembly with molecular chaperones. *Nature*, 370, 111-117.

FRYDMAN, J. and HÖHFELD, J. (1997). Chaperones get in touch: the Hip-Hop Connection. *Trends in Biochemical Sciences*, 22, 87-92.

FUJIOKA, H., DAS, A., SYIN, C., ZHENG, H., GOLDMAN, N., AIKAWA, M. and KUMAR, N. (1998). Molecular Characterisation and Ultrastructural Localisation of *Plasmodium falciparum* Hsp60. *Tokai Journal of Experimental and Clinical Medicine,* 23, 93

FUJIOKA, H. and AIKAWA, M. (2002). Malaria Parasites and Disease: Structure and Life Cycle. *Chemical Immunology*, 80, 1-26.

FUNG, K.L, HILGENBERG, K., WANG, N.M., and CHIRICO, W.J. (1996). Conformations of the nucleotide and polypeptide binding domains of a cytosolic Hsp70 molecular chaperone are coupled. *The Journal of Biological Chemistry*, 271, 21559-21565.

FÜZERY, A.J., TONELLI, M., TA, D.T., CORNILESCU, G., VICKERY, L.E. and MARKLEY, J.L. (2008). Solution structure of the iron-sulfur cluster cochaperone HscB and its binding surface for the iron-sulfur assembly scaffold protein IscU. *Biochemistry*, 47, 9394-9404.

GAITANARIS, G.A., VYSOKANOV, A., HUNG, S.C., GOTTESMAN, M.E. and GRAGEROV, A. (1994). Successive action of *Escherichia coli* chaperones *in vivo*. *Molecular Microbiology*, 14, 861-869.

GAO, B., EISENBERG, E. and GREENE, L. (1996). Effect of constitutive 70-kDa heat shock protein polymerization on its interaction with protein substrate. *The Journal of Biological Chemistry*, 28, 16792-16797.

GARDNER, M.J., HALL, N., FUNG, E., WHITE, O., BERRIMAN, M., HYMAN, R.W., CARLTON, J.M., PAIN, A., NELSON, K.E., BOWMAN, S., PAULSEN, I.T., JAMES, K., EISEN, J.A., RUTHERFORD, K., SALZBERG, S.L., CRAIG, A., KYES, S., CHAN., M.S., NENE, V., SHALLOM, S.J., SUH, B., PETERSON, J., ANGIUOLI, S., PERTEA, M., ALLEN, J., SELENGUT, J., HAFT, D., MATHER, M.W., VAIDYA, A.B., MARTIN, D.M., FAIRLAMB, A.H., FRAUNHOLZ, M.J., ROOS, D.S., RALPH, S.A., MCFADDEN, G.I., CUMMINGS, L.M., SUBRAMANIAN, G.M., MUNGALL, C., VENTER, J.C., CARUCCI, D.J., HOFFMAN, S.L., NEWBOLD, C., DAVIS, R.W., FRASER, C.M. and BARRELL, B. (2002). Genome sequence of the human malarial parasite *Plasmodium falciparum*. *Nature*, 419, 498-511.

GARDNER, M.J., BISHOP, R., SHAH, T., DE VILLIERS, E.P., CARLTON, J.M., HALL, N., REN, Q., PAULSEN, I.T., PAIN, A., BERRIMAN, M., WILSON, R.J., SATO, S., RALPH, S.A., MANN, D.J., XIONG, Z., SHALLOM, S.J., WEIDMAN, J., JIANG, L., LYNN, J., WEAVER, B., SHOAIBI, A., DOMINGO, A.R., WASAWO, D., CRABTREE, J., WORTMAN, J.R., HAAS, B., ANGIUOLI, S.V., CREASY, T.H., LU, C., SUH, B., SILVA, J.C., UTTERBACK, T.R., FELDBLYUM, T.V., PERTEA, M., ALLEN, J., NIERMAN, W.C., TARACHA, E.L., SALZBERG, S.L., WHITE, O.R., FITZHUGH, H.A., MORZARIA, S., VENTER, J.C., FRASER, C.M. and NENE, V. (2005). Genome sequence of *Theileria parva*, a bovine pathogen that transforms lymphocytes. *Science*, 309, 134–137.

GARIMELLA, R., LIU, X., QIAO, W., LIANG, X., ZUIDERWEG, E.R.P., RILEY, M.I. and VAN DOREN, S.R. (2006). Hsc70 contacts helix III of the J domain from polyomavirus T antigens: Addressing a dilemma in the chaperone hypothesis of how they release E2F from pRb. *Biochemistry*, 45, 6917-6929.

GARNIER, J., OSGUTHORPE, D.J. and ROBSON, B. (1978). Analysis of the accuracy and implication of simple methods predicting the secondary structure of globular proteins. *Journal of Molecular Biology*, 129, 97-120.

GARNIER, J., OSGUTHORPE, D.J. and ROBSON, B. (1996). GOR method for prediction of protein secondary structure from amino acid sequence. *Methods in Enzymology*, 266, 540-533.

GÄSSLER, C.S., BUCHBERGER, A., LAUFER, T., MAYER, M.P., SCHRÖDER, H., VALENCIA, A and BUKAU, B. (1998). Mutations in the DnaK chaperone affecting interaction with the DnaJ cochaperone. *Proceedings of the National Academy of Sciences*, 95, 15229-15234.

GEHDE, N., HINRICHS, C., MONTILLA, I., CHARPIAN, S., LINGELBACH, K. and PRZYBORSKI, J.M. (2009). Protein unfolding is an essential requirement for transport across the parasitophorous vacuolar membrane of *Plasmodium falciparum*. *Molecular Microbiology*, *In Press*, DOI: 10.1111/j.1365-2958.2008.06552.

GENEVAUX, P., WAWRZYNOW, A., ZYLICZ, M., GEORGEOPOULOS, C. and KELLEY, W.L. (2001). Dj1A is a third DnaK co-chaperone of *Escherichia coli*, and DjlA-mediated induction of colanic acid capsule requires DjlA-DnaK interaction. *The Journal of Biological Chemistry*, 276, 7906–7912.

GENEVAUX, P., SCHWAGER, F., GEORGOPOULOS, C. and KELLEY, W.L. (2002). Scanning Mutagenesis Identifies Amino Acid Residues Essential for the *in Vivo* Activity of the *Escherichia coli* DnaJ (Hsp40) J-Domain. *Genetics*, 162, 1045-1053.

GENEVAUX, P., LANG, F., SCHWAGER, F., VARTIKAR, J.V., RUNDELL, K., PIPAS, J.M., GEORGOPOULOS, C. and KELLEY, W.L. (2003). Simian Virus 40 T Antigens and J Domains: Analysis of Hsp40 Cochaperone Functions in *Escherichia coli*. *Journal of Virology*, 77, 10706-10713.

GEORGOPOULOS, C. and WELCH, W.J. (1993). Role of the Major Heat Shock Proteins as Molecular Chaperones. *American Journal of Biology*, 9, 601-634.

GINSBURG, H, FAMIN, O, ZHANG, J, KRUGLIAK, M. (1998). Inhibition of glutathione-dependent degradation of heme by chloroquine and amodiaquine as a possible basis for their antimalarial mode of action. *Biochemical Pharmacology*, 56, 1305–13.

GLOVER, J.R. and LINDQUIST, S. (1998). Hsp109, Hsp70, and Hsp40: a novel chaperone system that rescues previously aggregated proteins. *Cell*, 1998, 94: 73-82.

GLOVER, J. R. and TKACH, J. M. (2001). Crowbars and ratchets: Hsp100 chaperones as tools in reversing protein aggregation. *Biochemistry and Cell Biology,* 79, 557-568.

GOFFIN, L. and GEORGOPOULOS, C. (1998). Genetic and biochemical characterisation of mutations affecting the carboxy-terminal domain of the *Escherichia coli* molecular chaperone DnaJ. *Molecular Microbiology*, 30, 329-340.

GORMLEY, J.A., HOWARD, R.J. and TARASCHI, T.F. (1992). Trafficking of Malarial Proteins to the Host Cell Cytoplasm and Erythrocyte Surface Membrane Involves Multiple Pathways. *The Journal of Cell Biology*, 119, 1481-1495.

GOULOBINOFF, P, MOGK, A., ZVI, A.P., TOMOYASU, T. and BUKAU, B. (1999). Sequential mechanism of solubilisation and refolding of stable protein aggregates by a bichaperone network. *Proceedings of the National Academy of Sciences*, 96, 13732-13737.

GOWDA, D.C. and DAVIDSON, E.A. (1999). Protein glycosylation in the malaria parasite. *Parasitology Today*, 15, 147-152.

GRAGEROV, A. and GOTTESMAN, M.E. (1994). Different peptide binding specificities of hsp70 family members. *Journal of Molecular Biology*, 241, 133-135.

GRAGEROV, A., ZENG, L., ZHAO, X., BURKHOLDER, W., GOTTESMAN, M.E. (1994). Specificity of DnaK-peptide binding. *Journal of Molecular Biology*, 235, 848-854.

GRÄSLUND, S., NORDLUND, P., WEIGELT, J., BRAY, J., GILEADI, O., KNAPP, S., OPPERMANN, U., ARROWSMITH, C., HUI, R., MING, J., DHE-PAGANON, S., PARK, H.-W., SAVCHENKO, A., YEE, A., EDWARDS, A., VINCENTELLI, R., CAMBILLAU, C., KIM, R., KIM, S.-H., RAO, Z., SHI, Y., TERWILLIGER, T.C., KIM, C.-Y., HUNG, L.-W., WALDO, G.S., PELEG, Y., ALBECK, S., UNGER, T., DYM, O., PRILUSKY, J., SUSSMAN, J.L., STEVENS, R.C., LESLEY, S.A., WILSON, I.A., JOACHIMIAK, A., COLLART, F., DEMENTIEVA, I., DONNELLY, M.I., ESCHENFELDT, W.E., KIM, Y., STOLS, L., WU, R., ZHOU, M., BURLEY, S.K., EMTAGE, J.S., SAUDER, J.M., THOMPSON, D., BAIN, K., LUZ, J., GHEYI, T., ZHANG, F., ATWELL, S., C ALMO, S., BONANNO, J.B., FISER, A., SWAMINATHAN, S., STUDIER, F.W., CHANCE, M.R., SALI, A., ACTON, T.B., XIAO, R., ZHAO, L., MA, L.C., HUNT, J.F., TONG, L., CUNNINGHAM, K., INOUYE, M., ANDERSON, S., JANJUA, H., SHASTRY, R., HO, C.K., WANG, D., WANG, H., JIANG, M., MONTELIONE, G.T., STUART, D.I., OWENS, R.J., DAENKE, S., SCHÜTZ, A., HEINEMANN, U., YOKOYAMA. S., BÜSSOW, K. and GUNSALUS, K.C. (2008). Protein production and purification. *Nature Methods*, 5, 135-146.

GREENE, M.K., MASKOS, K. and LANDRY, S.J. (1998). Role of the J-domain in the cooperation of Hsp40 and Hsp70. *Proceedings of the National Academy of Sciences*, 95, 6108-6113.

GROSSMAN, A.D., STRAUS, D.B., WALTER, W.A. and GROSS, C.A. (1987). σ^{32} synthesis can regulate the synthesis of heat shock proteins in *Escherichia coli. Genes and Development*, 1, 179-184.

GRUSCHUS, J.M., GREENE, L.E., ESIENBERG, E. and FERRETTI, J.A. (2004). Experimentally biased model structure of the Hsc70/auxilin complex: Substrate transfer and interdomain structural change. *Protein Science*, 13, 2029-2044.

GUNASEKERA, A.M., MYRICK, A., MILITELLO, K.T., SIMS, J.S., DONG, C., GIERAHN, T., LE ROCH, K., WINZELER, E. and WIRTH, D.F. (2007). Regulatory motifs uncovered among gene expression clusters in *Plasmodium falciparum*. *Molecular and Biochemical Parasitology*, 153, 19-30

GUSEV, N.B., BOGATCHEVA, N.V. and MARSTON, S.B. (2002). Structure and properties of small heat shock proteins (sHsp) and their interaction with cytoskeleton proteins. *Biochemistry (Moscow)*, 67, 511-519.

HALDAR, K., HILLER, N.L., VAN OOIJ, C. and BHATTACHARJEE, S. (2005). *Plasmodium* parasite proteins and the infected erythrocyte. *Trends in Parasitology*, 21, 402-403.

HALL, T.A. (1999). BioEdit: a user-friendly biological sequence alignment editor and analysis program for Windows 95/98/NT. *Nucleic Acids Symposium Series,* 41, 95-98.

HALL, N., KARRAS, M., RAINE, J.D., CARLTON, J.M., KOOIJ, T.W., BERRIMAN, M., FLORENS, L., JANSSEN, C.S., PAIN, A., CHRISTOPHIDES, G.K., JAMES, K., RUTHERFORD, K., HARRIS, B., HARRIS, D., CHURCHER, C., QUAIL, M.A., ORMOND, D., DOGGETT, J., TRUEMAN, H.E., MENDOZA, J., BIDWELL, S.L., RAJANDREAM, M.A., CARUCCI, D.J., YATES, J.R., KAFATOS, F.C., JANSE, C.J., BARRELL, B., TURNER, C.M., WATERS, A. P.

and SINDEN, R.E. (2005). A comprehensive survey of the *Plasmodium* life cycle by genomic, transcriptomic, and proteomic analyses. *Science,* 307, 82–86.

HAN, W. and CHRISTEN, P. (2001). Mutations in the interdomain linker region of DnaK abolish the chaperone action of the DnaK/DnaJ/GrpE system. *FEBS Letters*, 497, 55-58.

HAN, W. and CHRISTEN, P. (2003). Mechanism of the Targeting Action of DnaJ in the DnaK Molecular Chaperone System. *The Journal of Biological Chemistry*, 278, 19038-19043.

HANAI, R. and MASHIMA, K. (2003). Characterization of two isoforms of a human DnaJ homologue, HSJ2. *Molecular Biology Reports*, 30, 149-153.

HARRISON, C.J., HAYER-HARTL, M., DI LIBERTO, M., HARTL, F.U. and KURIYAN, J. (1997). Crystal structure of the nucleotide exchange factor GrpE bound to the ATPase domain of the molecular chaperone DnaK. *Science*, 276, 431-435.

HARTL, F.U. (1996). Molecular chaperones in cellular protein folding. *Nature*, 381, 571-579.

HARTL, F.U. and HAYER-HARTL, M. (2002). Molecular chaperones in the cytosol: from nascent chain to folded protein. *Science*, 295, 1852-1858.

HEIGES, M., WANG, H., ROBINSON, E., AURRECOECHEA, C., GAO, X., KALUSKAR, N., RHODES, P., WANG, S., HE, C.Z., SU, Y., MILLER, J., KRAEMER, E. and KISSINGER, J.C. (2006). CryptoDB: a Cryptosporidium bioinformatics resource. *Nucleic Acids Research*, 34, D419-422.

HENDRICK, J.P., LANGER, T., DAVIS, T.A., HARTL, F.U. and WIEDMANN, M. (1993). Control of the folding and membrane translocation by binding of the chaperone DnaJ to nascent polypeptides. *Proceedings of the National Academy of Sciences,* 90, 10216-10220

HENDRICK, J.P. and HARTL, F.U. (1993). Molecular chaperone functions of heat-shock proteins. *Annual Review of Biochemistry*, 62, 349-384.

HENDRICK, J.P. and HARTL, F.U. (1995). The role of molecular chaperones in protein folding. *FASEB Journal*, 9, 1559-1569.

HENNESSY, F., CHEETHAM, M.E., DIRR, H.W. and BLATCH, G.L. (2000). Analysis of the levels of conservation of the J domain among the various types of DnaJ-like proteins. *Cell Stress and Chaperones*, 5, 347-358.

HENNESSY, F., BOSHOFF, A. and BLATCH, G.L. (2005a). Rational mutagenesis of a 40 kDa heat shock protein from *Agrobacterium tumefaciens* identifies amino acid residues critical to its in vivo function. *The International Journal of Biochemistry and Cell Biology*, 37, 177-191.

HENNESSY, F., NICOLL, W.S., ZIMMERMANN, R., CHEETHAM, M.E., and BLATCH, G.L. (2005b). Not all J domains are created equal: implications for the specificity of Hsp40-Hsp70 interactions. *Protein Science*, 14, 1697-1709.

HERNÁNDEZ, M.P., SULLIVAN, W.P. and TOFT, D.O. (2002). The assembly and intermolecular properties of the hsp70-Hop-hsp90 molecular chaperone complex. *The Journal of Biological Chemistry*, 277, 38294-38304.

HIGHTOWER, L.E., HAGEMAN, J., VOS, M.J., KUBOTA, H., TANGUAY, R.M., BRUFORD, E.A., CHEETHAM, M.E., CHEN, B. and KAMPINGA, H. (2009). Guidelines for the nomenclature of the human heat shock proteins. *Cell Stress and Chaperones*, 14, 105-111.

HILLER, N.L., BHATTACHARJEE, S., VAN OOIJ, C., LIOLIOS, K., HARRISON, T., LOPEZ-ESTRANO, C., HALDAR, K. (2004). A host-targeting signal in virulence proteins reveals a secretome in malarial infection. *Science*, 306, 1897-1898.

HILLIER, C.J., WARE, L.A., BARBOSA, A., ANGOV, E., LYON, J.A., HEPPNER, D.G. and LANAR, D.E. (2005). Process Development and Analysis of Liver-Stage Antigen 1, a Preerythrocyte-Stage Protein-Based Vaccine for *Plasmodium falciparum*. *Infection and Immunity*, 73, 2109-2115.

HOE, K.E., WON, M., CHUNG, K.S., JANG, Y.J., LEE, S.B., KIM, D.U., LEE., J.W., YUN, J.H. and YOO, H.S. (1998). Isolation of a new member of DnaJ-like heat shock protein 40 (Hsp40) from human liver. *Biochimica et Biophysica Acta*, 1383, 4-8.

HOFFMANN, K. and HANDSCHUMACHER, R.E. (1995). Cyclophilin-40: evidence for a dimeric complex with hsp90. *Biochemistry Journal*, 307, 5-8.

HOFFMAN, H.J., LYMAN, S.K., LU, C., PETIT, M.A. and ECHOLS, H. (1992). Activity of the Hsp70 chaperone complex—DnaK, DnaJ, and GrpE—in initiating phage lambda DNA replication by sequestering and releasing lambda P protein. *Proceedings of the National Academy of Sciences*, 89, 12108-12111.

HÖHFELD, J., MINAMI, Y. and HARTL, F.U. (1995). Hip, a novel cochaperone involved in the eukaryotic Hsc70/Hsp40 reaction cycle. *Cell*, 83, 589-598.

HÖHFELD, J. and JENTSCH, S. (1997). GrpE-like regulation of the Hsc70 chaperone by the anti-apoptopic protein BAG-1. *The EMBO Journal*, 16, 6209-6216.

HÖHFELD, J., CYR, D.M. and PATTERSON, C. (2001). From the cradle to the grave: molecular chaperones that may choose between folding and degradation. *EMBO Reports*, 885-890.

HÖHFELD, J., BÖHSE, K., GENAU, M. and WESTHOFF, B. (2006). From Creator to Terminator: Co-chaperones That Link Molecular Chaperones to the Ubiquitin/Proteasome System. *In* Blatch, G.L. (ed), *Networking of Chaperones by Co-Chaperones*. Georgetown, Texas, U.S.A.: Landes Bioscience, p. 109-121.

HOLDER, A.A., SINDEN, R.E., YATES, J.R. and CARUCCI, D.J. (2002). A proteomic view of the *Plasmodium falciparum* life cycle. *Nature,* 419, 520-526.

HOLLOWAY, S.P., MIN, W. and INSELBERG, J.W. (1994). Isolation and characterization of a chaperonin 60 gene of the human malaria parasite *Plasmodium falciparum*. *Molecular and Biochemical Parasitology*, 64, 25-32.

HOLT, R.A., SUBRAMANIAN, G.M., HALPERN, A., SUTTON, G.G., CHARLAB, R., NUSSKERN, D.R., WINCKER, P., CLARK, A.G., RIBIERO, J.M.C., IDES, R., SALZBERG, S.L., LOFTUS, B., YANDELL, M., MAJOROS, W.H., RUSCH, D.B., LAI, Z., KRAFT, C.L., ABRIL, J.F., ANTHOUARD, V., ARENSBURGER, P., ATKINSON, P.W., BADEN, H., DE BERARDINIS, V., BALDWIN, D., BENES, V., BIEDLER, J., BLASS, C., BOLANOS, R., BOSCUS, D., BARNSTEAD, M., CAI, S., CENTER, A., CHATUVERDI, K., CHRISTOPHIDES, G.L., CHRYSTAL, M.A., CLAMP, M., CRAVCHIK, A., CURWEN, V., DANA, A., DELCHER, A., DEW, I., EVANS, C.A., FLANIGAN, M., GRUNDSCHOBER-FREIMOSER, A., FRIELDI, L., GU, Z., GUAN, P., GUIGO, R., HILLENMEYER, M.E., HLADUN, S.L., HOGAN, J.R., HONG, Y.S., HOOVER, J., JAILLON, O., KE, Z., KODIRA, C., KOKOZA, E., KOUTSOS, A., LETUNIC, I., LEVITSKY, A., LIANG, Y., Lin, J., LOBO, N.F., LOPEZ, J.R., MALEK, J.A., MCINTOSH, T.C., MEISTER, S., MILLER, J., MOBARRY, C., MONGIN, E., MURPHY, S.D., O'BROCHTA, D., PFANNKOCH, C., QI, R., REGIER, M.A., REMINGTON, K., SHAO, H., SHARAKHOVA, M.V., SITTER, C.D., SHETTY, J., SMITH, T.J., STRONG, R., SUN, J., THOMASOVA, D., TON, L.Q., TOPALIS, P., TU., Z., UNGER, M.F., WALENZ, B., WANG, A., WANG, J., WANG, M., WANG, X., WOODFORD, K.J., WORTMAN, J.R., WU, M., YAO, A., ZDOBNOV, E.M., ZHANG, H., ZHAI, Q., ZHAO, S., ZHY, S.C., ZHIMULEV, U., COLUZZI, M., DELLA TORRE, A., ROTH, C.W., LOUIS, C., KALUSH, F., MURAL, R.J., MYERS, E.W., ADAMS, M.D., SMITH, H.O., BRODER, S., GARDNER, M.J., FRASER, C.M., BIRNEY, E., BORK, P., BREY, P.T., VENTER, J.C., WEISSENBACH, J., KAFATOS, F.C., COLLINS, F.H. and HOFFMAN, S.L. (2002). The Genome Sequence of the Malaria Mosquito *Anopheles Gambiae*. *Science*, 298, 129-149.

HOOFT, R.W.W., VRIEND, G., SANDER, C. and ABOLA, E.E. (1996). Errors in protein structures. *Nature*, 381-272-272.

HOOVER, D.M. and LUBKOWSKI, J. (2002). DNAWorks: an automated method for designing oligonucleotides for PCR-based gene synthesis. *Nucleic Acids Research*, 30, e43.

HOPP, T.P. and WOODS, K.R. (1981). Prediction of protein antigenic determinants from amino acid sequences. *Proceedings of the National Academy of Sciences*, 78, 3824-3828.

HORROCKS, P. and NEWBOLD, C.I. (2000). Intraerythrocytic polyubiquitin expression in *Plasmodium falciparum* is subjected to developmental and heat-shock control. *Molecular and Biochemical Parasitology*, 105, 115-125.

HORROCKS, P. and MUHIA, D. (2005). PEXEL/VTS: a protein export motif in erythrocytes infected with malaria parasites. *Trends in Parasitology,* 21, 396- 399.

HORWITZ, J. (1992) Alpha-crystallin can function as a molecular chaperone. *Proceedings of the National Academy of Sciences*, 89, 10449–10453.

HOURY, W.A., FRISHMAN, D., ECKERSKORN, C., LOTTSPEICH, F. and HARTL, F.U. (1999). Identification of in vivo substrates of the chaperonin GroEL. *Nature*, 402, 147-154.

HU, J., WU, Y., LI, J., QIAN, X., FU, Z. and SHA, B. (2008). The crystal structure of the putative peptide-binding fragment from the human Hsp40, Hdj1. *BMC Bioinformatics*, 8, 3.

HUANG, K., FLANAGAN, J.M. and PRESTEGARD, J.H. (1998). The influence of C-terminal extension on the structure of the J domain in *E. coli* DnaJ. *Protein Science*, 8, 203-214.

IMAI, K., MARUYA, M., YASHIRODA, H., YAHARA, I. and TANAKA, K. (2003). The molecular chaperone Hsp90 plays a role in the assembly and maintenance of the 26S proteasome. *The EMBO Journal*, 22, 3557-3567.

INGOLIA, T. and CRAIG, E.A. (1982). *Drosophila* gene related to the major heat shock-induced gene is transcribed at normal temperatures and not induced by heat shock. *Proceedings of the National Academy of Sciences*, 79, 525-529.

JAKOB, U., GAESTEL, M., ENGEL, K. and BUCHNER, J. (1993). Small heat shock proteins are molecular chaperones. *The Journal of Biological Chemistry*, 268, 1517-1520.

JAMESON, B.A., and WOLF, H. (1988). The antigenic index: A novel algorithm for predicting antigenic determinants. *Computer Applications in the Biosciences*, 4, 181-186.

JENSEN, R.E. and JOHNSON, A.E. (1999). Protein translocation: is Hsp70 pulling my chain. *Current Biology*, 9, R779-R782.

JIANG, J., PRASAD, K., LAFER, E, M. and SOUSA, R. (2005). Structural Basis of Interdomain Communication in the Hsc70 Chaperone. *Molecular Cell*, 20, 513-524.

JIANG, J., MAES, E., TAYLOR, A., WANG, L., HINCK, A., LAFER, E. and SOUSA, R. (2007). Structural Basis of J Cochaperone Binding and Regulation of Hsp70. *Molecular Cell*, 28, 422-433.

JOHNSON, J.L. and CRAIG, E.A. (2000). A role for the Hsp40 Ydj1 in repression of basal steroid receptor activity in yeast. *Molecular and Cellular Biology*, 20, 3027-3036.

JOHNSON, J.L. and CRAIG, E.A. (2001). An Essential Role for the Substrate-binding Region of Hsp40s in *Saccharomyces cerevisiae*. *The Journal of Cell Biology,* 152, 851-856.

JOINER, K.A. (1991). Rhoptry lipids and parasitophorous vacuole formation: a slippery issue. *Parasitology Today*, 7, 226-227.

JONES, D.T. (1999). GenTHREADER: an efficient and reliable protein fold recognition method for genomic sequences. *Journal of Molecular Biology*, 287, 797-815.

JORDAN, R. and MCMACKEN, R. (1995). Modulation of the ATPase Activity of the Molecular Chaperone DnaK by Peptides and the DnaJ and GrpE Heat Shock Proteins. *The Journal of Biological Chemistry,* 270, 4563-4569.

JOSHI, B., BISWAS, S. and SHARMA. Y.D. (1992). Effect of heat-shock on *Plasmodium falciparum* viability, growth and expression of the heat-shock protein 'PFHSP70-I' gene. *FEBS Letters*, 312, 91-94.

KABANI, M., BECKERICH, J.-M. and GAILLARDIN, C. (2000). Sls1p stimulates Sec63p-mediated activation of Kar2p in a conformation-dependent manner in the yeast endoplasmic reticulum. *Molecular and Cellular Biology*, 20, 6923-6934.

KABANI, M., BECKERICH, J.-M. and BRODSKY, J.L. (2002). Nucleotide exchange factor for the yeast Hsp70 molecular chaperones Ssa1p. *Molecular and Cellular Biology*, 22, 4677-4689.

KABANI, M., BECKERICH, J.-M. and BRODSKY, J.L. (2003). The yeast Sls1p and Fes1p proteins define a new family of Hsp70 nucleotide exchange factors. *Current Genomics*, 4, 465-473.

KABANI, M. and MARTINEAU, C. (2008). Multiple Hsp70 Isoforms in the Eukaryotic Cytosol: Mere Redundancy or Functional Specificity? *Current Genomics*, 9, 338-348.

KADEKOPPALA, M., O'DONNELL, R.A., GRAINGER, M., CRABB, B.S. and HOLDER, A.A. (2008). Deletion of the *Plasmodium falciparum* Merozoite Surface Protein 7 Gene Impairs Parasite Invasion of Erythrocytes. *Eukaryotic Cell*, 7, 2123-2132.

KAISER, K., CAMARGO, N. And KAPPE, S.H.I. (2003). Transformation of sporozoites into early exoerythrocytic malaria parasites does not require host cell. *Journal of Experimental Medicine*, 197, 1045-1050.

KANEHISA, M. and BORK, P. (2003). Bioinformatics in the post-sequence era. *Nature Genetics*, 33, 305-310.

KANG, Y., TALDONE, T., CLEMENT, C.C., FEWELL, S.W., AGUIRRE, J., BRODSKY, J.L. and CHIOSIS, G. (2008). Design of a fluorescence polarization assay platform for the study of human Hsp70. *Bioorganic & Medicinal Chemistry Letters*, 18, 3749-3751.

KAPPES, B., SUETTERLIn, B.W., HOFER-WARBINEK, R., HUMAR, R. and FRANKLIN, R.M. (1993). Two major phosphosproteins of *Plasmodium falciparum* are heat shock proteins. *Molecular and Biochemical Parasitology*, 59, 83-94.

KARPLUS, P.A. and SCHULTZ, G.E. (1988). Prediction of chain flexibility in proteins. *Naturwissenschaften*, 72, 212-213.

KAUTH, C.W., WOEHLBIER, U., KERN, M., MEKONNEN, Z., LUTZ, R., MÜCKE, N., LANGOWSKI, J. and BUJARD, H. (2006). Interactions between Merozoite Surface Proteins 1,6, and 7 of the Malaria Parasite *Plasmodium falciparum*. *The Journal of Biological Chemistry*, 281, 31517-31527.

KELLEY, L.A., MACCALLUM, R.M. and STERNBERG, M.J.E. (2000). Enhanced Genome Annotation using Structural Profiles in the Program 3D-PSSM. *Journal of Molecular Biology*, 299, 499-520.

KELLEY, P.M. and SCHLESINGER, M.J. (1982). Antibodies to Two Major Chicken Heat Shock Proteins Cross-React with Similar Proteins in Widely Divergent Species. *Molecular and Cellular Biology*, 2, 267-274.

KELLEY, W.L. and GEORGOPOULOS, C. (1997). The T/t common exon of the simian virus 40, JC and BK polyomavirus T antigens can functionally replace the J domain of the *Escherichia coli* DnaJ molecular chaperone. *Proceedings of the National Academy of Sciences*, 94, 3679-3684.

KELLEY, W.L. (1998). The J-domain family and the recruitment of chaperone power. *Trends in Biological Sciences*, 23, 222-227.

KELLEY, W.L. (1999). Molecular Chaperones: How J domains turn on Hsp70s. *Current Biology*, 9, 305-308.

KIM, H.-Y., AHN, B.-Y. and CHO, Y. (2001). Structural basis for the inactivation of retinoblastoma tumor suppressor by SV40 large T antigen. *The EMBO Journal*, 20, 295-304.

KISSINGER, J. C., GAJRIA, B., LI, L., PAULSEN, I. T. and ROOS, D. S. (2003). ToxoDB: accessing the *Toxoplasma gondii* genome. *Nucleic Acids Research*, 31, 234-236.

KLUCK, C.J., PATZELT, H., GENEVAUX, P., BREHMER, D., RIST, W., SCHNEIDER-MERGENER, J., BUKAU, B. and MAYER, M.P. (2002). Structure–function analysis of HscC, the *Escherichia coli* member of a novel subfamily of specialized Hsp70 chaperones. *The Journal of Biological Chemistry*, *277*, 41060–41069.

KOOIJ, T.W.A., JANSE, C.J. and WATERS, A.P. (2006). *Plasmodium* post-genomics: better the bug you know? *Nature Reviews Microbiology*, 4, 344-57.

KUMAR, N., ZHAO, Y., GRAVES, P., PEREZ FOLGAR, J., MALOY, L. and ZHENG, H. (1990). Human immune response directed against *Plasmodium falciparum* heat shock-related proteins. *Infection and Immunology*, 58, 1408-1414.

KUMAR, N., KOSKI, G., HARADA, M., AIKAWA, M. and ZHENG, H. (1991). Induction and localization of *Plasmodium falciparum* stress proteins related to the heat shock protein 70 family. *Molecular and Biochemical Parasitology*, 48, 47-58.

KUMAR, N. and ZHENG, H. (1992). Nucleotide sequence of a *Plasmodium falciparum* stress protein with similarity to mammalian 78-kDa glucose-related protein. *Molecular and Biochemical Parasitology*, 56, 353-356.

KUMAR, R., MUSIYENKO, A. and BARIK, S. (2005). *Plasmodium falciparum* calcineurin and its association with heat shock protein 90: mechanisms for the antimalarial activity of cyclosporin A and synergism with geldanamycin. *Molecular and Biochemical Parasitology*, 141, 29-37.

KUMAR, R., PAVITHRA, S.R. and TATU, U. (2007). Three-dimensional structure of heat shock protein 90 from *Plasmodium falciparum*: molecular modelling approach to rational drug design against malaria. *Journal of Biosciences*, 32, 531-536.

KROGH, A., LARSSON, B., VON HEIJNE, G. and SONNHAMMER, E.L.L. (2001). Predicting transmembrane protein topology with a hidden Markov model: application to complete genomes. *Journal of Molecular Biology*, 305, 567–580.

KYTE, J. and DOOLITTLE, R.F. (1982). A simple method for displaying the hydropathic character of a protein. *Journal of Molecular Biology*, 157, 105-132.

LACOUNT, D.J., VIGNALI, M., CHETTIER, R., PHANSALKAR, A., BELL, R., HESSELBERTH, J.R., SCHOENFELD, L.W., OTA, I., SAHASRABUDHE, S., KURSCHNER, C., FIELDS, S. and HUGHES, R.E. (2005). A protein interaction network of the malaria parasite *Plasmodium falciparum*. *Nature*, 438, 103-107.

LAMBROS, C. and VANDERBERG, J.P. (1979). Synchronization of *Plasmodium falciparum* erythrocytic stages in culture. *Journal of Parasitology*, 65, 418-420.

LANDRY, S.J. (2003). Structure and energetic of an allele-specific genetic interaction between *dnaJ* and *dnaK:* Correlation of nuclear magnetic resonance chemical perturbations in the J-domain of Hsp40/DnaJ with binding affinity for the ATPase domain of Hsp70/DnaK. *Biochemistry*, 42, 4926-4936.

LANZER, M., WICKERT, H., KROHNE, G., VINCENSINI, L. and BRAUN-BRETON, C. (2006). Maurer's clefts: A novel multi-functional organelle in the cytoplasm of *Plasmodium falciparum*-infected erythrocytes. *International Journal for Parasitology*, 36, 23-36.

LASKEY, R.A., HONDA, B.M., MILLS, A.D. and FINCH, J.T. (1978). Nucleosomes are assembled by an acidic protein which binds histones and transfers them to DNA. *Nature*, 275, 416-420.

LASKOWSKI, R.A., MACARTHUR, M.W., MOSS, D.S., and THORNTON, J.M. (1993). PROCHECK: a program to check the stereochemical quality of protein structures. *Journal of Applied Crystallography*, 26, 283-291.

LAUFEN, T., MAYER, M.P., BEISEL, C., KLOSTERMEIER, D., MOGK, A., REINSTEIN, J. and BUKAU, B. (1999). Mechanism of regulation of Hsp70 chaperones by DnaJ cochaperones. *Proceedings of the National Academy of Sciences*, 96, 5452-5457.

LEE, S., FAN, C.Y., YOUNGER, J.M., REN, H. and CYR, D.M. (2002). Identification of essential residues in the type II Hsp40 Sis1 that function in polypeptide binding. *The Journal of Biological Chemistry*, 277, 21675-21682.

LE ROCH, K.G., ZHOU, Y., BLAIR, P.L., GRAINGER, M., MOCH, J.K., HAYNES, J.D., DE LA VEGA, P., HOLDER, A.A., BATALOV, S., CARUCCI, D.J. and WINZELER, E.A. (2003). Discovery of gene function by expression profiling of the malaria parasite lifecycle. *Science*, 301, 1487-1488.

LELJ-GAROLLA, B. and MAUK, A.G. (2005). Self-association of a Small Heat Shock Protein. *Journal of Molecular Biology*, 345, 631-642.

LI, H., SÖDERBÄRG, K., HOUSHMAND, H., YOU, Z.Y. and MAGNUSSON, G. (2001). Effect on polyomavirus T-antigen function of mutations in a conserved Leucine-rich segment of the DnaJ domain. *Journal of Virology*, 75, 2253-2261.

LI, J., QIAN, X. and SHA, B. (2003). The crystal structure of the yeast Hsp40 Ydj1 complexed with its peptide substrate. *Structure*, 11, 1475-1483.

LI, J. and SHA, B., (2005). Structure-based mutagenesis studies of the peptide substrate binding fragment of type I heat-shock protein 40. *Biochemistry Journal*, 386, 453-460.

LI, J., WU, Y., QIAN, X. and SHA, B. (2006). Crystal structure of yeast Sis1 peptide-binding fragment and Hsp70 Ssa1 C-terminal complex. *Biochemistry Journal*, 398, 353-360.

LIBEREK, K., MARSZALEK, J., ANG, D., GEORGOPOULOS, C. and ZYLICZ, M. (1991). *Escherichia coli* DnaJ and GrpE heat shock proteins jointly stimulate ATPase activity of DnaK. *Proceedings of the National Academy of Sciences*, *88*, 2874-2878.

LINDENTHAL, C. and KLINKERT, M.Q. (2002). Identification and biochemical characterisation of a protein phosphatase 5 homologue from *Plasmodium falciparum*. *Molecular and Biochemical Parasitology*, 120, 257-268.

LINDQUIST, S. (1986). The Heat-Shock Response. *Annual Review of Biochemistry*, 55, 1151-1191.

LINGELBACH, K., and PRZYBORSKI, J.M. (2006). The long and winding road: Protein trafficking mechanisms in the *Plasmodium falciparum*-infected erythrocyte. *Molecular and Biochemical Parasitology*, 147, 1-8.

LINKE, K., WOLFRAM, T., BUSSEMER, J. And JAKOB, U. (2003). The Roles of Two Zinc Binding Sites in DnaJ. *The Journal of Biological Chemistry*, 278, 44457-44466.

LOPEZ, N., ARON, R. and CRAIG, E.A. (2003). Specificity of Class II Hsp40 Sis1 in Maintenance of Yeast Prion [RNQ+]. *Molecular Biology of the Cell*, 14, 1172-1181.

LOTZ, G.P., LIN, H., HARST, A. and OBERMAN, W.M.J. (2003). Aha1 Binds to the Middle Domain of Hsp90, Contributes to Client Protein Activation, and Stimulates the ATPase Activity of the Molecular Chaperone. *The Journal of Biological Chemistry*, 278, 17288-17235.

LOVEGROVE, F.E., PENA-CASTILLO, L., LILES, W.C., HUGHES, T.R. and KAIN, K.C. (2007). *Plasmodium falciparum* shows transcriptional versatility within the human host. *Trends in Parasitology*, 24, 288-291.

LU, Z. and CYR, D.M. (1998a). The conserved carboxyl terminus and zinc finger-like domain of the co-chaperone Ydj1 assist Hsp70 in protein folding. *The Journal of Biological Chemistry*, 273, 5970-5978.

LU, Z. and CYR, D.M. (1998b). Protein Folding Activity of Hsp70 Is Modified Differentially by the Hsp40 Co-chaperones Sis1 and Ydj1. *The Journal of Biological Chemistry*, 273, 27824-27830.

LUM, R., TKACH, J.M., VIERLING, E. and GLOVER, J.M. (2004). Evidence for an Unfolding/Threading Mechanism for Protein Disaggregation by *Saccharomyces cerevisiae* Hsp104. *The Journal of Biological Chemistry*, 279, 29139-29146.

MAGLIERY, T.J., WILSON, C.G.M., PAN, W., MISHLER, D., GHOSH, I., HAMILTON, A.D. and REGAN, L. (2005). Detecting protein-protein interactions with a Green Fluorescent Protein Fragment Reassembly Trap: Scope and Mechanism. *Journal of the American Chemical Society*, 127, 146-157.

MAHAJAN, B., NOIVA, R., YADAVA, N., ZHENG, H., MAJAM, V., MOHAN, K.V., MOCH, J.K., HAYNES, J.D., NAKHASI, H. and KUMAR, S. (2006). Protein disulfide isomerase assisted protein folding in malaria parasites. *International Journal for Parasitology*, 36, 1037-1048.

MAIER, A.G., RUG, M., O'NEILL, M.T., BEESON, J.G., MARTI, M., REEDER, J. and COWMAN, A.F. (2007). Skeleton-binding protein 1 functions at the parasitophorous vacuole membrane to traffic PfEMP1 to the *Plasmodium falciparum*-infected erythrocyte surface. *Blood*, 109, 1289-1297.

MAIER, A.G., RUG, M., O'NEILL, M.T., BROWN, M., CHAKRAVORTY, S., SZESTAK, T., CHESSON, J., WU, Y., HUGHES, K., COPPEL, R.L., NEWBOLD, C., BEESON, J.G., CRAIG, A, CRABB, B.S. and COWMAN, A.F. (2008). Exported Proteins Required for Virulence and Rigidity of *Plasmodium falciparum*-Infected Human Erythrocytes. *Cell*, 134, 48-61.

MARCHLER-BAUER, A. and BRYANT, S.H. (2004). CD-Search: protein domain annotations on the fly. *Nucleic Acids Research*, 32, 327-331.

MARCUS, N.Y., MARCUS, R.A., SCHMIDT, B.Z. and HASLAM, D.B. (2007). Contribution of the HEDJ/ERdj3 cysteine-rich domain to substrate interactions. *Archives of Biochemistry and Biophysics*, 468, 147-158.

MARTI, M., GOOD, R.T., RUG, M., KNUEPFER, E. and COWMAN, A.F. (2004). Targeting malaria virulence and remodeling proteins to the host erythrocyte. *Science*, 306, 1930-1933.

MARTI-RENOM, M.A., STUART, A., FISER, A., SÁNCHEZ, R., MELO, F., and SALI, A. (2000). Comparative protein structure modelling of genes and genomes. *Annual Review of Biophysics and Biomolecular* Structures, 29, 291-325.

MARTINEZ-YAMOUT, M., LEGGE, G.B., ZHANG, O., WRIGHT, P.E., DYSON, H.J. (2000). Solution Structure of the Cysteine-rich Domain of the *Escherichia coli* Chaperone Protein DnaJ. *Journal of Molecular Biology*, 300, 805-818.

MATAMBO, T.S., ODUNUGA, O.O., BOSHOFF, A. and BLATCH, G.L. (2004). Overproduction, purification, and characterization of the *Plasmodium falciparum* heat shock protein 70. *Protein Expression and Purification*, 33, 214-222.

MAYER, M.P. and BUKAU, B. (1998). Hsp70 chaperone systems: Diversity of cellular functions and mechanism of action. *Biological Chemistry*, 379, 261-268.

MAYER, M.P., LAUFEN, T., PAAL, K., MCCARTY, J.S. and BUKAU, B. (1999). Investigation of the Interaction between DnaK and DnaJ by Surface Plasmon Resonance Spectroscopy. *Journal of Molecular Biology,* 289, 1131-1144.

MAYER, M.P., RÜDIGER, S. and BUKAU, B. (2000). Molecular basis for interactions of the DnaK chaperone with substrates. *Biological Chemistry*, 381, 866-885.

MAYER, M.P. and BUKAU, B. (2005). Hsp70 chaperones: Cellular functions and molecular mechanisms. *Cellular and Molecular Life Sciences*, 62, 670-684.

MCCARTY, J.S., BUCHBERGER, A., REINSTEIN, J. and BUKAU, B. (1995). The role of ATP in the functional cycle of the DnaK chaperone system. *Journal of Molecular Biology*, 249, 126-137.

MCDONOUGH, H. and PATTERSON, C. (2003). CHIP: a link between the chaperone and proteasome systems. *Cell Stress and Chaperones*, 8, 303-308.

MCLAUGHLIN, S.H., SOBOTT, F., YAO, Z.-P., ZHANG, W., NIELSEN, P.R., GROSSMANN, J.G., LAUE, E.D., ROBINSON, C.V and JACKSON, S.E. (2006). The Co-chaperone p23 Arrests the Hsp90 ATPase Cycle to Trap Client Proteins. *Journal of Molecular Biology*, 356, 746-758.

MCNAMARA, C. (2006). Characterisation of Human Hsj1a: An Hsp40 Molecular Chaperone Similar to Malarial Pfj4. MSc Thesis, Rhodes University, Grahamstown, South Africa.

MEHLIN, C., BONI, E., BUCKNER, F.S., ENGEL, L., FEIST, T., GELB, M.H., HAJI, L., KIM, D., LIU, C., MUELLER, N., MYLER, P.J., REDDY, J.T., SAMPSON, J.N., SUBRAMANIAN, E., VAN VOORHIS, W.C., WORTHEY, E., ZUCKER, F. and HOL, W.G.J. (2006). *Molecular and Biochemical Parasitology*, 148, 144-160.

MEYER, P., PRODROMOU, C., HU, B., VAUGHAN, C., ROE, S.M., PANARETOU, B., PIPER, P.W. and PEARL, L.H. (2003). Crystal structure and functional analysis of the middle segment of Hsp90: *Molecular Cell*, 11, 647-658.

MICHALAK, P. (2008). Coexpression, coregulation, and cofunctionality of neighbouring genes in eukaryotic genomes. *Genomics*, 3, 243-248.

MILITELLO, K.T., DODGE, M., BETHKE, L. and WIRTH, D.F. (2004). Identification of regulatory elements in the *Plasmodium falciparum* genome. *Molecular and Biochemical Parasitology*, 134, 75-88.

MINAMI, Y., HOHFELD, J OHTSUKA, K. and HARTL, F.-U. (1996). Regulation of the heat-shock protein 70 reaction cycle by the mammalian DnaJ homology, Hsp40. *The Journal of Biological Chemistry*, 271, 19617-19624.

MISSELWITZ, B., STAECK, O. And RAPOPOR, T.A. (1998). J proteins catalytically activate Hsp70 molecules to trap a wide range of peptide sequences. *Molecular Cell*, 2, 593-603.

MOGK, A., TOMOYASU, T., GOLOUBINOFF, P., RÜDIGER, S., RODER, D., LANGEN, H., and BUKAU, B. (1999). Identification of thermolabile *Escherichia coli* proteins: prevention and reversion of aggregation by DnaK and ClpB. *The EMBO Journal,* 18, 6934-6949.

MOGK, A., DEUERLING, E., VORDERWÜHLBECKE, S., VIERLING, E. and BUKAU, B. (2003). Small heat shock proteins, ClpB and the DnaK system in reversing protein aggregation. *Molecular Microbiology*, 50, 585-595.

MOKRANJAC, D., BOURENKOV, G., HELL, K., NEUPERT, W., and GROLL, M. (2006). Structure and function of Tim14 and Tim16, the J and J-like components of the mitochondrial protein import motor. *The EMBO Journal*, 25, 4675-4685.

MONAGHAN, P. and BELL, A. (2005). A *Plasmodium falciparum* FK506-binding protein (FKBP) with peptidyl-prolyl *cis-trans* isomerase and chaperone activities. *Molecular and Biochemical Parasitology*, 139, 185-195.

MORISHIMA, Y., KANELAKIS, K.C., MURPHY, P.J., LOWE, E.R., JENKINS, G.J., OSAWA, Y., SUNAHARA, R.J. and PRATT, W.B. (2003). The hsp90 cochaperone p23 is the limiting component of the multiprotein hsp90/hsp70-based chaperone system in vivo where it acts to stabilize the client protein: hsp90 complex. *The Journal of Biological Chemistry*, 278, 48754-48763.

MUNRO, S. and PELHAM, H.R.B. (1987). A C-terminal signal prevents secretion of luminal ER proteins. *Cell*, 48, 899-907.

MURPHY, P.J., MORISIHIMA, Y., CHEN, H., GALIGNIANA, M.D., MANSFIELD, J.F., SIMONS, S.S., PRATT, W.B. (2003). Visualization and mechanism of assembly of a glucocorticoid receptor.Hsp70 complex that is primed for subsequent Hsp90-dependent opening of the steroid binding cleft. *The Journal of Biological Chemistry*, 278, 34764-34773.

NAKAI, K. and HORTON, P. (1999). PSORT: a program for detecting the sorting signals of proteins and predicting their subcellular localization. *Trends in Biochemical Sciences*, 24, 34-35.

NAYLOR, D.J., STINES, A.P., HOOGENRAAD, N.J. and HOJ, P.B. (1998). Evidence for the existence of distinct mammalian cytosolic, microsomal, and two mitochondrial GrpE-like proteins, the co-chaperones of specific Hsp70 members. *The Journal of Biological Chemistry,* 273, 21169-21177.

NEMOTO, T., OHARA-NEMOTO, Y., OTA, M., TAKAGI, T. and YOKOYAMA, K. (1995). Mechanism of dimer formation of the 90-kDa heat-shock protein. *European Journal of Biochemistry*, 233, 1-8.

NGOSUWAN, J., WANG, N.M., FUNG, K.L. and CHIRICO, W.J. (2003). Roles of Cytosolic Hsp70 and Hsp40 Molecular Chaperones in Post-translational Translocation of Presecretory Proteins in the Endoplasmic Reticulum. *The Journal of Biological Chemistry*, 278, 7034-7042.

NICOLL, W.S., BOSHOFF, A., LUDEWIG, M.G., HENNESSY, F., JUNG, M. and BLATCH, G.L. (2006). Approaches to the isolation and characterization of molecular chaperones. *Protein Expression and Purification*, 46, 1-15.

NICOLL, W.S., BOTHA, M., MCNAMARA, C., SCHLANGE, M., PESCE, E.R., BOSHOFF, A., LUDEWIG, M.H., ZIMMERMAN, R., CHEETHAM, M.E., CHAPPLE, J.P. and BLATCH, G.L. (2007). Cytosolic and ER J-domains of mammalian and parasitic origin can functionally interact with DnaK. *International Journal of Biochemistry and Cell Biology*, 39, 736-751.

NIELSEN, H., ENGELBRECHT, J., BRUNAK, S. and VON HEIJNE, G. (1997). Identification of prokaryotic and eukaryotic signal peptides and prediction of their cleavage sites. *Protein Engineering*, 10, 1-6.

NIELSEN, H. and KROGH, A. (1998). Prediction of signal peptides and signal anchors by a hidden Markov model. In Proceedings of the Sixth International Conference on Intelligent Systems for Molecular Biology (ISMB 6), AAAI Press, Menlo Park, California, 122-130.

NOLLEN, E.A., KABAKOV, A.E., BRUNSTING, J.F., KANON, B., HÖHFELD, J. and KAMPINGA, H.H. (2001). Modulation of in vivo HSP70 chaperone activity by Hip and Bag-1. *The Journal of Biological Chemistry*, 276, 4677-4682.

NUNN, C.M., DJORDJEVIC, S., HILLAS, P.J., NISHIDA, C.R. and ORTIZ DE MONTELLANO, P.R. (2002). The Crystal Structure of *Mycobacterium tuberculosis* Alkylhydroperoxidase AhpD, a Potential Target for Antitubercular Drug Design. *The Journal of Biological Chemistry*, 277, 20033-20040.

NYALWIDHE, J., BAUMEISTER, S., HIBBS, A.R., TAWILL, S., PAPAKRIVOS, J, VÖLKER, U. and LINGELBACH, K. (2002). A Nonpermeant Biotin Derivative Gains Access to the Parasitophorous Vacuole in *Plasmodium falciparum*-infected Erythrocytes Permeabilized with Streptolysin O. *The Journal of Biological Chemistry*, 277, 40005-40011.

NYALWIDHE, J., MAIER, U.-G., and LINGELBACH, K. (2003). Intracellular parasitism: cell biological adaptations of parasitic protozoa to a life inside cells. *Zoology*, 106, 341-348.

NYALWIDHE, J. and LINGELBACH, K. (2006). Proteases and chaperones are the most abundant proteins in the parasitophorous vacuole of *Plasmodium falciparum*-infected erythrocytes. *Proteomics*, 6, 1563-1573.

OAKLEY, M.S.M., KUMAR, S., ANANTHARAMAN, V., ZHENG, H., MAHAJAN, B., HAYNES, J.D., MOCH, J.K., FAIRHURST, R., MCCUTCHAN, T.F. and ARAVIND, L. (2007). Molecular Factors and Biochemical Pathways Induced by Febrile Temperature in Intraerythrocytic *Plasmodium falciparum* Parasites. *Infection and Immunity*, 75, 2012-2025.

ODUNUGA, O.O., LONGSHAW, V.M. and BLATCH, G.L. (2004). Hop: more than an Hsp70/Hsp90 adaptor protein. *BioEssays*, 26, 1058-1068.

OTTO, H., CONZ, C., MAIER, P., WOLFE, T., SUZUKI, C.K., JENO, P., RUCKNAGEL, P., STAHL, J. and ROSPERT, S. (2005). The chaperones MPP11 and Hsp70L1 form the mammalian ribosome-associated complex. *Proceedings of the National Academy of Sciences*, 102, 10064-10069.

PACHEBAT, J.A., KADEKOPPALA, M., GRAINGER, M., DLUZEWSKI, A.R., GUNARATNE, R.S., SCOTT-FINNIGAN, T.J., OGUN, S.A., LING, I.T., BANNISTER, L.H., TAYLOR, H.M., MITCHELL, G.H. and HOLDER, A.A. (2007). Extensive proteolytic processing of the merozoite surface protein 7 during biosynthesis and parasite release from erythrocytes. *Molecular and Biochemical Parasitology*, 151, 59-69.

PAGE, R. D. M. (1996). TREEVIEW: An application to display phylogenetic trees on personal computers. C*omputer Applications in the Biosciences*, 12, 357-358.

PAK, M. and WICKNER, S. (1997). Mechanism of protein remodeling by ClpA chaperone. *Proceedings of the National Academy of Sciences*, 94, 4901-4906.

PAIN, A., RENAULD, H., BERRIMAN, M., MURPHY, L., YEATS, C.A., WEIR, W., KERHORNOU, A., ASLETT, M., BISHOP, R., BOUCHIER, C., COCHET, M., COULSON, R.M., CRONIN, A., DE VILLIERS, E.P., FRASER, A., FOSKER, N., GARDNER, M., GOBLE, A., GRIFFITHS-JONES, S., HARRIS, D.E., KATZER, F., LARKE, N., LORD, A., MASER, P., MCKELLAR, S., MOONEY, P., MORTON, F., NENE, V., O'NEIL, S., PRICE, C., QUAIL, M.A., RABBINOWITSCH, E., RAWLINGS, N.D., RUTTER, S., SAUNDERS, D., SEEGER, K., SHAH, T., SQUARES, R., SQUARES, S., TIVEY, A., WALKER, A.R., WOODWARD, J., DOBBELAERE, D.A., LANGSLEY, G., RAJANDREAM, M.A., MCKEEVER, D., SHIELS, B., TAIT, A., BARRELL, B. and HALL, N. (2005). Genome of the host-cell transforming parasite *Theileria annulata* compared with *T. parva*. *Science*, 309, 131–133.

PASINI, E.M., KIRKEGAARD, M., MORTENSEN, P., LUTZ, H.U., THOMAS, A.W. and MANN, M. (2006). In-depth analysis of the membrane and cytosolic proteome of red blood cells. *Blood*, 108, 791-801.

PAPWORTH, C. BAUER, J. C., BRAMAN, J. and WRIGHT, D. A. (1996). Site-directed mutagenesis in one day with greater than 80% efficiency. *Strategies*, 9, 3–4.

PATANKAR, S., MUNASINGHE, A., SHOAIBI, A., CUMMINGS, L.M. and WIRTH, D.F. (2001). Serial analysis of gene expression in *Plasmodium falciparum* reveals the global expression profile of erythrocytic stages and the presence of anti-sense transcripts in the malarial parasite *Molecular Biology of the Cell*, 12, 3114–3125.

PAVITHRA, S.R., BANUMATHY, G., JOY, O., SINGH, V. and TATU, U. (2004). Recurrent fever promotes *Plasmodium falciparum* development in human erythrocytes. *The Journal of Biological Chemistry*, 279, 46692-46699.

PAVITHRA, S.R., KUMAR, R. and TATU, U. (2007). Systems Analysis of Chaperone Networks in the Malarial Parasite *Plasmodium falciparum*. *PLoS Computational Biology,* 3, 1701-1715.

PELHAM, H. R. (1982). A regulatory upstream promoter element in the *Drosophila hsp70* heat-shock gene. *Cell,* 30, 517–528

PELLECCHIA, M., SZYPERSKI, T., WALL, D., GEORGOPOULOS, C. and WÜTHRICH, K. (1996). NMR Structure of the J-domain and the Gly/Phe-rich Region of the *Escherichia coli* DnaJ Chaperone. *Journal of Molecular Biology*, 260, 236-250.

PELLECCHIA, M., MONTGOMERY, D.L., STEVENS, S.Y., VAN DER KOOI, C.W., FENG, H.-P., GIERASCH, L.M. and ZUIDERWEG, E.R.P. (2000). Structural insights into substrate binding by the molecular chaperone DnaK. *Nature Structural Biology*, 7, 298-303.

PENKETT, C.J., MORRIS, J.A., WOOD, V. and BÄHLER, J. (2006). YOGY: a web-based, integrated database to retrieve protein and associated Gene Ontology terms. *Nucleic Acids Research*, 34, 330-334.

PETERSON, M.G., CREWTHER, P.E., THOMPSON, J.K., CORCORAN, L.M., COPPEL, R.L., BROWN, G.V., ANDERS, R.F. and KEMP, D.J. (1988). A second antigenic heat shock protein of *Plasmodium falciparum*. *DNA*, 7, 71-78.

PICARD, D., KHURSHEED, B. GARABEDIAN, M.J., FORTIN, M.G., LINDQUIST, S. and YAMAMOTO, K.R. (1990). Reduced levels of hsp90 compromise steroid receptor action in vivo. *Nature*, 348, 166-168.

PIERPAOLI, E.V., SANDMEIER, E., BAICI, A., SCHÖNFIELD, H., GISLER, S. and CHRISTEN, P. (1997). The Power Stroke of the DnaK/DnaJ/GrpE Molecular Chaperone System. *Journal of Molecular Biology*, 269, 757-768.

PIERPAOLI, E.V., SANDMEIER, E., SCHÖNFELD, H.-J., and CHRISTEN, P. (1998). Control of the DnaK chaperone cycle by substoichiometric concentrations of the co-chaperones DnaJ and GrpE. Journal of Biological Chemistry *273*, 6643-6649.

PIZZI, E. and FRONTALI, C. (2001). Low-complexity regions in *Plasmodium falciparum* proteins. *Genome Research*, 11, 218-229.

PRATT, W.B. and TOFT, D.O. (1997). Steroid Receptor Interactions with Heat Shock Protein and Immunophilin Chaperones. *Endocrine Reviews*, 18, 306-360.

PRATT, W.B. and TOFT, D.O. (2003). Regulation of signalling protein function and trafficking by the hsp90/hsp70-based chaperone machinery. *Experimental Biology and Medicine*, 228, 111-133.

PRÖLS, F., MAYER, M.P., RENNER, O., CZARNECKI, P.G., AST, M., GÄSSLER, C, WILTING, J., KURZ, H. and CHRIST, B. (2001). Upregulation of the cochaperone Mdg1 in endothelial cells is induced by stress and during *in vitro* angiogenesis. *Experimental Cell Research*, *269*, 42–53.

PRODROMOU, C., ROE, S.M., O'BRIEN, R., LADBURY, J.E., PIPER, P.W. and PEARL, L.H. (1997). Identification and structural characterization of the ATP/ADP-binding site in the Hsp90 molecular chaperone. *Cell*, 90, 65-75.

PRODROMOU, C., PANARETOU, B., BHOHAN, S., SILIGARDI, G., O'BRIEN, R., LADBURY, J.E., ROE, S.M., PIPER, P.W. and PEARL, L.H. (2000). The ATPase cycle of Hsp90 drives a molecular 'clamp' via transient dimerization of the N-terminal domains. *The EMBO Journal*, 19, 4383-4392.

PRZYBORSKI, J.M., WICKERT, H., KROHNE, G. and LANZER, M. (2003). Maurer's clefts – a novel secretory organelle? *Molecular and Biochemical Parasitology*, 132, 17-26.

PRZYBORSKI, J.M. and LANZER, M. (2005). Protein transport and trafficking in *Plasmodium falciparum*-infected erythrocytes. *Parasitology, 130*, 373-388.

QAZI, K.R., WIKMAN, N., VASCONCELOS, N.-M., BERZINS, K., STAHL, S. and FERNANDEZ, C. (2005). Enhancement of DNA vaccine potency by linkage of Plasmodium falciparum malarial antigen gene fused with a fragment of HSP70 gene. *Vaccine*, 23, 1114-1125.

QIAN, Y.Q., PATEL, D. HARTL, F.-U., and MCCOLL, D.J. (1996). Nuclear magnetic resonance solution structure of the human Hsp40 (HDJ-1) J domain. *Journal of Molecular Biology*, 260, 224-235.

QIAN, X., HOU, W., ZHENGANG, L. and SHA, B. (2002). Direct interactions between molecular chaperones heat-shock protein (Hsp) 70 and Hsp40: yeast Hsp70 Ssa1 binds the extreme C-terminal region of yeast Hsp40 Sis1. *Biochemistry Journal*, 361, 27-34.

QIU, X.-B., SHAO, Y.-M., MIAO, S. and WANG, L. (2006). The diversity of the DnaJ/Hsp40 family, the crucial partners for Hsp70 chaperones. *Cellular and Molecular Life Sciences*, 63, 2560-70.

RAMOS, C.H., OLIVEIRA, C.L., FAN, C.Y., TORRIANI, I.L. and CYR, D.M. (2008). Conserved central domains control the quaternary structure of type I and II Hsp40 molecular chaperones. *Journal of Molecular Biology*, 383, 155-166.

RAMYA, T.N.C., SUROLIA, N.N. and SUROLIA, A. (2006). 15-Deoxyspergualin modulates *Plasmodium falciparum* heat shock protein function. *Biochemical and Biophysical Research Communications,* 348**,**585-592.

RANSON, N., FARR, G., ROSEMAN, A., GOWEN, B., FENTON, W., HORWICH, A. and SAIBIL, H. (1999). ATP-Bound States of GroEL Captures by Cryo-Electron Microscopy. *Cell*, 107, 869-879.

RAYNER, J.C., TRAN, T.M., CORREDOR, V., HUBER, C.S., BARNWELL, J.W. and GALINSKI, M.R. (2005). Dramatic difference in diversity between *Plasmodium falciparum* and *Plasmodium vivax* reticulocyte binding-like genes. *American Journal of Tropical Medicine and Hygiene*, 72, 666-674.

RICHTER, T., SOROKA, J., SKALNIAK, L., LESKOVAR, A., HESSLING, M., REINSTEIN, J. and BUCHNER, J. (2008). Conserved conformational changes in the ATPase cycle of human Hsp90. *The Journal of Biological Chemistry*, 283, 17757-17765.

RITOSSA, F. (1962). A new puffing pattern induced by temperature shock and DNP in *Drosophila*. *Experientia***,** 18, 571-473.

RODRIGUEZ, F., ARSÈNE-PLOETZE, F., RIST, W., RÜDIGER, S., SCHNEIDER-MERGENER, J., MAYER, M.P. and BUKAU, B. (2008). Molecular basis for regulation of the heat shock transcription factor sigma32 by the DnaK and DnaJ chaperones. *Molecular Cell*, 32, 347-358.

ROE, S.M., ALI, M.M.U., MEYE, P., VAUGHAN, C.K., PANARETOU, B., PIPER, P.W., PRODROMOU, C. and PEAR, L.H (2004). The mechanism of Hsp90 regulation by the protein kinase-specific cochaperone $p50_{cdc37}$. *Cell*, 116, 87-98.

RÖMISCH, K. (2005). Protein Targeting from Malaria Parasites to Host Erythrocytes. *Traffic*, 6, 706-709.

ROOS, D. (2001). Bioinformatics – Trying to Swim in a Sea of Data. *Science*, 291, 1260-1261.

ROSSER, M.F.N. and CYR, D.M. (2006). Do Hsp40s Act as Chaperones or Co-Chaperones? *In* BLATCH, G.L. (ed.), *Networking of Chaperones by Co-Chaperones*. Georgetown, Texas, U.S.A.: Landes Bioscience, 38-51.

RÜDIGER, S., GERMEROTH, L., SCHNEIDER-MERGENER, J. and BUKAU, B. (1997). Substrate specificity of the DnaK chaperone determined by screening cellulose peptide libraries. *The EMBO Journal*, 16, 1501-1507.

RÜDIGER, S., SCHNEIDER-MERGENER, J. and BUKAU, B. (2001). Its substrate specificity characterizes the DnaJ co-chaperone as a scanning factor for the DnaK chaperone. *The EMBO Journal*, 20, 1042-1050.

RUG, M., WICKHAM, M.E., FOLEY, M., COWMAN, A.F. and TILLEY, L. (2004). Correct promoter control is needed for trafficking of the ring-infected erythrocyte surface antigen to the host cytosol in transfected malaria parasites. *Infection and Immunity*, 72, 6095-6105.

RYAN, M.T. and PFANNER, N. (2002). Hsp70 proteins in protein translocation. *Advances in Protein Chemistry*, 59, 223-242.

SAHI, C. and CRAIG, E.A. (2007). Network of general and speciality J protein chaperones of the yeast cytosol. *Proceedings of the National Academy of Sciences*, 104, 7163-7168.

SALI, A. and BLUNDELL, T.A. (1993). Comparative protein modelling by satisfaction of spatial restraints. Journal *of Molecular Biology*, 234, 779-815.

SAM-YELLOWE, T., FLORENS, L., JOHNSON, J.R., WANG, T., DRAZBA, J.A., LE ROCH, K.G., BATALOV, S., CARUCCI, D.J., WINZELER, E.A. and YATES, J.R. (2004). A Plasmodium Gene Family Encoding Maurer's Cleft Membrane Proteins: Structural Properties and Expression Profiling. *Genome Research*, 14, 1052-1059.

SANCHEZ, Y. and LINDQUIST, S.L. (1990). Hsp104 required for induced thermotolerance. *Science*, 248, 1112-1115.

SARIDAKI, T., SANCHEZ, D.O., PFAHLER, J. and LANZER, M. (2008). A conditional export system provides new insights into protein export in *Plasmodium falciparum*-infected erythrocytes. *Cell Microbiology*, 10, 2483-2495.

SARGEANT, T.J., MARTI, M., CALER, E., CALRTON, J.M., SIMPSON, K., SPEED, T.P. and COWMAN, A.F. (2006). Lineage-specific expansion of proteins exported to erythrocytes in malaria parasites. *Genome Biology*, 7, R12.1-R12.22.

SATI, S.P., SINGH, S.K., KUMAR, N. and SHARMA, A. (2002). Extra terminal residues have a profound effect on the folding and solubility of a *Plasmodium falciparum* sexual stage-specific protein over-expressed in *Escherichia coli*. *European Journal of Biochemistry*, 269, 5259-5263.

SCHEUFLER, C., BRINKER, A., BOURENKOV, G., PEGARARO, S., MORODER, L., BARTUNIK, H., HARTL, F.U., MOAREFI, I. (2000). Structure of TPR domain-peptide complexes: critical elements in the assembly of the Hsp70-Hsp90 multichaperone machine. *Cell*, 101, 199-210.

SCHLENSTEDT, G., HARRIS, S., RISSE, B., LILL, R. and SILVER, P.A. (1995). A yeast DnaJ homologue, Scj1p, can function in the endoplasmic reticulum with BiP/Kar2p via a conserved domain that specifies interactions with Hsp70s. *The Journal of Cell Biology*, 129, 979-988.

SCHLITZER, M. (2005). Inhibition of Farnesyltransferase as a Strategy for the Development of Novel Anti-Malarials. *Current Medical Chemistry – Anti-Infective Agents*, 4, 277-286.

SCHNAIDER, T., SOTI, C., CHEETHAM, M.E., MIYATA, Y., YAHARA, I., CSERMELY, P. (2000). Interaction of the human DnaJ homologue, HSJ1b with the 90 kDa heat shock protein, Hsp90. *Life Sciences*, 67, 1455-1465.

SCHNEIDER, E.L., KING, D.S. and MARLETTA, M.A. (2005). Amino acid substitution and modification resulting from *Escherichia coli* expression of recombinant *Plasmodium falciparum* histidine-rich protein II. *Biochemistry*, 44, 987-995.

SCHÖNFELD, H.-J., SCHMIDT, D., SCHRÖDER, H. and BUKAU, B. (1995). The DnaK Chaperone System of *Escherichia coli*: Quaternary Structures and Interactions of the DnaK and GrpE Components. *The Journal of Biological Chemistry*, 270, 2183-2189.

SCHWEDE, T., KOPP, J., GUEX, N., and PEITSCH, M.C. (2003). SWISS-MODEL: an automated protein homology modeling server. *Nucleic Acids Research*, *31*, 3381-3385.

SEARLS, D.B. (2000). Bioinformatics Tools for Whole Genomes. *Annual Review of Genomics and Human Genetics*, 1, 251-279.

SHA, B., LEE, S. and CYR, D.M. (2000). The crystal structure of the peptide binding fragment from the yeast Hsp40 protein Sis1. *Structure*, 8, 799-807.

SHARMA, Y.D. (1991). Knobs, knob proteins and cytoadherence in falciparum malaria. *The International Journal of Biochemistry*, 23, 775-789.

SHARMA, Y.D. (1992). Structure and Possible Function of Heat-Shock Proteins in *Plasmodium falciparum* Malaria. *Comparative Biochemistry and Physiology*, 102, 437-444.

SHERMAN, I.W., CRANDALL, I.E., GUTHRIE, N. and LAND, K.M. (1995). The Sticky Secrets of Sequestration. *Parasitology Today*, 11, 378-384.

SHI, Y., HONG, X. and WANG, C. (2005). The C-terminal (331-376) Sequence of *Escherichia coli* DnaJ Is Essential For Dimerization and Chaperone Activity: A Small Angle X-Ray Scattering Study in Solution. *The Journal of Biological Chemistry*, 280, 22761-22768.

SHIAU, A.K., HARRIS, S.F., SOUTHWORTH, D.R. and AGARD, D.A. (2006). Structural Analysis of *E. coli* hsp90 Reveals Dramatic Nucleotide-Dependent Conformational Rearrangements. *Cell*, 127, 329-340.

SHONHAI, A., BOSHOFF, A. and BLATCH, G.L. (2005). *Plasmodium falciparum* heat shock protein 70 is able to suppress the thermosensitivity of an *Escherichia coli* DnaK mutant strain. *Molecular Genetics and Genomics*, 274, 70-78.

SHONHAI, A. (2007). Molecular Characterisation of the Chaperone Properties of *Plasmodium falciparum* Heat Shock Protein 70. PhD Thesis, Rhodes University, Grahamstown, South Africa.

SHONHAI, A., BOSHOFF, A. and BLATCH, G.L. (2007). The structural and functional diversity of Hsp70 proteins from *Plasmodium falciparum*. *Protein Science*, 16, 1803-1818.

SHONHAI, A., BOTHA, M., DE BEER, T.J., BOSHOFF, A. and BLATCH, G.L. (2008). Structure-Function Study of a *Plasmodium falciparum* Hsp70 Using Three Dimensional Modelling and *In Vitro* Analyses. *Protein and Peptide Letters*, 15, 1117-1125.

SILIGARDI, G., PANARETOU, B., MEYER, P., SINGH, S., WOOLFSON, D.N., PIPER, P.W., PEARL, L.H. and PRODROMOU, C. (2002). Regulation of Hsp90 ATPase activity by the co-chaperone p50/Cdc37. *The Journal of Biological Chemistry,* 277, 20151-2159.

SILVA, M.D., COOKE, B.M., GUILLOTTE, M., BUCKINGHAM, D.W., SAUZET, J.P., LE SCANF, C., CONTAMIN, H., DAVID, P., MERCEREAU-PUIJALON, O. and BONNEFOY, S. (2005). A role for the *Plasmodium falciparum* RESA protein in resistance against heat shock demonstrated using gene disruption. *Molecular Microbiology*, 56, 990-1003.

SIPPL, M.J. (1993). Recognition of Errors in Three-Dimensional Structures of Proteins. *Proteins*, 17, 355-362.

ŠLAPETA, J. and KEITHLY, J.S. (2004). *Cryptosporidium parvum* mitochondrial-type Hsp70 targets homologous and heterologous mitochondria. *Eukaryotic Cell*, 3, 483-494.

SMITH, D.F., WHITESELL, L. and KATSANIS, E. (1998). Molecular Chaperones: Biology and Prospects for Pharmacological Intervention. *Pharmacological Reviews*, 50, 493-511.

SONDERMANN, H., SCHEUFLER, C., SCHNEIDER, C., HÖHFLED, J., HARTL, F.U. and MOAREFI, I. (2001). Structure of a Bag/Hsc70 complex: convergent functional evolution of Hsc70 nucleotide exchange factors. *Science*, 291, 1553-1557.

SØRENSEN, H.P. and MORTENSEN, K.K. (2005). Soluble expression of recombinant proteins in the cytoplasm of *Escherichia coli*. *Microbial Cell Factories*, 4:1.

SŐTI, C., PÁL, C., PAPP, B. and CSERMELY, P. (2005). Molecular chaperones as regulatory elements of cellular networks. *Current Opinion in Cell Biology*, 17, 210-215.

SPIELMANN, T., HAWTHORNE, P.L., DIXON, M.W.A., HANNEMANN, M., KLOTZ, K., KEMP, D.J., KLONIS, N., TILLEY, L., TRENHOLME, K.R. and GARDINER, D.L. (2006). A Cluster of Ring Stage–specific Genes Linked to a Locus Implicated in Cytoadherence in *Plasmodium falciparum* Codes for PEXEL-negative and PEXEL-positive Proteins Exported into the Host Cell. *Molecular Biology of the Cell*, 17, 3613-3624.

SPYCHER, C., KLONIS, N., SPIELMANN, T., KUMP, E., STEIGER, S., TILLEY, L. and BECK, H.P. (2003). MAHRP-1, a novel *Plasmodium falciparum* histidine-rich protein, binds ferriprotoporphyrin IX and localizes to the Maurer's clefts. *The Journal of Biological Chemistry*, 278, 35373-35383.

SPYCHER, C., RUG, M., KLONIS, N., FERGUSON, D.J.P., COWMAN, A.F., BECK, H.-P. and TILLEY, L. (2006). Genesis of and Trafficking to the Maurer's Clefts of *Plasmodium falciparum*-Infected Erythrocytes. *Molecular and Cellular Biology*, 26, 4074-4085.

STEMMER, W.P.C., CRAMERI, A., HA, K.D., BRENNAN, T.M., and HEYNEKER, H.L. (1995). Single-step assembly of a gene and entire plasmid from large numbers of oligodeoxyribonucleotides. *Gene*, 164, 49-53.

STRAUS, D.B., WALTER, W.A., and GROSS, C. (1987). The heat shock response of *E. coli* is regulated by changes in the concentration of sigma-32.

STRAUS, D.B., WALTER, W.A. and GROSS, C. (1990). DnaK, DnaJ, and GrpE heat-shock proteins negatively regulate heat-shock gene expression by controlling synthesis and stability of sigma 32. *Genes and Development*, 4, 2202-2209.

SU, X.Z., HEATWOLE, V.M., WERTHEIMER, S.P., GUINET, F., HERRFELDT, J.A., PETERSON, D.S., RAVETCH, J.A. and WELLEMS, T.E. (1995). The large diverse gene family *var* encodes proteins involved in cytoadherence and antigenic variation of *Plasmodium falciparum*-infected erythrocytes. *Cell*, 82, 89-100.

SUGAWARA, H., OGASAWARA, O., OKUBO, K., GOJOBORI, T. and TATENO, Y. (2008). DDBJ with new system and face. *Nucleic Acids Research,* 36, D22-24.

SUH, W., BURKHOLDER, W.F., LU, C.Z., ZHAO, X., GOTTESMAN, M.E. and GROSS, C.A. (1998). Interaction of the Hsp70 molecular chaperone, DnaK, with its cochaperone DnaJ. *Proceedings of the National Academy of Sciences*, 95, 15223-15228.

SUH, W.-C., LU, C.Z., and GROSS, C.A. (1999). Structural features required for the interaction of the Hsp70 molecular chaperone DnaK with its cochaperone DnaJ. *The Journal of Biological Chemistry*, 274, 30534-30539.

SULLIVAN, C.S., TREMBLAY, J.D., FEWELL, S.W., LEWIS, J.A., BRODSKY, J.L. and PIPAS, J.M. (2000). Species-specific elements in the large T antigen J domain are required for cellular transformation and DNA replication by simian virus 40. *Molecular and Cellular Biology*, 20, 5749-5757.

SUTHRAM, S., SITTLER, T. and IDEKER, T. (2005). The *Plasmodium* protein network diverges from those of other eukaryotes. *Nature Letters*, 438, 108-112.

SYIN, C. and GOLDMAN, N.D. (1996). Cloning of a *P. falciparum* gene related to the human 60 kDa heat shock protein. *Molecular and Biochemical Parasitology*, 79, 13-19.

SYKEN, J., DE-MEDINA, T. and MUNGER, K. (1999). *TID1*, a human homolog of the *Drosophila* tumor suppressor l(*2*)tid, encodes two mitochondrial modulators of apoptosis with opposing functions*. Proceedings of the National Academy of Sciences*, 96, 8499–8504.

SZABO, A., LANGER, T., SCHRODER, H., FLANAGAN, J., BUKAU, B., and HARTL, F.U. (1994). The ATP hydrolysis-dependent reaction cycle of the *Escherichia coli* Hsp70 system DnaK, DnaJ, GrpE. *Proceedings of the National Academy of Sciences,* 91, 10345-10349.

SZABO, A., KORSZUN, R., HARTL, F.U. and FLANAGAN, J. (1996). A zinc-finger like motif domain of the molecular chaperone DnaJ is involved in binding to denatured substrates. *The EMBO Journal*, 15, 408-417.

TAKAYAMA, S., BIMSTON, D.N., MATSUZAWA, S., FREEMAN, B.C., AIME-SEMPE, C., XIE, Z., MORIMOTO, R. and REED, J.C. (1997). BAG-1 modulates the chaperone activity of Hsp70/Hsc70. *The EMBO Journal*, 16, 4886-4896.

TARASCHI, T.F., TRELKA, D., MARTINEZ, S., SCHNEIDER, T. and O'DONNELL, M.E. (1991). Vesicle-mediated trafficking of parasite proteins to the host cell cytosol and erythrocyte surface membrane in *Plasmodium falciparum* infected erythrocytes. *International Journal of Parasitology*, 31, 1381-1391.

TARDIEUX, I., BAINES, I., MOSSAKOWSKA, M. and WARD, G. E. (1998) Actin-binding proteins of invasive malaria parasites and the regulation of actin polymerization by a complex of 32/34-kDa proteins associated with heat shock protein 70kDa. *Molecular and Biochemical Parasitology,* 93, 295-308.

TEMPLETON, T.J. and DEITSCH, K.W. (2005). Targeting malaria parasite proteins to the erythrocyte. *Trends in Parasitology*, 21, 399-402.

TERADA, K. and MORI, M. (2000). Human DnaJ Homologs dj2 and dj3, and bag-1 Are Positive Cochaperones of hsc70. *The Journal of Biological Chemistry*, 275, 24728-24734.

THOMAS, J.G., AYLING, A. and BANEYX, F. (1997). Molecular chaperones, folding catalysts, and the recovery of active recombinant proteins from *E. coli*. To fold or to refold. *Applied Biochemistry and Biotechnology*, 66, 197-238.

THULASIRAMAN, V., YANG, C.F. and FRYDMAN, J. (1999). *In vivo* newly translated polypeptides are sequestered in a protected folding environment. *The EMBO Journal*, 18, 85-95.

TODD, M.J., VIITANEN, P.V. and LORIMER, G.H. (1994). Dynamics of the chaperonin ATPase cycle: implications for facilitated protein folding. *Science*, 265, 659-666.

TOMOYASU, T., OGURA, T., TATSUTA, T. and BUKAU, B. (2002). Levels of DnaK and DnaJ provide tight control of heat shock gene expression and protein repair in *Escherichia coli*. *Molecular Microbiology*, 30, 567-581.

TRABBIC-CARLSON, K., LIU, L., KIM, B., CHILKOTI, A. (2004). Expression and purification of recombinant proteins from *Escherichia coli*: Comparison of an elastin-like polypeptide fusion with an oligohistidine fusion. *Protein Science,* 13, 3274-3284.

TSAI, J. and DOUGLAS, M.G. (1996). A Conserved HPD Sequence of the J-domain is Necessary for YDJ1 Stimulation of Hsp70 ATPase Activity at a Site Distinct from Substrate Binding. *The Journal of Biological Chemistry*, 271, 9347-9354.

TUTAR, Y., SONG, Y. and MASISON, D.C. (2005). Primate chaperones Hsc70 (constitutive) and Hsp70 (induced) differ functionally in supporting growth and prion propagation in *Saccharomyces cerevisiae*. *Genetics*, 172, 851-861.

TUTEJA, R. (2007a). Malaria – an overview. *FEBS Journal*, 274, 4670-4679.

TUTEJA, R. (2007b). Unraveling the components of protein translocation pathway in human malaria parasite *Plasmodium falciparum. Archives of Biochemistry and Biophysics*, 467, 249-260.

UEGUCHI, C., SHIOWAZA, T., KAKEDA, M., YAMADA, H. and MIZUNO, T. (1995). A study of the double mutation of dnaJ and cbpA, whose gene products function as molecular chaperones in *Escherichia coli. Journal of Bacteriology*, 177, 3894-3896.

USHIODA, R., HOSEKI, J., ARAKI, K., JANSEN, G., THOMAS, D.Y. and NAGATA, K. (2008). ERdj5 is required as a disulfide reductase for degradation of misfolded proteins in the ER. *Science*, 321, 569-672.

UNGEWICKELL, E., UNGEWICKELL, H., HOLSTEIN S.E., LINDER, R., KONDURY, P., BAROUCH, W., MARTINI, B., GREENE, L.E. and EISENBERG, E. (1995). Role of auxilin in uncoating clathrin-coated vesicles. *Nature,* 378, 632–635.

VAN HUIZEN, R., MARTINDALE, J.L., GOROSPE, M. and HOLBROOK, N.J. (2003). P58^{IPK}, a Novel Endoplasmic Reticulum Stress-inducible Protein and Potential Negative Regulator of eIF2α Signaling. *The Journal of Biological Chemistry*, 278, 15558-15564.

VEDADI, M., LEW, J., ARTZ, J., AMANI, M., ZHAO, Y., DONG, A., WASNEY, G.A., GAO, M., HILLS, T., BROKX, S., QIU, W., SHARMA, S., DIASSITI, A., ALAM, Z., MELONE, M., MULICHAK, A., WERNIMONT, A., BRAY, J., LOPPNAU, P., PLOTNIKOVA, O., NEWBERRY, K., SUNDARARAJAN, E., HOUSTON, S., WALKER, J., TEMPEL, W., BOCKHAREV, A., KOZIERADZKI, I., EDWARDS, A., ARROWSMITH, C., ROOS, D., KAIN, K. AND HUI, R. (2007). Genome-scale protein expression and structural biology of *Plasmodium falciparum* and related Apicomplexan organisms. *Molecular and Biochemical Parasitology*, 151, 100-110.

VIITANEN, P.V., LUBBEN, T.H., REED, J., GOLOUBINOFF, P., O'KEEFE, D.P. and LORIMER, G.H. (1990). Chaperonin-facilitated refolding of ribulose bisphosphate carboxylase and ATP hydrolysis by chaperonin 60 (groEL) are K+ dependent. *Biochemistry*, 29, 5665-5671.

VINCENSINI, L., RICHERT, S., BLISNICK, T., VAN DORSSELAER, A., LEIZE-WAGNER, E., RABILLOUD, T. and BRAUN-BRETON, C. (2005). Proteomic Analysis Identifies Novel Proteins of the Maurer's Clefts, a Secretory Compartment Delivering *Plasmodium falciparum* Proteins to the Surface of Its Host Cell. *Molecular and Cellular Proteomics,* 4.4, 582-593.

VONLAUFEN, N., KANZOK, S.M., WEK, R.C. and SULLIVAN, W.J. (2008). Stress response pathways in protozoan parasites. *Cellular Microbiology*, 10, 2387-2399.

VOS, M.J., HAGEMAN, J., CARRA, S., and KAMPINGA, H.H. (2008). Structural and Functional Diversities between Members of the Human HSPB, HSPH, HSPA, and DNAJ Chaperone Families*. Biochemistry*, 47, 7001-7011.

WADHWA, R., TAIRA, K. and KAUL, S.C. (2002). An Hsp70 family chaperone, mortalin/mthsp70/PBP74/Grp75: what, when, and where? *Cell Stress and Chaperones*, 7, 309-316.

WALL, D., ZYLICZ, M. and GEORGOPOULOS, C. (1994). The NH_2-terminal 108 amino acids of the *Escherichia coli* DnaJ protein stimulate the ATPase activity of DnaK and are sufficient for lambda replication. *The Journal of Biological Chemistry*, 269, 5446-5451.

WALL, D., ZYLICZ, M. and GEORGOPOULOS, C. (1995). The Conserved G/F Motif of the DnaJ Chaperone Is Necessary for the Activation of the Substrate Binding Properties of the DnaK Chaperone. *The Journal of Biological Chemistry*, 270, 2139-2144.

WALSH, P., BURSAC, D., LAW, Y.C., CYR, D. and LITHGOW, T. (2004). The J-protein family: modulating protein assembly, disassembly and translocation. *EMBO Reports*, 5, 567-571.

WATANABE, J. (1997). Cloning and characterization of heat shock protein DnaJ homologues from *Plasmodium falciparum* and comparison with ring infected erythrocyte surface antigen. *Molecular and Biochemical Parasitology*, 88, 253-258.

WEGELE, H., MÜLLER, L. and BUCHNER, J. (2004). Hsp70 and Hsp90 – A relay team for protein folding. *Reviews of Physiology, Biochemistry and Pharmacology*, 151, 1-44.

WHITE, N.J. (2008). *Plasmodium knowlesi*: the fifth human malaria parasite. *Clinical Infectious Diseases*, 46, 165-171.

WICKERT, H, GOTTLER, W., KROHNE, G. and LANZER, M. (2004). Maurer's cleft organization in the cytoplasm of *Plasmodium falciparum*-infected erythrocytes: new insights from three-dimensional reconstruction of serial ultrathin sections. *The European Journal of Cell Biology,* 83, 567-582.

WICKHAM, M.E., RUG, M., RALPH, S.A., KLONIS, N., MCFADDEN, G.I., TILLEY, L. and COWMAN, A.F. (2001). Trafficking and assembly of the cytoadherence complex in *Plasmodium falciparum*-infected human erythrocytes. *The EMBO Journal*, 20, 5636-5649.

WIRTH, D.F. (2002). The parasite genome: Biological revelations. *Nature*, 419, 495-496.

WISER, M.F., LANNERS, H.N., BAFFORD, R.A. and FAVOLORO, J.M. (1997). A novel alternate secretory pathway for the export of *Plasmodium* proteins into the host erythrocyte. *Proceedings of the National Academy of Sciences*, 94, 9108-9113.

WISER, M.F., LANNERS, H.N. and BAFFORD, R.A. (1999). Export of *Plasmodium* Proteins via a Novel Secretory Pathway. *Parasitology Today*, 15, 194-198.

WITTUNG-STAFSHEDE, P., GUIDRY, J., HORNE, B.E. and LANDRY, S.J. (2003). The J-Domain of Hsp40 Couples ATP Hydrolysis to Substrate Capture in Hsp70. *Biochemistry*, 42, 4937-4944.

WOEHLBIER, U., EPP, C., KAUTH, C.W., LUTZ, R., LONG, C.A., COULIBALY, B., KOUYATÉ, B., AREVALO-HERRERA, M., HERRERA, S. and BUJARD, H. (2006). Analysis of Antibodies Directed Against Merozoite Surface Protein 1 of the Human Malaria Parasite *Plasmodium falciparum*. *Infection and Immunity*, 74, 1313-1322.

WRIGHT, C.M., CHOVATIYA, R.J., JAMESON, N.E., TURNER, D.M., ZHU, G., WERNER, S., HURYN, D.M., PIPAS, J.M., DAY, B.W., WIPF, P., and BRODSKY, J.L. (2008). Pyrimidinone-peptoid hybrid molecules with distinct effects on molecular chaperone function and cell proliferation. *Bioorganic & Medicinal Chemistry*, 16, 3291-3301.

WU, X., JÖRNVALL, H., BERNDT, K.D. and OPPERMAN, U. (2004). Codon optimization reveals critical factors for high level expression of two rare codon genes in *Escherichia coli*: RNA stability and secondary structure but not tRNA abundance. *Biochemical and Biophysical Research Communications*, 313, 89-96.

WU, Y., LI, J., JIN, Z., FU, Z. and SHA, B. (2005). The Crystal Structure of the C-terminal Fragment of Yeast Hsp40 Ydj1 Reveals Novel Dimerization Motif for Hsp40. *Journal of Molecular Biology,* 346, 1005-1011.

XU, Y. and LINDQUIST, S. (1993). Heat shock protein hsp90 governs the activity of pp60v-src kinase. *Proceedings of the National Academy of Sciences*, 90, 7074-7078.

XU, Z.H., HORWICH, A.L. and SIGLER, P.B. (1997). The crystal structure of the asymmetric GroEL-GroES-$(ADP)_7$ chaperonin complex. *Nature*, 388, 741-750.

XU, Z.H. and SIGLER, P.B. (1998). GroEL/GroES: Structure and Function of a Two-Stroke Folding Machine. *Journal of Structural Biology*, 124, 129-141.

XU, P., WIDMER,G., WANG, Y., OZAKI, L.S., ALVES, J.M., SERRANO, M.G., PUIU, D., MANQUE, P., AKIYOSHI, D., MACKEY, A.J., PEARSON, W.R., DEAR, P.H., BANKIER, A.T., PETERSON, D.L., ABRAHAMSEN, M.S., KAPUR, V., TZIPORI, S. and BUCK, G.A. (2004). The genome of *Cryptosporidium hominis*. *Nature*, 431, 1107-1112.

YADAVA, A. and OCKENHOUSE, C.F. (2003). Effect of codon optimization on expression levels of a functionally folded malaria vaccine candidate in prokaryotic and eukaryotic expression systems. *Infection and Immunity*, 71, 4961-4969.

YAN, W., and CRAIG, E.A. (1999). The glycine-phenylalanine-rich region determines the specificity of the yeast Hsp40 Sis1. *Molecular and Cellular Biology*, 19, 7751-7758.

YAN, W., GALE, M.J., TAN, S.-L., and KATZE, M.G. (2002). Inactivation of the PKR Protein Kinase and Stimulation of mRNA Translation by the Cellular Co-Chaperone P58IPK Does Not Require J Domain Function. *Biochemistry*, 41, 4938-4945.

YOUNG, J.C., OBERMANN, W.M.J. and HARTL, F.U. (1998). Specific Binding of the Tetratricopeptide Repeat Proteins to the C-terminal 12kDa Domain of hsp90. *The Journal of Biological Chemistry*, 273, 18007-18010.

YOUNG, J.C. and HARTL, F.U. (2000). Polypeptide release by Hsp90 involves ATP hydrolysis and is enhanced by the co-chaperone p23. *The EMBO Journal*, 19, 5930-5940.

YOUNG, J.C., MOAREFI, I. and HARTL, F.U. (2001). Hsp90: a specialized but essential protein-folding tool. *The Journal of Cell Biology*, 154, 267-273.

YOUNG, J.C., BARRAL, J.M., and HARTL, F.U. (2003). More than folding: localized functions of cytosolic chaperones. *Trends in Biochemical Sciences*, 28, 541-547.

YOUNG, J.C., AGASHE, V.R., SIEGERS, K. and HARTL, F.U. (2004). Pathways of Chaperone-mediated Protein Folding in the Cytosol. *Molecular Cell Biology*, 5, 781-791.

YOUKER, R.T., WALSH, P., BEILHARZ, T., LITHGOW, T. and BRODSKY, J.L. (2004). Distinct Roles for the Hsp40 and Hsp90 Molecular Chaperones during Cystic Fibrosis Transmembrane Conductance Regulator Degradation in Yeast. *Molecular Biology of the Cell*, 15, 4787-4797.

ZHOU, A., SCHNAKE, P., XIAO, K. and LAL, A.A. (2004). Enhanced expression of a recombinant malaria candidate vaccine in *Escherichia coli* by codon optimization. *Protein Expression and Purification*, 34, 87-94.

ZHU, X., XHAO, X., BURKHOLDER, W., GRAGEROV, A., OGATA, C.M., GOTTESMAN, M.E. and HENDRICKSON, W.A. (1996). Structural analysis of substrate binding by the molecular chaperone, DnaK. *Science*, 272, 1606-1614.

ZIMMERMAN, S.B. and MINTON, A.P. (1993). Macromolecular crowding: biochemical, biophysical and physiological consequences. *Annual Review of Biophysics and Biomolecular Structure*, 22, 27-65.

ZUEGGE, J., RALPH, S., SCHMUKER, M., MCFADDEN, G.I. and SCHNEIDER, G. (2001). Deciphering apicoplast targeting signals - feature extraction from nuclear-encoded precursors of *Plasmodium falciparum* apicoplast proteins. *Gene*, 280, 19-26.